The role of lung tissue-resident memory T cells in protection against tuberculosis

Naomi Bull

Harris Manchester College

University of Oxford

A thesis submitted for the degree of

Doctor of Philosophy

Trinity 2017

Word count: ~ 30,000

THE JENNER INSTITUTE
DEVELOPING INNOVATIVE VACCINES

Animal & Plant Health Agency

The role of lung tissue-resident memory T cells in protection against tuberculosis

Naomi Bull, Harris Manchester College

Thesis submitted for the degree of Doctor of Philosophy, Trinity Term 2017

Abstract

Tuberculosis (TB) is a global health problem, which is proving extremely difficult to control in the absence of an effective vaccine. Bacille Calmette-Guérin (BCG), the only vaccine currently licensed against TB, demonstrates variable efficacy in humans and cattle. A greater understanding of what constitutes a protective host immune response is required in order to aid the development of improved vaccines. Tissue-resident memory T cells (T_{RM}) are a recently-identified subset of T cells, which may represent an important aspect of protective immunity to TB. This thesis aims to characterise the role of lung T_{RM} in BCG-induced protection against TB. In a mouse model, intravascular staining allowed discrimination between lung-vascular and lung-parenchymal T cells. Experiments demonstrated that BCG vaccination induced a population of antigen-specific lung-parenchymal $CD4^+$ T cells, a putative tissue-resident population. This lung-parenchymal population was significantly increased in frequency following mucosal BCG vaccination, compared to systemic BCG vaccination. This correlated with enhanced protection against *Mycobacterium tuberculosis* (*M.tb*) infection in the lungs of mice receiving mucosal BCG, compared to those receiving systemic BCG. Mucosal BCG induced lung-parenchymal $CD4^+$ T cells with enhanced proliferative capacity and a $PD1^+KLRG1^-$ cell-surface phenotype, a memory-like phenotype associated with improved protection against *M.tb* infection. These cells may represent a BCG-induced lung T_{RM} population responsible for the enhanced protection observed following mucosal BCG. Overall, this thesis highlights the potential of mucosal vaccination to elicit lung T_{RM} and identifies this as a possible immunological mechanism underlying enhanced protection against *M.tb* infection. These cells may constitute an important target for future vaccination strategies.

Acknowledgements

I would like to thank my supervisors, Professor Helen McShane and Dr Philip Hogarth, for giving me the opportunity to undertake this DPhil and for all their support and guidance throughout the project. It has been a fantastic 3 years, made even more enjoyable by the wonderful colleagues and friends that I have met in the labs both at Oxford and APHA. Special thanks go to Elena, Nawamin, Janet and Rachel for all their help with challenge experiments and for making time spent in CL3 such good fun. Also enormous thanks to Daryan and Carmen for teaching me many new techniques and for all their help in the lab. The cell-sorting experiments would have been impossible without the skill and patience of Daryan and Drew, and I am very grateful to the dedicated staff in the FGF and ASU for all their assistance with the mouse work.

I am extremely fortunate to have an incredibly supportive family who have always encouraged me and believed in me. I would not have got to this point without them and I am truly thankful for everything they have done for me. I would like to dedicate this thesis to my Dad, Arthur 'Keith' Bull. He may not be here to see it completed but I have no doubt he would be immensely proud.

Finally, thank you to Jon for supporting my decision to do this DPhil and for driving many miles on a regular basis to see me while we have been apart. I'm lucky to have found someone so special to share my life with.

Contents

List of figures

List of abbreviations

Ag85A	antigen 85A
APC	antigen presenting cell
APC	allophycocyanin
AF	Alexa Fluor
BAL	bronchoalveolar lavage
BCG	bacille Calmette-Guérin
Bcl6	B cell lymphoma 6 protein
BV	Brilliant Violet
CCR	CC-chemokine receptor
CD	cluster of differentiation
CFU	colony forming units
ChAd	chimpanzee adenovirus
Cy	cyanine
CXCR	CXC-chemokine receptor
DC	dendritic cell
DOTS	directly-observed treatment short course
EdU	5-ethynyl-2’-deoxyuridine
ESAT-6	early secreted antigenic target 6
FITC	fluorescein isothiocyanate
FBS	foetal bovine serum
GM-CSF	granulocyte macrophage colony-stimulating factor
GTP	guanosine triphosphate
HBSS	Hank’s balanced salt solution

H&E	haematoxylin and eosin
HIV	human immunodeficiency virus
iBALT	inducible bronchus-associated lymphoid tissue
ICOS	inducible T cell co-stimulator
ICS	intracellular cytokine staining
ID	intradermal
IFN	interferon
IL	interleukin
IN	intranasal
KLRG1	killer cell lectin-like receptor G1
LN	lymph node
iNOS	inducible nitric oxide synthase
mAB	monoclonal antibody
M.bovis	*Mycobacterium bovis*
MDR-TB	multidrug-resistant TB
MHC	major histocompatibility complex
MRI	magnetic resonance imaging
M.tb	*Mycobacterium tuberculosis*
MVA	modified Vaccinia virus Ankara
NHP	non-human primate
NK	natural killer
NTM	non-tuberculous mycobacteria
PBS	phosphate buffered saline
PE	R-phycoerythrin
PerCP	peridinin chlorophyll protein

PET	positron emission tomography
PPD	purified protein derivative
RBC	red blood cell
S1PR1	sphingosine-1-phosphate receptor 1
SEM	standard error of the mean
SPECT	single photon emission computed tomography
SPF	specific-pathogen-free
T-bet	T-box expressed in T cells
TB	tuberculosis
T_{CM}	central memory T cell
TCR	T cell receptor
T_{EM}	effector memory T cell
Th1	T helper 1
TNF	tumour necrosis factor
T_{RM}	tissue-resident memory T cell
WHO	World Health Organisation
XDR-TB	extensively drug-resistant TB

Chapter 1.

Introduction

1.1. Tuberculosis

Tuberculosis (TB), resulting from infection with *Mycobacterium tuberculosis (M.tb)*, was responsible for 1.8 million deaths in 2015, making it the leading cause of human mortality from an infectious disease worldwide[1]. *M.tb* is a highly successful pathogen which is estimated to infect one third of the world's population and causes a devastating disease burden in endemic areas, largely located in tropical and sub-tropical regions of the globe[2]. However, disease is not limited to these areas and countries with high levels of immigration from endemic regions are also experiencing increased numbers of cases within this population[3], meaning that TB remains truly a disease of global importance.

The World Health Organisation (WHO) has developed the 'End TB Strategy', aiming to reduce TB incidence by 80% and deaths by 90% by 2030[4]. However, efforts to control this ongoing pandemic have been hindered by the lack of an effective vaccine, discussed in greater detail later, and the emergence of drug-resistant TB. Multidrug-resistant TB (MDR-TB) and the even more severe form, extensively drug-resistant TB (XDR-TB), present a major obstacle to effective care and prevention, as well as increasing the economic burden on both an individual and national level[5]. Another challenge facing the control effort is the increased risk of developing TB for people infected with human immunodeficiency virus (HIV). TB is the most common presenting illness of people with HIV and is the major cause of HIV-related deaths, even among those taking antiretroviral treatment[6]. This dual epidemic is of particular consequence for the developing world, especially Sub-Saharan Africa, which accounted for 75% of deaths from HIV-associated TB in 2015[7].

Mycobacterium bovis (M.bovis), another member of the *M.tb* complex, primarily causes TB disease in cattle, although it is a zoonotic pathogen and there are estimates that *M.bovis* may be responsible for up to 7% of human TB cases in endemic areas[8, 9]. Due to the genetic homology between *M.tb* and *M.bovis*, both humans and cattle stand to benefit from development of an improved vaccine[10, 11]. Bovine TB (bTB) results in substantial production losses for farmers and presents a serious global threat to health and socioeconomic development. The UK government alone has spent £500 million of taxpayers' money in efforts to combat the disease over the last decade and this is estimated to rise to £1 billion over the next decade if no further action is taken[12]. Control of bTB is made much more difficult by the ability of *M.bovis* to infect wildlife species, forming a reservoir of disease which is extremely challenging to address. In the UK, this disease reservoir is primarily located within the European badger population, although brushtail possums in New Zealand and white-tailed deer in the USA present similar problems[13].

1.2. Vaccination against TB

There are a number of important interventions being employed in the battle against TB in humans, including development of new drugs to treat infection[14, 15], implementation of the directly observed treatment short course (DOTS) strategy[16] and development of new diagnostic tests such as the Xpert MTB/RIF[17]. In cattle, attempts to control the disease have focussed on nationwide test and slaughter measures[12]. It is widely accepted that vaccination offers the most sustainable and cost-effective solution for long-term control of any infectious disease. The only vaccine currently available against TB is bacille Calmette-Guérin (BCG), an attenuated strain of *M. bovis* developed through serial *in vitro* passage[18,

[19]. It has been used as a vaccine in humans since 1921 and has now been administered to over 4 billion people worldwide[20]. However, clinical trials investigating the protective efficacy of BCG in humans have found that it ranges from 0% to 80% depending on the population studied, as summarised in a recent meta-analysis[21]. The most variable efficacy in humans is reported against pulmonary TB in adults, but BCG does provide some protection against severe disseminated forms of the disease in childhood[22]. Interestingly, within some populations, such as American Indians and Alaskan Natives, BCG has been shown to remain efficacious for a very long period of time, up to 50-60 years[23]. Field trials of BCG in cattle have also demonstrated a large variability in protective efficacy (reviewed in[24]).

Several theories have been proposed as explanations for this variability in efficacy, including vaccine-related factors such as BCG strain and viability, as well as recipient-related factors such as nutrition, genetics, exposure to environmental non-tuberculous mycobacteria (NTM) and presence of co-infection with helminths[25-28]. The explanation best supported by the existing literature is that of previous exposure to NTM, which may result in pre-existing immunity to antigens that are common to NTM and *M.tb*[21, 29-36]. It is hypothesised that this may lead to 'masking', where previous sensitisation confers a level of protection against TB which masks the effect of BCG, or 'blocking', where the pre-existing immune response prevents the host from generating an effective immune response against BCG[35, 37, 38].

TB was declared a global emergency by the WHO in the early 1990s and since this time significant focus has been placed on the development of improved vaccines. More than 12 novel TB vaccine candidates have now been evaluated or are in the process of being

evaluated in human clinical trials, and new strategies are still under development at the pre-clinical stages[26, 39, 40]. There are generally three broad approaches which have been taken: improvement of BCG through the addition or over-expression of highly immunogenic *M.tb* antigens[41, 42], attenuation of *M.tb* through gene deletions in pathways required for full virulence or survival[43, 44] and finally the use of prime-boost strategies employing a subsequent immunisation to amplify an initial protective immune response[45-50]. Prime-boost strategies have tended to focus on the use of BCG as the primary immunisation, given its proven efficacy against disease in childhood and the discovery that it may provide additional non-specific health benefits resulting in reduced childhood mortality[51-54]. Progress is severely hampered by the absence of reliable immunological correlates of protection and uncertainty surrounding the predictive value of animal models, necessitating empirical testing of vaccine candidates in lengthy and expensive efficacy trials[55].

An ideal vaccine candidate would be one capable of inducing sterile immunity, however opinion is divided as to whether or not this is achievable[56-58]. Most infected individuals remain healthy but also latently infected for the duration of their lives. Consequently, if new vaccines are to be developed with the goal of sterile eradication of *M.tb*, they must out-perform natural immunity in resistant individuals. Alternatively, vaccine development could target the 10% of latently-infected individuals at risk of disease reactivation and could function to induce an immune response in these susceptible individuals matching that of resistant individuals. Prevention of transmission through enforcement of latency can be seen as a more realistic approach. However, in order to achieve this goal, a better understanding of the nature of protective immunity must remain a key focus. Selecting

appropriate target populations for new vaccines will also be critical. Creating an effective vaccine for infants is important considering the high burden of disease in this population. However, mass vaccination of adolescents and young adults will likely have the greatest impact on disease transmission, and may therefore be considered a more effective strategy[59, 60].

1.3. Pathogenesis

Transmission of *M.tb* occurs via aerosol droplets containing bacteria which are inhaled and deposited in the distal alveoli of the lung[57, 61]. Members of the *M.tb* complex are intracellular bacteria, capable of infecting many different cell types including neutrophils[62] and dendritic cells (DCs)[63], although alveolar macrophages are considered the primary target for *M.tb* upon entry into the lung[64-67]. Following phagocytosis, *M.tb* is able to persist in the macrophage through a number of immune evasion strategies involving manipulation of major histocompatibility complex (MHC) class II antigen processing and presentation pathways. These include transcriptional downregulation of MHC class II molecules, interference with intracellular trafficking of MHC class II molecules, disruption of dendritic cell maturation and inhibition of phagolysosomal fusion and phagosome acidification[68-76]. These mechanisms allow *M.tb* to generate an intracellular niche in which to survive and avoid the antibacterial effects mediated by antibodies[65, 77].

Alveolar macrophages are thought to be the initiators of granuloma formation in the lung, the hallmark of infection with *M.tb*[78]. These organised, dynamic structures contain lymphocytes, macrophages, epithelial cells and fibroblasts and are thought to be a means of initially controlling the infection through walling off the pathogen and limiting its spread

to other organs(reviewed in [79, 80]). However, recent studies have provided evidence that granuloma formation may in fact favour bacterial growth, with infected macrophages able to leave the primary granuloma and establish secondary granulomas at other sites[81, 82]. The paradox of TB is that in spite of the concentration of host immune responses in granulomas, sterilising immunity often fails to develop and bacterial persistence can continue indefinitely in apparently immunocompetent people[83-85]. This latent infection presents a real challenge for TB control strategies, as such a large proportion of the population of the globe is latently infected that is it impossible to test and treat all these individuals[2]. A means of targeting treatment to those most likely to go on to develop active disease, estimated at between 5 and 10% of latently infected individuals, is currently being sought[86, 87].

A balance of pro-inflammatory and anti-inflammatory immune responses is thought to be critical for the control of bacterial proliferation within granulomas and for the resolution of these lesions over time. However, dysregulation in the immune response e.g. in the case of HIV infection, malnutrition or cancer leads to granuloma progression and active disease, with granuloma enlargement, loss of structural integrity and development of a necrotic, caseated centre. Collapse of the granuloma releases virulent bacilli into the tissue, resulting in formation of further granulomas[88]. In the lung, the granuloma may erode into the airways, facilitating subsequent spread of bacteria to other individuals when the host coughs[80]. It is the loss of lung functionality resulting from this pathological progression that eventually leads to death of the host in the most common form of TB disease, pulmonary TB. Although pulmonary TB accounts for 70% of cases, *M.tb* can also cause extrapulmonary

disease through dissemination to other tissues including bone, lymph nodes and meninges[89].

1.4. Animals as experimental models

Experimental animal models of TB are a vital part of research furthering our understanding of the disease. Human challenge studies with virulent *M.tb* strains are impossible given the unpredictable nature of disease development following *M.tb* infection and the lengthy and complex treatment period required. In order to overcome this barrier, utilisation of BCG as a substitute challenge organism in humans has been described, and has demonstrated the ability to detect differences in antimycobacterial immunity induced by vaccination[90]. However, in this model BCG is administered intradermally, rather than being inhaled as with natural *M.tb* infection, and this doesn't allow for the study of local mucosal immunity in the lung. Field efficacy trials of new candidate vaccines relying on natural *M.tb* exposure require large numbers of volunteers and lengthy follow-up, which is both logistically challenging and extremely costly. In light of these challenges and the lack of correlates of protection for vaccine efficacy[55], the use of animal models forms an important part of the vaccine development process[91].

Mouse models generally offer the best tools for studying the immune response to pathogens due to the wealth of genetics and reagents available. However, the commonly used strains of mice such as BALB/c and C57BL/6, do not replicate the pathology found in human disease. In contrast to human granulomas, the murine equivalent is poorly organised and lacks fibrosis, hypoxia and caseation[92, 93]. Additionally, the model lacks the range of latency to active disease observed in humans, as bacterial counts remain relatively

high but stable throughout the course of infection and all mice ultimately die from progressive disease[86]. In spite of this, low dose aerosol infection with *M.tb* in mice, guinea pigs, rabbits and non-human primates (NHPs) does exhibit a number of the important features of human disease, including induction of an antigen-specific $CD4^+$ T cell response, initial suppression of bacterial accumulation in the lungs and persistent infection controlled immunologically for many months[94-97].

Use of inbred strains of mice with genetic deletions allowed identification of interferon-gamma (IFN-γ), tumour necrosis factor-alpha (TNF-α) and interleukin-12 (IL-12) as critical factors for a protective immune response in mice[98-100]. These findings have subsequently been validated in human disease studies, demonstrating the similarities in host-protective factors between mice and humans[101-104]. The importance of $CD4^+$ T cells in protection has also been proven in the mouse model as well as in human studies[105-110]. Certain strains of mice which are highly susceptible to *M.tb* infection exhibit lung pathology more closely resembling the pathology found in human disease and these represent a tool for investigating mechanisms of pathogenesis[111-113]. These models may reveal previously unknown factors important in the development of active disease.

Alternative models of TB include the use of guinea pigs, NHPs and cattle. There are fewer reagents available for studies in these species and the costs involved in challenge studies in larger animals are greater than those for murine studies, so these species are used less commonly. However, they do have some advantages over the mouse model depending on the aspect of disease to be studied, as the pathology seen in these species more closely mirrors active human TB[96, 97, 114-118]. NHPs are also able to provide a model for latent infection[96, 97].

Animal models of TB also allow application of techniques not possible in humans. Within the context of TB research, samples routinely collected from human clinical trial participants would usually be limited to peripheral blood and bronchoalveolar lavage (BAL) fluid, although it is also possible to perform lung biopsies, as has been done for the study of respiratory syncytial virus[119]. Use of a murine model allows the injection of an intravascular stain to identify populations of tissue-resident cells within the parenchyma of the lung[120-125], as well as adoptive transfer of cells from a donor mouse to a recipient mouse to determine protective capacity of different cell subsets[120, 126, 127]. Use of these techniques is providing valuable insight into local protective immune responses against *M.tb* infection, which may prove critical to the design of an effective new vaccine.

1.5. Current understanding of cell-mediated immune response to tuberculosis

The initial stages of *M.tb* infection involve innate immune responses, characterised by recruitment of inflammatory cells to the lung[128]. Here, antigen-presenting cells (APCs), such as dendritic cells (DCs), phagocytose the bacteria and its antigen before migrating to the lung-draining lymph nodes (LNs) to present antigen to naïve T cells[129]. These T cells become activated, proliferate and are able to differentiate into populations of effector cells with defined functions including the ability to produce cytokines[129-132]. Generation of these antigen-specific T cells marks the initiation of the adaptive immune response.

Upon entry to the lung, *M.tb* is able to impair DC-mediated antigen presentation and the migration of DCs to the draining LNs, thereby limiting the development of an effective

adaptive immune response[63, 129, 133-135]. This mechanism of immune evasion enables the bacterial population to expand within the lung for up to 18-20 days before antigen-specific T cells accumulate in sufficient numbers to inhibit bacterial growth[78, 129, 131, 136, 137]. Griffiths *et al.* have demonstrated that delivery of activated *M.tb* antigen-primed DCs into the lungs of vaccinated mice, at the same time as exposure to *M.tb*, overcomes this delay[138]. This period presents an opportunity for vaccine strategies targeting the generation of local lung immune responses, to control the early phase of *M.tb* growth. It has previously been shown that in the mouse, parenteral immunisation allows *M.tb* to grow logarithmically in the lung for >10 days, while mucosal immunisation inhibits *M.tb* growth in the early phase after challenge[139, 140].

There is strong evidence that a T helper 1 (Th1) -polarised $CD4^+$ T cell response plays a critical role in protection against *M.tb*. The requirement for $CD4^+$ T cells was initially established through the use of knockout mice and adoptive transfer experiments[105-107] and further substantiated by the observation that HIV-infected individuals, with reduced $CD4^+$ T cell counts, are at increased risk of developing active TB[108-110]. A central role for IFN-γ was determined by the fact that mice lacking this cytokine are extremely susceptible to *M.tb*[98, 141]. Genetic studies in humans confirmed a role for IFN-γ in people. It was identified that mutations in the IL-12-IFN-γ-signal transducer and activator of transcription 1 (STAT1) axis resulted in inherited susceptibility to disseminated infections caused by NTM and BCG[102-104, 142, 143]. Additionally, Cheallaigh *et al.*[144] recently reported that the common human Mal S180L polymorphism, which attenuates IFN-γ signalling, impairs responses to *M.tb* infection. IFN-γ is able to activate macrophages to kill intracellular bacteria through a number of downstream antimicrobial effector pathways. These include phagosomal

maturation and acidification, autophagy, inducible nitric oxide synthase (iNOS), vitamin D receptor signalling and IFN-γ-inducible GTPases[145-150]. Fletcher *et al.*[151] have shown that in BCG-immunised infants, the presence of BCG-specific T cells secreting IFN-γ correlates with reduced risk of TB disease. Put together, these discoveries lead to the establishment of the 'central dogma' of TB immunity, which is that production of IFN-γ by $CD4^+$ T cells activates macrophages to kill intracellular *M.tb*.

Despite widespread acceptance that $CD4^+$ T cells and IFN-γ are key players in the immune response against *M.tb*, further discoveries and developments in our understanding of the complex nature of TB immunity has called the central dogma into question. For example, a number of studies in mice have shown that several knockout strains, including TNF-α, IL-1- and IL-6-knockout mice, die very quickly following *M.tb* challenge despite retaining production of IFN-γ[100, 152-154]. In humans, it has been reported that administration of anti-TNF-α antibody for the treatment of Crohn's disease and rheumatoid arthritis can lead to reactivation of latent TB[101]. Also important to note is the fact that the majority of individuals who develop active TB have no identifiable deficiencies in their T cell compartment and are perfectly capable of mounting an *M.tb*-specific IFN-γ response. This indicates that whilst $CD4^+$ T cells and IFN-γ are certainly required for successful immunity against *M.tb*, they are not necessarily sufficient to prevent the development of active disease.

Comparable conclusions can be reached from vaccination studies demonstrating that the frequency of *M.tb*- or *M.bovis*-specific Th1 cells in the blood and lymphoid organs of humans, mice and cattle does not correlate with protection[155-158]. Similarly, magnitude and frequency of vaccine-induced IFN-γ responses fail to predict immunity[155, 156, 158-161]. This lack

of a robust correlate of protection presents a major hurdle to the development of improved TB vaccines.

In light of this, the field is now looking past the central dogma to identify other protective immunological functions. Potentially important mediators that activate macrophages and therefore may play a significant role include the cytokines TNF-α, IL-1β and granulocyte macrophage colony-stimulating factor (GM-CSF) as well as vitamins C and D[100, 101, 152, 153, 162-168]. Other cell types with suggested roles in the adaptive immune response include $CD8^+$ T cells and Th17 cells[169-175]. Sousa *et al.*[176] used knockout mouse strains to demonstrate that mice lacking $CD8^+$ T cells display increased susceptibility to *M.tb* infection. Importantly, unlike $CD4^+$ T cells, $CD8^+$ T cells have the ability to recognise non-phagocytic cells infected with *M.tb* such as epithelial cells, allowing them to conduct surveillance of a broader range of cell types[177]. In addition to production of Th1 cytokines, they are able to secrete granules containing cytotoxic molecules to lyse infected host cells and can induce apoptosis through ligation of Fas[178, 179]. Current evidence for Th17 cells supports a role in the early phase of protection against aerosol *M.tb* infection in mice[135, 173, 174], although the precise mechanisms leading to their activation and differentiation remain unclear.

The cells of the innate immune system, such as neutrophils, macrophages and natural killer (NK) cells are also hypothesised to play a key role. In fact, it may be the case that the functional limitations of an individual's innate cells are one of the deciding factors in the outcome of a TB infection (reviewed in [64]). Several genetic studies support the importance of T cell-independent intrinsic bactericidal activity of macrophages[180-183] and NK cells may be responsible for non-specific production of IFN-γ in the early stages of infection, prior to the development of adaptive T cell immunity[184-186].

Type I interferons (IFNs) have also been suggested to play a role in *M.tb* infection. Moreira-Teixeira *et al.* used a mouse model to demonstrate that in the absence of IFN-γ, type I IFN suppressed alternative macrophage activation, resulting in macrophages retaining a more-protective classically-activated phenotype[187]. It has been suggested that low levels of type I IFN may be required during the early stages of bacterial infection to initiate cell-mediated immune responses[188]. However, there is also *in vivo* evidence for exacerbation of disease by type I interferons. Mice lacking the receptor common to all type I IFNs, *Ifnar1*$^{-/-}$, have reduced bacterial load and increased survival following *M.tb* infection[188-190]. Additionally, mice treated with anti-type I IFN antibody also demonstrated increased survival post-*M.tb* infection[191].

1.6. CD4$^+$ T cell Memory

Establishment of immunological memory, a hallmark of the adaptive immune response, is the underlying principle behind vaccination. Following an infection or immunisation, an adaptive effector response is generated and subsequently resolves, leaving behind it a pool of long-lived antigen-specific lymphocytes with specialised characteristics. When a memory lymphocyte recognises its cognate antigen, it is able to generate a quantitatively and qualitatively superior effector response compared to naïve lymphocytes. Memory responses also occur more rapidly than naïve responses, generally enabling efficient control of disease upon re-exposure to a pathogen[192, 193].

Despite evidence demonstrating a critical role for CD4$^+$ T cells in protection against TB, far less is known about memory CD4$^+$ T cells than is known about their CD8$^+$ counterparts. In spite of the fact that CD4$^+$ T cells outnumber CD8$^+$ T cells in the body[194], most of our

knowledge about T cell memory generation comes from acute viral models of infection where the $CD4^+$ T cell response is generally much lower in magnitude[195-197]. This, combined with a relative lack of availability of effective MHC class II tetramers to detect antigen-specific $CD4^+$ T cells by flow cytometry[198], has made them a more challenging population to study. Care must be taken when determining the relevance of studies of $CD8^+$ T cells, as it is known that the requirements for memory development, as well as survival, differ between $CD4^+$ and $CD8^+$ T cells[197].

A specific characteristic of *M.tb* infection is its chronic nature, resulting in prolonged antigen exposure[127]. Immunisation with BCG mimics this situation due to the persistence of live BCG bacilli in the host[199, 200]. In both cases, this microenvironment of prolonged antigen exposure and chronic inflammation may lead to immune exhaustion, cell death and potentially the generation of dysfunctional or exhausted effector T cells instead of memory T cells[201, 202].

Several subsets of memory T cells have been proposed but it has proved difficult to characterise these precisely on the basis of either phenotype or cytokine profile, and we currently have a limited understanding of the specifics of their generation and maintenance.

A seminal study conducted in 1999 by Sallusto *et al*. described two distinct memory T cell compartments, differing in effector function, proliferative capacity and anatomical location[203]. Central memory T cells (T_{CM}) are predominantly located in the secondary lymphoid organs, express the cell-surface markers CCR7 and CD62L, produce IL-2 and proliferate extensively. Effector memory T cells (T_{EM}) are able to recirculate through

peripheral tissues, lack CCR7 and CD62L expression and are capable of producing a range of effector cytokines.

The relative importance of these two subsets of $CD4^+$ memory T cells to protective immunity against TB has been investigated through adoptive transfer experiments in mice. Several studies have suggested that $CD4^+$ T_{CM} mediate enhanced protection against TB[204-207] and it has been hypothesised that the lack of protection afforded by BCG against adult pulmonary TB may be due to it inducing T_{EM} rather than T_{CM}[208]. Interestingly, it has been shown that aerosol delivery of BCG to rhesus macaques resulted in expansion of the $CD4^+$ T_{CM} population in the peripheral blood[209]. This suggests that the route of antigen exposure, i.e. mucosal or systemic, may play a role in determining the development of different memory subsets.

1.7. Tissue-resident memory T cells

Recently, a new subset of memory T cells has been described, tissue-resident memory T cells (T_{RM}). As the name implies, the defining feature of these T_{RM} cells is their persistence in non-lymphoid tissues and lack of re-circulation through the body. They were first identified in the skin following infection with herpes simplex virus[210] and have since been described in a number of other tissues including small intestinal mucosa, brain and lung[120, 211, 212]. Development of an *in vivo* labelling technique to discriminate between cells present within the vasculature of an organ and those truly resident within the tissue has allowed definitive identification of these T_{RM} cells[120-125]. Lung T_{RM} may represent an important aspect of protective immunity to *M.tb*, as they have been shown to be present locally at the site of infection, have the ability to rapidly respond to pathogenic challenge *in situ*

independently of T cell recruitment from the blood and are able to coordinate recruitment of immune cells to tissue sites[120, 123, 212-214].

Teijaro *et al*. were able to demonstrate through the use of a mouse parabiosis model that $CD4^+$ T_{RM} are present in the murine lung following influenza infection[120]. These cells were shown to provide enhanced protection against influenza when compared to memory cells from the spleen, despite the ability of the splenic cells to migrate to the lung. This suggests that tissue localisation may be a critical factor for induction of protective immune responses against lung infections. More recently, additional work on the generation of $CD4^+$ T_{RM} following influenza infection found high expression levels of CD69 and CD11a within the T_{RM} population, whilst imaging has revealed these virus-specific T_{RM} cells are subsequently maintained in compartmentalised niches near the airways in the lungs of both mice and humans[123].

A seminal study by Sakai *et al.*[126] was the first to use the intravascular staining method to identify a population of $CD4^+$ T cells present within the lung-parenchyma post-*M.tb* infection. These cells were able to provide superior protection against *M.tb* challenge upon transfer to a lymphopoenic recipient, compared to $CD4^+$ T cells transferred from the lung-vasculature. Interestingly, this study found that the parenchymal $CD4^+$ T cells produced less IFN-γ than those present in the vasculature of the lung, suggesting that the location of the cell, rather than the quantity of cytokine it produces, is the critical factor in generating a protective immune response. The study also found that TB-specific lung-parenchymal $CD4^+$ T cells induced following *M.tb* infection were able to rapidly migrate back into the lung parenchyma upon adoptive transfer into infection-matched recipient mice, suggesting that these cells exhibit a tropism for lung tissue.

Maintenance of a lung-parenchymal $CD4^+$ T cell population during chronic *M.tb* infection has since been demonstrated[127]. Additionally, in order to investigate the survival of this subset in the absence of ongoing antigenic stimulation, lung-parenchymal cells were removed and transferred into naïve recipient animals where they persisted for 28 days, the duration of the experiment[127].

Many studies have described a phenotype associated with lung-parenchymal $CD4^+$ T_{RM}, although there has yet to be definitive characterisation of a phenotype unique to this population. They have so far been identified as $CXCR3^{hi}$[126], $CD69^+$ and $CD11a^{hi}$[123], $PD1^+$[127] and $CD103^+$[215]. Interestingly, the lung-vascular $CD4^+$ T cell population has also been described as having a characteristic phenotype, with expression of CX3CR1 and KLRG1 being reported on this subset[126, 215].

The possibility of exploiting development of lung T_{RM} in the design of improved vaccines against TB is an exciting new prospect. The finding that BCG-immunised mice were protected against challenge with BCG despite administration of fingolimod, a molecule preventing lymphocyte egress from secondary lymphoid organs, implies that T_{RM} present in the lung following vaccination are sufficient for protection[216]. However, few studies have investigated the induction of T_{RM} following vaccination against TB, focussing instead on their induction following infection. A number of studies that have investigated lung T_{RM} in the context of vaccination have neglected to utilise the intravascular staining technique to truly identify only lung-parenchymal cells[207, 216, 217]. This is critically important as it has been shown that even when utilising lung perfusion to 'remove' lung-vascular lymphocytes, the vast majority of $CD8^+$ T cells isolated from the lungs of perfused mice were in fact stained

positively for intravascular antibody, indicating that they were actually present within the vasculature of the lungs[122].

So far, just one study has employed the use of the intravascular staining technique to investigate responses to a subunit vaccine against TB. Woodworth *et al.*[218] found that immunised mice generated polyfunctional $CD4^+$ T cells which preferentially localised to the parenchyma of *M.tb*-infected lungs upon adoptive transfer, and also expressed reduced levels of KLRG1 on their cell surface, a phenotype associated with tissue-residence and enhanced control of bacterial growth[126, 207, 215]. Vaccination also resulted in an enrichment of $KLRG1^-$ cells in the lung-vascular $CD4^+$ population and the peripheral circulation, which the authors suggest represent a population of circulating $CD4^+$ T cells able to selectively home to the lung. The vaccine conferred durable protection against *M.tb* infection, further highlighting the exciting potential role of this subset in protective immunity.

It is important to understand the factors regulating the generation and maintenance of lung-parenchymal $CD4^+$ T cells, if we are to consider novel vaccine strategies targeting their induction. A recent study by Moguche *et al.* found that during *M.tb* infection in mice, the lung-homing parenchymal population were dependent on Bcl6 and ICOS and were retained in the lung at least in part through CXCR5[127]. Sallin *et al.* report that T-bet supresses development of $CD4^+$ T cells with a tissue-resident phenotype in the lungs of mice infected with *M.tb*, but together with IL-12 is essential for the generation of lung-vascular $CD4^+$ $KLRG1^+$ T cells which persist poorly and are not capable of controlling *M.tb* growth[215]. This may indicate that $CD4^+$ T cells which are less polarised towards the Th1 lineage are better able to protect against *M.tb* infection. However, in the same study the authors also found that IFN-γ derived from Th1 cells inhibited the accumulation of the non-protective lung-

vascular $CD4^+$ T cell population, adding a further layer of contrasting complexity to our current understanding of these populations[215].

Determining the importance of T_{RM} for protective immunity in humans is much more challenging. It has so far been shown that T_{RM} are present in human lung and that this population is enriched for memory cells able to respond to a number of common respiratory pathogens, such as influenza virus[219]. Additionally, BAL samples taken from patients with latent *M.tb* infection have been found to contain antigen-specific memory T cells[220]. Using bronchoscopic challenge with purified protein derivative of *M.tb* (PPD-T), one group investigated the role of lung homing in *M.tb*-specific recall responses and demonstrated rapid mobilisation of $CD4^+$ T cells into the airways of latently infected individuals, resulting in a significant increase in antigen-specific T cells[221]. These findings suggest that local mucosal immunity may play a crucial role in protective responses against *M.tb* infection in humans, although further work is needed to clarify the exact nature of their contribution.

1.8. Aims of this thesis

The overall aim of this project was to identify and characterise lung $CD4^+$ T_{RM}, induced by BCG immunisation, in a BALB/c mouse model of vaccine-induced immunity against *M.tb* infection. The specific objectives included:

1. Utilisation of intravascular staining to identify $CD4^+$ T_{RM} in the lungs of immunised mice

2. Phenotypic and functional characterisation of $CD4^+$ T_{RM}, with the goal of identifying features uniquely associated with this population

3. Investigation of the effect of different routes of delivery of BCG on development of the $CD4^+$ T_{RM} population

4. Determination of the role of $CD4^+$ T_{RM} in vaccine-induced protection against *M.tb* infection

Chapter 2.

Materials and Methods

2.1. Animals

2.1.1. Ethics

All animal work was undertaken in accordance with the UK Animal (Scientific Procedures) Act 1986, under the appropriate Project and Personal licences.

2.1.2. Mice

Female specific-pathogen-free (SPF) BALB/c mice were supplied by Charles River UK Ltd or Harlan UK Ltd and used at eight weeks of age unless otherwise specified. For some experiments, female BALB/c mice from a congenic colony maintained at the Animal and Plant Health Agency, Weybridge, were used in order to allow flow cytometric discrimination of their T cells by expression of CD90.1 surface marker rather than the usual CD90.2 marker expressed by BALB/c. Animals were housed in appropriate biological containment.

2.1.3. Immunisation

Mice were immunised with the human vaccine strain *M.bovis* BCG Danish 1331 prepared as per manufacturer's instructions (Statens Serum Institut, Denmark) or grown to mid-log phase in Middlebrook 7H9 broth (Appendix – Reagent details) and subsequently frozen at -80°C. BCG was grown by Dr Carmen Garcia-Pelayo at the Animal and Plant Health Agency. A single dose of $2x10^5$ colony forming units (CFU) of BCG in 50µl inoculum was administered by intradermal injection in either the tail base or the ear, or by the intranasal route. For

intranasal immunisation, mice were anaesthetised with inhaled isofluorane (Sigma) and 50ul total inoculum was delivered to both nares. Control mice were immunised with 50µl Hanks' Balanced Salt Solution (HBSS) (Gibco) via the intradermal route.

2.1.4. Intravascular stain

An injection of 100µl of PE-conjugated anti-CD45 monoclonal antibody (eBioscience) at 0.75µg/ml or FITC-conjugated anti-CD4 monoclonal antibody (Biolegend) at 6µg/ml in HBSS was given via the lateral tail vein one minute prior to euthanasia, unless otherwise stated, to allow flow-cytometric discrimination between lung-vascular cells (accessible to the stain) and lung-parenchymal cells (inaccessible to the stain). Mice were warmed in a heat box prior to injection to aid visualisation of the vein.

2.1.5. Tissue collection

At various time points post-immunisation, mice were euthanased and the lungs and spleens were harvested into complete medium (Appendix – Reagent details) on ice and homogenised. Peripheral blood was collected from some animals and mixed with 10µl of Heparin Sodium (1000 I.U./ml Wockhardt, UK). Bronchoalveolar lavage (BAL) cells were isolated from some animals prior to removal of lungs. This was performed through *in situ* catherisation of the trachea and flushing of the airways twice with individual volumes of 0.5ml phosphate buffered saline (PBS) (Sigma), which were subsequently pooled. Prior to removal, lungs from some animals underwent perfusion via the injection of 10ml HBSS into the right ventricle of the heart.

2.1.6. *M.tb* challenge

Mice were challenged using a Biaera AeroMP®-controlled nebuliser (Biaera technologies; Hagerstown, USA) contained in a Biosafety level 3 TCOL isolator (Total Containment Oxford Ltd). Animals were loaded in nose-only restrainers and exposed to aerosolised *M.tb* Erdman K01 (TMC107) (BEI resources; Manassas USA), prepared at $1x10^6$ CFU/ml in the nebuliser. The programme was run for 10 minutes followed by a 5 minute purge, airflow 12 L/min, and pressure 20 psig. Mice were infected with 50-100 CFU, verified 24 hours after challenge in two mice per experiment.

2.1.7. Adoptive transfer

Lung and spleen cells previously harvested from donor mice and sorted using fluorescence activated cell sorting (FACS) as described below were transferred in 100µl PBS by intravenous injection into the lateral tail vein of recipient mice. Mice were warmed in a heat box prior to injection to aid visualisation of the vein. Number of cells transferred was variable and is stated for each experiment.

2.2. Colony forming unit (CFU) determination

To determine vaccine-induced protection, mice were euthanased four weeks post-challenge with *M.tb*. Lungs and spleens were harvested into 1ml PBS in CK28-R tubes containing 2.8mm ceramic beads (Stretton Scientific) and homogenised twice for 20s/5500rpm using a Precellys 24 (Stretton Scientific). Homogenates were serially diluted in

PBS, plated in duplicate on Modified 7H11 agar plates (Appendix – Reagent details) and incubated for four weeks at 37°C before counting colonies.

2.3. Immunological assays

2.3.1. Cell isolations

Spleen cells were isolated by passage through a 40µm cell strainer into complete medium (Appendix – Reagent details). Cells were washed (300g/8min/4°C), counted using a CASY® TT Cell Counter (Roche Innovatis AG) and then re-suspended at $10x10^6$/ml in complete medium for assays.

Lung cells were isolated either through manual mincing with fine scissors or mechanically through use of a GentleMACS™ tissue dissociator and C tubes, using Lung_02 machine pre-setting (Miltenyi Biotech). Cells were re-suspended into 25ml digestion medium (Appendix – Reagent details) and agitated at 37°C for 1 hour. Suspensions were passed through a 100µm cell strainer, washed (300g/8min/4°C), passed through a 40µm cell strainer, washed (300g/8min/4°C), counted in Trypan Blue (Sigma) using a haemocytometer and re-suspended at $5x10^6$/ml in complete medium for assays. For samples undergoing fluorescence-activated cell sorting (FACS), the addition of 5ml of 1X red blood cell (RBC) lysis buffer (eBioscience) for 5 minutes was performed in between washes.

Peripheral blood cells were isolated through incubation for 10 minutes at room temperature with MACS rinsing buffer (Miltenyi Biotech) and anti-Ter119-biotin (eBioscience) at 6.7µg/ml, followed by addition of EasySep™ mouse streptavidin RapidSpheres™ (STEMCELL Technologies Inc.) at 174µl/ml and placement on EasySep™

magnet for 5 minutes. Supernatants were poured off, cells washed (300g/8min/4°C), counted using a CASY® TT Cell Counter and re-suspended at $2x10^6$/ml in complete medium for assays.

BAL cells were washed (300g/5min/4°C), counted using a CASY® TT Cell Counter and re-suspended in 200µl complete medium for assays.

2.3.2. Antigen stimulations

Purified Protein Derivative of *M.tb* (PPD-T) (Statens Serum Institut, Denmark) was used for the majority of antigen stimulations, at a final concentration of 10µg/ml. For selected experiments, where stated, cells were cultured with Rv0288 (TB10.4) peptide 4 = $TB10.4_{19-34}$: AGYAGTLQSLGAEIAV ($CD8^+$) and peptide 13 = $TB10.4_{73-88}$: SSTHEANTMAMMARDT ($CD4^+$) antigens to stimulate both $CD4^+$ and $CD8^+$ responses, each at a final concentration of 2µg/ml for all assays.

2.3.3. Flow cytometry – surface staining and intracellular cytokine staining (ICS)

Cells isolated from spleen, lungs, BAL or peripheral blood were cultured with antigen, 1µg/ml anti-CD28 (BD Biosciences, UK) and 10µg/ml Brefeldin A (Sigma) for 16 hours, unless otherwise stated, at 37°C/5% CO_2. Cells were washed (300g/5min/4°C) in flow wash buffer (Appendix – Reagent details) and surface stained with fluorochrome-labelled monoclonal antibodies (Appendix – Flow cytometry antibodies) for 15min/4°C in the dark. Cells were then washed, fixed for 1hr/4°C with Cytofix™ (BD Biosciences), permeabilised for

1hr/4°C with Cytoperm™ (BD Biosciences) and stained intracellularly for 20 min/4°C with antibodies listed in Appendix – Flow cytometry antibodies. Cells were washed again and analysed using an LSRFortessa™ analyser with FACSDiva™ software (BD Biosciences). Final analysis was performed using FlowJo® software (Tree Star Inc.) on a minimum of 100,000 live lymphocytes (50,000 for BAL and peripheral blood).

2.3.4. Fluorescence-activated cell sorting (FACS)

Cells from spleen and lung were isolated and stained as described above for flow cytometry surface staining without the initial antigen stimulation step. Cells were sorted using either a MoFlo® or MoFlo® Astrios™ (both Beckman Coulter) with Summit software (Cytomation, Inc.) into complete medium supplemented with 40% FBS (Appendix – Reagent details), washed (300g/8min) and resuspended either in PBS for transfer into recipient mice or in complete medium (Appendix – Reagent details) for antigen-stimulation assays. Cell sorting was performed by Dr Daryan Kaveh and Dr Andrew Worth.

2.3.5. Tetramer staining

Cells isolated from the lungs were stained for 45min/37°C/5% CO_2 in complete medium with a major histocompatibility complex (MHC) class II-peptide tetramer complex loaded with Rv0288 (TB10.4) peptide 13 (amino acids 73-88: SSTHEANTMAMMARDT) labelled with APC. Tetramer was provided by NIH MHC Tetramer Core Facility, USA. After staining, cells were washed (300g/8min) before surface staining with antibodies as described above for flow cytometry.

2.3.6. EdU incorporation assay

To identify antigen-stimulated proliferation by EdU incorporation, cells isolated from spleen and lungs were cultured with and without antigen (TB10.4 peptides or PPD-T) with the addition of 1µg/ml anti-CD28 for three days at 37°C/5% CO_2. EdU (Click-iT® Plus EdU Flow Cytometry Assay Kit, Invitrogen) was added at 0.125µl/ml for the final 24 hours and cell surface staining was performed for flow cytometric analysis as described above. Following surface staining, cells were fixed for 1hr/4°C with Cytofix™ before washing (300g/5min/4°C), resuspending in EdU kit perm buffer and incubating for 20min/4°C. Click-iT® reaction buffer cocktail was prepared as per manufacturer's instructions through addition of picoylazide AF647, copper protectant and reaction buffer additive to PBS. Cells were resuspended in reaction buffer cocktail and incubated for 30min/room temperature in the dark before washing twice in EdU kit perm buffer (300g/5min/4°C) and resuspending in flow wash buffer (Appendix – Reagent details) for analysis.

2.3.7. Ki67 expression

Purified $CD4^+$ T cell populations obtained from spleen and lung through FACS were stimulated with antigen as described above for the EdU incorporation assay in co-culture with adherent spleen-derived antigen presenting cells (APCs) from a naïve congenic BALB/c mouse. These cells were excluded from final flow cytometric analysis through expression of CD90.1 cell-surface marker. Following three days of culture at 37°C/5% CO_2, cell-surface staining was performed as described above for flow cytometry. Following surface staining, cells were washed twice in flow wash buffer (300g/5min/4°C), supernatant was discarded and 3ml cold 70% ethanol was added to the cell pellet while vortexing. Cells were

incubated for 1hr/-20°C before washing three times in flow wash buffer (300g/5min/4°C) and resuspending in 100µl flow wash buffer. PE-conjugated anti-Ki67 monoclonal antibody (Appendix – flow cytometry antibodies) was added and cells were incubated for 30min/room temperature in the dark. Cells were washed twice in flow wash buffer (300g/5min/4°C) before analysis.

2.4. Histology

After removal from the mouse, lungs were placed in fixative (10% neutral buffered formalin) for 7 days before embedding in paraffin wax. Sections were cut and stained with haematoxylin and eosin (H&E) for histological examination by light microscopy and digital image acquisition (Lucia; Laboratory Imaging Ltd, Prague, Cz). Histology was performed by the pathology department at the Animal and Plant Health Agency.

2.5. Statistical analysis

All data were analysed using GraphPad Prism 6 statistical package (GraphPad, USA). The statistical test used is described for each figure. When comparing two groups, an unpaired Student's two-tailed *t*-test was performed. With three or more treatment groups the data were analysed by one-way ANOVA with appropriate multiple comparisons test as stated. Where two independent variables were compared, data were analysed by two-way ANOVA with appropriate multiple comparisons test as stated. Mycobacterial counts were $\log_{10}$ transformed before the statistical analysis. For all data, * represents $\rho \leq 0.05$, ** represents $\rho \leq 0.01$, *** represents $\rho \leq 0.001$ and **** represents $\rho \leq 0.0001$.

Chapter 3.

Optimisation of the intravascular staining technique and other assays

3.1. Introduction

The ability to clearly discriminate between lung-vascular and lung-parenchymal populations is critical to the separate analysis of these two compartments. Identifying T cells present within the lung tissue is necessary in order to define them as T_{RM}, a subset of T cells which may play an important role in protection against *M.tb* infection. Anderson *et al.* recently published a protocol for intravascular staining, allowing the definitive identification of these two populations through intravenous injection of fluorescently-labelled monoclonal antibody (mAb)[121]. The antibody circulates throughout the bloodstream, labelling cells present within the blood vessels, including those that are within the organ tissue itself, but the antibody does not exit the vasculature. This allows the subsequent flow cytometric identification of two populations of cells present within organs; one population labelled fluorescently, indicating that those cells were present in the vasculature of the organ, and one population of unlabelled cells that were inaccessible to the vascular stain, indicating that they were present within the parenchyma of the organ.

This technique has now been used by several groups to identify tissue-resident T cells in the lung[120-122, 124, 126, 127, 215, 218, 222, 223]. In order to maximise discrimination between populations and achieve high reproducibility between experiments, it is critical to ensure that all elements of the technique are optimised to reduce staining variability. In order to achieve this, experiments were conducted to titrate the concentration of antibody injected and the injection-euthanasia interval, as well as trialling different methods of tissue homogenisation.

Perfusion of the lungs prior to their removal is a method commonly employed to remove blood from the vasculature of the lungs. This is performed with the intention of eliminating the lung-vascular cell populations prior to analysis, in order to ensure that only lung-parenchymal cells are being studied. However, perfusion has been shown to disrupt tissue architecture through loss of inducible bronchus-associated lymphoid tissue (iBALT) and alveolar tissue aggregates[121]. Therefore, experiments described within this chapter were performed in order to determine whether perfusion was necessary to achieve good intravascular stain definition.

Identification of antigen-specific T cells is possible through two methods: antigenic stimulation followed by intra-cellular cytokine staining (ICS) to identify cells producing cytokine in response to cognate antigen, or use of a major histocompatibility complex (MHC)-peptide tetramer complex loaded with cognate antigen which binds to the T cell receptor (TCR) of cells specific to that antigen. In order to optimise detection of antigen-specific T cells, experiments were conducted in order to quantify background cytokine production from unstimulated cells, optimise antigen-stimulation length, compare different antigens used for stimulation and assess whether tetramer staining was a viable method for detection of antigen-specific T cells.

In summary, the aim of this chapter was to optimise techniques and assays that would be used throughout the remainder of the project, ensuring that subsequent experiments would result in high quality, reproducible data.

3.2. Results

3.2.1. Optimisation of intravascular staining technique

Experiments were conducted to optimise the intravascular staining technique and maximise discrimination between intravascular stain-positive lung-vascular cells, and intravascular stain-negative lung-parenchymal cells (a putative tissue-resident population) when analysed by flow cytometry (Appendix – Flow cytometry gating strategy).

3.2.1.1. Manual vs mechanical lung tissue homogenisation

Comparison between manual and mechanical (GentleMACS™) homogenisation revealed no significant difference between the total numbers of lymphocytes extracted from the lungs of naïve BALB/c mice (Figure 3.1). Therefore GentleMACS™ homogenisation was adopted for all further studies to ensure consistency of processing between samples.

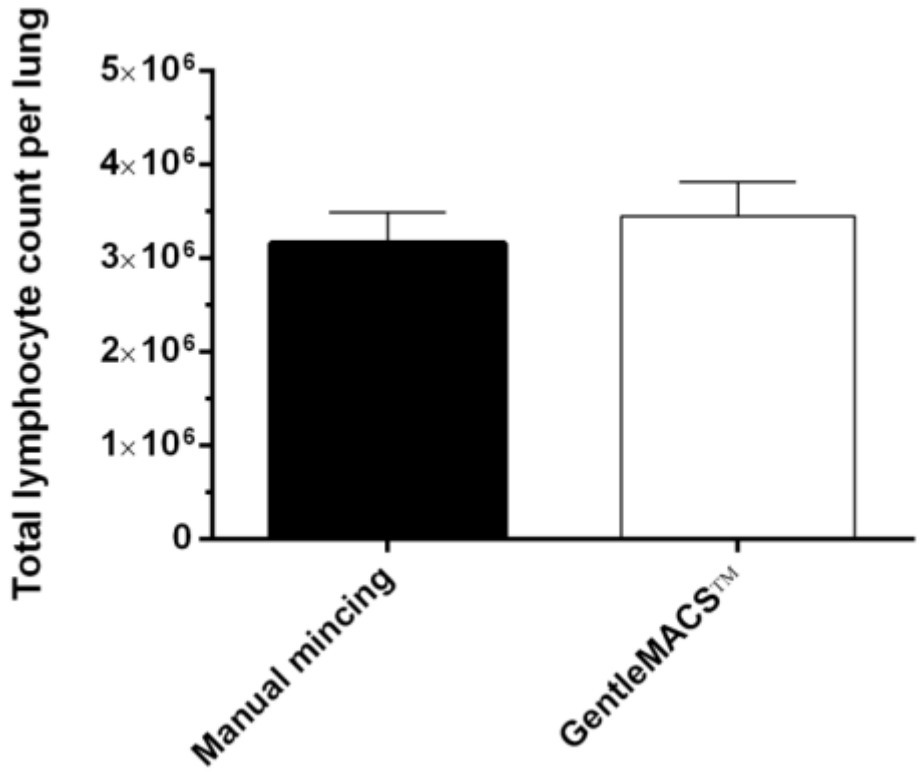

Figure 3.1 - Total number of lymphocytes isolated from murine lungs following manual or GentleMACS™ mechanical homogenisation. Naïve BALB/c mice were euthanased and lungs were harvested before undergoing manual or mechanical tissue homogenisation. Cells isolated from lungs homogenised by each method were counted manually using a haemocytometer. Bars represent mean values (n=6) and error bars show SEM. Unpaired *t*-test, comparing methods.

3.2.1.2. Titration of time to euthanasia and antibody concentration

Different lengths of time between intravascular injection of PE-conjugated anti-CD45 antibody and euthanasia were compared. One minute, 2 minutes and 3 minutes were tested and 1 minute was selected in order to achieve optimal discrimination by flow cytometry (Figure 3.2). Concentration of antibody injected was also titrated for each antibody used for intravascular staining. Representative plots are shown for FITC-conjugated anti-CD4 mAB, which allowed selection of 6μg/ml as the optimal concentration for this antibody (Figure 3.3).

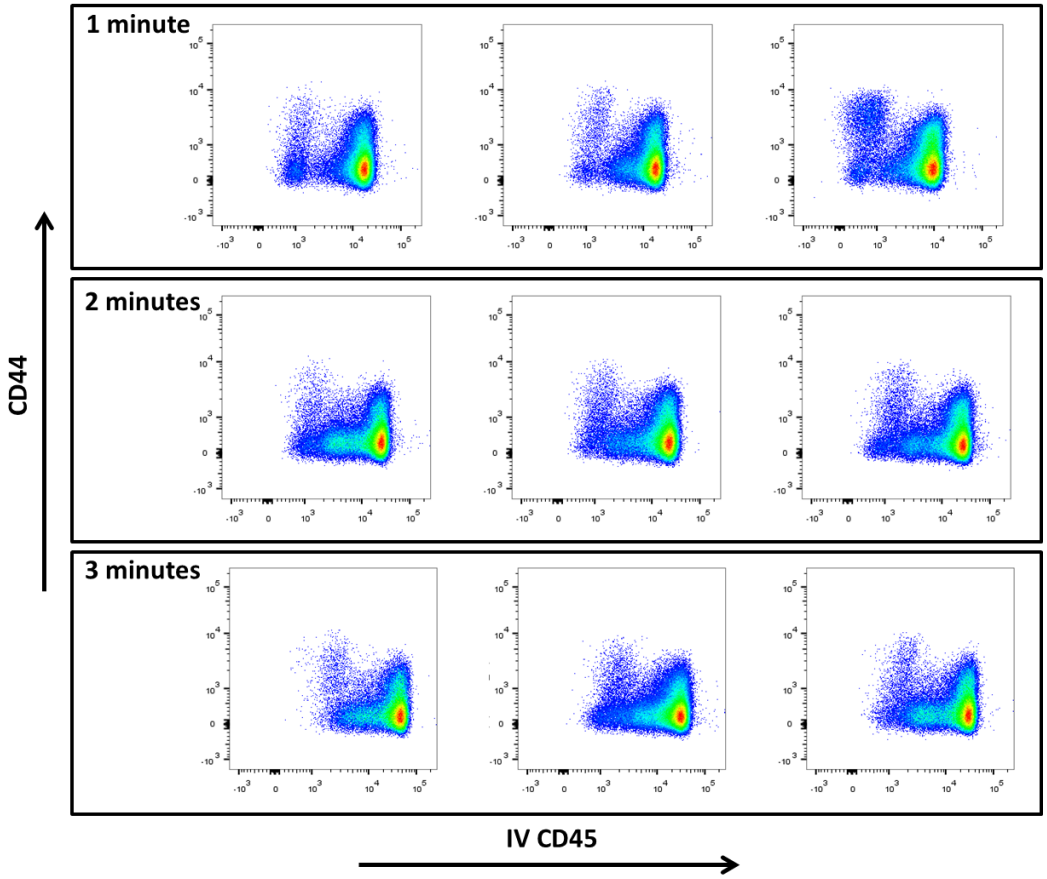

Figure 3.2 - Titration of time between intravenous injection and euthanasia. BALB/c mice were immunised intradermally with BCG and 6 weeks later were euthanased at different time points: 1 minute, 2 minutes and 3 minutes, following intravenous injection of anti-CD45 mAb to identify populations of lung-parenchymal and lung-vascular $CD4^+$ T cells. Representative plots are shown for 3 mice at each timepoint. Plots are pre-gated on $CD4^+$ T cells.

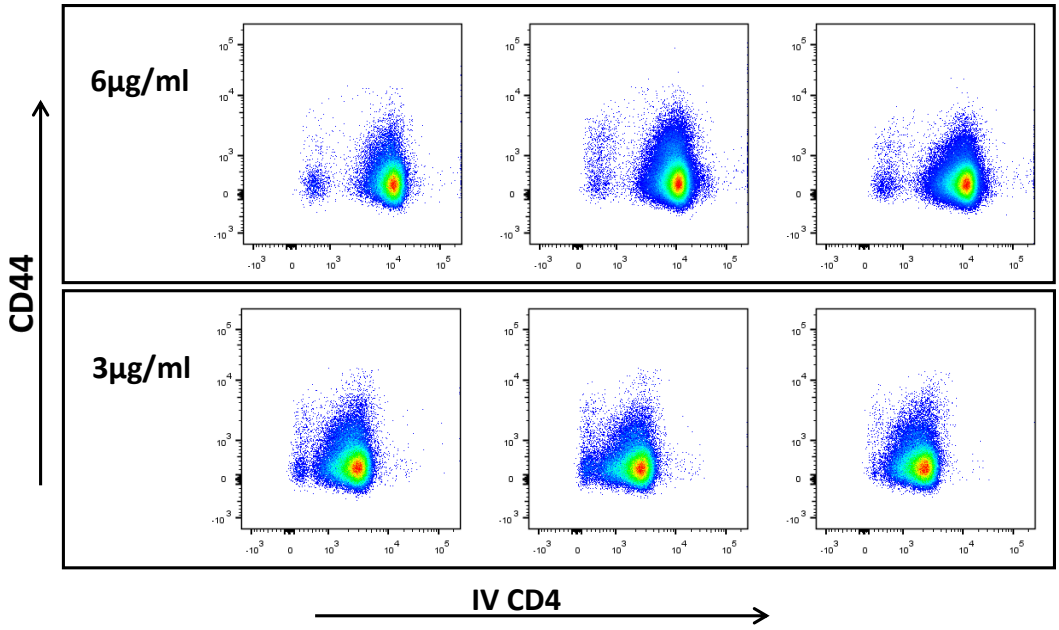

Figure 3.3 - Titration of intravascular stain concentration. Naïve BALB/c mice were euthanased following intravenous injection of different concentrations of anti-CD4 mAb to identify populations of lung-parenchymal and lung-vascular $CD4^+$ T cells. Representative plots are shown for 3 mice at each concentration. Plots are pre-gated on $CD4^+$ T cells.

3.2.2. Effect of pulmonary perfusion

Perfusion of the lungs prior to removal from the mouse is a method commonly employed to remove blood from the lungs, but it has been shown to disrupt tissue architecture[121]. To assess whether or not it was necessary to perfuse lungs in order to achieve good intravascular stain discrimination, a comparison was made between perfusing and not-perfusing. Groups of 12 mice were vaccinated intradermally with BCG or placebo and lungs harvested 6 weeks later, following intravascular staining. Six mice per group underwent perfusion and 6 did not. To identify antigen-specific cells through intra-cellular cytokine staining (ICS), the isolated cells were stimulated with TB10.4 peptides and analysed by flow cytometry (Appendix – Flow cytometry panel 1 & Flow cytometry gating strategy).

3.2.2.1. Effect of perfusion on total number of lymphocytes extracted from the lung

Comparison between perfusion and non-perfusion revealed no significant difference between the total numbers of lymphocytes extracted from the lung (Figure 3.4a).

3.2.2.2. Effect of perfusion on frequency of lung-vascular and lung-parenchymal $CD4^+$ and $CD8^+$ T cells

There was no significant difference in frequency of lung-vascular or lung-parenchymal $CD4^+$ or $CD8^+$ T cells isolated from perfused or non-perfused lungs (Figure 3.4b). For representative flow cytometry plots see Figure 8.2a.

3.2.2.3. Effect of perfusion on frequency of lung-vascular and lung-parenchymal cytokine-producing $CD4^+$ and $CD8^+$ T cells

In BCG-vaccinated mice, non-perfused lungs showed a significantly higher frequency of TB10.4 peptide-specific $CD4^+$ T cells producing IFN-γ, IL-2 or TNF-α, or any combination of these (cytokine$^+$) in the lung-vascular compartment compared with perfused lungs (Figure 3.4c). For representative flow cytometry plots see Figure 8.2b. BCG failed to induce a significant antigen-specific $CD8^+$ T cell response in either perfused or non-perfused lungs.

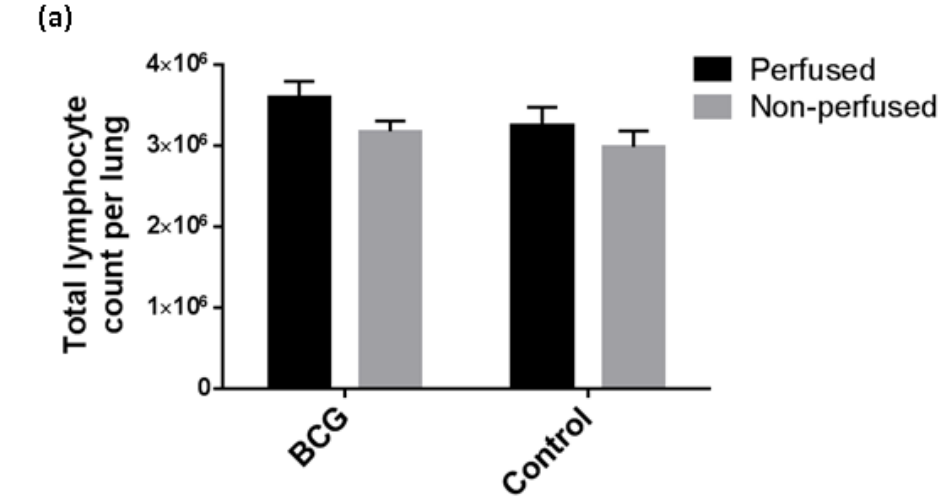
(a)
Total lymphocyte count per lung
4×10⁶
3×10⁶
2×10⁶
1×10⁶
0
Perfused
Non-perfused
BCG
Control

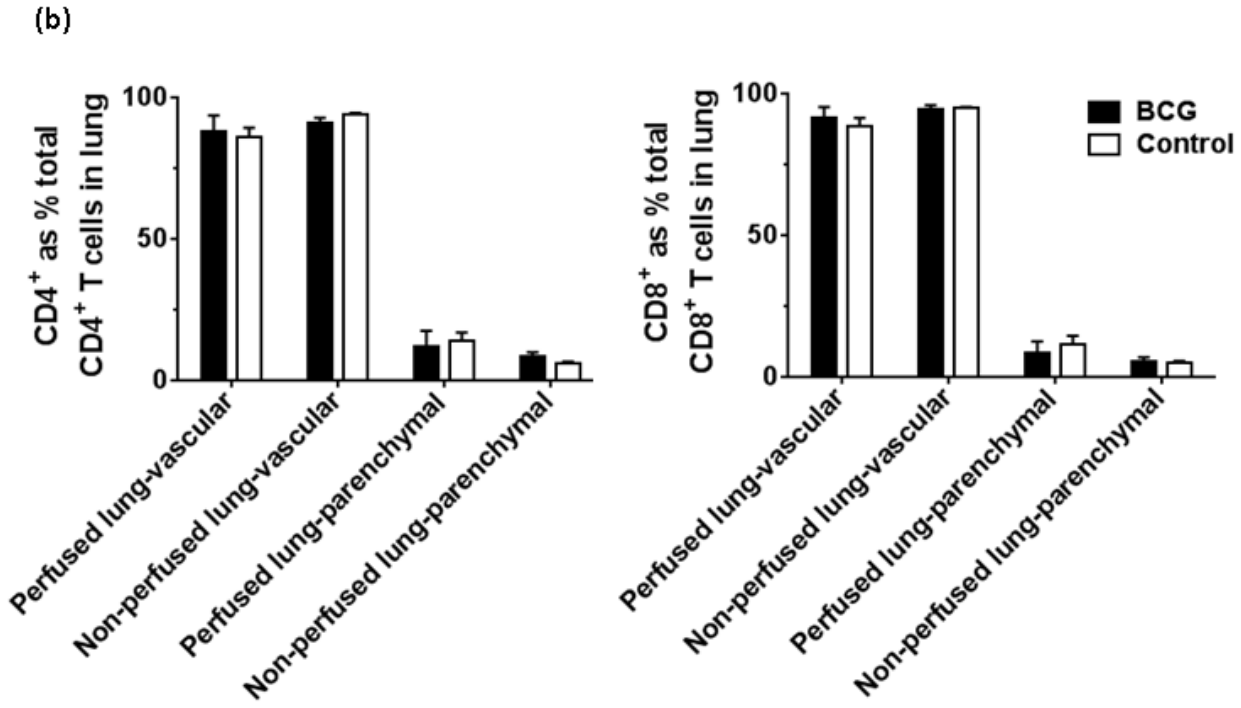
(b)
CD4⁺ as % total CD4⁺ T cells in lung
100
50
0
Perfused lung-vascular
Non-perfused lung-vascular
Perfused lung-parenchymal
Non-perfused lung-parenchymal
CD8⁺ as % total CD8⁺ T cells in lung
BCG
Control

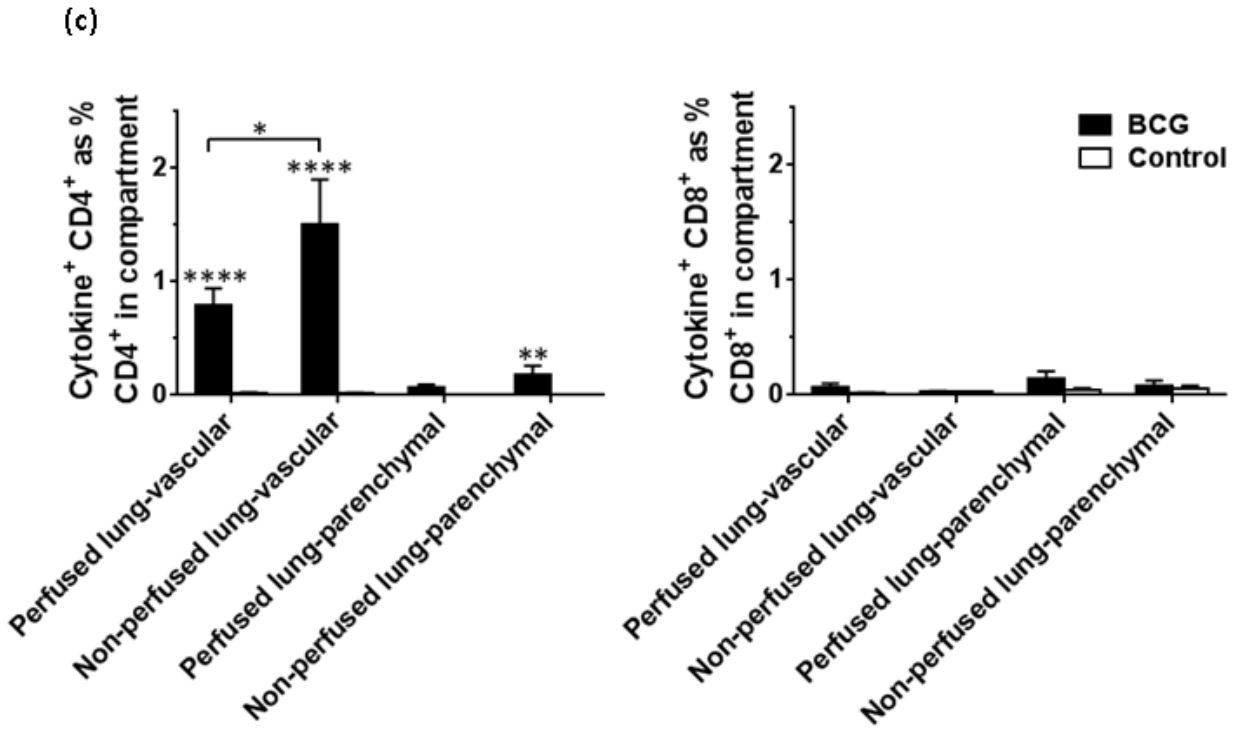

Figure 3.4 - Effect of perfusion on lung compartments. BALB/c mice received intradermal BCG or placebo immunisation and were euthanased 6 weeks later. Intravascular staining followed by ICS was used to identify populations of lung-parenchymal and lung-vascular TB10.4 peptide-specific $CD4^+$ and $CD8^+$ T cells. Equal numbers of mice per group had lungs perfused, or not perfused, prior to removal. Cells were analysed by flow cytometry. (a) Total number of lymphocytes isolated from murine lung following perfusion or non-perfusion. Cells were counted manually using a haemocytometer. (b) Relative proportions of lung-vascular and lung-parenchymal $CD4^+$ or $CD8^+$ T cells as a % of total $CD4^+$ or $CD8^+$ T cells isolated from the lung. (c) Frequency of BCG-induced TB10.4 peptide-specific $CD4^+$ or $CD8^+$ T cells producing IFNγ, IL-2 or TNF-α (cytokine$^+$) as a % of total $CD4^+$ or $CD8^+$ T cells in the lung-vascular and lung-parenchymal compartments. Statistical comparison is shown between BCG and control and between perfusion and non-perfusion for the same compartment. For all graphs, bars represent mean values (n=6) and error bars show SEM. * $\rho \leq 0.05$, **** $\rho \leq 0.0001$, two-way ANOVA with Sidak's post-test.

3.2.3. Comparison between unstimulated and TB10.4 peptide-stimulated $CD4^+$ T cells

In order to establish whether unstimulated control samples were required in experiments involving ICS, it was necessary to identify whether there was any non-specific cytokine-production from unstimulated T cells. A comparison was made between cytokine-production from $CD4^+$ T cells incubated overnight with TB10.4 peptides and those incubated overnight in the absence of peptides. Groups of 6 mice were vaccinated intradermally with BCG or placebo and lungs and spleen harvested 6 weeks later, following intravascular staining. Lymphocytes from each compartment were either stimulated or left unstimulated before ICS to identify $CD4^+$ T cells producing IFN-γ, TNF-α, IL-2 or any combination of these ($cytokine^+$) (Appendix – Flow cytometry panel 1).

3.2.3.1. Cytokine production by TB10.4 peptide-stimulated and unstimulated $CD4^+$ T cells

There were significant populations of $cytokine^+$ $CD4^+$ T cells present in both lung compartments and the spleen of BCG-immunised mice following overnight peptide-stimulation (Figure 3.5). In the absence of peptide-stimulation, there were no significantly detectable populations of $cytokine^+$ $CD4^+$ T cells present in the lung or spleen of BCG-immunised mice. For representative flow cytometry plots see Figure 8.3. Having established that there was no significant detectable non-specific cytokine production from unstimulated $CD4^+$ T cells it was decided that inclusion of unstimulated samples was unnecessary for future experiments.

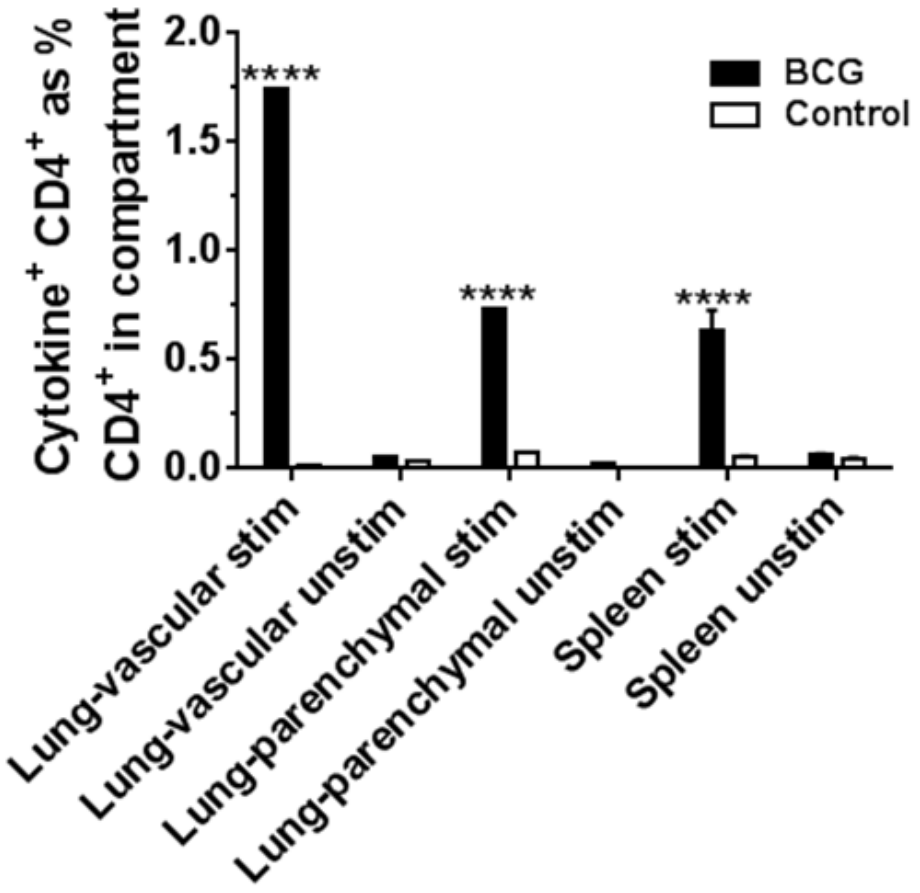

Figure 3.5 - Cytokine production by TB10.4 peptide-stimulated and unstimulated $CD4^+$ T cells. BALB/c mice received BCG or placebo immunisation and 6 weeks later, intravascular staining following by ICS was used to identify populations of lung-parenchymal and lung-vascular TB10.4 peptide-specific $CD4^+$ T cells. Cells from the lung and spleen were either stimulated by TB10.4 peptides in overnight culture or left unstimulated during overnight culture. Bars represent mean values (n=6) and error bars show SEM. **** $\rho \leq 0.0001$, two-way ANOVA with Sidak's post-test, comparing BCG and control.

3.2.4. Comparison between TB10.4 peptide-stimulation and purified protein derivative of TB (PPD-T) protein-stimulation

In the existing literature, TB10.4 peptides and PPD-T protein are both used as antigenic stimuli to induce cytokine-production by T cells[199, 224-227]. In order to establish whether there were any differences in phenotype or function of cells recovered from the same animals following stimulation with either antigen, a comparison was made between the two. Groups of 6 mice were vaccinated intradermally with BCG or placebo and lungs and spleen harvested 6 weeks later, following intravascular staining. Lymphocytes from each compartment were either stimulated overnight with TB10.4 peptides 4 and 13 (see materials and methods for further details) or PPD-T protein before ICS to identify cytokine$^+$ CD4$^+$ T cells (Appendix – Flow cytometry panel 1).

3.2.4.1. Cytokine production by TB10.4 peptide-stimulated and PPD-T-stimulated CD4$^+$ T cells

Both TB10.4 peptide- and PPD-T-stimulation resulted in significant populations of cytokine$^+$ CD4$^+$ T cells in both lung compartments and the spleen of BCG-vaccinated mice compared to control (Figure 3.6a). In the lung-vascular compartment, there was a significantly greater frequency of cytokine$^+$ CD4$^+$ T cells when cells were stimulated with TB10.4 peptides compared to PPD-T. In all other compartments, the frequency of cytokine$^+$ CD4$^+$ T cells was not significantly different comparing stimulation-types. For representative flow cytometry plots see Figure 8.4a&b.

3.2.4.2. Cell-surface immunophenotyping of BCG-induced TB10.4 peptide-specific and PPD-T-specific CD4$^+$ T cells

Following both TB10.4 peptide- and PPD-T-stimulation, cytokine$^+$ CD4$^+$ T cells in both lung compartments and the spleen all displayed a CD44^{hi}CD62L^{lo}CD27$^-$ phenotype (Figure 3.6b). For representative flow cytometry plots see Figure 8.4c. In the lung-vascular compartment and the spleen, TB10.4 peptide-stimulation resulted in a greater frequency of cytokine$^+$ CD4$^+$ T cells with a CD44^{hi}CD62L^{lo}CD27$^-$ phenotype compared to PPD-T-stimulation (Figure 3.6c).

3.2.4.3. Functionality of BCG-induced TB10.4 peptide-specific and PPD-T-specific CD4$^+$ T cells

Boolean gating analysis was used to identify populations of TB10.4 peptide-specific or PPD-T-specific CD4$^+$ T cells producing IFN-γ, IL-2, TNF-α or any combination of the three. In both lung compartments and spleen of BCG-vaccinated mice, stimulation with TB10.4 peptides resulted in a greater frequency of IFNγ$^+$IL-2$^+$TNF-α$^+$ CD4$^+$ T cells compared to stimulation with PPD-T (Figure 3.6d). In the lung-vascular compartment, stimulation with TB10.4 peptides resulted in a greater frequency of BCG-induced IFNγ$^+$IL-2$^-$TNF-α$^+$ CD4$^+$ T cells compared to PPD-T stimulation. Only PPD-T-stimulation resulted in significant populations of IFNγ$^-$IL-2$^+$TNF-α$^+$ CD4$^+$ T cells in the lung-parenchyma and IFNγ$^-$IL-2$^-$TNF-α$^+$ CD4$^+$ T cells in the spleen, comparing vaccinated animals with control.

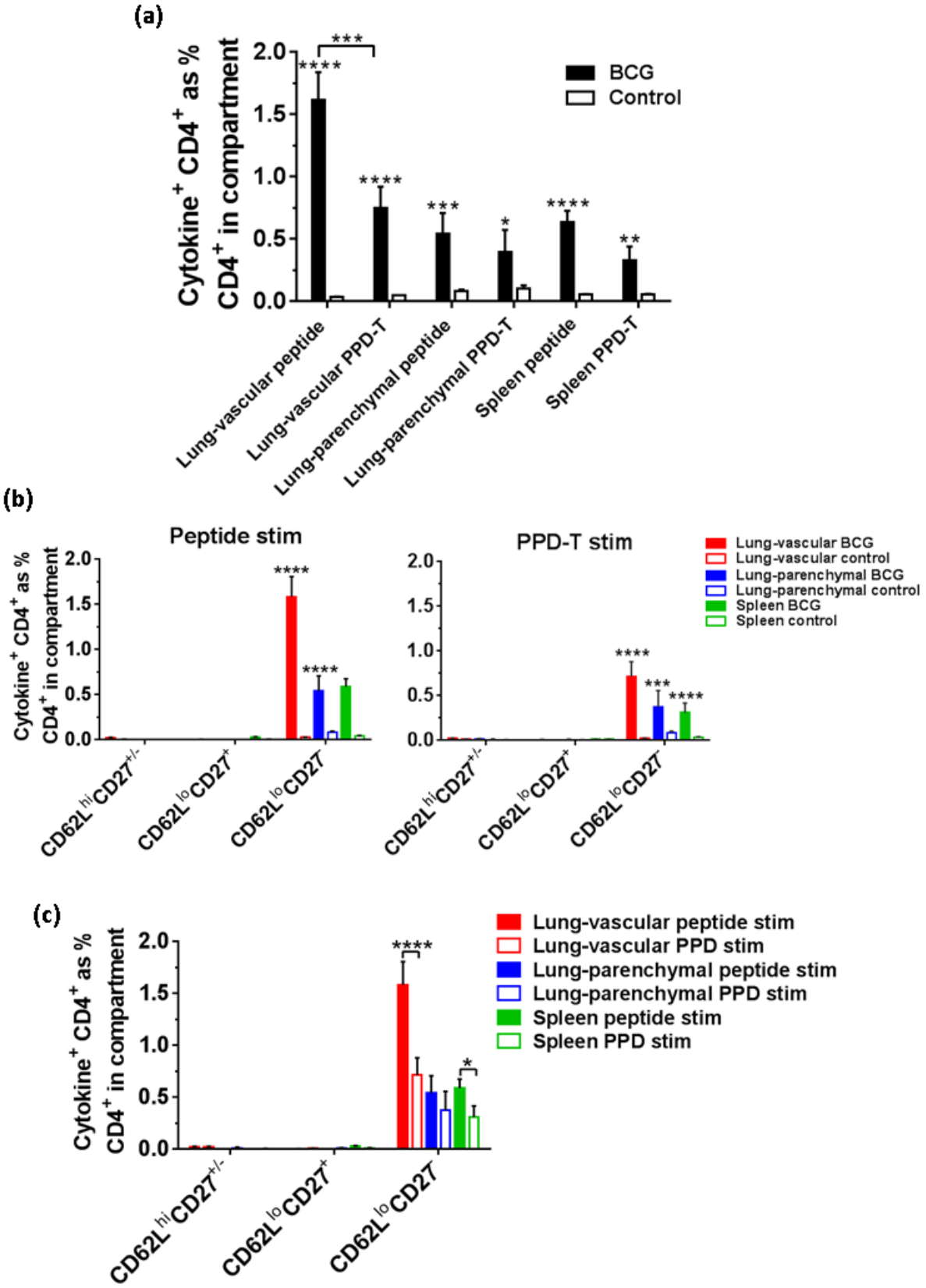
(a)
Cytokine+ CD4+ as % CD4+ in compartment
BCG
Control
Lung-vascular peptide
Lung-vascular PPD-T
Lung-parenchymal peptide
Lung-parenchymal PPD-T
Spleen peptide
Spleen PPD-T
(b)
Peptide stim
PPD-T stim
Lung-vascular BCG
Lung-vascular control
Lung-parenchymal BCG
Lung-parenchymal control
Spleen BCG
Spleen control
CD62L hiCD27+/-
CD62L loCD27+
CD62L loCD27-
(c)
Lung-vascular peptide stim
Lung-vascular PPD stim
Lung-parenchymal peptide stim
Lung-parenchymal PPD stim
Spleen peptide stim
Spleen PPD stim

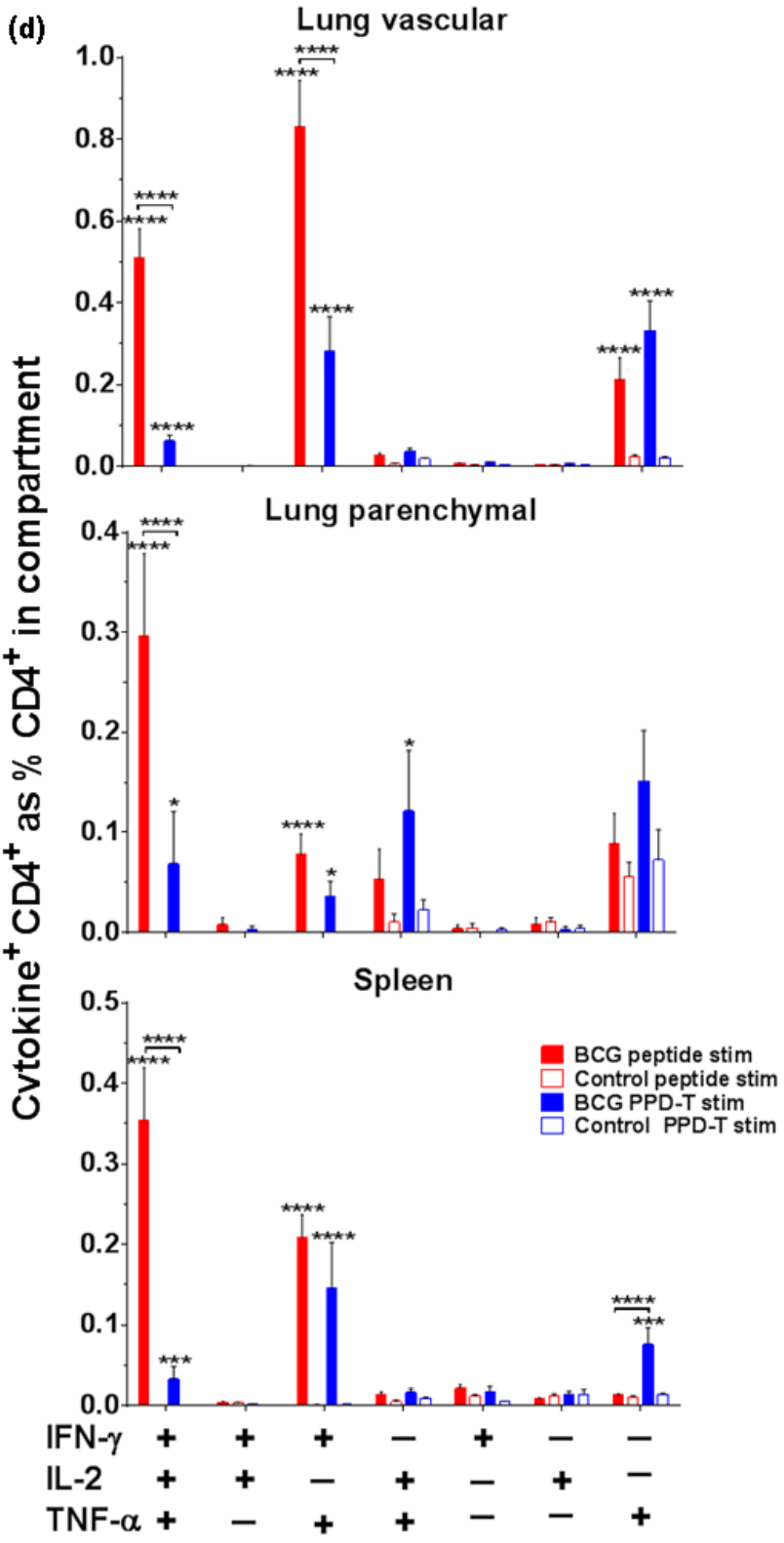

Figure 3.6 - Comparison between TB10.4 peptide-stimulation and PPD-T protein-stimulation. BALB/c mice received intradermal BCG or placebo immunisation and 6 weeks

later, intravascular staining was used to identify populations of lung-parenchymal and lung-vascular T cells. Cells from the lung and spleen were either stimulated by TB10.4 peptides or PPD-T in overnight culture. ICS was used to identify populations of TB10.4 peptide-specific or PPD-T-specific $CD4^+$ T cells producing IFNy, IL-2 or TNF-α (cytokine$^+$). (a) Frequency of cytokine$^+$ peptide- or PPD-T-specific $CD4^+$ T cells as a % of total $CD4^+$ T cells in compartment. Statistical comparison is between BCG with control and peptide with PPD-T stimulation in each compartment. (b) Frequency of cytokine$^+$ peptide- or PPD-T-specific $CD4^+$ $CD44^{hi}$ T cells in all compartments displaying combinations of CD62L and CD27 cell surface markers as a % of total $CD4^+$ T cells in that compartment. Statistical comparison is between BCG and control for each compartment. (c) Frequency of BCG-induced cytokine$^+$ peptide- or PPD-T-specific $CD4^+$ $CD44^{hi}$ T cells in all compartments displaying combinations of CD62L and CD27 cell surface markers as a % of total $CD4^+$ T cells in that compartment. Statistical comparison is between peptide and PPD-T stimulation in each compartment. (d) Frequencies of BCG-induced peptide- or PPD-T-specific $CD4^+$ T cells in all compartments producing IFN-γ, IL-2 or TNF-α plus combinations of all three as a % of the total $CD4^+$ T cells in the same compartment. Statistical comparison is between BCG with control and peptide with PPD-T stimulation. For all graphs, bars represent mean values (n=6) and error bars show SEM. * $\rho \leq 0.05$, ** $\rho \leq 0.01$, *** $\rho \leq 0.001$, **** $\rho \leq 0.0001$, two-way ANOVA with Sidak's post-test.

3.2.5. Comparison between different antigen-stimulation lengths

In order to establish the optimal length of time for which cells should be stimulated with cognate antigen, a comparison was made between stimulation for 6 hours and overnight stimulation. Groups of 6 mice were vaccinated intradermally with BCG or placebo and lungs and spleen harvested 6 weeks later, following intravascular staining. It was not possible to obtain a sufficient number of lung lymphocytes to allow a comparison between 6 hour and overnight stimulation with both antigens. Therefore, lymphocytes from both lung compartments were either stimulated for 6 hours or overnight with TB10.4 peptides 4 and 13 whilst lymphocytes from the spleen were stimulated for 6 hours or overnight with TB10.4 peptides or PPD-T protein, before ICS to identify cytokine$^+$ CD4$^+$ T cells (Appendix – Flow cytometry panel 1).

3.2.5.1. Cytokine-production by lung CD4$^+$ T cells following different antigen-stimulation lengths

There was no significant difference in the frequency of BCG-induced cytokine$^+$ CD4$^+$ T cells, in both lung compartments, following 6 hour or overnight stimulation with TB10.4 peptides (Figure 3.7a).

3.2.5.2. Cytokine-production by spleen CD4$^+$ T cells following different antigen-stimulation lengths

There was a significantly higher frequency of BCG-induced cytokine$^+$ CD4$^+$ T cells in the spleen following overnight stimulation with PPD-T compared to 6 hour stimulation with PPD-T (Figure 3.7b). There was no significant difference in the frequency of BCG-induced cytokine$^+$ CD4$^+$ T cells in the spleen following 6 hour or overnight stimulation with TB10.4 peptides.

3.2.5.3. Cell-surface immunophenotyping of BCG-induced antigen-specific lung CD4$^+$ T cells following different antigen-stimulation lengths

Following TB10.4 peptide-stimulation for 6 hours or overnight, cytokine$^+$ CD4$^+$ T cells in both lung compartments all displayed a CD44^{hi}CD62L^{lo}CD27$^-$ phenotype (Figure 3.7c). There was no difference in frequency of CD44^{hi}CD62L^{lo}CD27$^-$ CD4$^+$ T cells when comparing stimulation lengths within the same compartment.

3.2.5.4. Cell-surface immunophenotyping of BCG-induced antigen-specific spleen CD4$^+$ T cells following different antigen-stimulation lengths

Stimulation with PPD-T overnight resulted in a greater frequency of CD44^{hi}CD62L^{lo}CD27$^-$ CD4$^+$ T cells when compared to stimulation with PPD-T for 6 hours (Figure 3.7d). Frequency of CD44^{hi}CD62L^{lo}CD27$^-$ CD4$^+$ T cells did not differ following stimulation with TB10.4 peptides for either 6 hours or overnight.

3.2.5.5. Functionality of BCG-induced antigen-specific spleen CD4$^+$ T cells following different antigen-stimulation lengths

Boolean gating analysis was used to identify populations of TB10.4 peptide-specific or PPD-T-specific CD4$^+$ T cells producing IFN-γ, IL-2, TNF-α or any combination of the three.

Stimulation with PPD-T overnight resulted in significantly higher frequencies of IFNγ$^+$IL-2$^+$TNF-α$^+$ and IFNγ$^+$IL-2$^-$TNF-α$^+$ CD4$^+$ T cells compared to stimulation for 6 hours (Figure 3.7e). Stimulation with TB10.4 peptides for either 6 hours or overnight resulted in no significant differences in frequency of any of the populations of cytokine$^+$ CD4$^+$ T cells.

(a)

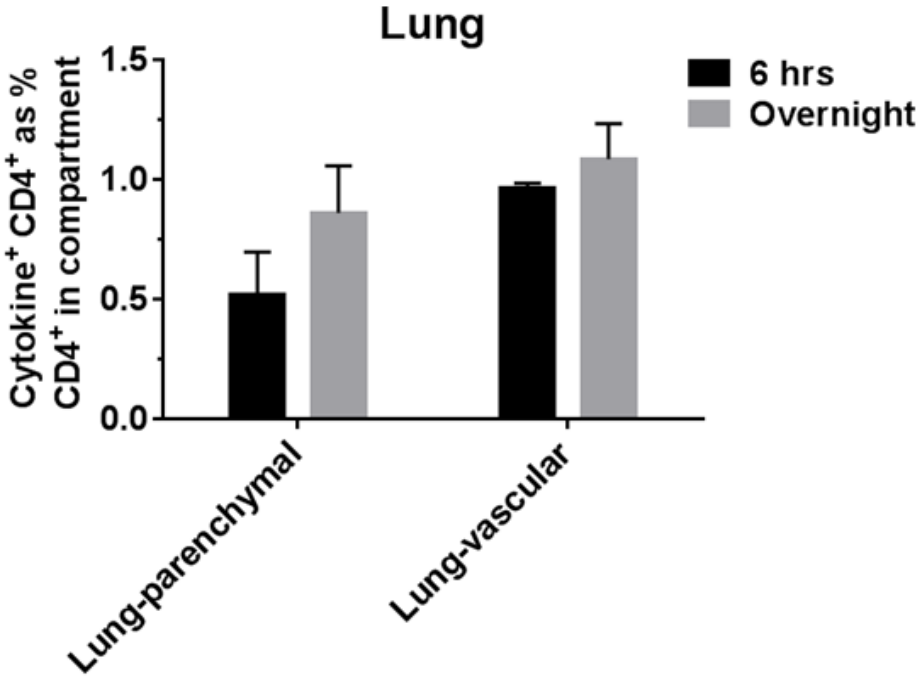
Lung
6 hrs
Overnight
Cytokine+ CD4+ as % CD4+ in compartment
1.5
1.0
0.5
0.0
Lung-parenchymal
Lung-vascular

(b)

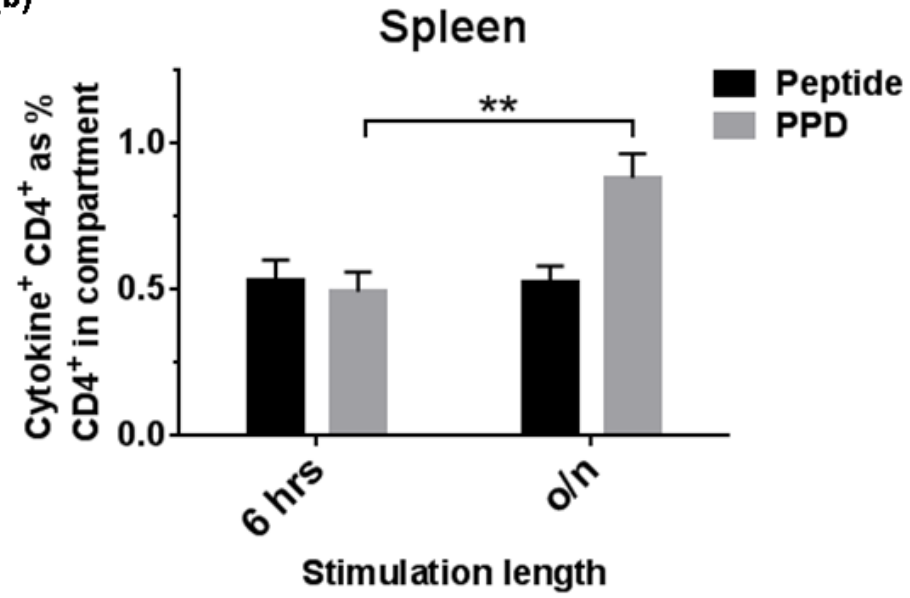
Spleen
Peptide
PPD
**
Cytokine+ CD4+ as % CD4+ in compartment
1.0
0.5
0.0
6 hrs
o/n
Stimulation length

(c)

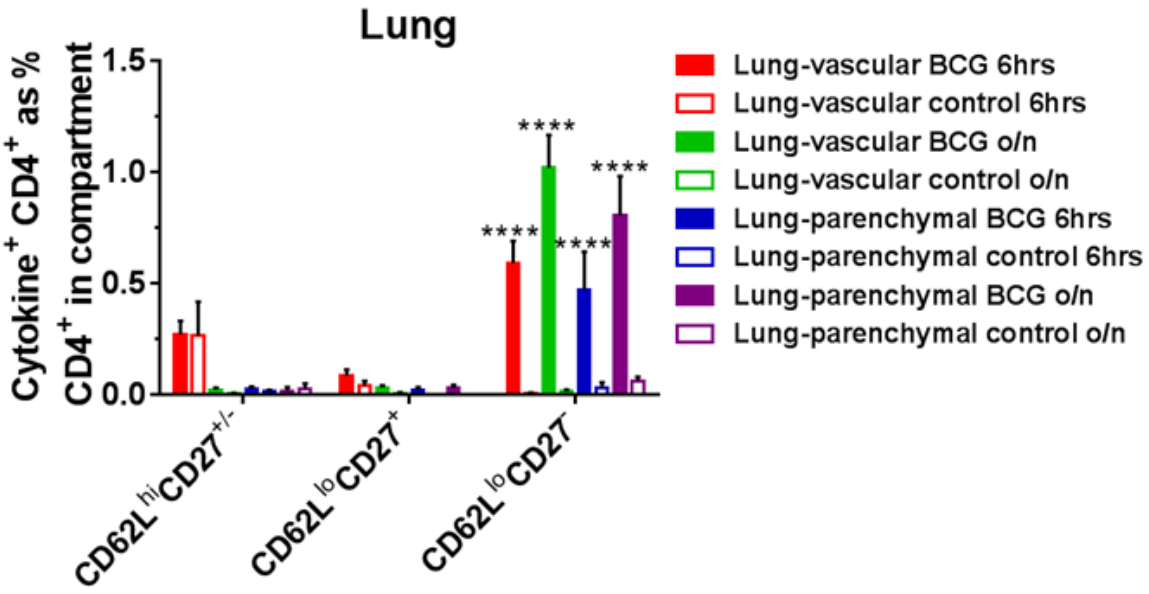
Lung
Cytokine+ CD4+ as % CD4+ in compartment
1.5
1.0
0.5
0.0
****
****
****
****
CD62L hiCD27+/-
CD62L loCD27+
CD62L loCD27-
Lung-vascular BCG 6hrs
Lung-vascular control 6hrs
Lung-vascular BCG o/n
Lung-vascular control o/n
Lung-parenchymal BCG 6hrs
Lung-parenchymal control 6hrs
Lung-parenchymal BCG o/n
Lung-parenchymal control o/n

(d)

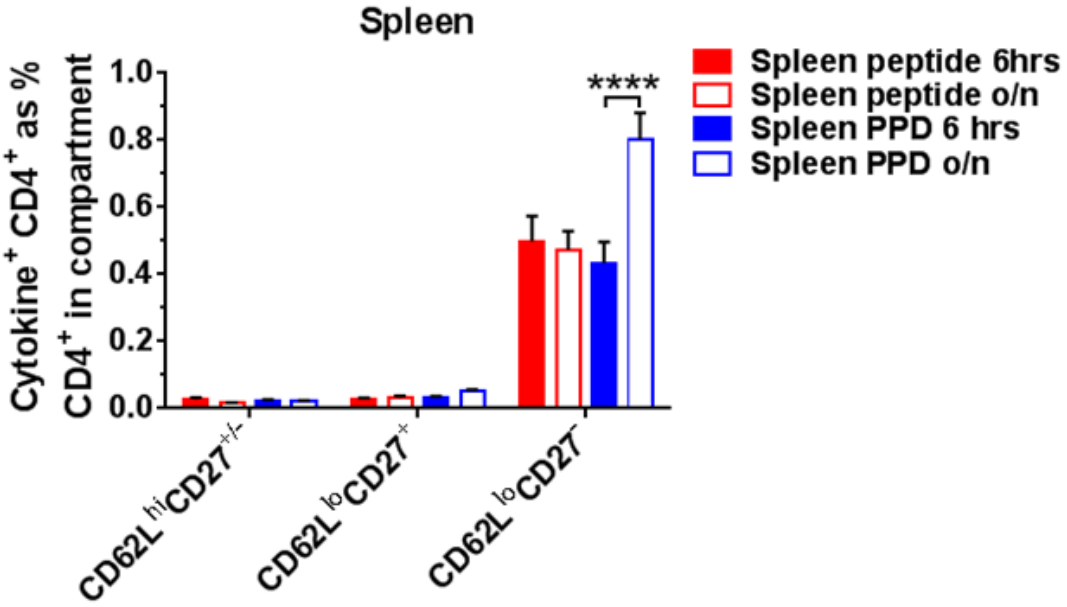
Spleen
Cytokine+ CD4+ as % CD4+ in compartment
1.0
0.8
0.6
0.4
0.2
0.0
****
CD62L hiCD27+/-
CD62L loCD27+
CD62L loCD27-
Spleen peptide 6hrs
Spleen peptide o/n
Spleen PPD 6 hrs
Spleen PPD o/n

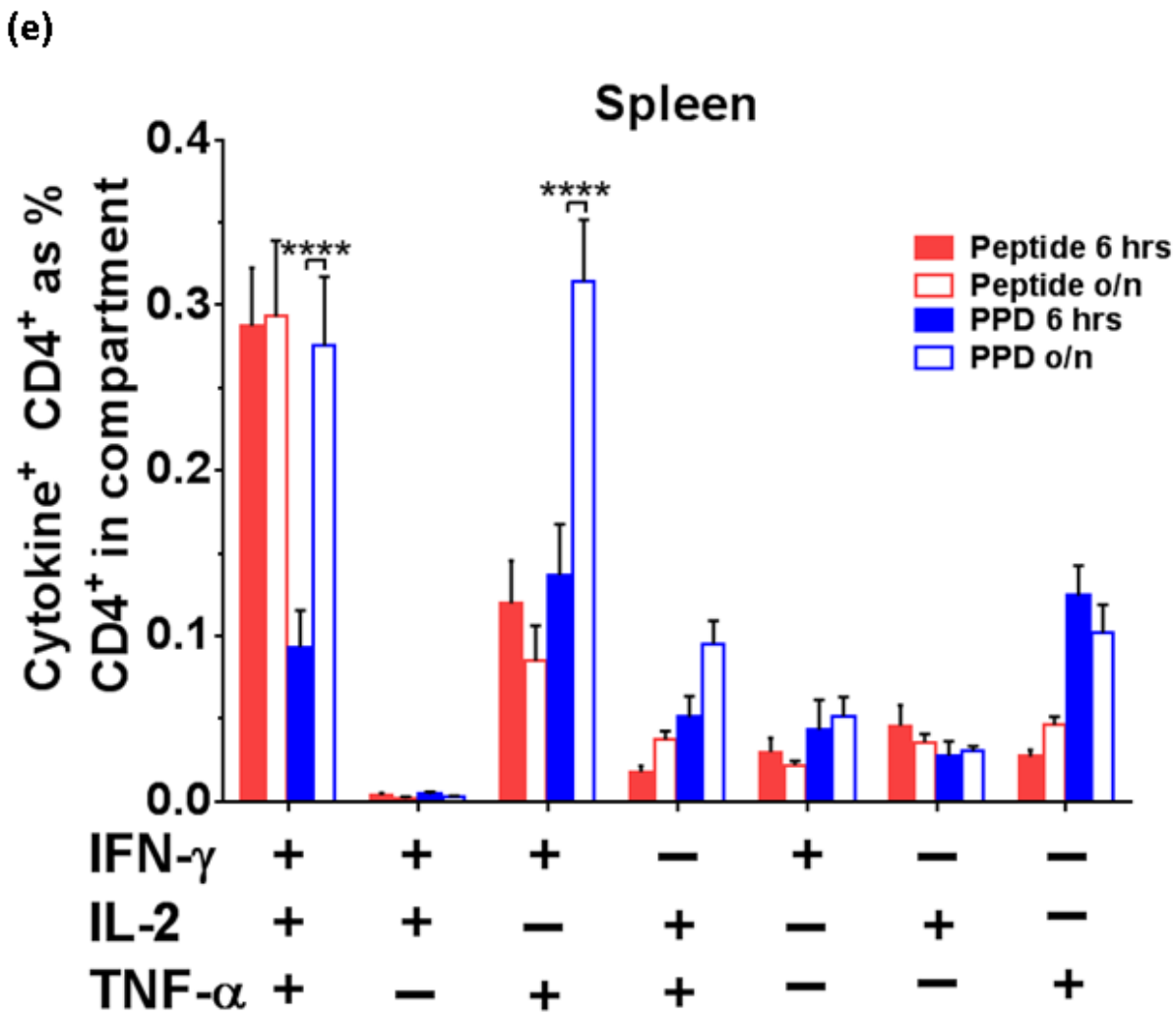

Figure 3.7 - Comparison of stimulation lengths. BALB/c mice received BCG or placebo immunisation and 6 weeks later, intravascular staining was used to identify populations of lung-parenchymal and lung-vascular T cells. Cells from the lung were stimulated by TB10.4 peptides in 6 hour or overnight culture. Cells from the spleen were stimulated by TB10.4 peptides or PPD-T in 6 hour or overnight culture. ICS was used to identify populations of TB10.4 peptide-specific or PPD-T-specific $CD4^+$ T cells producing IFNy, IL-2 or TNF-α ($cytokine^+$). (a) Frequency of lung $cytokine^+$ peptide-specific $CD4^+$ T cells as a % of total $CD4^+$ T cells in compartment, following 6 hour and overnight peptide culture . (b) Frequency of spleen $cytokine^+$ peptide- or PPD-T-specific $CD4^+$ T cells as a % of total $CD4^+$ T cells in the spleen, following 6 hour and overnight culture. Statistical comparison is between peptide and PPD-T stimulation and stimulation length. (c) Frequency of $cytokine^+$ peptide-specific

$CD4^+$ $CD44^{hi}$ T cells in the lung displaying combinations of CD62L and CD27 cell surface markers as a % of total $CD4^+$ T cells in that compartment, following 6 hour and overnight peptide culture. Statistical comparison is between BCG with control and stimulation length within compartment. (d) Frequency of cytokine$^+$ peptide- or PPD-T-specific $CD4^+$ $CD44^{hi}$ T cells in the spleen displaying combinations of CD62L and CD27 cell surface markers as a % of total $CD4^+$ T cells in the spleen, following TB10.4 peptide-stimulation or PPD-T-stimulation for 6 hours or overnight. Statistical comparison is between BCG with control. (e) Frequency of BCG-induced cytokine$^+$ peptide- or PPD-T-specific $CD4^+$ $CD44^{hi}$ T cells in the spleen displaying combinations of CD62L and CD27 cell surface markers as a % of total $CD4^+$ T cells in the spleen, following 6 hour and overnight culture. Statistical comparison is between stimulation type and length. (e) Frequencies of BCG-induced peptide- or PPD-T-specific $CD4^+$ T cells in the spleen producing IFN-γ, IL-2 or TNF-α plus combinations of all three as a % of the total $CD4^+$ T cells in the spleen, following 6 hour and overnight culture. Statistical comparison is between stimulation type and length. For all graphs, bars represent mean values (n=6) and error bars show SEM. * $\rho \leq 0.05$, ** $\rho \leq 0.01$, *** $\rho \leq 0.001$, **** $\rho \leq 0.0001$, two-way ANOVA with Sidak's post-test.

3.2.6. Identification of antigen-specific $CD4^+$ T cells through tetramer staining

Identification of antigen-specific T cells through ICS requires fixation and permeabilisation steps which kill the cells and make further analysis impossible. Use of a tetramer allows for identification without damage to the cells, which opens up further experimental possibilities. A comparison was made between ICS using TB10.4 peptide-stimulation, and use of tetramer staining with the same specificity, as techniques for identification of antigen-specific $CD4^+$ T cells. Groups of 6 mice were vaccinated intradermally with BCG or placebo and lungs and spleen harvested 6 weeks later, following intravascular staining. Lymphocytes from each compartment were either stimulated overnight with TB10.4 peptide 13 before ICS to identify $cytokine^+$ $CD4^+$ T cells, or stained with a MHC class II-peptide tetramer complex loaded with TB10.4 peptide 13 to identify $tetramer^+$ $CD4^+$ T cells (Appendix – Flow cytometry panel 1 and tetramer panel).

3.2.6.1. Identification of antigen-specific $CD4^+$ T cells through tetramer staining or ICS

Tetramer staining identified a significant population of antigen-specific $CD4^+$ T cells in the lung-vascular compartment but not the lung-parenchyma or spleen of BCG-vaccinated mice compared to controls (Figure 3.8a). ICS identified significant populations of antigen-specific $CD4^+$ T cells in both lung compartments and the spleen of BCG-vaccinated mice compared to controls (Figure 3.8b).

3.2.6.2. Frequency of antigen-specific CD4$^+$ T cells identified by ICS or tetramer staining

In both lung compartments, ICS identified a significantly higher frequency of antigen-specific CD4$^+$ T cells compared to tetramer staining (Figure 3.8c). In the spleen there was no difference in the frequency of antigen-specific CD4$^+$ T cells identified by either method. This indicates that ICS on peptide-stimulated cells provides greater sensitivity for detection of antigen-specific CD4$^+$ T cells in the lungs.

(a)

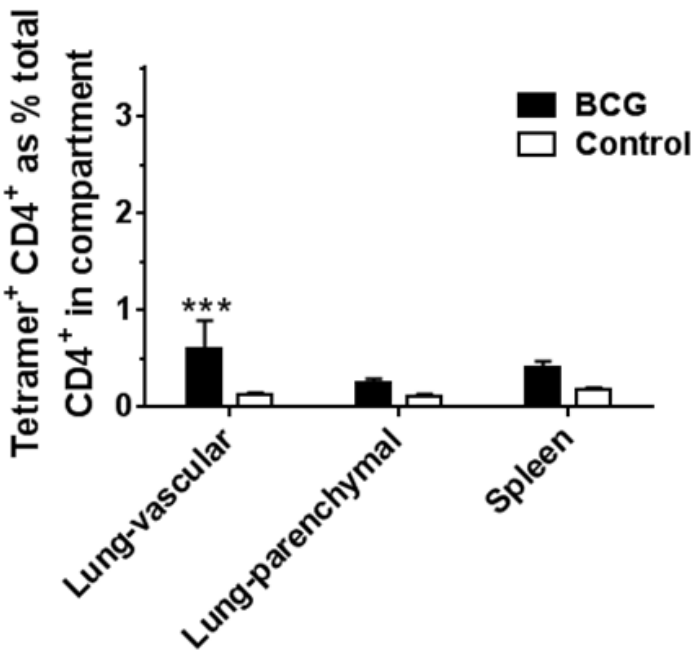
Tetramer+ CD4+ as % total CD4+ in compartment
BCG
Control
***
0
1
2
3
Lung-vascular
Lung-parenchymal
Spleen

(b)

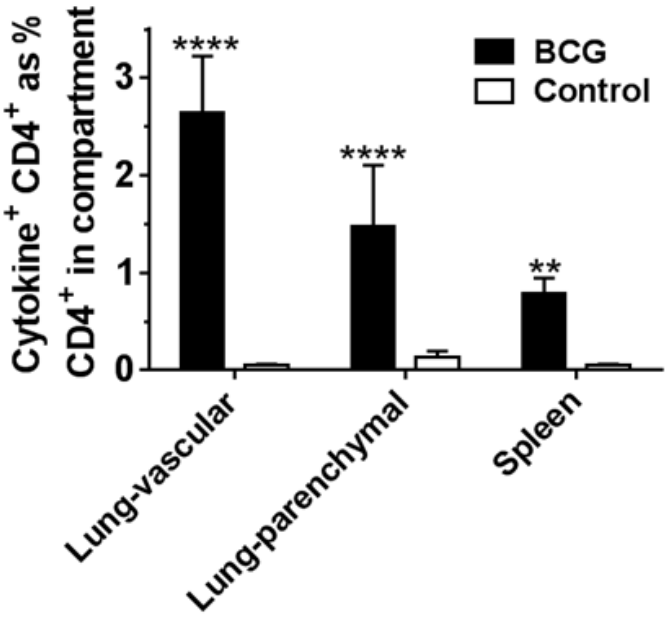
Cytokine+ CD4+ as % CD4+ in compartment
BCG
Control
****
****
**
0
1
2
3
Lung-vascular
Lung-parenchymal
Spleen

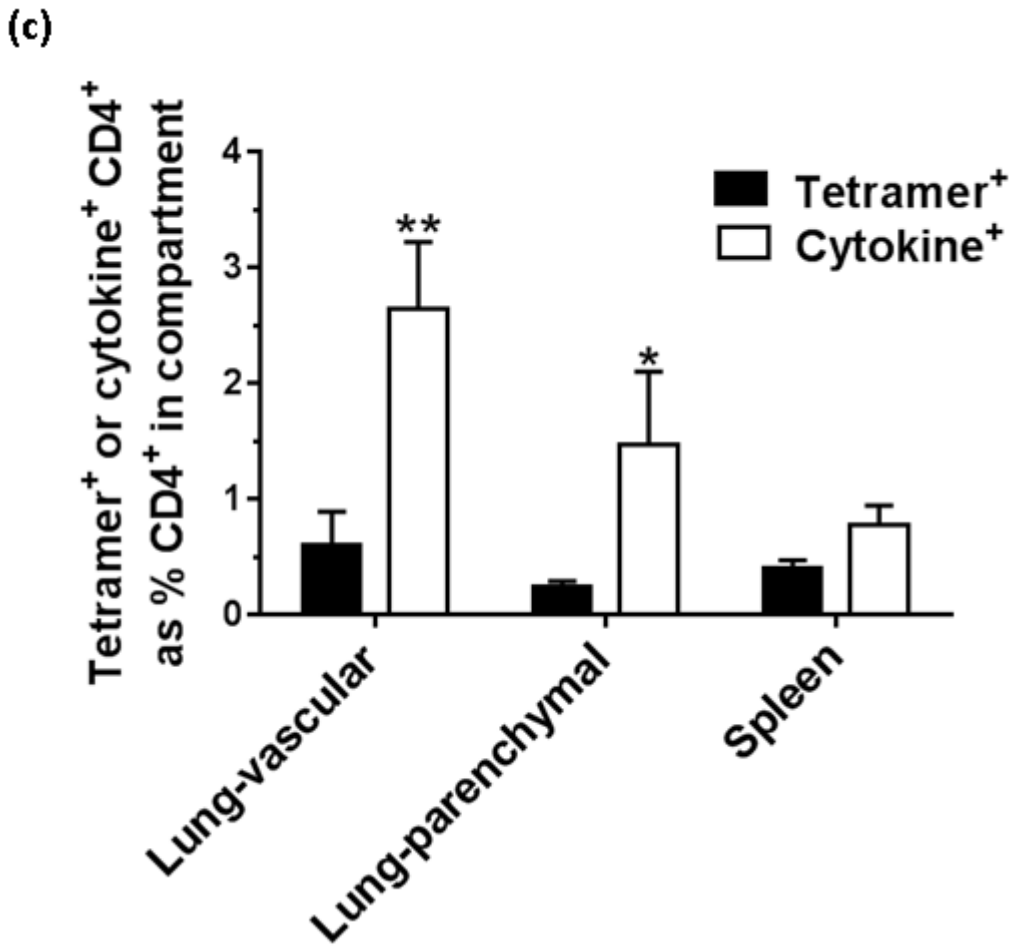

Figure 3.8 - Tetramer staining following TB10.4 peptide-stimulation. BALB/c mice received BCG or placebo immunisation and 6 weeks later, intravascular staining was used to identify populations of lung-parenchymal and lung-vascular T cells. Cells from the lung and spleen were stimulated by TB10.4 peptide 13 in overnight culture. ICS was used to identify populations of TB10.4 peptide-specific $CD4^+$ T cells producing IFNy, IL-2 or TNF-α ($cytokine^+$). MHC class II tetramer was used to identify TB10.4 peptide 13-specific $CD4^+$ T cells. (a) Frequency of $tetramer^+$ TB10.4 peptide-specific $CD4^+$ T cells in lung and spleen as a % of total $CD4^+$ T cells in compartment. Statistical comparison is between BCG and control. (b) Frequency of $cytokine^+$ TB10.4 peptide-specific $CD4^+$ T cells in lung and spleen identified by ICS as a % of total $CD4^+$ T cells in compartment. Statistical comparison is between BCG

and control. (c) Frequency of tetramer$^+$ and cytokine$^+$ TB10.4 peptide-specific CD4$^+$ T cells in lung and spleen as a % of total CD4$^+$ T cells in compartment. Statistical comparison is between tetramer$^+$ and cytokine$^+$ for the same compartment. For all graphs, bars represent mean values (n=6) and error bars show SEM. * $\rho \leq 0.05$, ** $\rho \leq 0.01$, *** $\rho \leq 0.001$, **** $\rho \leq 0.0001$, two-way ANOVA with Sidak's post-test.

3.3. Discussion

The purpose of the experiments described in this chapter was to optimise the techniques and assays underpinning the study of lung T_{RM}, with the goal of establishing robust protocols to take forward for the remainder of the project. Of critical importance to this was refining the intravascular staining technique, in order to allow for clear differentiation between lung-vascular and lung-parenchymal populations.

Utilisation of the intravascular staining technique introduced a requirement for fast processing of organs upon removal from the animal, in order to ensure that any excess antibody was swiftly diluted and rinsed away[121]. Mechanical homogenisation using the GentleMACS^{TM} machine was shown to have no detrimental effect on live lymphocyte yield from the lungs when compared to manual homogenisation with scissors. Therefore, mechanical homogenisation was adopted for all further studies to ensure swift and consistent processing. Each antibody used intravascularly was titrated to identify optimal antibody concentration, and different intervals of time between injection of the antibody and euthanasia were also compared to ensure that discrimination between populations was as clear as possible.

Studying cell populations in the context of anatomical location requires minimal disruption to the tissue architecture. Perfusion of the lungs prior to harvest, a method of removing blood, has been shown to result in a marked reduction in the abundance of iBALT and alveolar tissue aggregates, as well as decreased cell recovery[121]. By design, perfusion also results in loss of the blood within the lungs. This was previously necessary in order to

ensure that only lung-parenchymal cells were being harvested and analysed. However, with the introduction of intravascular staining, it is now possible to study the cells within this vascular compartment separately from those in the parenchyma, and it has been demonstrated that these vascular cells in the lungs and other tissues may play critical roles in protective immune responses[126, 228-231]. In addition, it has been demonstrated that perfusion itself is imperfect, failing to remove all vascular cells from the lung[122].

Data presented in this chapter demonstrate no effect on total lymphocyte yield or on the frequency of $CD4^+$ or $CD8^+$ T cells recovered from either lung compartment when not perfusing. In fact, not perfusing increased frequencies of BCG-induced TB10.4 peptide-specific $CD4^+$ T cells producing IFN-γ, IL-2 or TNF-α in the lung-vascular compartment, suggesting selective removal by perfusion. As these cells are of potential significance, perfusion was not performed for future experiments, allowing a more complete analysis of this compartment.

Whilst BCG induced a significant antigen-specific $CD4^+$ T cell response in both compartments of the lung, compared to naïve animals, it failed to induce a significant antigen-specific $CD8^+$ T cell response. BCG and *M.tb* preferentially reside in phagosomes within APCs. This dictates trafficking of their antigen through the MHC class II pathway, resulting in preferential stimulation of $CD4^+$ T cells[232-234]. Nevertheless, BCG immunisation of BALB/c mice has been shown previously to induce $CD8^+$ T cells specific to TB10.4[235]. However, these cells were detected by their cytolytic ability rather than through cytokine-production. This implies that detection of antigen-specific $CD8^+$ T cells following BCG vaccination may require the use of additional assays detecting other effector molecules specific for cytotoxic T lymphocyte effector functionality. BCG has also been reported to

induce weak antigen-specific $CD8^+$ T cell responses in humans[42, 236]. In fact, one strategy for the improvement of protective efficacy afforded by BCG has involved engineering recombinant BCG strains to result in greater $CD8^+$ T cell stimulation[42]. As $CD4^+$ T cells are the primary cells implicated in a protective immune response against *M.tb*, future experiments within this thesis focus solely on induction and detection of antigen-specific $CD4^+$ T cells.

The number of lymphocytes available to analyse through flow cytometry is limited by the number recovered from each organ. In particular, lymphocyte yield from the lung, usually ~$3x10^6$, limits the number of samples able to be analysed through ICS, with each sample comprising $1x10^6$ lymphocytes. Identification of antigen-specific T cells through ICS involves stimulation with cognate antigen and identification of cytokine production through flow cytometry. In order to maximise the number of samples available for analysis, it was important to establish whether or not unstimulated control samples were required. If unstimulated cells produced cytokine, they would need to be included in order to subtract this non-specific production from true antigen-specific production. Data presented here show that unstimulated cells do not produce significant levels of non-specific cytokine, allowing future experiments to be conducted without the inclusion of unstimulated control samples.

Published studies use both TB10.4 peptides and PPD-T protein as antigens to stimulate cytokine-production from $CD4^+$ T cells[199, 224-227]. TB10.4 is an immunodominant antigen conserved in BCG and *M.tb* and therefore use of these peptides allows tracking of defined clonal T cell responses to both vaccination and challenge[237, 238]. PPD-T is a preparation of purified *M.tb* proteins, also known as tuberculin, and is the reagent used for tuberculin skin

testing to identify individuals infected with *M.tb*[239]. Data included in this chapter demonstrates that both antigens were capable of stimulating comparable antigen-specific responses in cells isolated from BCG-immunised mice, with cytokine-production detected from significant populations of $CD4^+$ T cells in both lung compartments and the spleen, all sharing a $CD44^{hi}CD62L^{lo}CD27^-$ cell-surface phenotype. These phenotypic markers were selected as they have been described previously in the context of BCG-induced antigen-specific $CD4^+$ T cells[225]. Their importance is discussed in greater detail in chapter 4, in the context of their evaluation in a larger study. In addition to comparisons between antigens, length of stimulation was also optimised. It was determined that in order to achieve the highest frequencies of cytokine$^+$ $CD4^+$ T cells when using PPD-T, overnight stimulation rather than 6 hour stimulation was required. This difference may be explained by the fact that T cells are able to present peptide antigen to other T cells without the involvement of professional APCs[240-242], whereas protein antigen requires uptake and processing by APCs before it can be presented to T cells[243, 244]. Therefore, with peptide stimulation, a shorter stimulation length is required, compared to PPD-T-stimulation, to measure a similar frequency of cytokine$^+$ $CD4^+$ T cells. Stimulation length had no impact on cell-surface immunophenotyping. These experiments provided evidence that use of either TB10.4 peptide- or PPD-T-stimulation was acceptable in order to identify antigen-specific $CD4^+$ T cells and that overnight stimulation was optimal in order to identify the highest frequencies of antigen-specific cells.

Identification of antigen-specific T cells through ICS involves fixation and permeabilisation of the cells, killing them in the process. Identification through a MHC-peptide tetramer complex has the advantage of not damaging the cells, so that they may be used in

subsequent assays or even adoptively transferred into other animals. However, use of MHC class II tetramers can be challenging as they have been shown to have lower sensitivity of detection compared to their MHC class I counterparts, due in part to their inferior binding characteristics[198, 245]. In this chapter, a MHC class II-peptide tetramer complex loaded with TB10.4 peptide failed to identify a significant population of antigen-specific $CD4^+$ T cells in either the lung-parenchyma or the spleen, compared to naïve animals. ICS performed alongside, following peptide-stimulation with the same TB10.4 peptide included in the tetramer complex, did identify significant populations of $cytokine^+$ $CD4^+$ T cells in these tissue compartments. This was at least partly due to the higher levels of background staining present within the tetramer-stained control samples. Within the lung-vascular compartment, both tetramer staining and ICS identified significant populations of antigen-specific $CD4^+$ T cells; however, the frequency of antigen-specific cells detected was significantly greater using ICS. Therefore, ICS was adopted as the method of detection of antigen-specific $CD4^+$ T cells for subsequent experiments.

In conclusion, results presented in this chapter allowed for significant optimisation of the intravascular staining technique, maximising discrimination between lung-vascular and lung-parenchymal populations for all future experiments. Additionally, comparison of different conditions for identification of antigen-specific $CD4^+$ T cells has resulted in establishment of standard protocols to be utilised throughout the remainder of the project.

Chapter 4.

Development of lung tissue-resident $CD4^+$ T cells following intradermal BCG immunisation

4.1. Introduction

Several studies have investigated $CD4^+$ T_{RM} within the context of a respiratory viral infection[120, 123, 219, 246-249] and a smaller number within the context of *M.tb* infection[126, 127, 215, 250], but there are no data published on their induction following BCG vaccination utilising the intravascular staining technique. One study, involving the administration of fingolimod to BCG-immunised mice to prevent lymphocyte egress from secondary lymphoid organs, suggests that BCG-induced protection depends on lymphocyte migration to the lungs and retention of lung memory $CD4^+$ T cells[216]. However, this study did not analyse lung-vascular and lung-parenchymal cells separately, so it remains unclear exactly which cells were responsible for providing protection.

The phenotype of $CD4^+$ T cells induced by BCG vaccination has been described by several studies[199, 205, 225], but it is not known whether or not these phenotypic descriptions apply to $CD4^+$ T cells present in the parenchyma or the vasculature of the lung as the studies do not separately identify these two populations. It is important to establish whether BCG-induced lung-parenchymal cells exhibit a unique phenotype, identifying them as tissue-resident cells. It is also important to establish whether the phenotype of these cells can provide any information about their memory capacity, as they have been suggested to potentially play an important role in vaccine-mediated protection against *M.tb* infection[218].

The aim of this chapter was to utilise the intravascular staining technique to investigate the development of $CD4^+$ T_{RM} in the lungs of mice over the course of 12 months following intra-dermal BCG immunisation. This included phenotypic and functional characterisation of

these cells as well as comparison between $CD4^+$ T_{RM} and $CD4^+$ T cells located in the lung-vasculature, spleen and peripheral blood of the immunised mice, with the goal of identifying unique features of $CD4^+$ T_{RM}.

4.2. Results

4.2.1. Development of a putative tissue-resident lung-parenchymal $CD4^+$ T cell population following intradermal BCG vaccination

To investigate the development of a population of lung-parenchymal $CD4^+$ T cells following BCG immunisation, groups of 6 mice were vaccinated intradermally with BCG or placebo. Lungs, spleen and peripheral blood were harvested 1, 3, 5, 6, 12, 26 and 52 weeks later, following intravascular staining. To identify antigen-specific $CD4^+$ T cells within these organs, isolated cells were stimulated with TB10.4 peptides 4 and 13 (see materials and methods for details) and analysed by flow cytometry (Appendix – Flow cytometry panels 1 and 2). ICS was used to identify TB10.4 peptide-specific $CD4^+$ T cells producing IFN-γ, IL-2, TNF-α or any combination of these (cytokine$^+$ $CD4^+$ T cells) (Appendix – Flow cytometry gating strategy).

4.2.1.1. Frequency of $CD4^+$ T cells in the lung-vascular compartment is greater than in the lung-parenchymal compartment post-BCG or placebo immunisation

For the first 12 weeks post-BCG or placebo immunisation, the frequency of $CD4^+$ T cells in the lung-vascular and lung-parenchymal compartments as a percentage of the total $CD4^+$ T cells isolated from the lung did not alter significantly (Figure 4.1a). During this time, the frequency of $CD4^+$ T cells in the lung-vascular compartment was approximately 9-fold greater than in the lung-parenchymal compartment. At 26 and 52 weeks post-BCG or placebo immunisation, the frequency of lung-parenchymal $CD4^+$ T cells was significantly

greater when compared with all previous time points for both immunised and control mice, and the frequency of lung-vascular $CD4^+$ T cells was significantly lower when compared with all previous time points for both immunised and control mice. The frequency of $CD4^+$ T cells in both compartments did not alter significantly between 26 and 52 weeks post-immunisation, for both immunised and control mice. At all time points investigated, the frequency of lung-vascular $CD4^+$ T cells was significantly greater than lung-parenchymal $CD4^+$ T cells in both BCG-vaccinated and control animals, and there was no significant difference in frequency of $CD4^+$ T cells in either compartment comparing BCG with control at each time point. The actual number of $CD4^+$ T cells in the lung-parenchymal compartment did not alter significantly between any of the time points measured post-BCG or placebo immunisation (Figure 4.1b). There were significantly fewer $CD4^+$ T cells in the lung-vascular compartment at week 26 compared to weeks 1 and 6 in both BCG and placebo-immunised mice. The number of lung-vascular $CD4^+$ T cells was significantly greater than the number of lung-parenchymal $CD4^+$ T cells at all time points.

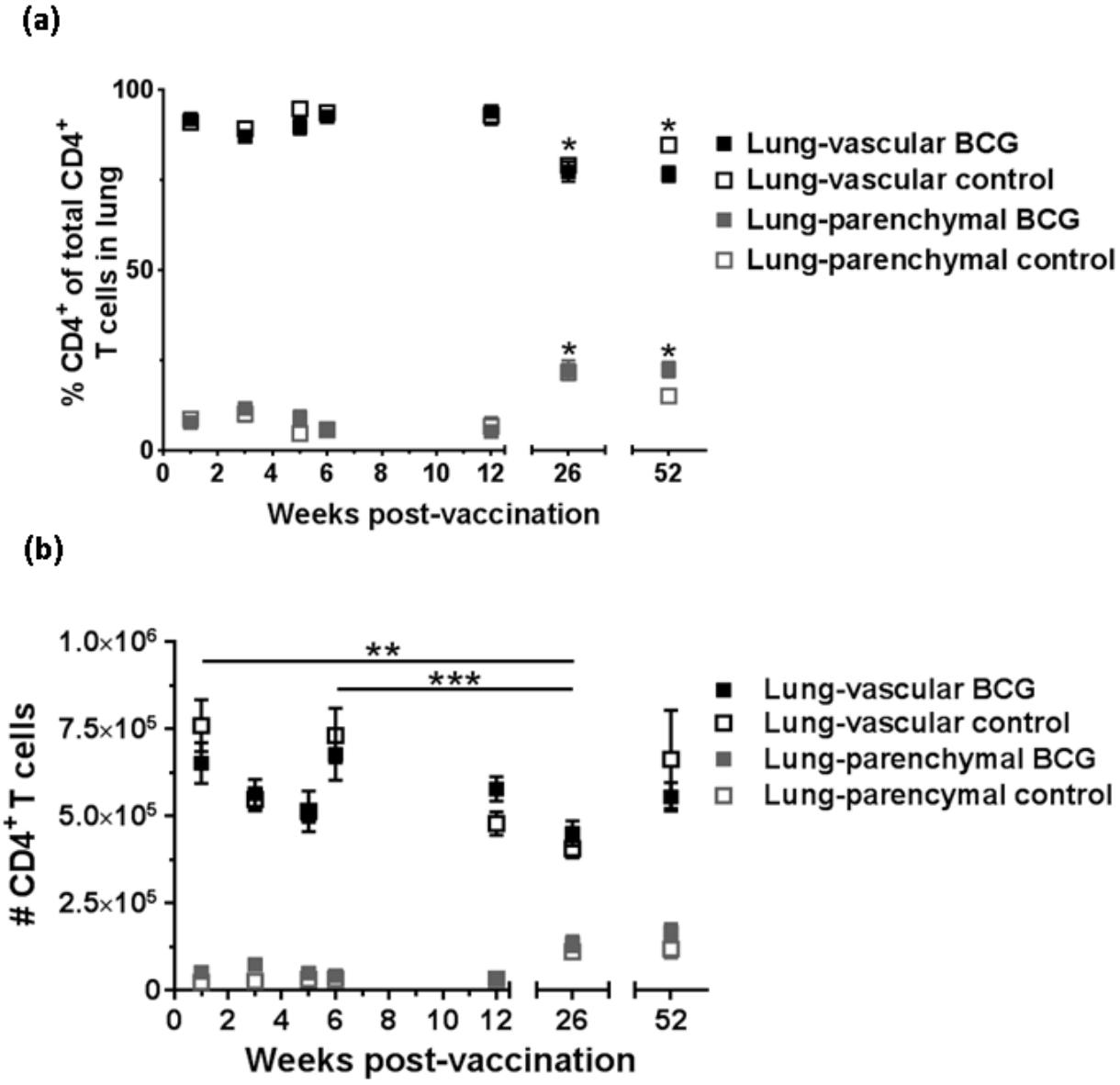

Figure 4.1 - Analysis of $CD4^+$ T cells in lung-vascular and lung-parenchymal compartments. BALB/c mice received BCG or placebo immunisation and at various time points post-immunisation, intravascular staining was used to identify populations of lung-parenchymal and lung-vascular $CD4^+$ T cells. Cells were analysed by flow cytometry. (a) Frequency of lung-vascular and lung-parenchymal $CD4^+$ T cells is shown as a % of total $CD4^+$ T cells isolated from the lung. (b) Number of $CD4^+$ T cells in the lung-parenchymal and lung-vascular compartments. For both graphs, points represent mean values (n=6) and error bars show SEM. Two-way ANOVA with Sidak's post-test, comparing each time point within the same compartment (shown on graph, * $\rho \leq 0.05$, ** $\rho \leq 0.01$, *** $\rho \leq 0.001$), BCG with

control and lung-parenchymal with lung-vascular (not shown on graph, for all time points frequency of lung-vascular $CD4^+$ T cells exceeded lung-parenchymal $CD4^+$ T cells in both BCG-immunised and control mice by **** $p \leq 0.0001$).

4.2.1.2. BCG vaccination induces cytokine$^+$ CD4$^+$ T cells in lung, spleen and peripheral blood

BCG vaccination induced significant populations of cytokine$^+$ CD4$^+$ T cells in the lung, spleen and peripheral blood (Figure 4.2a). Cytokine$^+$ CD4$^+$ T cells were identified from week 3 post-BCG vaccination in the lung-vascular compartment and from 5 weeks post-BCG vaccination in the lung-parenchymal compartment, spleen and peripheral blood.

4.2.1.3. BCG induces the highest frequencies of cytokine$^+$ CD4$^+$ T cells in the lung, with no difference in frequency between lung compartments

There was no significant difference between relative proportions of cytokine$^+$ CD4$^+$ T cells present in the lung-vascular and lung-parenchymal compartments at any time point post-BCG vaccination (Figure 4.2b). At week 5 post-vaccination, both lung compartments contained significantly higher frequencies of cytokine$^+$ CD4$^+$ T cells when compared to both spleen and peripheral blood. At week 12 post-vaccination, only the lung-parenchymal compartment contained significantly higher frequencies of cytokine$^+$ CD4$^+$ T cells compared to spleen and peripheral blood. At week 52 post-vaccination, only the lung-vascular compartment contained significantly higher frequencies of cytokine$^+$ CD4$^+$ T cells compared to spleen and peripheral blood.

(a)

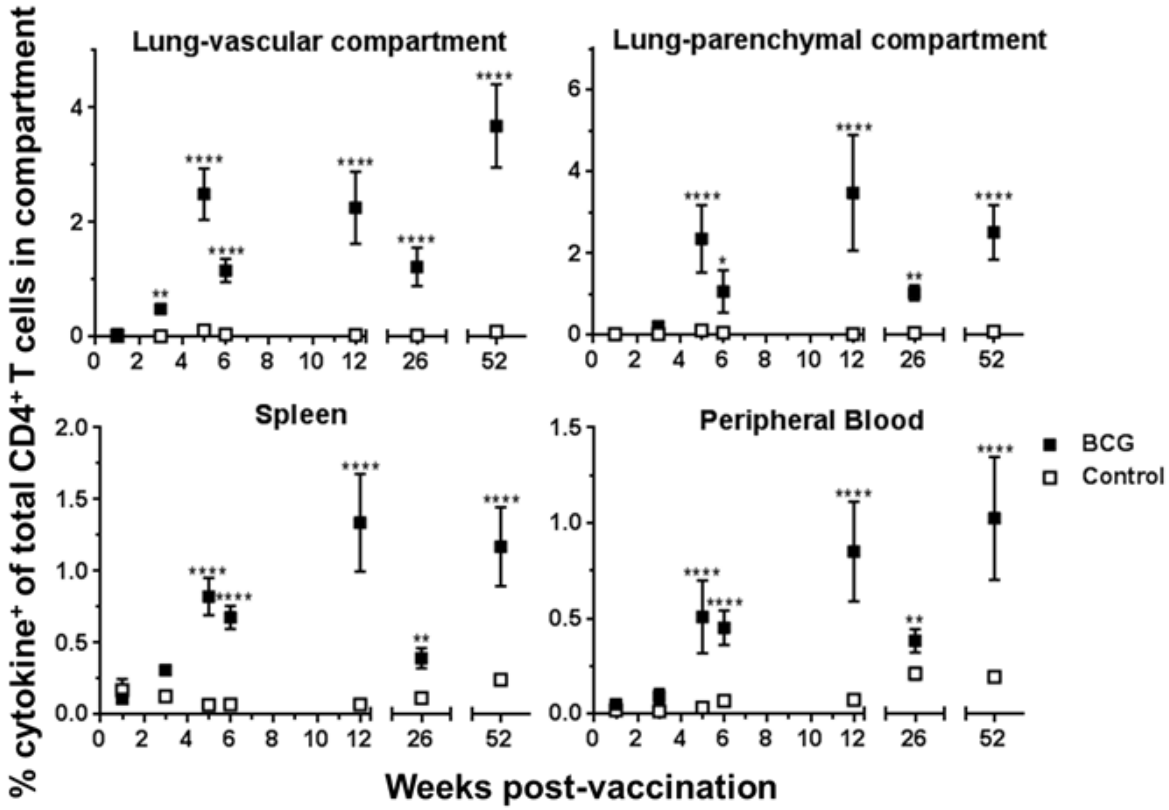

(b)

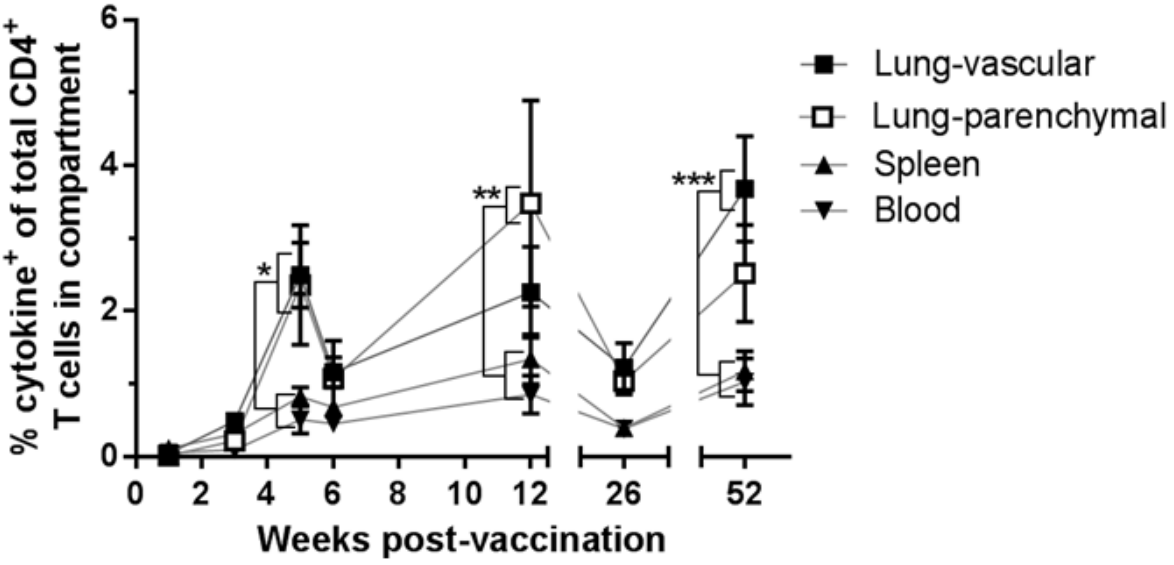

Figure 4.2 - **Analysis of cytokine$^+$ CD4$^+$ T cells in different tissue compartments.** BALB/c mice received BCG or placebo immunisation and at various time points post-immunisation

intravascular staining followed by ICS was used to identify populations of lung-parenchymal and lung-vascular TB10.4 peptide-specific $CD4^+$ T cells in the lungs, spleen and peripheral blood. **(a)** Graphs show frequencies of $cytokine^+$ $CD4^+$ T cells in all compartments as a % of the total number of $CD4^+$ T cells in the same compartment. Statistical comparison is between BCG and control at each time point. **(b)** Frequency of $cytokine^+$ $CD4^+$ T cells from all compartments in BCG-vaccinated animals expressed as a % of the total number of $CD4^+$ T cells in the same compartment. Statistical comparison is between frequency of BCG-induced $cytokine^+$ $CD4^+$ T cells in all compartments at each time point. For all graphs, points represent mean values (n=6) and error bars show SEM. Two-way ANOVA with Sidak's post-test was used. * $\rho \leq 0.05$, ** $\rho \leq 0.01$, *** $\rho \leq 0.001$, **** $\rho \leq 0.0001$.

4.2.1.4. Cell-surface immunophenotyping of antigen-specific $CD4^+$ T cells at different time points post-vaccination

i. BCG-induced cytokine$^+$$CD4^+$ T cells express a $CD44^{hi}CD62L^{lo}CD27^-$ phenotype in all compartments

At all time points from week 3 post-BCG vaccination, cytokine$^+$ $CD4^+$ T cells in both lung compartments, spleen and peripheral blood all displayed a $CD44^{hi}CD62L^{lo}CD27^-$ phenotype (Figure 4.3). At week 1 post-BCG vaccination there were no significant populations of cytokine$^+$ $CD4^+$ T cells in any compartment.

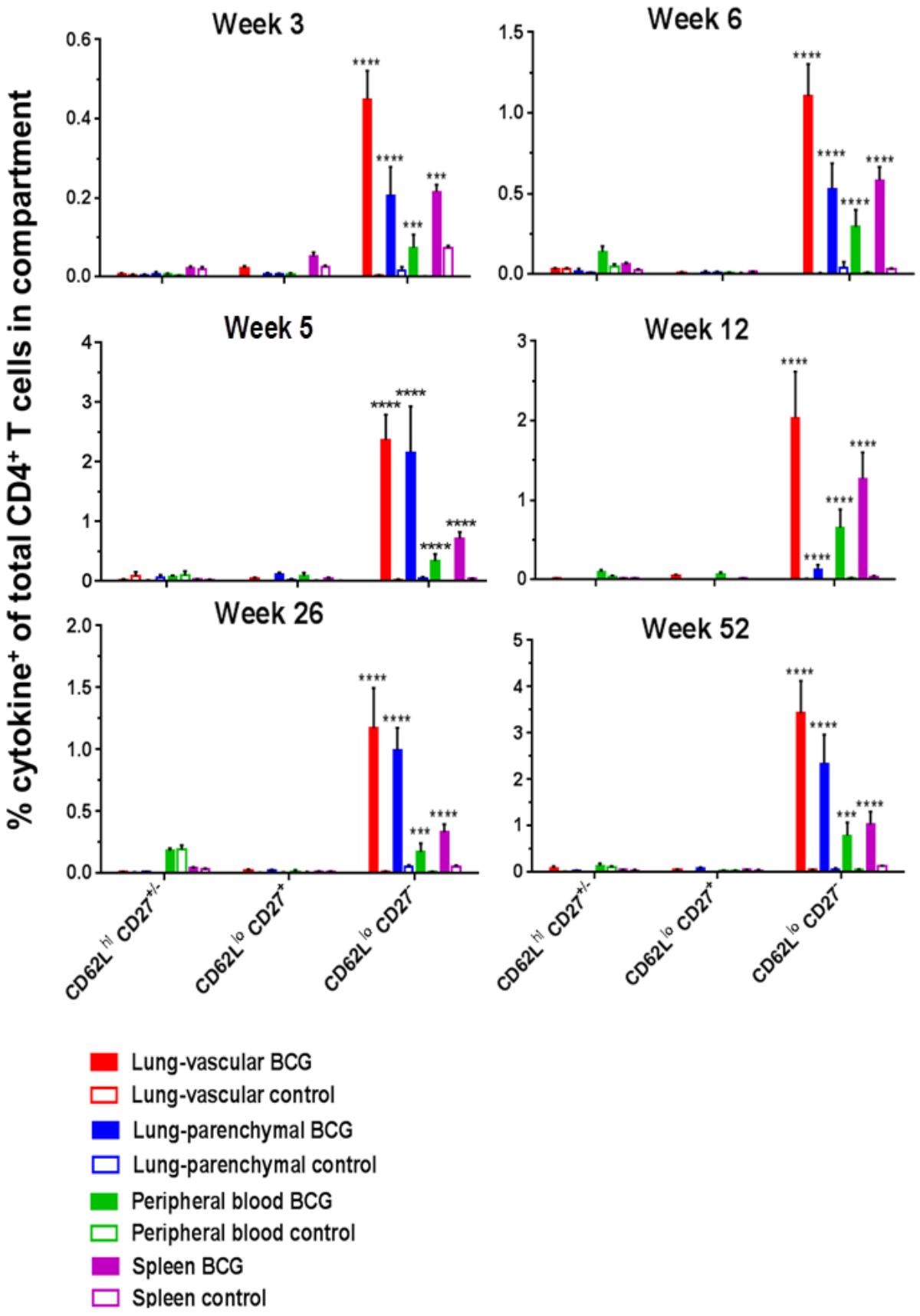
Week 3
Week 6
Week 5
Week 12
Week 26
Week 52
% cytokine+ of total CD4+ T cells in compartment
CD62L hi CD27+/-
CD62L lo CD27+
CD62L lo CD27-
Lung-vascular BCG
Lung-vascular control
Lung-parenchymal BCG
Lung-parenchymal control
Peripheral blood BCG
Peripheral blood control
Spleen BCG
Spleen control

Figure 4.3 - Phenotype analysis of cytokine^{+} CD4^{+} CD44^{hi} T cells post-vaccination. BALB/c mice received BCG or placebo immunisation and at various time points post-immunisation intravascular staining followed by ICS was used to identify populations of lung-parenchymal and lung-vascular TB10.4 peptide-specific CD4^{+} T cells in the lungs, spleen and peripheral blood. Graph shows frequency of cytokine^{+} CD4^{+} CD44^{hi} T cells in all compartments displaying combinations of CD62L and CD27 cell surface markers as a % of total CD4^{+} T cells in that compartment. Bars represent mean values (n=6) and error bars show SEM. *** $\rho \leq 0.001$, **** $\rho \leq 0.0001$, two-way ANOVA with Sidak's post-test, comparing BCG and control.

ii. BCG-induced cytokine$^+$ CD4$^+$ T cells are CCR7$^-$ but heterogeneous for CD69 and CD127 in lung and spleen

At all time points from week 3 post-BCG vaccination, cytokine$^+$ CD4$^+$ T cells in both lung compartments, spleen and peripheral blood were all CCR7$^-$, either CD69$^+$ or CD69$^-$ and either CD127^{hi} or CD127^{lo} (Figure 4.4). There were significantly higher frequencies of CD127^{lo} cytokine$^+$ CD4$^+$ T cells in both lung compartments and spleen at weeks 3, 5 and 6. There were significantly higher frequencies of CD69$^+$ cytokine$^+$ CD4$^+$ T cells in both lung compartments and spleen at weeks 12 and 26 and in the lung-vascular compartment alone at week 3. There were significantly higher frequencies of CD69$^-$ cytokine$^+$ CD4$^+$ T cells in the lung-vascular compartment and the spleen at week 52. At week 1 post-BCG vaccination there were no significant populations of cytokine$^+$ CD4$^+$ T cells in any compartment.

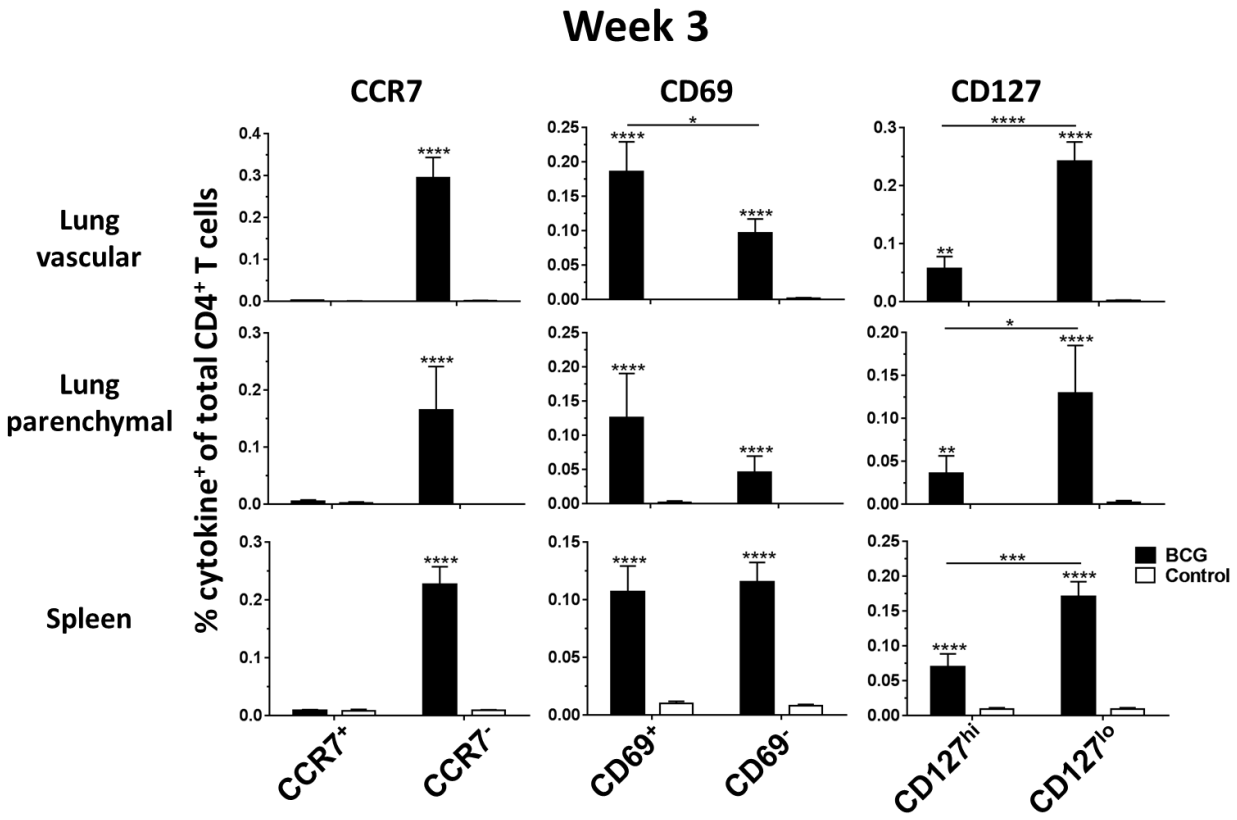
Week 3
CCR7
CD69
CD127
Lung vascular
Lung parenchymal
Spleen
% cytokine+ of total CD4+ T cells
BCG
Control
CCR7+
CCR7-
CD69+
CD69-
CD127hi
CD127lo

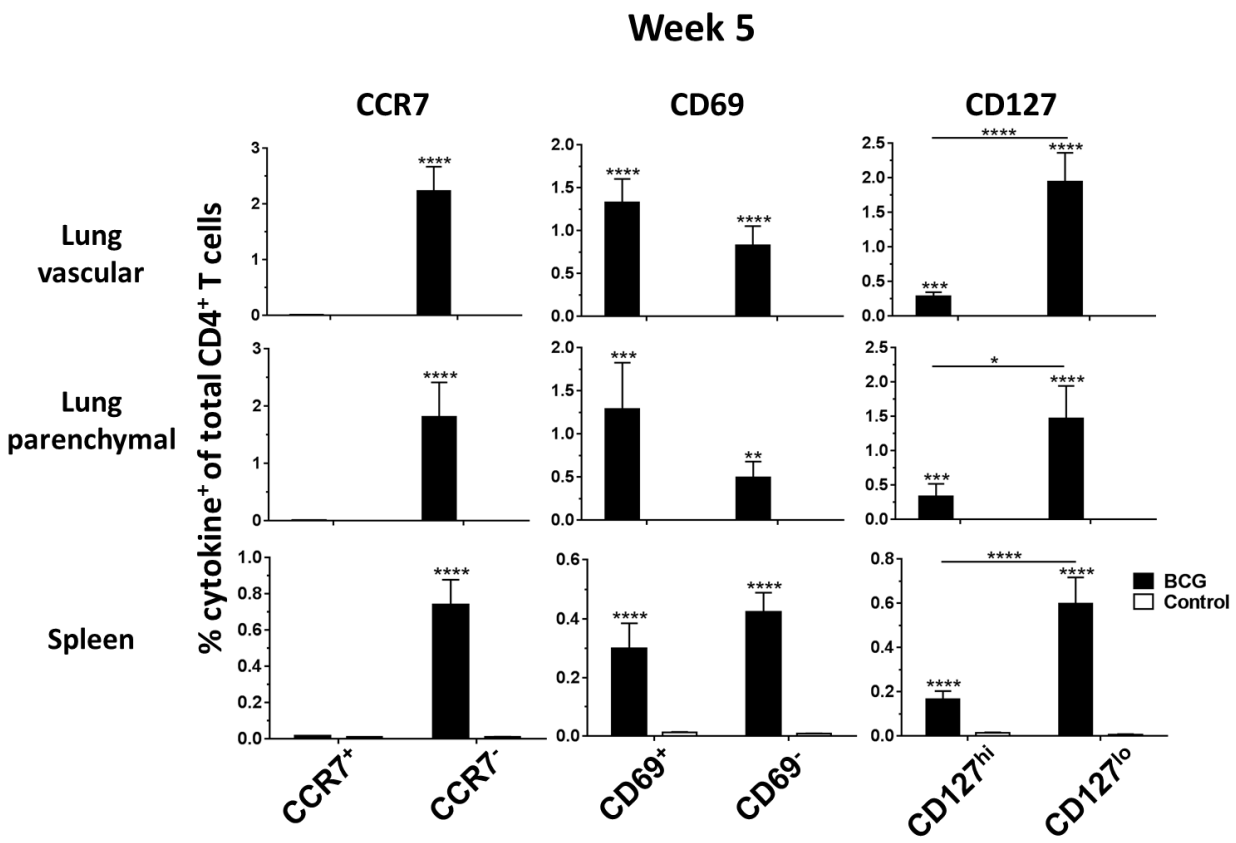
Week 5
CCR7
CD69
CD127
Lung vascular
Lung parenchymal
Spleen
% cytokine+ of total CD4+ T cells
BCG
Control
CCR7+
CCR7-
CD69+
CD69-
CD127hi
CD127lo

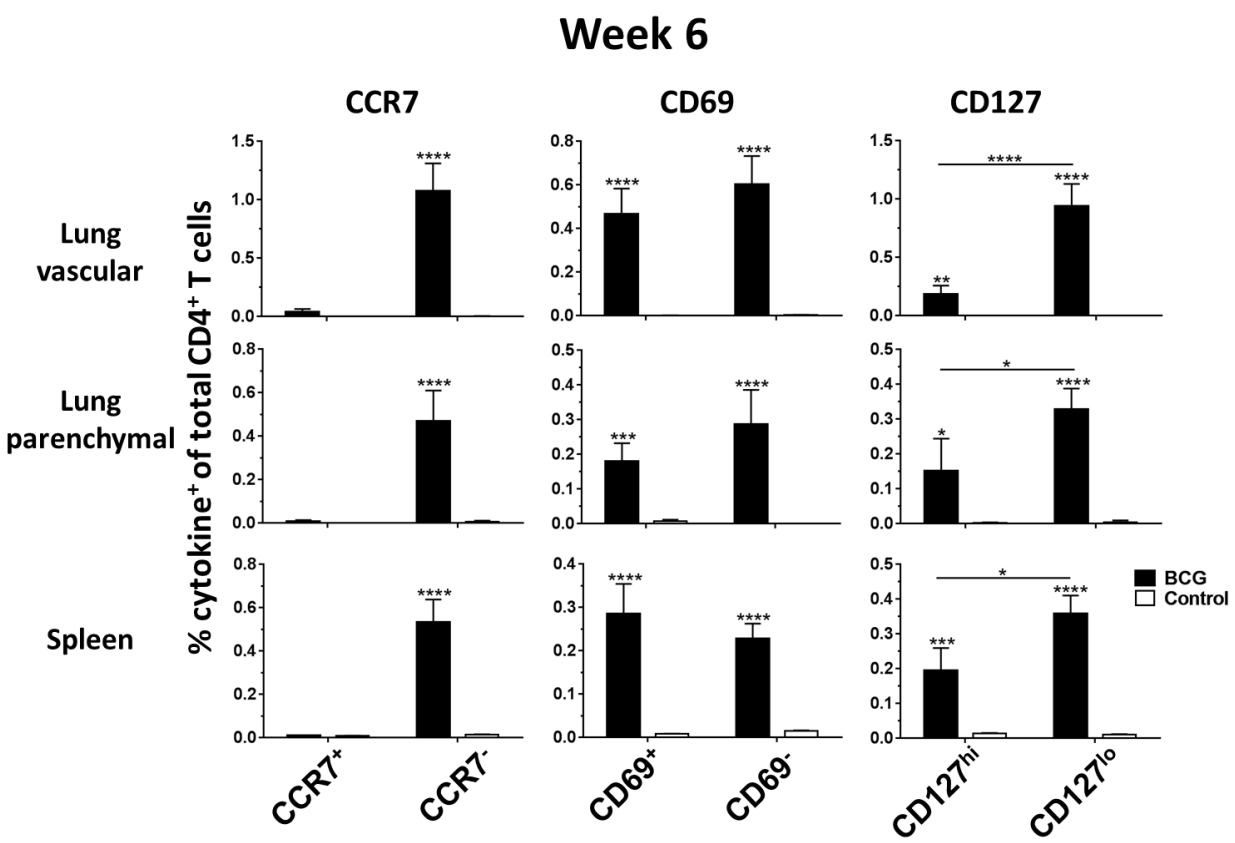
Week 6
CCR7
CD69
CD127
Lung vascular
Lung parenchymal
Spleen
% cytokine+ of total CD4+ T cells
BCG
Control
CCR7+
CCR7-
CD69+
CD69-
CD127hi
CD127lo

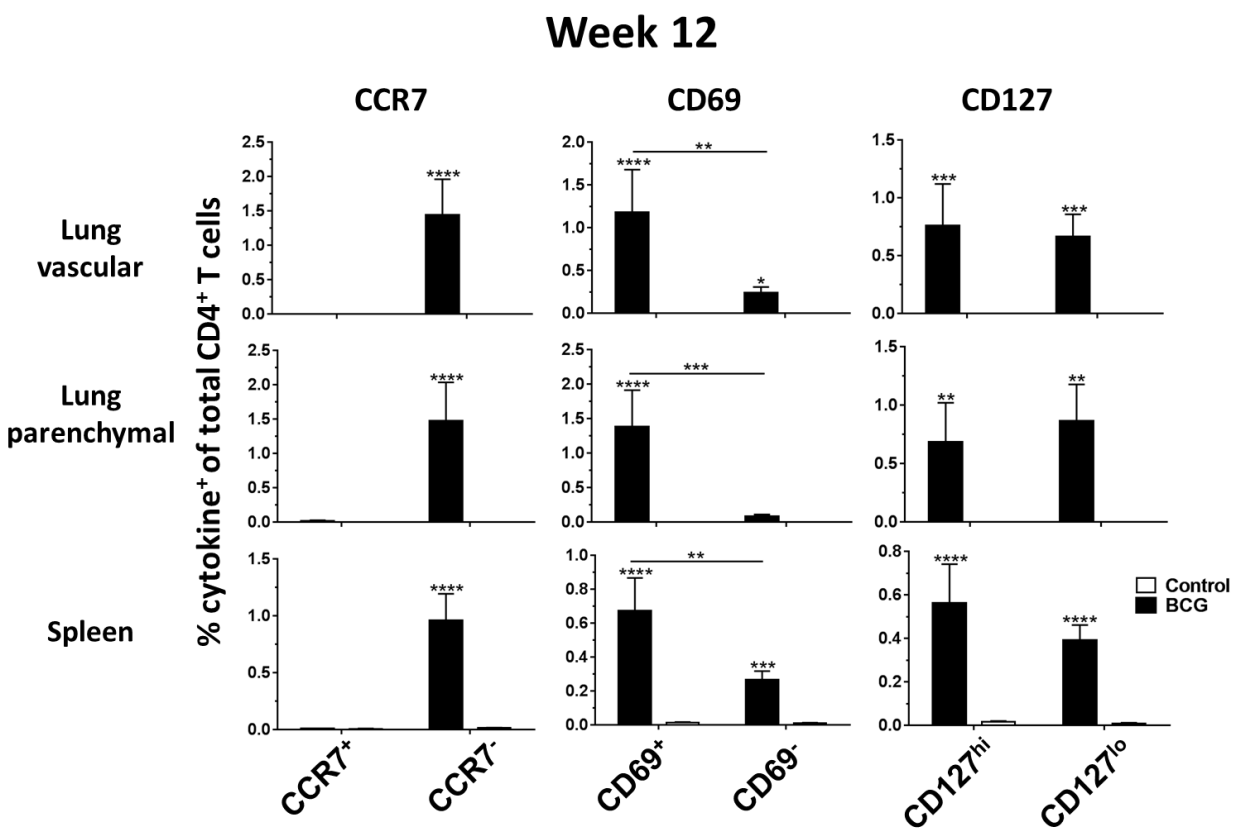
Week 12
CCR7
CD69
CD127
Lung vascular
Lung parenchymal
Spleen
% cytokine+ of total CD4+ T cells
Control
BCG
CCR7+
CCR7-
CD69+
CD69-
CD127hi
CD127lo

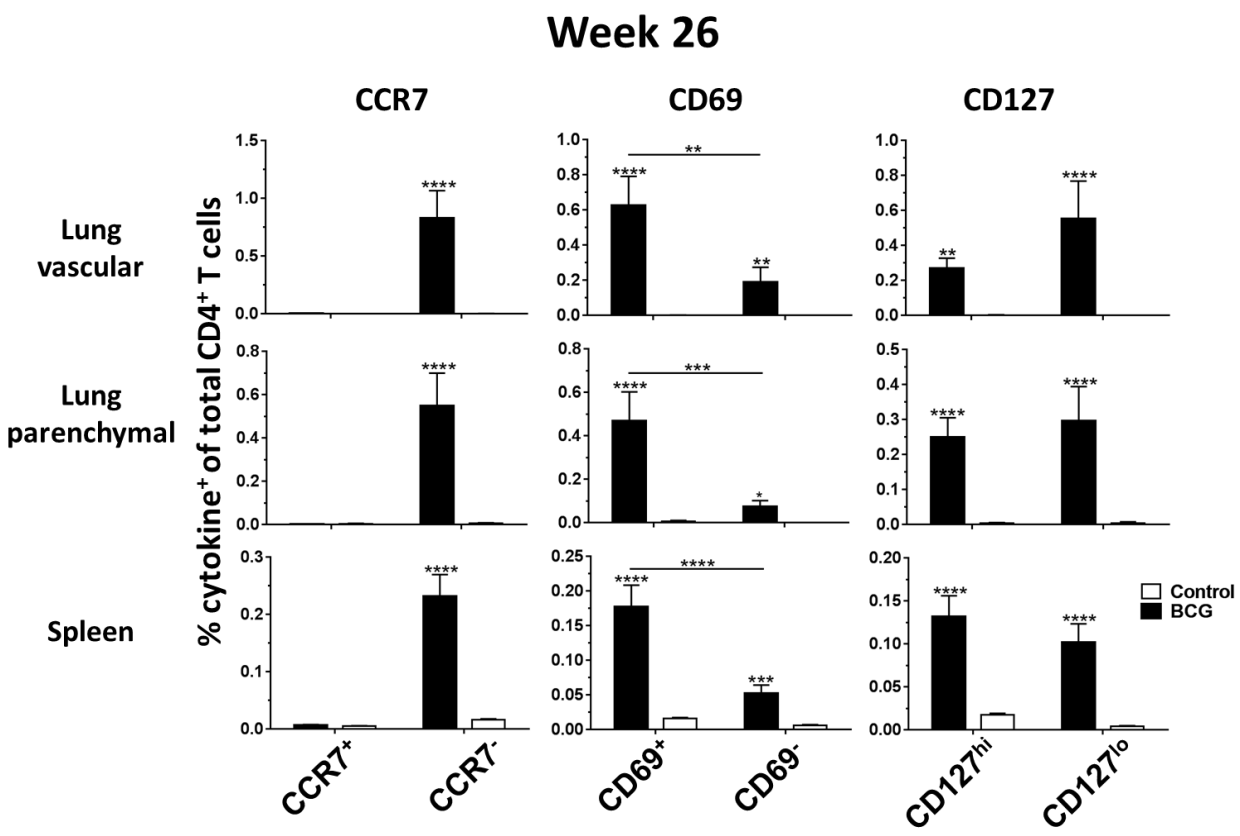
Week 26
CCR7
CD69
CD127
Lung vascular
Lung parenchymal
Spleen
% cytokine+ of total CD4+ T cells
Control
BCG
CCR7+
CCR7-
CD69+
CD69-
CD127hi
CD127lo

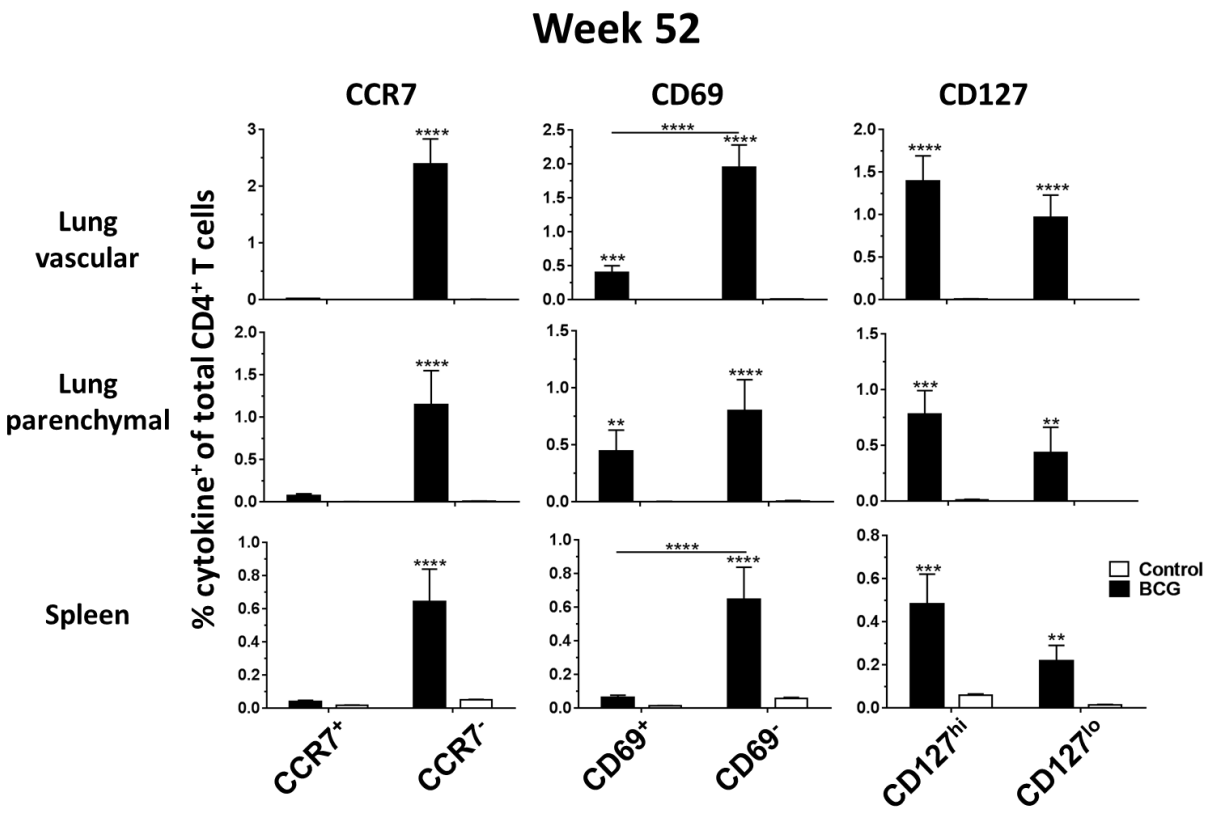

Figure 4.4 - Phenotype analysis of cytokine$^+$ CD4$^+$ CD62L^{lo} T cells post-vaccination. BALB/c mice received BCG or placebo and at various time points post-immunisation intravascular staining followed by ICS was used to identify populations of lung-parenchymal and lung-vascular TB10.4 peptide-specific CD4$^+$ T cells in the lungs and spleen. Graphs show frequencies of cytokine$^+$ CD4$^+$ CD62L^{lo} T cells in all compartments displaying CCR7, CD69 and CD127 cell surface markers as a % of total CD4$^+$ T cells in that compartment. For all graphs, bars represent mean values (n=6) and error bars show SEM. * $\rho \leq 0.05$, ** $\rho \leq 0.01$, *** $\rho \leq 0.001$, **** $\rho \leq 0.0001$, two-way ANOVA with Sidak's post-test comparing BCG with control and BCG with BCG.

4.2.1.5. BCG-induced cytokine$^+$ CD4$^+$ T cells in all compartments display a dominance of multifunctional cells

Boolean gating analysis was used to identify populations of TB10.4 peptide-specific CD4$^+$ T cells producing IFN-γ, IL-2, TNF-α or any combination of the three. IFNγ$^+$IL-2$^+$TNF-α$^+$ and IFNγ$^+$IL-2$^-$TNF-α$^+$ CD4$^+$ T cells were detectable in all compartments at all time points post-BCG vaccination except week 1, when there were no significant populations of cytokine$^+$ CD4$^+$ T cells in any compartment (Figure 4.5). IFNγ$^+$IL-2$^+$TNF-α$^-$ CD4$^+$ T cells were only detectable in the spleen at weeks 3 and 5. IFNγ$^-$IL-2$^+$TNF-α$^+$ CD4$^+$ T cells were detectable in the lung-vascular compartment at weeks 3, 12 and 52, in the lung-parenchymal compartment at weeks 12, 26 and 52 and in the spleen at week 12. IFNγ$^+$IL-2$^-$TNF-α$^-$ CD4$^+$ T cells were detectable in the lung-vascular compartment at weeks 3 and 5 and in the spleen at weeks 3, 5 and 6. IFNγ$^-$IL-2$^-$TNF-α$^+$ CD4$^+$ T cells were detectable in the lung-vascular compartment at weeks 3, 5, 6, 12 and 26 and in the lung-parenchymal compartment at weeks 26 and 52.

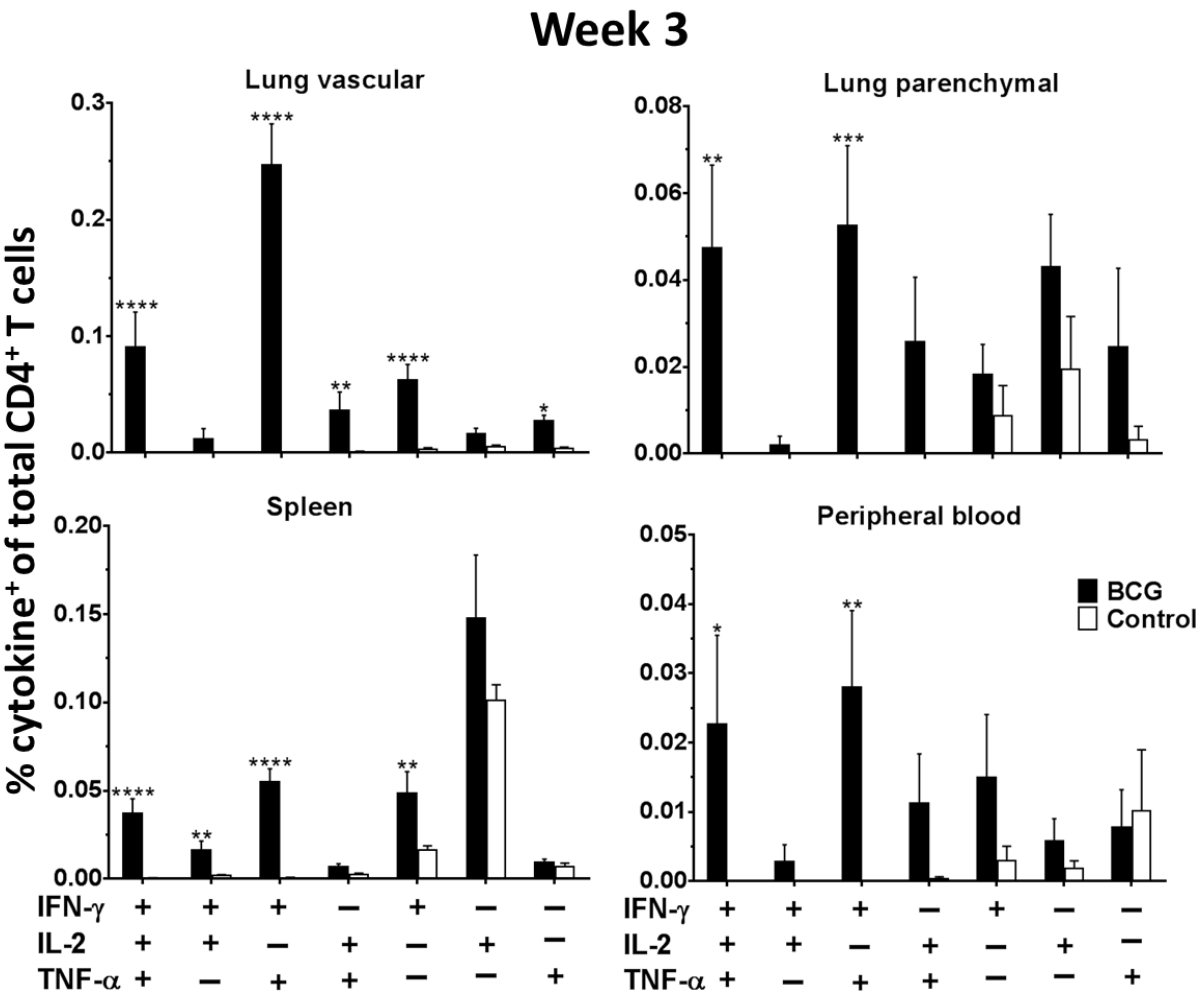
Week 3
Lung vascular
Lung parenchymal
Spleen
Peripheral blood
% cytokine+ of total CD4+ T cells
BCG
Control
IFN-γ
IL-2
TNF-α

Week 5

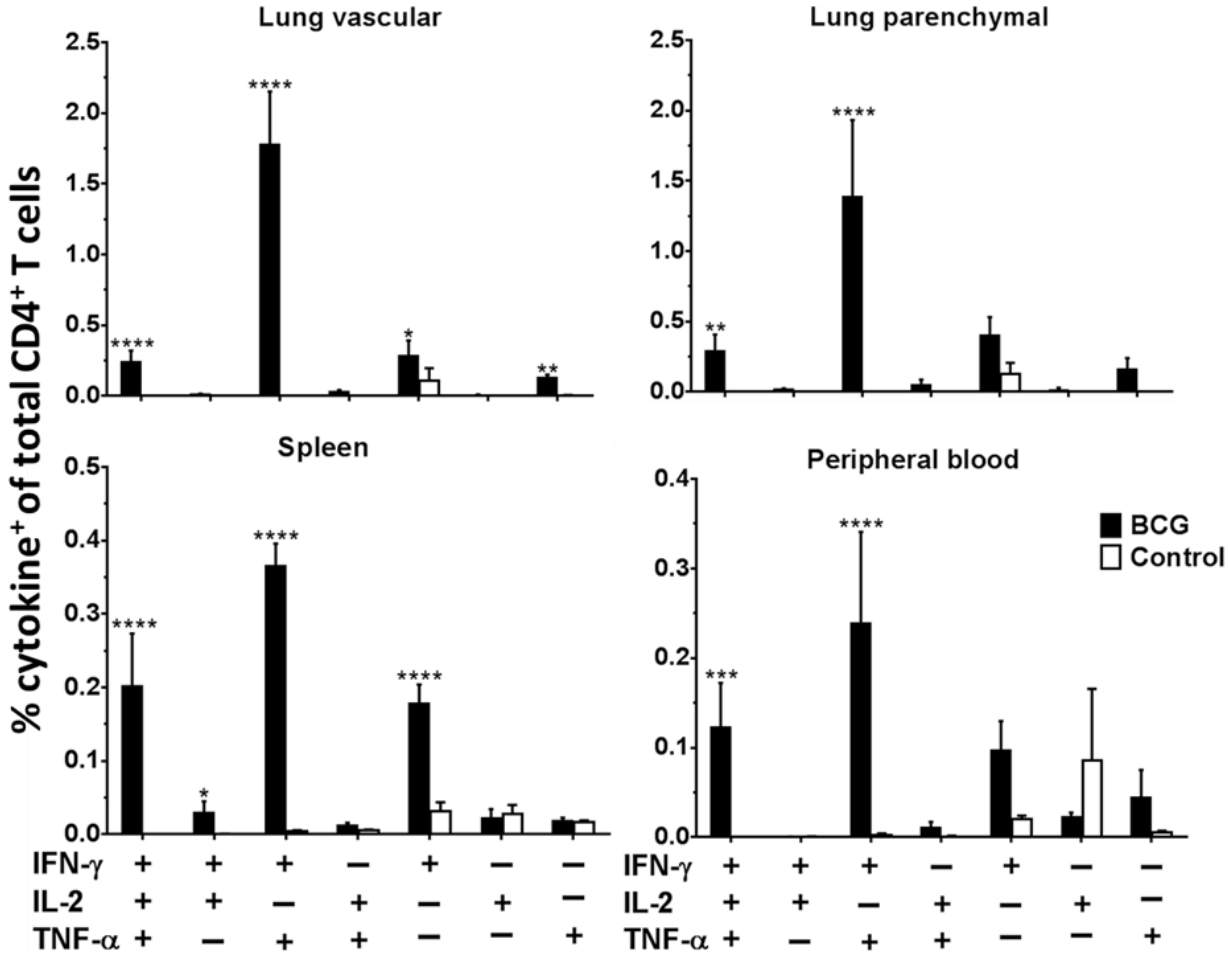
Lung vascular
Lung parenchymal
Spleen
Peripheral blood
% cytokine+ of total CD4+ T cells
BCG
Control
IFN-γ
IL-2
TNF-α

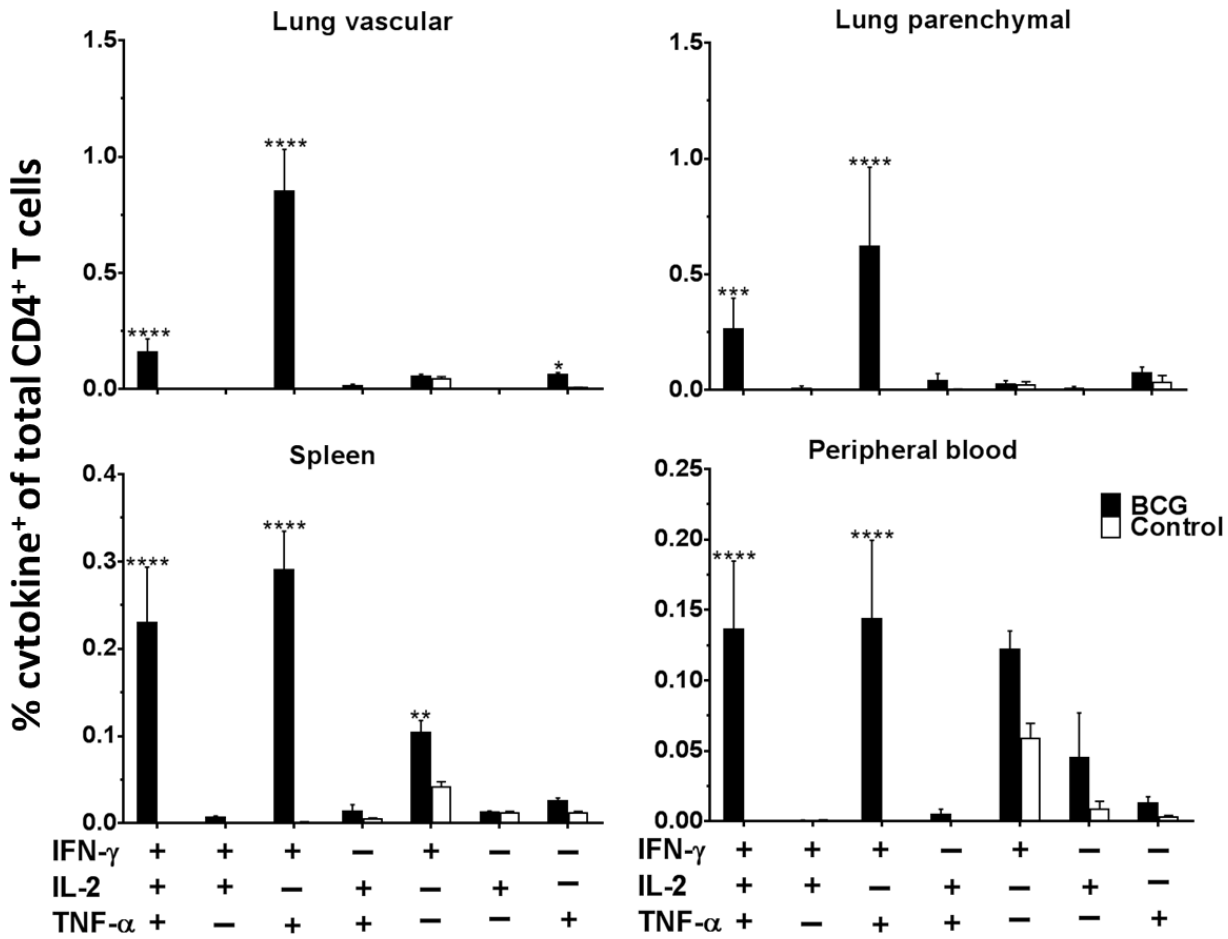
Week 6
Lung vascular
Lung parenchymal
Spleen
Peripheral blood
% cytokine+ of total CD4+ T cells
BCG
Control
IFN-γ
IL-2
TNF-α

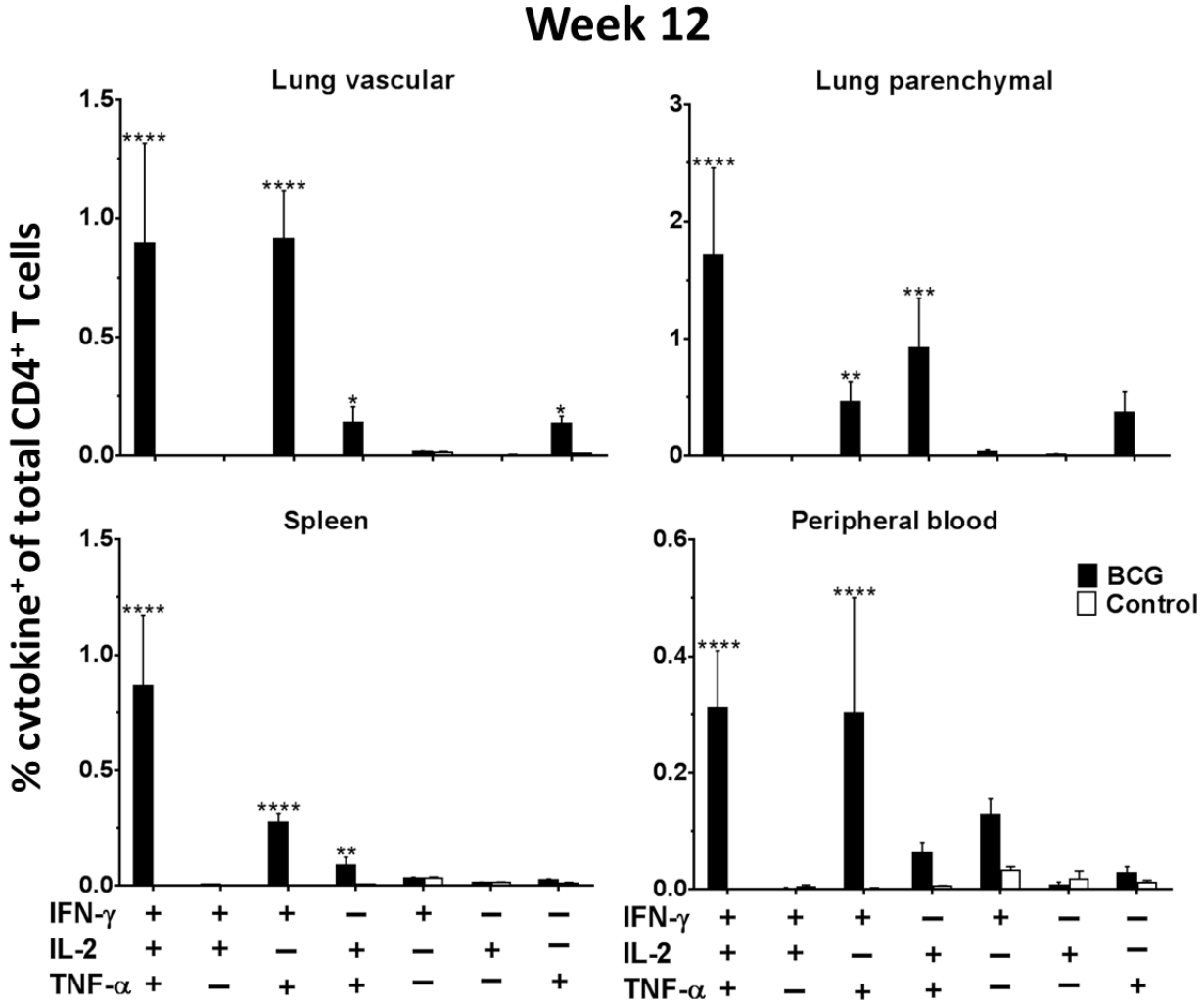
Week 12
Lung vascular
Lung parenchymal
Spleen
Peripheral blood
% cytokine+ of total CD4+ T cells
BCG
Control
IFN-γ
IL-2
TNF-α

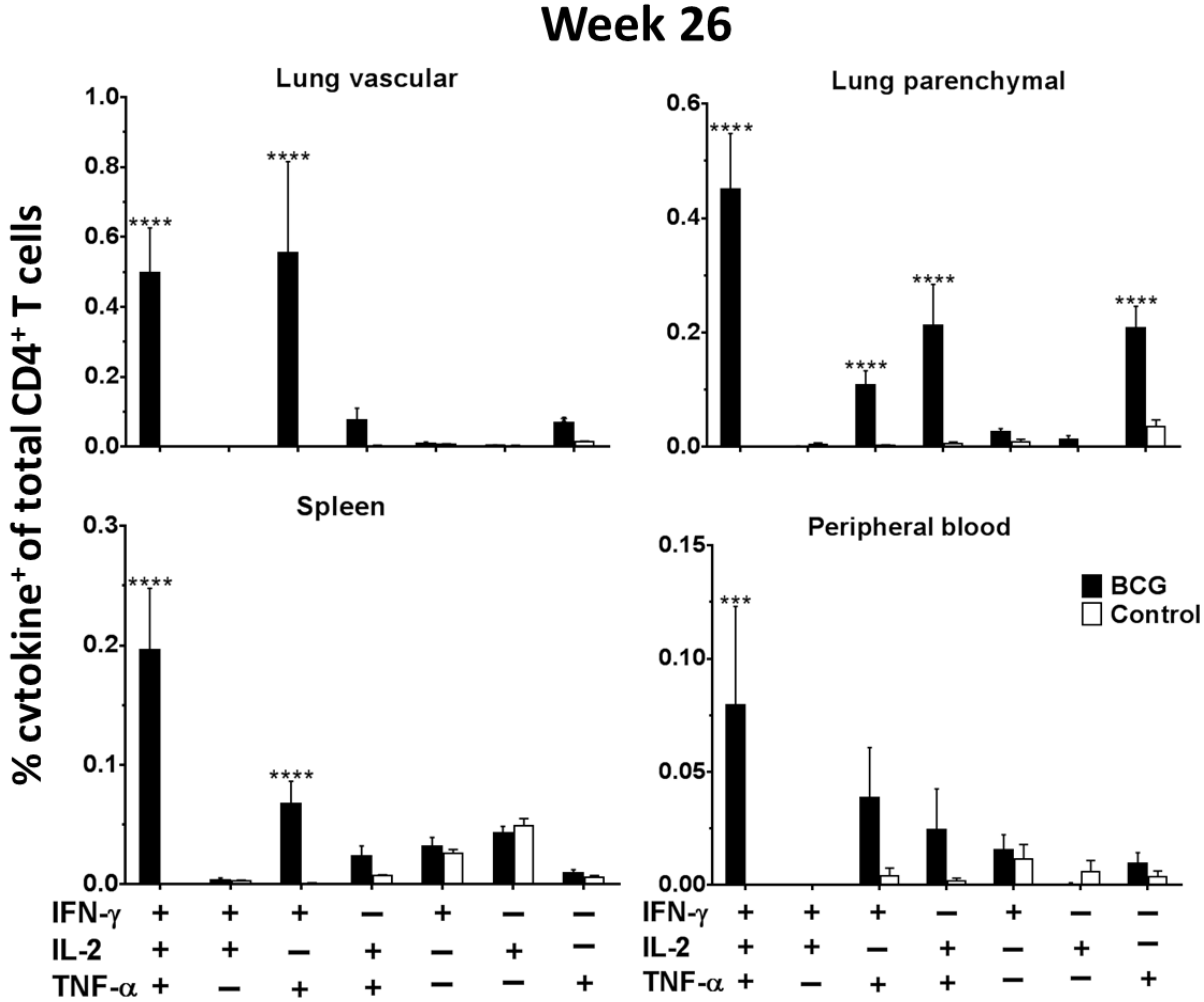
Week 26
Lung vascular
Lung parenchymal
Spleen
Peripheral blood
% cytokine+ of total CD4+ T cells
BCG
Control
IFN-γ
IL-2
TNF-α

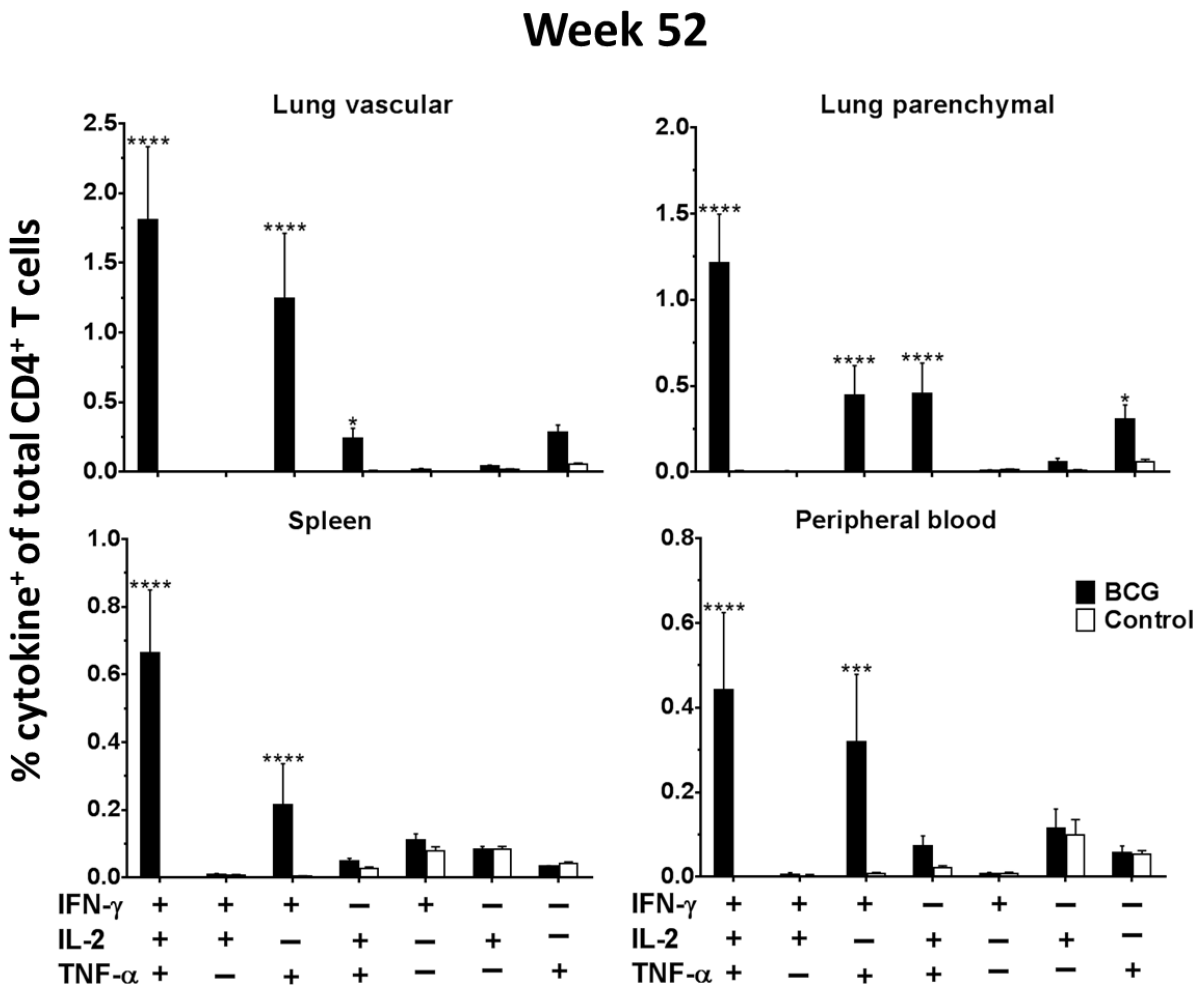

Figure 4.5 - Cytokine production by $CD4^+$ T cells post-vaccination. BALB/c mice received BCG or placebo and at various time points post-immunisation intravascular staining followed by ICS was used to identify populations of TB10.4 peptide-specific $CD4^+$ T cells in the lungs, spleen and peripheral blood. Graphs show frequencies of BCG-induced $CD4^+$T cells in all compartments producing IFN-γ, IL-2 or TNF-α plus combinations of all three as a % of the total $CD4^+$ T cells in the same compartment. For all graphs, bars represent mean values (n=6) and error bars show SEM. * $\rho \leq 0.05$, ** $\rho \leq 0.01$, *** $\rho \leq 0.001$, **** $\rho \leq 0.0001$, two-way ANOVA with Sidak's post-test comparing BCG and control.

4.2.2. Development of $CD4^+$ T cells with proliferative capacity in the spleen following BCG vaccination

In order to investigate the proliferative capacity of $CD4^+$ T cells, the EdU incorporation assay was performed as part of the previously-described study on splenic lymphocytes from groups of 6 mice at various time points post-BCG or placebo immunisation. Cells were stimulated with TB10.4 peptides and analysed by flow cytometry (Appendix – Flow cytometry EdU panel). Proliferating cells are identified as EdU^+.

4.2.2.1. BCG vaccination induces EdU^+ $CD4^+$ T cells in the spleen

Proliferating $CD4^+$ T cells were induced in the spleen from week 3 onwards in the BCG-vaccinated group, with the highest frequency observed at 12 weeks post-vaccination (Figure 4.6a).

4.2.2.2. BCG-induced EdU^+ $CD4^+$ T cells display a mixed phenotype

From week 3 post-BCG vaccination, all EdU^+ $CD4^+$ T cells at each time point were $CD27^+$ (Figure 4.6b). There were statistically significant populations of EdU^+ $CD4^+$ $CD27^+$ T cells with $CD62L^{hi}CCR7^+$, $CD62L^{lo}CCR7^+$ and $CD62L^{lo}CCR7^-$ phenotypes at all time points except weeks 26 and 52. At week 26 the only significant population of EdU^+ $CD4^+$ $CD27^+$ T cells had a $CD62L^{lo}CCR7^-$ phenotype and at week 52 there were significant populations of $CD62L^{hi}CCR7^+$ and $CD62L^{lo}CCR7^+$ T cells. Prior to week 3, there were no significant populations of EdU^+ $CD4^+$ T cells.

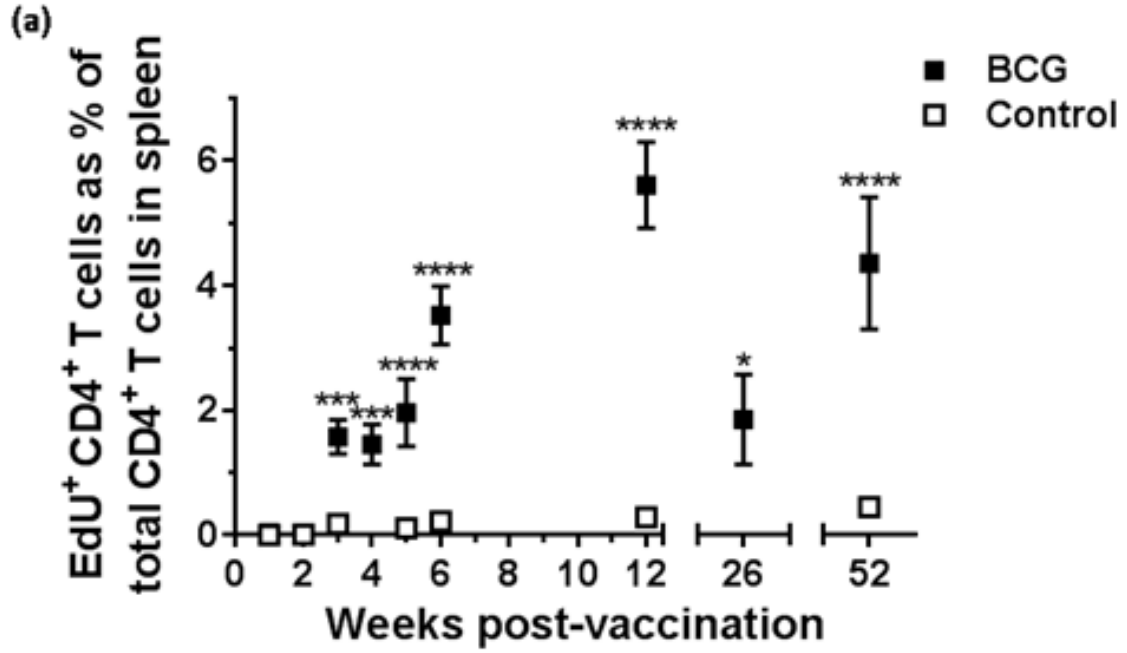
(a)
EdU+ CD4+ T cells as % of total CD4+ T cells in spleen
BCG
Control
0
2
4
6
***
***
****
****
****
*
****
0
2
4
6
8
10
12
26
52
Weeks post-vaccination

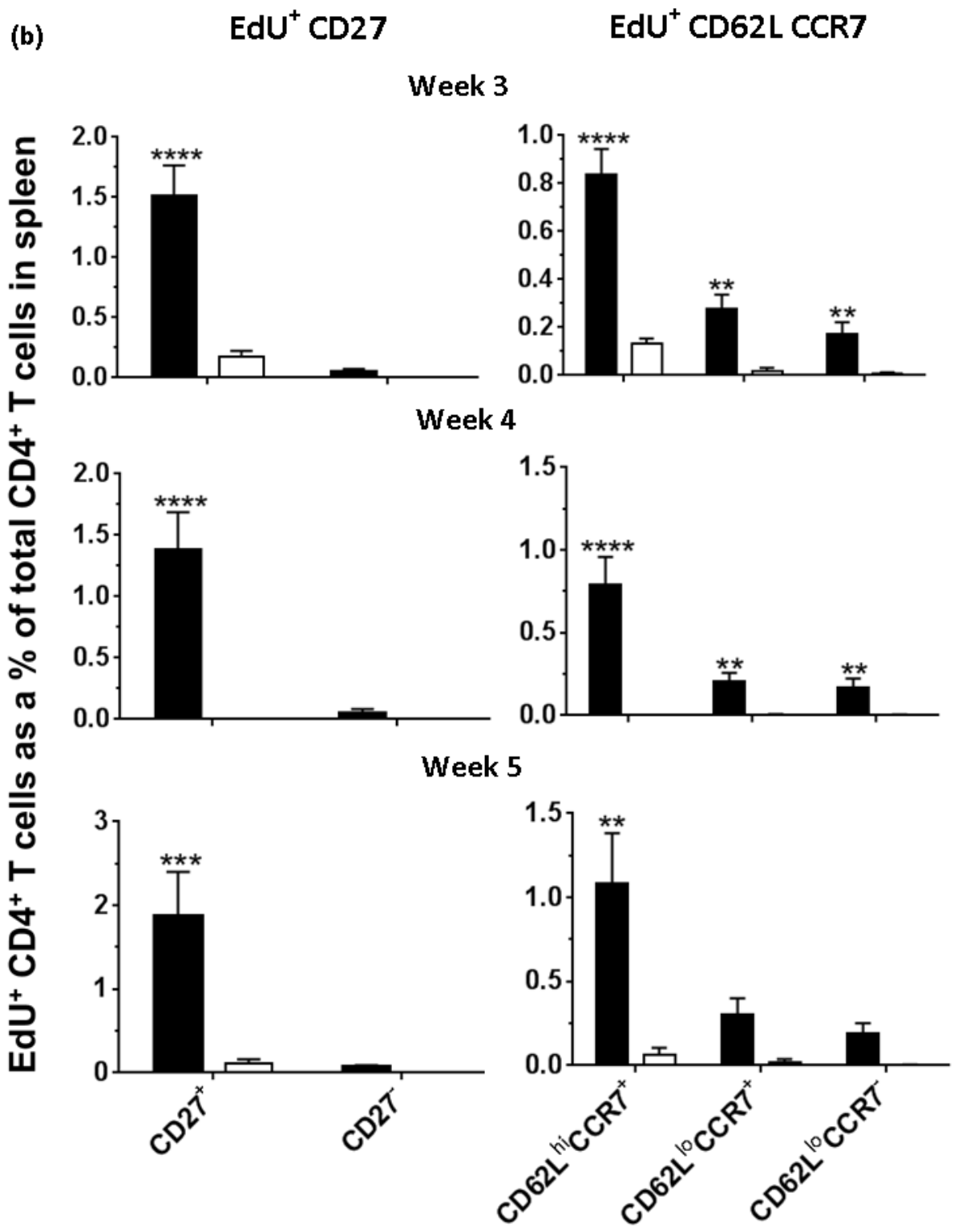
(b)
EdU+ CD27
EdU+ CD62L CCR7
Week 3
Week 4
Week 5
EdU+ CD4+ T cells as a % of total CD4+ T cells in spleen
CD27+
CD27-
CD62L hiCCR7+
CD62L loCCR7+
CD62L loCCR7-

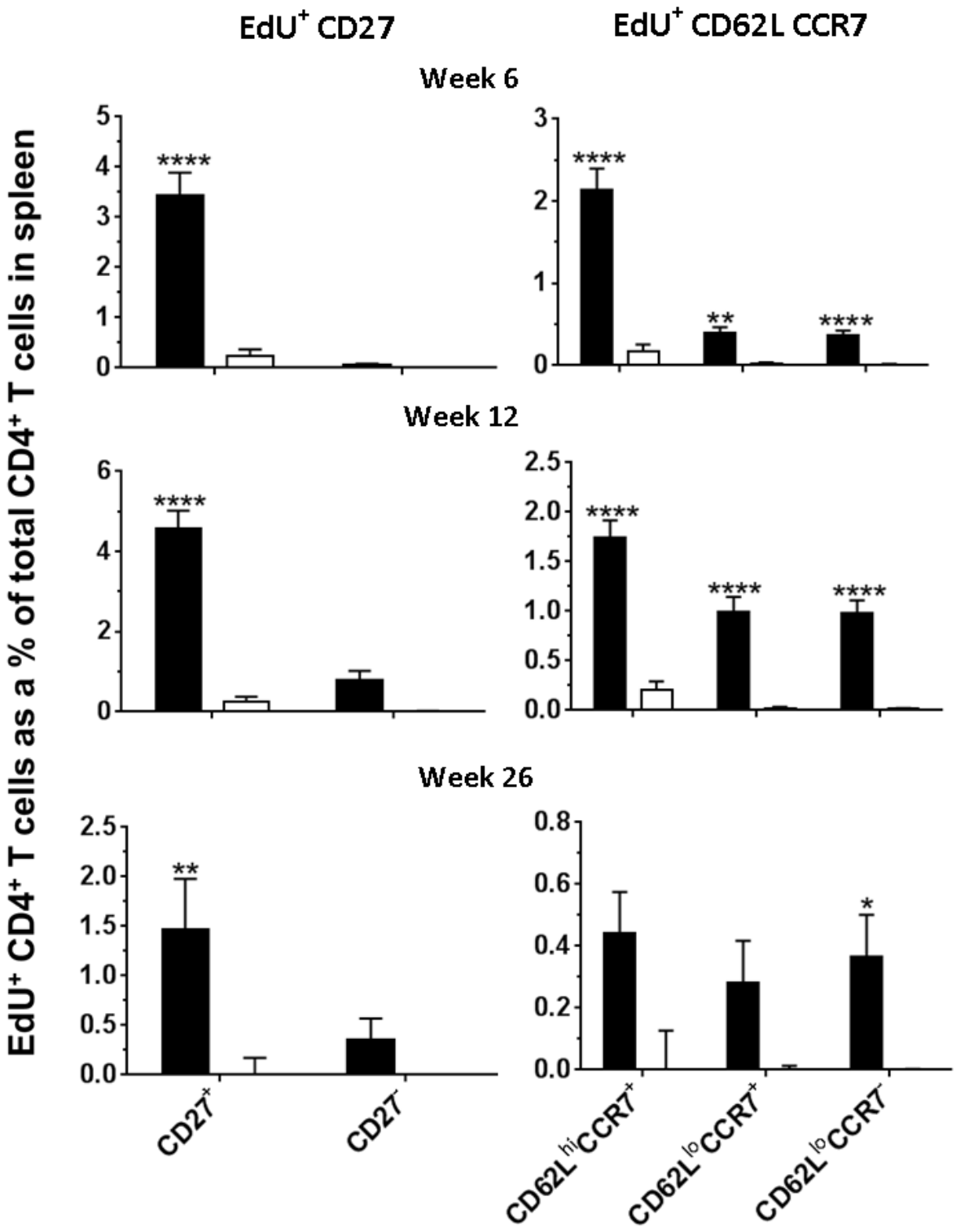
EdU+ CD27
EdU+ CD62L CCR7
Week 6
Week 12
Week 26
EdU+ CD4+ T cells as a % of total CD4+ T cells in spleen
****
**
*
CD27+
CD27-
CD62L hiCCR7+
CD62L loCCR7+
CD62L loCCR7-

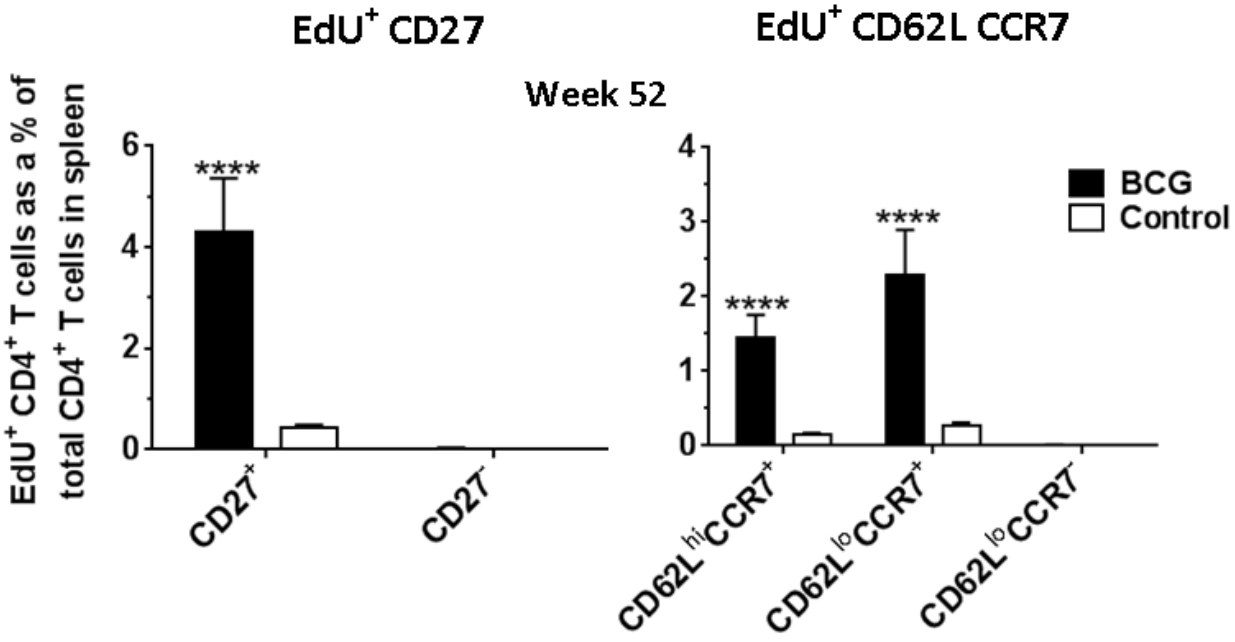

Figure 4.6 - EdU incorporation assay. BALB/c mice received BCG or placebo immunisation and were euthanased at various time points post-immunisation. The EdU proliferation assay was performed on splenic lymphocytes stimulated with TB10.4 peptides and cells were analysed by flow cytometry. (a) Frequency of EdU^+ $CD4^+$ T cells in the spleen as a % of total $CD4^+$ T cells in the spleen at each time point following immunisation. (b) Frequency of EdU^+ $CD4^+$ T cells expressing CD27 as a % of total $CD4^+$ T cells in the spleen and frequency of EdU^+ $CD4^+$ $CD27^+$ T cells expressing combinations of CD62L and CCR7 as a % of total $CD4^+$T cells in the spleen post-vaccination. For all graphs, bars or points represent mean values (n=6) and error bars show SEM. * $\rho \leq 0.05$, *** $\rho \leq 0.001$, **** $\rho \leq 0.0001$, two-way ANOVA with Sidak's post-test comparing BCG with control.

4.3. Discussion

The purpose of the study described in this chapter was to investigate the development of a putative lung tissue-resident $CD4^+$ T cell population following BCG vaccination and make phenotypic and functional comparisons between this and other tissue compartments. The cells are described as a 'putative' tissue-resident population, as it is not possible to determine from this study alone that these cells permanently reside in the lung parenchyma, only that they were detectable in the tissue at the time of euthanasia of the mice. This is one of the limitations of the intravascular staining technique; however, it does allow clear differentiation between lung-parenchymal and lung-vascular populations at that point in time, which gives a much greater level of insight into the characteristics of these two distinct populations.

BCG-induced TB10.4 peptide-specific $CD4^+$ T cells producing IFN-γ, IL-2 or TNF-α were identified from 3 weeks post-vaccination in the lung-vascular compartment and 5 weeks post-vaccination in the lung-parenchymal compartment. This may indicate that antigen-specific cells are migrating into the lung parenchyma from the lung vasculature. However, antigen-specific $CD4^+$ T cells were also undetectable in the peripheral blood until week 5 post-BCG vaccination, suggesting that the lung-vascular compartment is not simply an extension of the systemic circulation but may be thought of as a distinct compartment in its own right. This hypothesis is supported by several studies investigating the kinetics of migration of leukocytes through the vasculature of the lungs[251-256]. These studies indicate that leukocytes may take a substantial amount of time to travel through the capillary bed of the lung, causing them to be retained in the vasculature whilst migrating.

Notably, from week 5 post-BCG vaccination, frequencies of antigen-specific $CD4^+$ T cells in both lung compartments were comparable when analysed as a percentage of total $CD4^+$ T cells in the same compartment. This is spite of the fact that at all time points post-immunisation, the proportion of total lung $CD4^+$ T cells present in the lung-vasculature was significantly greater than the proportion present in the lung-parenchyma. By week 26 post-immunisation, the difference in proportion of total $CD4^+$ T cells between both lung compartments was reduced, although there was still a significantly greater proportion of the total $CD4^+$ T cell population present in the lung-vasculature. However, this was the case for both BCG- and placebo-immunised mice and therefore may reflect a physiological ageing change in the mice rather than a specific effect of BCG vaccination. This could be investigated further by repeating the experiment but starting with older mice. At week 5 post-vaccination, antigen-specific $CD4^+$ T cells in both lung compartments were observed more frequently than in either the spleen or peripheral blood, providing further evidence to support the existing literature that systemic BCG vaccination induces lung-specific responses[225].

Detailed analysis of the surface phenotype of the antigen-specific $CD4^+$ T cells reveals that all antigen-specific $CD4^+$ T cells, regardless of location, were $CD44^{hi}$ indicating antigen-experience[257] and $CD62L^{lo}CD27^-$ as described previously[225]. Whilst a $CD62L^{lo}$ phenotype is widely accepted to indicate an effector phenotype, there is less certainty about the significance of CD27 expression. CD27 has been described as a marker of functional heterogeneity in $CD4^+$ memory T cells. Schiott *et al*[258]. report $CD27^-$ as 'responding' vs $CD27^+$ as 'resting' $CD4^+$ memory T cells, suggesting that $CD27^-$ $CD4^+$ memory T cells are more differentiated and are able to rapidly secrete high levels of a broad panel of effector

cytokines in response to cognate antigen[258]. Pepper *et al.*[259] found that $CD27^-$ $CD4^+$ memory T cells were short-lived following adoptive transfer compared to $CD27^+$ $CD4^+$ memory T cells. Further work is needed in order to clarify the true implications of the lack of CD27 expression observed here following BCG vaccination.

Importantly, results presented in this chapter revealed that a significant proportion of antigen-specific $CD4^+$ T cells in both lung compartments as well as the spleen were $CD69^+$ and $CD69^-$. CD69 has been described as a putative marker of tissue-residence on T_{RM} after migration[260-262]. It has been suggested that the ability of CD69 to inhibit sphingosine-1-phosphate receptor 1 (S1PR1), which is required for T cells to exit secondary lymphoid organs via chemotactic gradients[263-265], may represent an important mechanism for maintenance of T_{RM} in tissues[262, 266]. However, this is not consistent with results shown here following BCG vaccination, as CD69 was not exclusively expressed by $CD4^+$ T cells in the lung parenchyma. This finding reinforces the need to utilise the intravascular staining technique to definitively identify lung-parenchymal cells, rather than relying on phenotypic markers alone for their identification.

Further phenotypic analysis has revealed that all antigen-specific $CD4^+$ T cells in the lung and spleen share a $CD62L^{lo}CCR7^-$ phenotype, described as being an 'effector' T cell phenotype[203, 267]. This is consistent with previous findings that BCG establishes antigen-specific populations of cells within the lung predominantly expressing an effector or effector memory phenotype[199, 267]. In fact, it has been suggested that the failure of BCG to provide durable long-term protection into adulthood may be due to its propensity to induce effector memory rather central memory T cells[208, 267]. Vogelzang *et al.* have reported

that central memory $CD4^+$ T cells are responsible for the superior protection mediated by a novel recombinant BCG vaccine[206].

Expression of CD127 (also known as IL-7 receptor subunit-α) was also investigated as part of the study presented in this chapter. IL-7 signalling has been shown to promote long-term survival of memory $CD4^+$ T cells as well as acting as a key regulator of survival during earlier stages, as resting memory cells develop from primary cells which have been exposed to antigen[268, 269]. Therefore, expression of high levels of CD127 has been used as an additional marker of effector T cell memory[270, 271]. It was found that there were significant populations of antigen-specific $CD127^{hi}$ $CD4^+$ T cells in the both the parenchyma and the vasculature of the lungs as well as the spleen and peripheral blood at all time points up to 12 months post-BCG vaccination, indicating that populations of memory T cells are maintained in these tissue sites. There were also significant populations of $CD127^{lo}$ $CD4^+$ T cells present at all time points in all tissue types, which may suggest an ongoing effector response mediated by chronic antigen exposure, due to the persistence of BCG[199, 200].

To assess the proliferative capacity of BCG-induced TB10.4 peptide-specific $CD4^+$ T cells in the spleen, a flow-cytometric EdU incorporation assay was performed at various time points post-BCG vaccination. Proliferative $CD4^+$ T cells were induced from week 3 post-BCG vaccination onwards and were still present at 52 weeks post-vaccination, the last time point investigated. The ability to proliferate suggests that these are long-term memory, rather than terminally-differentiated effector $CD4^+$ T cells. Interestingly, the phenotype of these cells differed dramatically from the cytokine-producing $CD4^+$ T cells identified through ICS. In contrast to the effector phenotype, the majority of proliferating cells at all time points except weeks 26 and 52 post-vaccination exhibited a $CD62L^{hi}CCR7^+$ central

memory phenotype[203] and were $CD27^+$, compared to the $CD27^-$ phenotype of $cytokine^+$ $CD4^+$ T cells. However, it is not possible to rule out a change in phenotype during *in vitro* culture and stimulation. To confirm these data definitively it will be necessary to conduct cell sorting based on surface phenotype prior to assessment of proliferative capacity.

These results may suggest the presence of another distinct population of antigen-specific cells, revealed by their ability to proliferate in response to cognate antigen. However, the results presented here do not determine whether these proliferative cells are present in the lung. It is important to determine this, as a limitation of the study described in this chapter is lack of demonstration of definitive memory phenotype of lung-parenchymal $CD4^+$ T cells. Memory can only truly be described when present in the absence of cognate antigen and previous work demonstrates BCG can persist for extended periods exceeding 18 months[199]. Demonstrating proliferative capacity is one way to establish memory potential whilst overcoming the challenge of persistent BCG.

In conclusion, results presented in this chapter indicate that BCG delivered systemically is capable of inducing antigen-specific $CD4^+$ T cells in the lung-parenchyma and lung-vasculature as well as the spleen and peripheral blood, which are still detectable up to 12 months post-vaccination. There is an enrichment of antigen-specific $CD4^+$ T cells in both lung compartments compared to the spleen and peripheral blood, but attempts to further characterise these subsets in terms of a distinct phenotype or functional profile were unsuccessful. This reveals high levels of heterogeneity in the $CD4^+$ memory T cell populations found in all compartments, and further reinforces the importance of using the intravascular staining technique as a definitive means of identifying $CD4^+$ T cells present in the lung-parenchyma.

Chapter 5.

Development of lung tissue-resident $CD4^+$ T cells following different routes of BCG delivery

5.1. Introduction

Mimicking the natural mucosal route of *M.tb* infection in the delivery of vaccines has been suggested as a possible means of improving their protective efficacy[272]. This approach is also being considered for other diseases with a mucosal route of transmission, such as brucellosis[273] and influenza[274]. It has already been shown by a number of studies in mice, guinea pigs and non-human primates that mucosal BCG vaccination, via the intranasal, intratracheal or aerosol route, is more protective against aerosol *M.tb* challenge than BCG delivered parenterally[217, 275-282]. Mucosal boosting of parenterally-delivered BCG with an adenovirus-vectored vaccine has also been shown to enhance protection over BCG alone[283-285].

Aerosol delivery of BCG to rhesus macaques has been demonstrated to expand $CD4^+$ T cells with a T_{CM} phenotype in the peripheral circulation[209]. This is in contrast to the preferential expansion of $CD4^+$ T_{EM} seen in the lungs, spleen and lymph nodes of mice receiving BCG subcutaneously or intradermally[225, 286]. Taken together, these results suggest that the route of antigen exposure may play an important role in determining which memory T cell subsets develop following immunisation.

It is also possible that delivery of a vaccine via a mucosal route has a direct effect on the local environment in the lung, specifically on the development of T_{RM}. A recent study by Perdomo *et al.* finds a link between mucosal delivery of BCG and generation of T_{RM} in the lung[217]. The authors describe an influx of antigen-specific $CD4^+$ and $CD8^+$ T cells into the parenchyma of the lung following intratracheal BCG. Interestingly, they describe this influx

as transient, with increased numbers of lung-parenchymal T cells present between days 22 and 45 post-vaccination in animals vaccinated mucosally, compared to those vaccinated systemically, but no difference between the two groups by day 60 post-vaccination. However, the authors define the lung-parenchymal population as all cells remaining in the lung once the BAL fluid has been removed, and previous studies[121, 122], as well as experiments in this thesis, reveal that use of intravascular staining identifies ≥50% of these T cells as being present in the vasculature of the lung rather than the parenchyma.

Lai *et al.* have shown that pulmonary administration of BCG to macaques induces higher frequencies of T cells in the lung, when compared to systemic delivery of BCG[287]. Kaushal *et al.* describe mucosal vaccination of macaques with attenuated *M.tb* resulting in significant development of iBALT, as well as recruitment of $CD4^+$ and $CD8^+$ T cells to the lung[288]. This suggests that mucosal BCG induces specific local effects on the cell populations present in the lung. However, as with the previous study, neither of these publications utilise the intravascular staining technique to differentiate between T cells in the parenchyma and vasculature of the lung. It is important to further dissect the immune response to mucosal BCG immunisation, utilising the intravascular staining technique in order to allow definitive identification of lung-parenchymal T cells and gain a greater understanding of their potentially pivotal role in protective immunity.

In the previous chapter of this thesis, experiments were conducted attempting to identify a cell-surface phenotype associated with lung-parenchymal $CD4^+$ T cells. However, it was not possible to define a unique phenotype expressed by this population, using the markers investigated. In light of this, it is important to continue to examine expression of other markers able to provide further information about this potentially important population.

PD-1, KLRG1 and CXCR3 have been previously described as markers able to define different subsets of $CD4^+$ T cells present during murine *M.tb* infection. PD-1-expressing $CD4^+$ T cells have been shown to represent a subset of less differentiated cells, exhibiting a greater proliferative and protective capacity than KLRG1-expressing cells[127, 289]. Expression of KLRG1 has been associated with terminal differentiation[289, 290] and lack of ability to migrate into the lung-parenchyma and protect against *M.tb* infection[126, 215]. Moguche *et al.*[291] have recently shown that chronic antigenic stimulation during *M.tb* infection promotes the maintenance of a large population of $CD4^+$ $KLRG1^+$ T cells which they describe as terminally-differentiated, functionally-exhausted cells. CXCR3 expression has been described as identifying a population of $CD4^+$ T cells capable of localising to the lung-parenchyma during *M.tb* infection[126].

These markers have been investigated in the context of vaccination as well as *M.tb* infection. Woodworth *et al.*[218] described a population of lung-resident $CD4^+$ T cells with reduced KLRG1 and increased CXCR3 expression, induced following subcutaneous immunisation with a candidate subunit TB vaccine. Lindenstrom *et al.*[207] identified a population of IL-2-producing $KLRG1^-$ $CD4^+$ T cells present in the draining lymph nodes following primary vaccination with BCG and booster vaccination with a subunit TB vaccine, both delivered subcutaneously. These cells were able to proliferate and produce cytokine when the animals were challenged with *M.tb* 2 years post-vaccination, leading the authors to suggest that they represent central memory T cells, capable of persisting long term in the body and replenishing T cells at the site of subsequent infection. Jeyanathan *et al.*[292] conducted experiments administering an adenovirus-vectored vaccine by mucosal and systemic routes and identified expression of CXCR3 on circulating T cells to be a critical

requirement for their subsequent entry to the lung-parenchyma and airways. Perdomo *et al.*[217] report induction of $CD4^+$ and $CD8^+$ T cells expressing CXCR3 in the airways of mice following intratracheal BCG vaccination. It is now important to investigate expression of these markers on the antigen-specific lung-parenchymal $CD4^+$ T cell population induced following BCG vaccination, and examine whether or not the route of administration of BCG has any impact on expression of these markers.

Alongside the work being done to characterise immune responses to mucosally-administered TB vaccines in animal models, there is increasing interest in administration of TB vaccines to humans via mucosal routes. A candidate modified vaccinia Ankara virus-vectored vaccine expressing antigen 85A (Ag85A), an immunodominant *M.tb* protein, has been administered to humans via aerosol and found to be safe and highly immunogenic[293]. Local immunogenicity in the lung was assessed through flow-cytometric analysis of cells harvested from the BAL fluid of participants. T cells present in the BAL fluid, airway luminal T cells, have been suggested to have an important role to play in vaccination-induced protection against *M.tb* infection[294]. In order to enable comparisons to be drawn between human studies and animal studies, which have the advantage of being able to assess protection against infection through *M.tb* challenge experiments, it is critical to assess similar measures of immunogenicity in both humans and animals. Therefore, in addition to identifying lung-parenchymal $CD4^+$ T cells using intravascular staining in the mouse model, it is also important to harvest $CD4^+$ T cells from the BAL fluid and assess whether there are any features of this population which are associated with enhanced protection against *M.tb* infection.

In summary, delivery of TB vaccines via mucosal routes appears to be a promising means of enhancing protective efficacy against *M.tb* infection in multiple animal models[217, 275-285], and administration of a candidate TB vaccine via aerosol to humans has been shown to be safe and immunogenic[293]. It is now important to investigate whether administration of BCG via different routes has any impact on the development of antigen-specific $CD4^+$ T cells in the lung-parenchyma and airways, and whether any observed differences appear to correlate with enhanced protection. As part of this, analysis of further phenotypic markers and their association with the location of $CD4^+$ T cells may provide additional information enabling better characterisation of these anatomically distinct populations.

5.2. Results

5.2.1. Protection against aerosol *M.tb* challenge in mice receiving BCG via the intradermal (ID) or intranasal (IN) route

In order to investigate protection against *M.tb* infection afforded by different routes of immunisation with BCG, groups of mice were vaccinated ID or IN with $2x10^5$ CFU BCG. A group of naïve mice formed the control group. Six weeks post-immunisation, all mice were challenged with 50-100 CFU *M.tb* Erdman via aerosol. Four weeks post-challenge lungs and spleens were harvested and plated to determine bacterial burden.

Aerosol BCG delivered by the human OMRON nebuliser device was also considered as a route of mucosal immunisation. However, this was found during optimisation experiments to be an inefficient route of delivery to the mice. In order to determine the number of CFU delivered to the lungs following nebulisation with BCG, 3 mice received a dose of $5x10^6$ CFU BCG and 1 hour later their lungs were harvested and plated to determine bacterial burden. An average of 125 CFU BCG were grown from the lungs of each mouse (data not shown). This was likely due to the difficulty in forming a suitable connection between the nebuliser and mouse restrainer, allowing for loss of aerosol during delivery. As it would not have been possible to deliver a high enough dose of BCG via aerosol to result in $2x10^5$ CFU BCG reaching the lungs, this route was not pursued.

5.2.1.1. IN BCG vaccination confers enhanced protection against M.tb infection in the lung

Mice vaccinated with BCG IN or ID had significantly lower bacterial burdens than control naïve mice in both their lungs and spleen (Figure 5.1). The lungs of control mice had a bacterial burden of 6.7 $\log_{10}$ CFU *M.tb* compared to 4.5 $\log_{10}$ CFU in IN BCG-immunised mice and 5.2 $\log_{10}$ CFU in ID-immunised mice ($p \leq 0.0001$). The spleens of control mice had a bacterial burden of 5.0 $\log_{10}$ CFU *M.tb* compared to 3.4 $\log_{10}$ CFU in IN BCG-immunised mice and 3.3 $\log_{10}$ CFU in ID-immunised mice ($p \leq 0.0001$). Mice vaccinated IN had significantly lower bacterial burdens in their lungs compared with mice receiving ID BCG, a 0.7 $\log_{10}$ reduction ($p \leq 0.01$). There was no significant difference in bacterial load in the spleens of mice receiving BCG by either route.

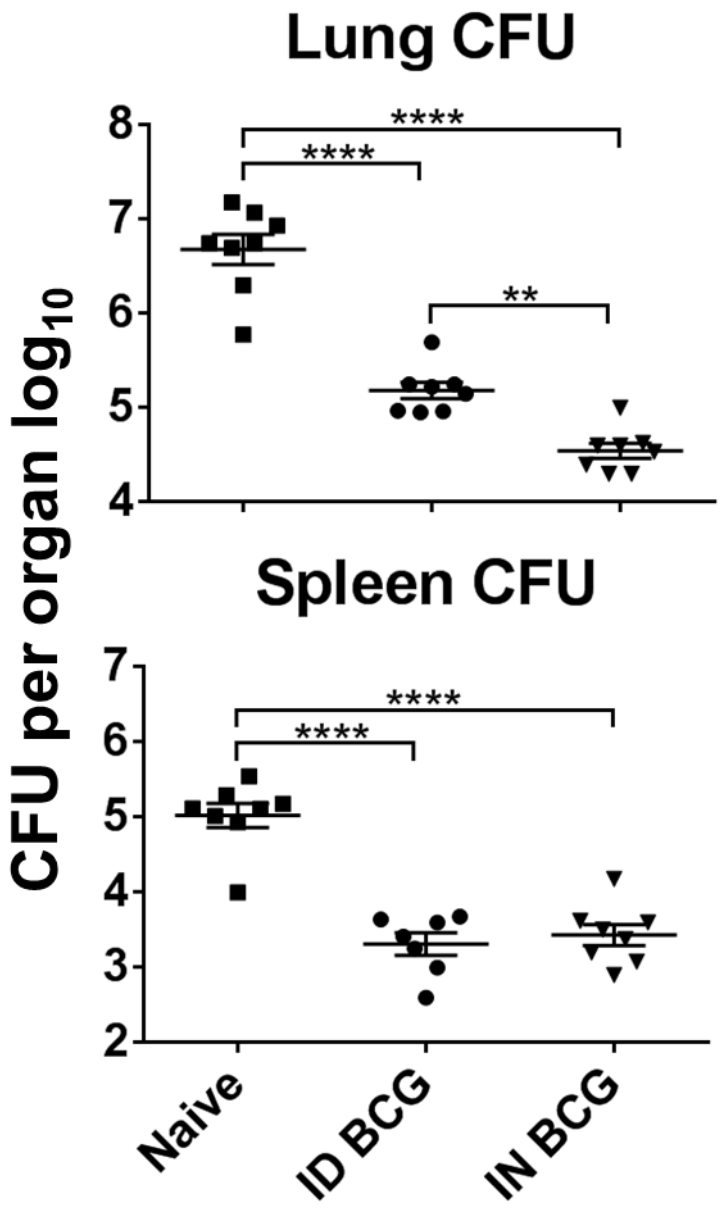

Figure 5.1 - Protection against aerosol *M.tb* challenge following different routes of immunisation with BCG. BALB/c mice were immunised IN or ID with BCG and challenged 6 weeks later with *M.tb* via aerosol. Four weeks post-challenge, lungs and spleen were removed for CFU enumeration. Individual $\log_{10}$ CFU counts are shown, with bars indicating mean and error bars showing SEM (n≥7). One-way ANOVA with Tukey's post-test for significance; **** $p \leq 0.0001$; ** $p \leq 0.01$. Data representative of two independent experiments with similar results.

5.2.2. Immunological differences following different routes of BCG vaccination

In order to investigate immunological differences resulting from BCG being delivered by different routes, groups of mice were vaccinated ID or IN with $2x10^5$ CFU BCG. A group of naïve mice formed the control group. Six weeks post-immunisation, lungs, spleen and BAL fluid were harvested following intravascular staining. Isolated cells were stimulated with PPD-T and analysed by flow cytometry (Appendix – Flow cytometry panels 1 and 3). ICS was used to identify PPD-T-specific $CD4^+$ T cells producing IFN-γ, IL-2, TNF-α or any combination of these (cytokine$^+$ $CD4^+$ T cells) (Appendix – Flow cytometry gating strategy).

5.2.2.1. IN BCG vaccination results in recruitment of $CD4^+$ T cells to the lung-parenchyma

Following IN BCG vaccination, lung-parenchymal $CD4^+$ T cells comprised a significantly greater proportion of the total $CD4^+$ T cell population isolated from the lung, when compared to naïve and ID BCG-vaccinated mice (Figure 5.2a&b). Analysis of the total numbers of $CD4^+$ T cells found in the lung-parenchyma and lung-vasculature revealed significantly greater numbers of cells in the parenchyma following IN BCG compared to ID BCG, with no difference in numbers present in the lung-vasculature between groups (Figure 5.2c). This suggests that $CD4^+$ T cells are being recruited to the parenchyma from the periphery following IN BCG vaccination.

(a)

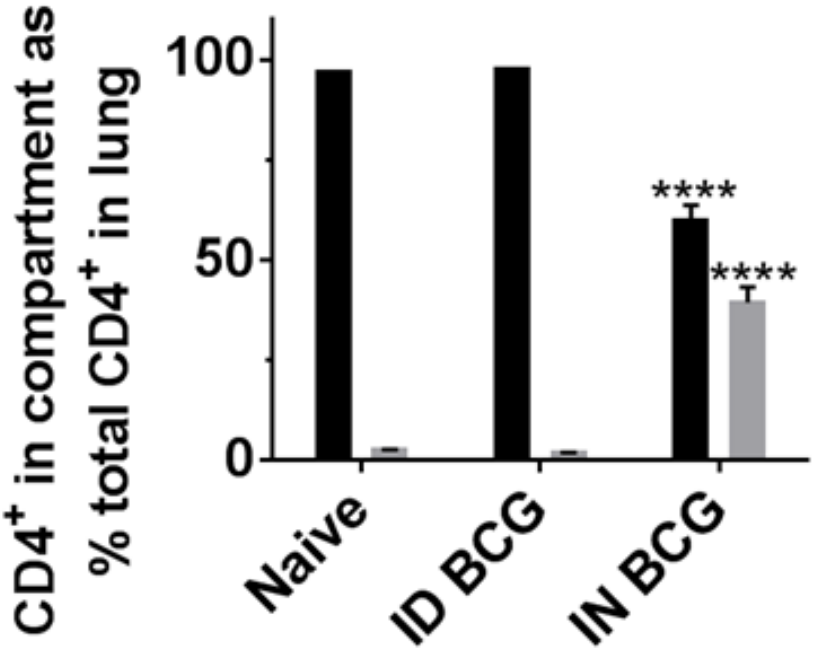
CD4+ in compartment as
% total CD4+ in lung
100
50
0
****
****
Naive
ID BCG
IN BCG

(b)

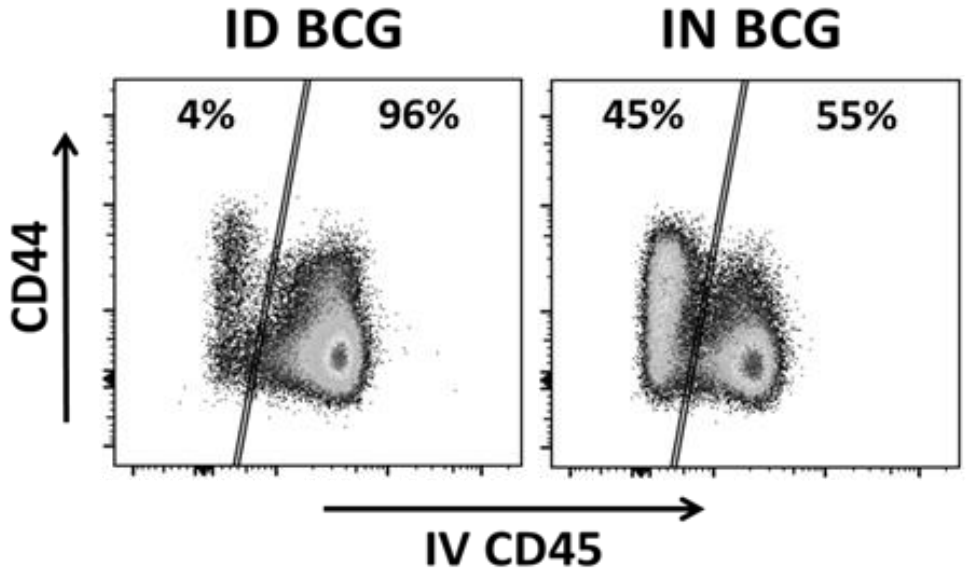
ID BCG
IN BCG
4%
96%
45%
55%
CD44
IV CD45

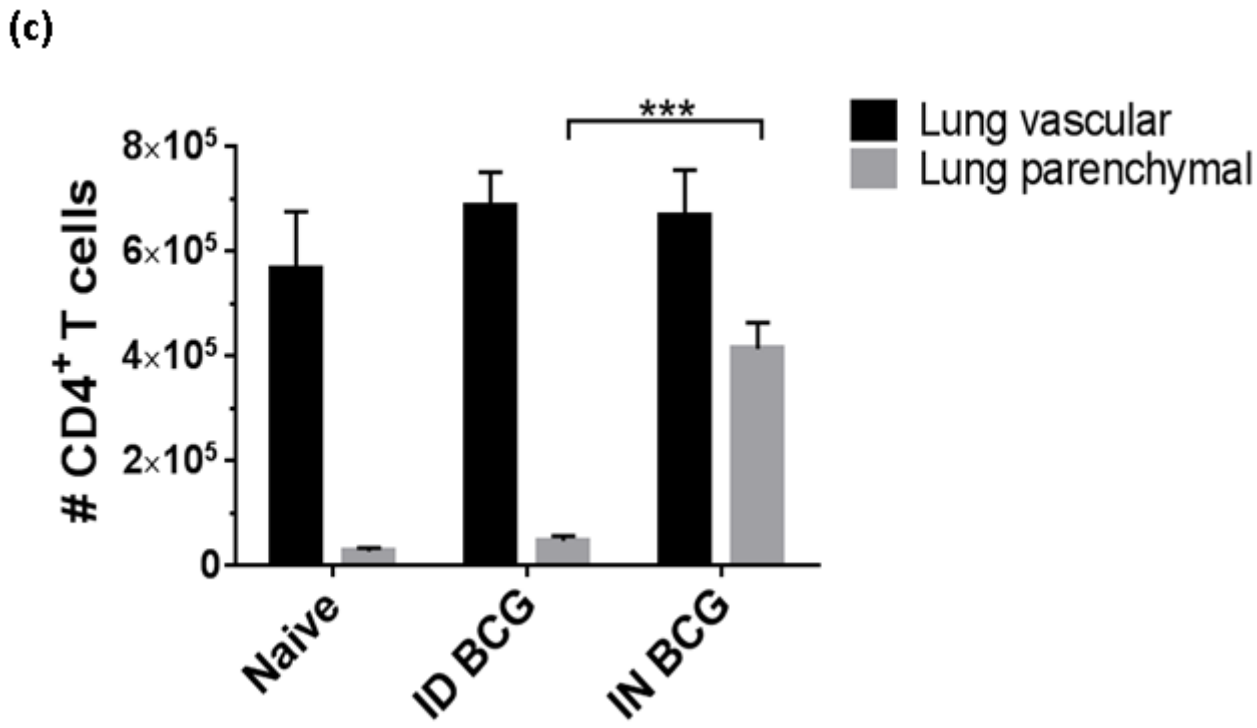

Figure 5.2 - Analysis of $CD4^+$ T cells in lung-vascular and lung-parenchymal compartments following mucosal or systemic BCG. BALB/c mice were immunised IN or ID with BCG and 6 weeks later intravascular staining was used to identify populations of lung parenchymal and lung vascular $CD4^+$ T cells. (a) Frequency of lung-parenchymal and lung-vascular $CD4^+$ T cells as a % of total $CD4^+$ T cells isolated from the lung. Statistical comparison is between frequency of $CD4^+$ T cells in both lung compartments compared with the same compartment across all groups. (b) Representative flow cytometry plots showing the proportions of lung-parenchymal and lung-vascular $CD4^+$ T cells in the lungs of ID or IN BCG-immunised mice. (c) Number of $CD4^+$ T cells in the lung-parenchymal and lung-vascular compartments of animals immunised with BCG IN or ID. Statistical comparison is between number of $CD4^+$ T cells in each compartment following ID BCG compared with the same compartment following IN BCG. For all graphs, bars represent mean values (n=6) and error bars show SEM. *** $\rho \leq 0.001$, **** $\rho \leq 0.0001$, two-way ANOVA with Sidak's post-test. Data representative of two independent experiments with similar results.

5.2.2.2. Accumulation of lymphocytes in the lungs following IN BCG vaccination

Examination of HE-stained histopathological tissue sections under light microscopy allowed evaluation of histological changes in the lung following IN BCG vaccination. In the lungs of vaccinated animals (Figure 5.3c&d), there were discrete clusters of lymphocytes present surrounding some blood vessels, including those in association with the airways. These clusters of lymphocytes were absent in the lungs of naïve animals (Figure 5.3a&b).

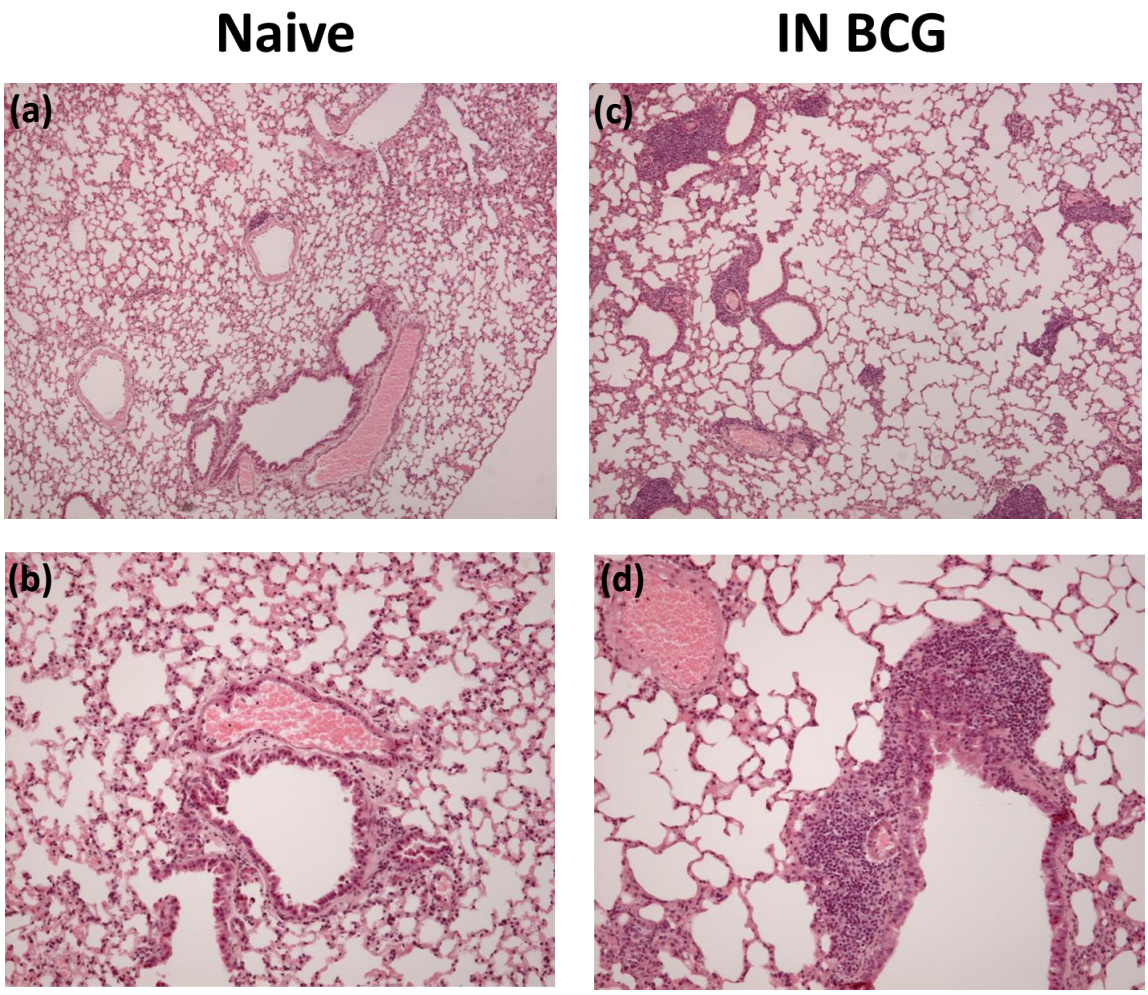

Figure 5.3 - Histopathological examination of the lungs of naïve and IN BCG-immunised mice. (a) and (b) Lung from naïve mouse. (c) and (d) Lung from IN BCG-immunised mouse 6 weeks post-immunisation. All images are H&E stained. (a) and (b) are x100 magnification, (c) and (d) are x400 magnification.

5.2.2.3. IN BCG vaccination induces cytokine$^+$ CD4$^+$ T cells in the BAL and results in increased frequency of cytokine$^+$ CD4$^+$ T cells in the lung-parenchyma

Both IN and ID BCG vaccination induced significant populations of cytokine$^+$ CD4$^+$ T cells in the lung-parenchyma, lung-vasculature and spleen compared to naïve mice (Figure 5.4). IN but not ID vaccination induced significant populations of cytokine$^+$ CD4$^+$ T cells in the BAL, compared to naïve mice. IN vaccination resulted in a significant increase in the frequency of cytokine$^+$ CD4$^+$ T cells in the lung-parenchyma, compared to ID vaccination. There was no difference in frequency of cytokine$^+$ CD4$^+$ T cells in the lung-vasculature between ID and IN-vaccinated groups.

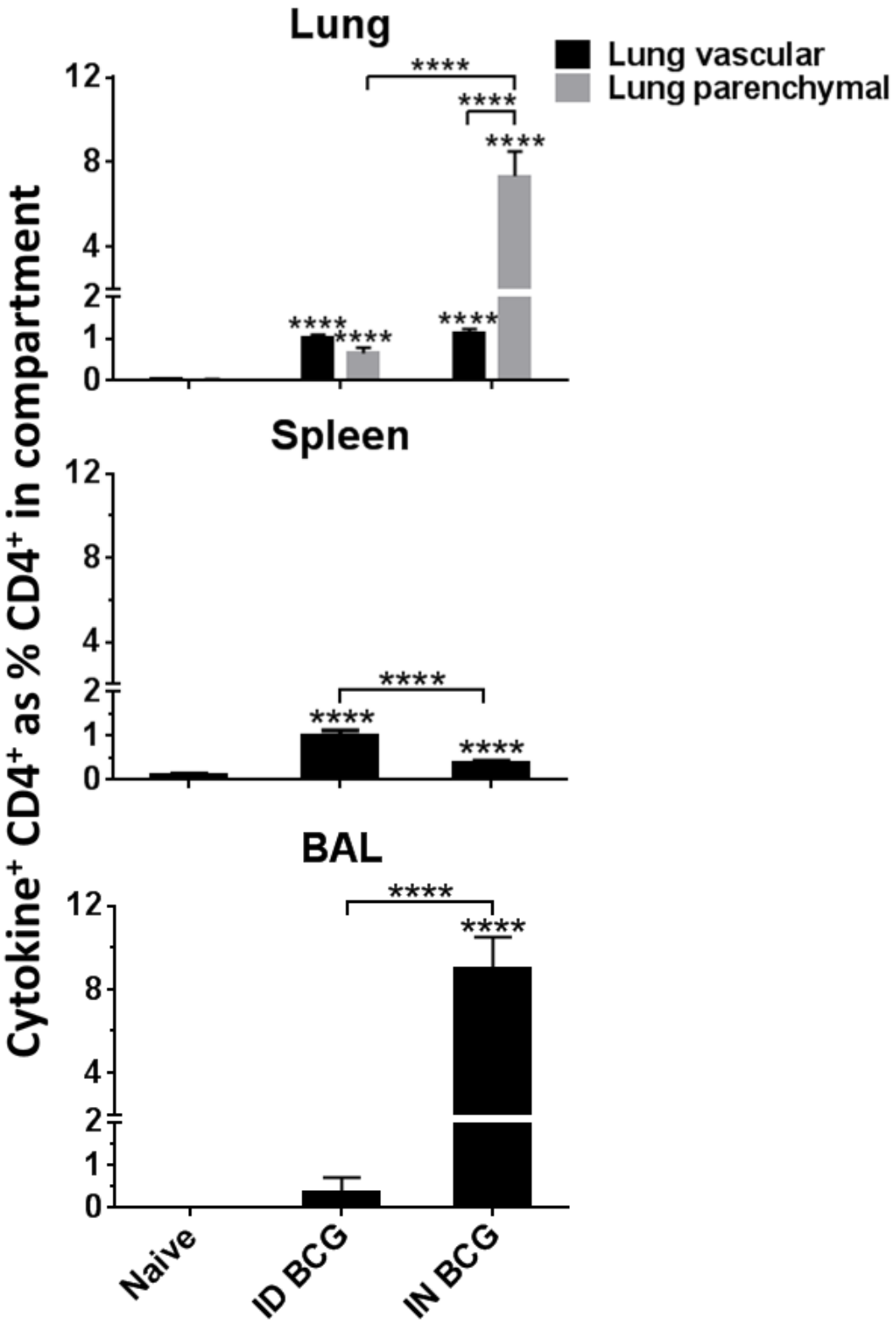

Figure 5.4 - Analysis of cytokine$^+$ CD4$^+$ T cells in different tissue compartments following ID or IN BCG. BALB/c mice were immunised IN or ID with BCG and 6 weeks later

intravascular staining followed by ICS was used to identify populations of lung-parenchymal and lung-vascular PPD-T-specific $CD4^+$ T cells producing IFN-γ, TNF-α or IL-2 alone or in combination ($cytokine^+$). Spleen and BAL were also harvested for ICS. Graphs show frequencies of $cytokine^+$ $CD4^+$ T cells in all compartments as a % of the total number of $CD4^+$ T cells in the same compartment. Statistical comparison is between naïve and BCG (stars) and between IN and ID BCG (stars with brackets). Bars represent mean values (n=6) and error bars show SEM. **** $\rho \leq 0.0001$, two-way ANOVA with Sidak's post-test for lung and one-way ANOVA with Tukey's post-test for Spleen and BAL. Data representative of two independent experiments with similar results.

5.2.2.4. Cell-surface immunophenotyping of antigen-specific CD4$^+$ T cells induced following IN or ID BCG vaccination

iii. Cytokine$^+$ CD4$^+$ T cells expressing a PD-1$^+$ KLRG1$^-$ phenotype were exclusively present within the lung parenchyma and BAL following IN BCG vaccination

Significant populations of cytokine$^+$ CD4$^+$ T cells expressing a PD-1$^+$ KLRG1$^-$ phenotype were present within the lung parenchyma and BAL following IN BCG vaccination compared to naïve, and were not induced following ID BCG vaccination (Figure 5.5b). Significant populations of cytokine$^+$ CD4$^+$ T cells expressing the opposing PD-1$^-$ KLRG1$^+$ phenotype were present in the lung-vascular compartment, lung-parenchymal compartment and BAL following IN BCG and in the lung-vascular compartment and spleen following ID BCG, both compared to naive. Representative flow cytometry plots show PD-1 and KLRG1 staining in the lung-parenchyma and lung-vasculature of IN-immunised animals, pre-gated on cytokine$^+$ CD4$^+$ T cells (Figure 5.5a).

iv. Cytokine$^+$ CD4$^+$ T cells expressing CXCR3 were exclusively present within the lung parenchyma following IN BCG vaccination

A significant population of cytokine$^+$ CXCR3$^+$ CD4$^+$ T cells was present in the lung-parenchyma following IN BCG, compared to naive (Figure 5.5c). Association of CXCR3 expression with PD-1 and KLRG1 expression was investigated. CXCR3 was expressed on lung-parenchymal cytokine$^+$ CD4$^+$ T cells with both a PD-1$^+$ KLRG1$^-$ and PD1$^-$ KLRG1$^+$ phenotype (Figure 5.5d). There was a significantly greater frequency of CXCR3$^+$ cells within the PD1$^+$ KLRG1$^-$ population.

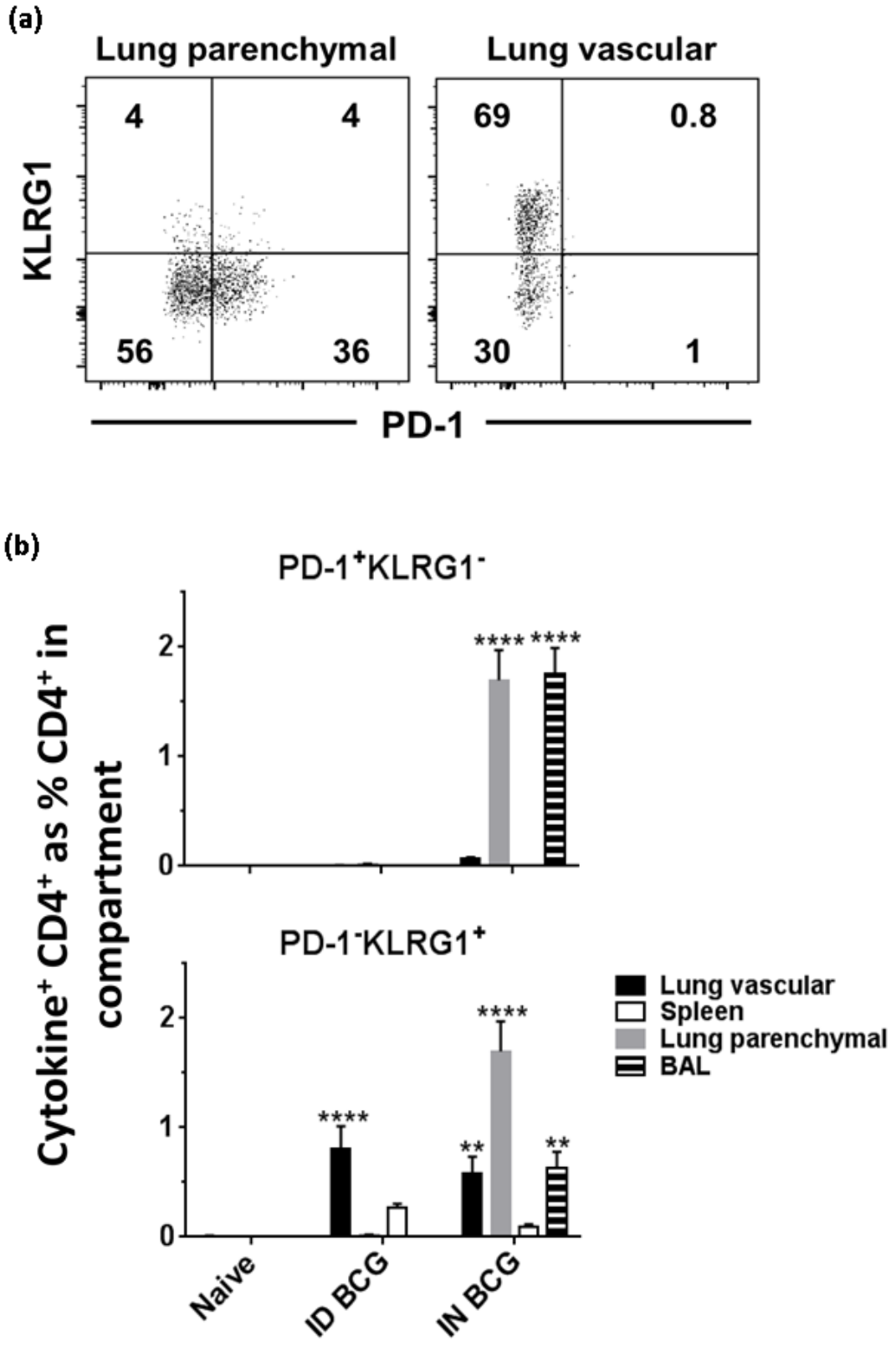
(a)
Lung parenchymal
Lung vascular
4
4
69
0.8
56
36
30
1
KLRG1
PD-1
(b)
PD-1+KLRG1-
PD-1-KLRG1+
Cytokine+ CD4+ as % CD4+ in compartment
****
****
****
**
**
Lung vascular
Spleen
Lung parenchymal
BAL
Naive
ID BCG
IN BCG

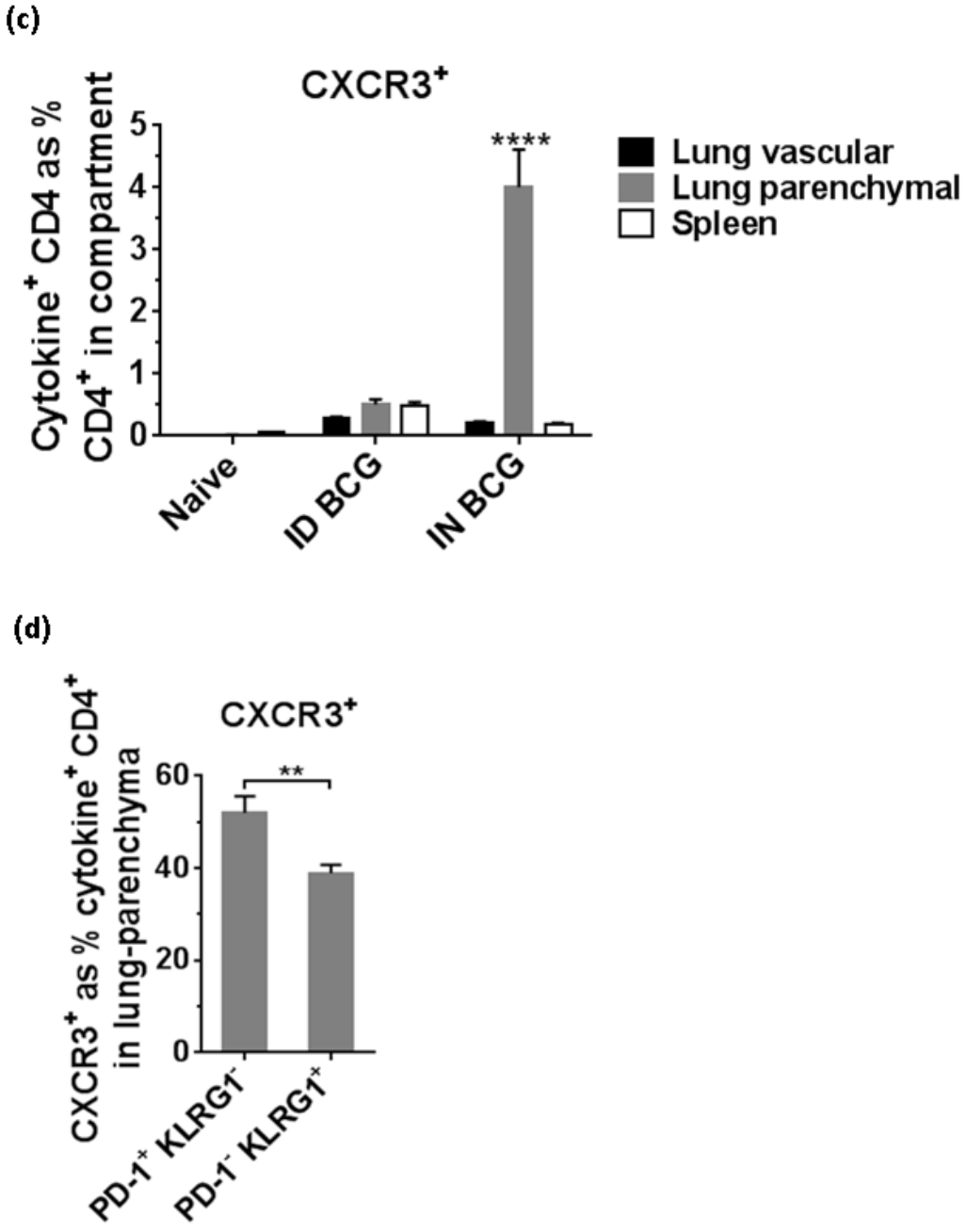

Figure 5.5 - Phenotype analysis of cytokine$^+$ CD4$^+$ T cells in different tissue compartments following ID or IN BCG. BALB/c mice were immunised IN or ID with BCG and 6 weeks later intravascular staining followed by ICS was used to identify populations of lung-parenchymal and lung-vascular PPD-T-specific CD4$^+$ T cells producing IFN-γ, TNF-α or IL-2 alone or in combination (cytokine$^+$). Spleen and BAL were also harvested for ICS. (a) Representative plots from an IN-immunised animal showing cytokine$^+$ CD4$^+$ T cells in the lung parenchymal and lung vascular compartments surface stained for PD-1 and KLRG1, pre-gated on

cytokine^{+} CD4^{+} T cells. (b) Frequency of cytokine^{+} CD4^{+} T cells expressing a PD-1^{+} KLRG1^{-} or PD-1^{-} KLRG1^{+} phenotype in mice receiving IN or ID BCG. Statistical comparison is between naïve and BCG-immunised groups for the same compartment. (c) Frequency of cytokine^{+} CD4^{+} T cells in the lungs and spleen expressing CXCR3 in mice receiving IN or ID BCG. Statistical comparison is between naïve and BCG-immunised groups for the same compartment. (d) Proportion of lung-parenchymal cytokine^{+} CD4^{+} T cells expressing CXCR3 as well as PD1 or KLRG1 in mice receiving IN BCG. For (b), (c) & (d) bars represent mean values (*n*=6) and error bars show SEM. Two-way ANOVA with Tukey's post-test (b) or Sidak's post-test (c); **** $p \leq 0.0001$, ***$p \leq 0.001$, ** $p \leq 0.01$. Unpaired t-test (d); ** $p \leq 0.01$. Data representative of two independent experiments with similar results.

5.2.2.5. BCG-induced cytokine$^+$ CD4$^+$ T cells display a dominance of multifunctional cells

Significant populations of IFNγ$^+$IL-2$^+$TNF-α$^+$ and IFNγ$^+$IL-2$^-$TNF-α$^+$ CD4$^+$ T cells are present in all compartments following IN BCG vaccination compared to naïve, and in the lung-vascular compartment, lung-parenchymal compartment and spleen following ID BCG vaccination compared to naïve (Figure 5.6). IFNγ$^-$IL-2$^+$TNF-α$^+$ and IFNγ$^+$IL-2$^-$TNF-α$^-$ CD4$^+$ T cells are present following IN BCG in the lung-parenchymal compartment, lung-vascular compartment and BAL compared to naïve. IFNγ$^-$IL-2$^+$TNF-α$^-$ CD4$^+$ T cells are present in the lung-parenchyma and BAL following IN BCG vaccination compared to naïve. IFNγ$^-$IL-2$^-$TNF-α$^+$ CD4$^+$ T cells are present in the lung-vascular and lung-parenchymal compartments following IN or ID BCG and in the BAL following IN BCG compared to naïve.

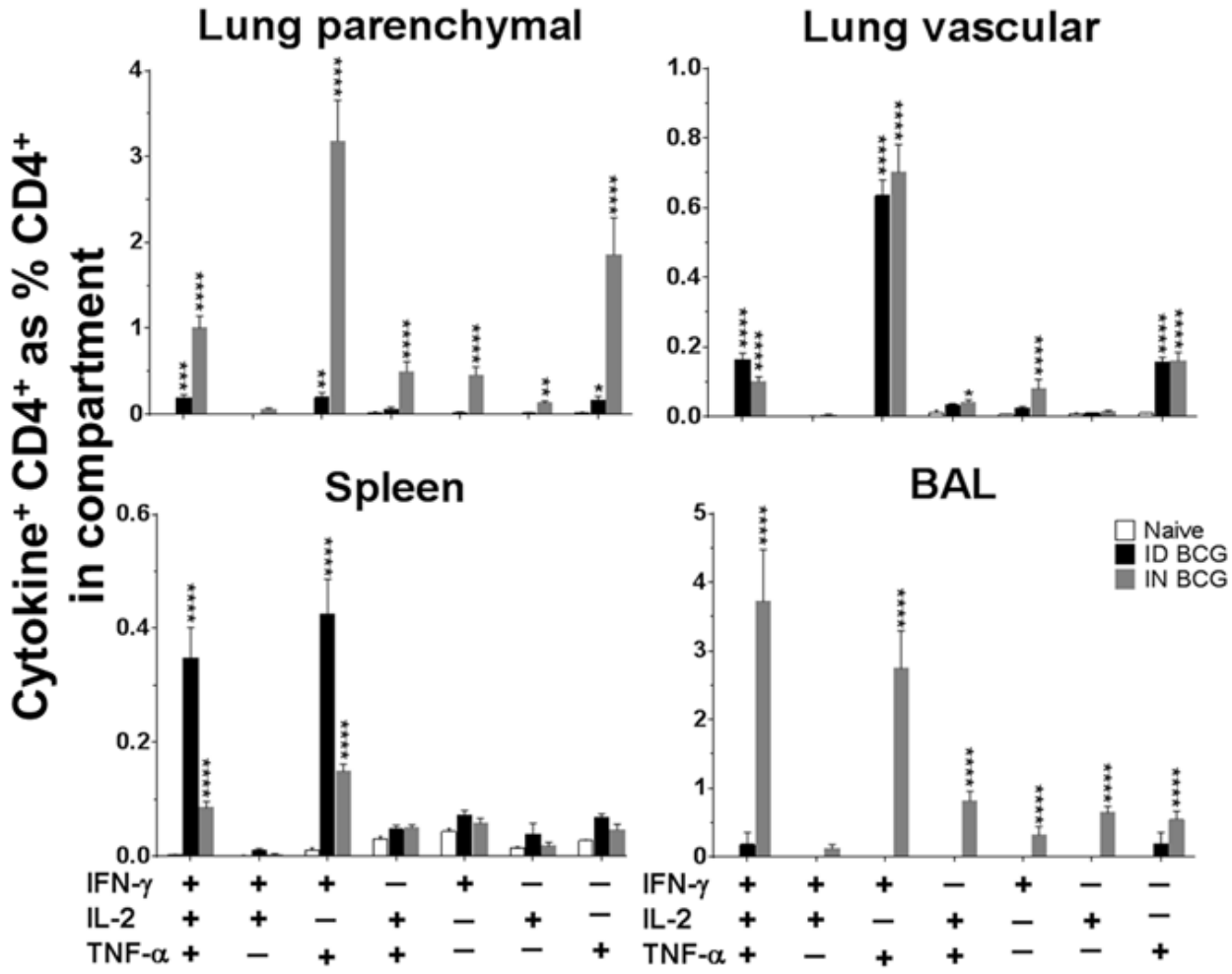

Figure 5.6 - Frequency of cytokine$^+$ CD4$^+$ T cells in the lungs, spleen and BAL producing each cytokine combination. BALB/c mice were vaccinated IN or ID with BCG. Six weeks post-vaccination lungs, spleen and BAL were harvested and lymphocytes stimulated with PPD-T before ICS to identify PPD-T-specific cells. Boolean gating analysis allowed identification of CD4$^+$ T cells producing IFN-γ, TNF-α or IL-2 alone or in combination. Bars represent mean values (n=6) and error bars show SEM. Statistical comparison is between naïve and BCG-immunised groups. * $\rho \leq 0.05$, ** $\rho \leq 0.01$, *** $\rho \leq 0.001$ **** $\rho \leq 0.0001$, two-way ANOVA with Sidak's post-test. Data representative of two independent experiments with similar results.

5.2.3. Protection against aerosol *M.tb* challenge in mice 26 weeks after IN or ID BCG vaccination

In order to investigate whether BCG delivered IN or ID resulted in durable protective responses, groups of mice were vaccinated ID or IN with $2x10^5$ CFU BCG and 26 weeks post-vaccination all mice were challenged with 50-100 CFU *M.tb* Erdman via aerosol. Four weeks post-challenge lungs and spleens were harvested and plated to determine bacterial burden. A group of age-matched naïve mice formed the control group.

5.2.3.1. IN and ID BCG vaccination confer protection against M.tb infection in the lung and spleen 26 weeks post-immunisation

Mice vaccinated with BCG IN or ID had significantly lower bacterial burdens than control naïve mice in both their lungs and spleen (Figure 5.7). The lungs of control mice had a bacterial burden of 6.2 $\log_{10}$ CFU *M.tb* compared to 5.1 $\log_{10}$ CFU in IN BCG-immunised mice and 5.4 $\log_{10}$ CFU in ID-immunised mice ($p \leq 0.0001$). The spleens of control mice had a bacterial burden of 5.4 $\log_{10}$ CFU *M.tb* compared to 3.1 $\log_{10}$ CFU in IN BCG-immunised mice and 3.7 $\log_{10}$ CFU in ID-immunised mice ($p \leq 0.0001$).

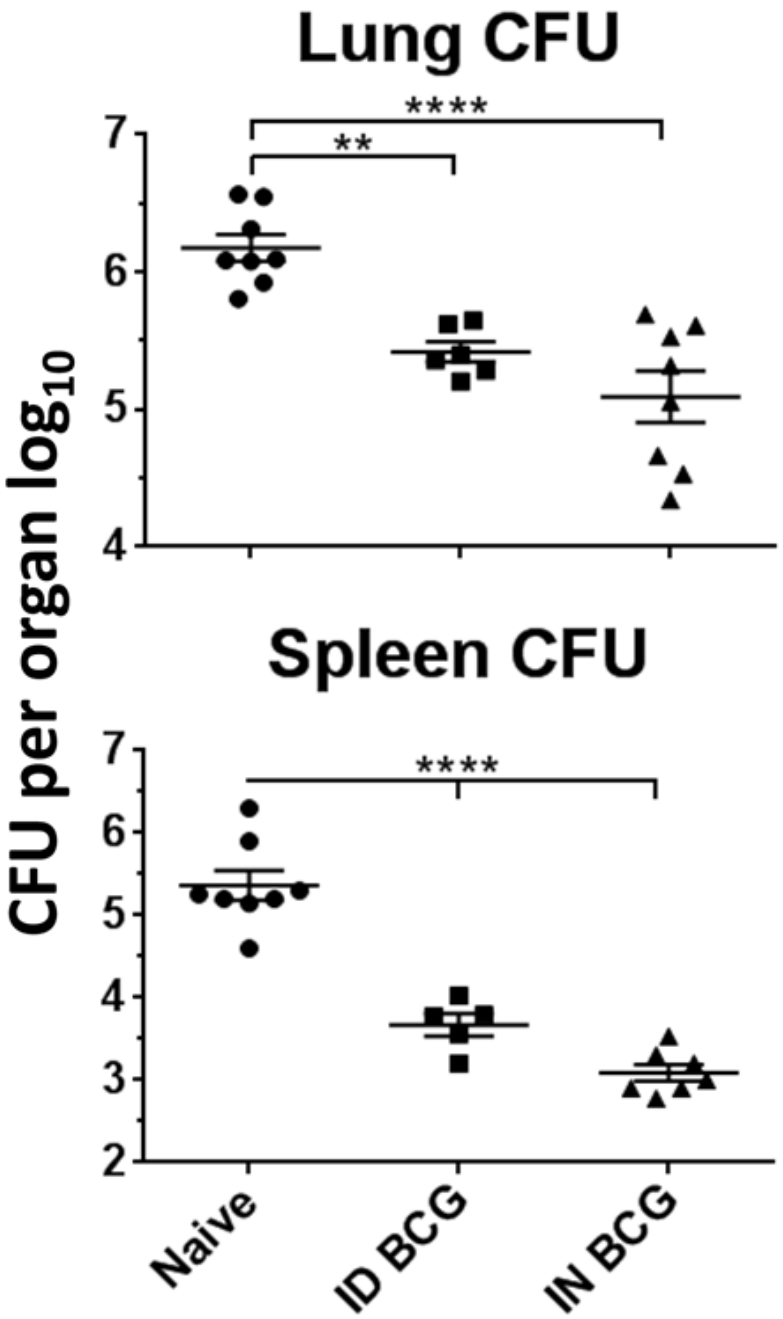

Figure 5.7 - Protection against *M.tb* challenge 26 weeks post-BCG immunisation. BALB/c mice were immunised IN or ID with BCG and challenged 26 weeks later with *M.tb* via aerosol. Four weeks post-challenge, lungs and spleen were harvested for CFU enumeration. Individual $\log_{10}$ CFU counts are shown with bars indicating mean and error bars showing SEM (n ≥7). One-way ANOVA with Tukey's post-test for significance; **** $p \leq 0.0001$; ** $p \leq 0.01$.

5.2.4. Immunological differences at different time points following IN or ID BCG vaccination

In order to investigate immunological changes over time following different routes of BCG vaccination, groups of mice were vaccinated IN or ID with $2x10^5$ CFU BCG. A group of naïve mice formed the control group. At 3, 6 and 26 weeks post-vaccination, lungs, spleen and BAL were harvested, following intravascular staining. Isolated cells were stimulated with PPD-T and analysed by flow cytometry (Appendix – Flow cytometry panels 1 and 3). ICS was used to identify PPD-T-specific $CD4^+$ T cells producing IFN-γ, IL-2, TNF-α or any combination of these ($cytokine^+$).

5.2.4.1. Frequency of lung-parenchymal $CD4^+$ T cells remains stable following IN BCG vaccination

Following IN BCG vaccination, lung-parenchymal $CD4^+$ T cells comprised a significantly greater proportion of the total $CD4^+$ T cell population isolated from the lung at weeks 3, 6 and 26 post-vaccination, when compared to naïve and ID-vaccinated groups (Figure 5.8a). Proportions of lung-parenchymal and lung-vascular $CD4^+$ T cells remain stable over time following IN BCG vaccination, with no significant differences when comparing animals at 3, 6 and 26 weeks post-vaccination (Figure 5.8b).

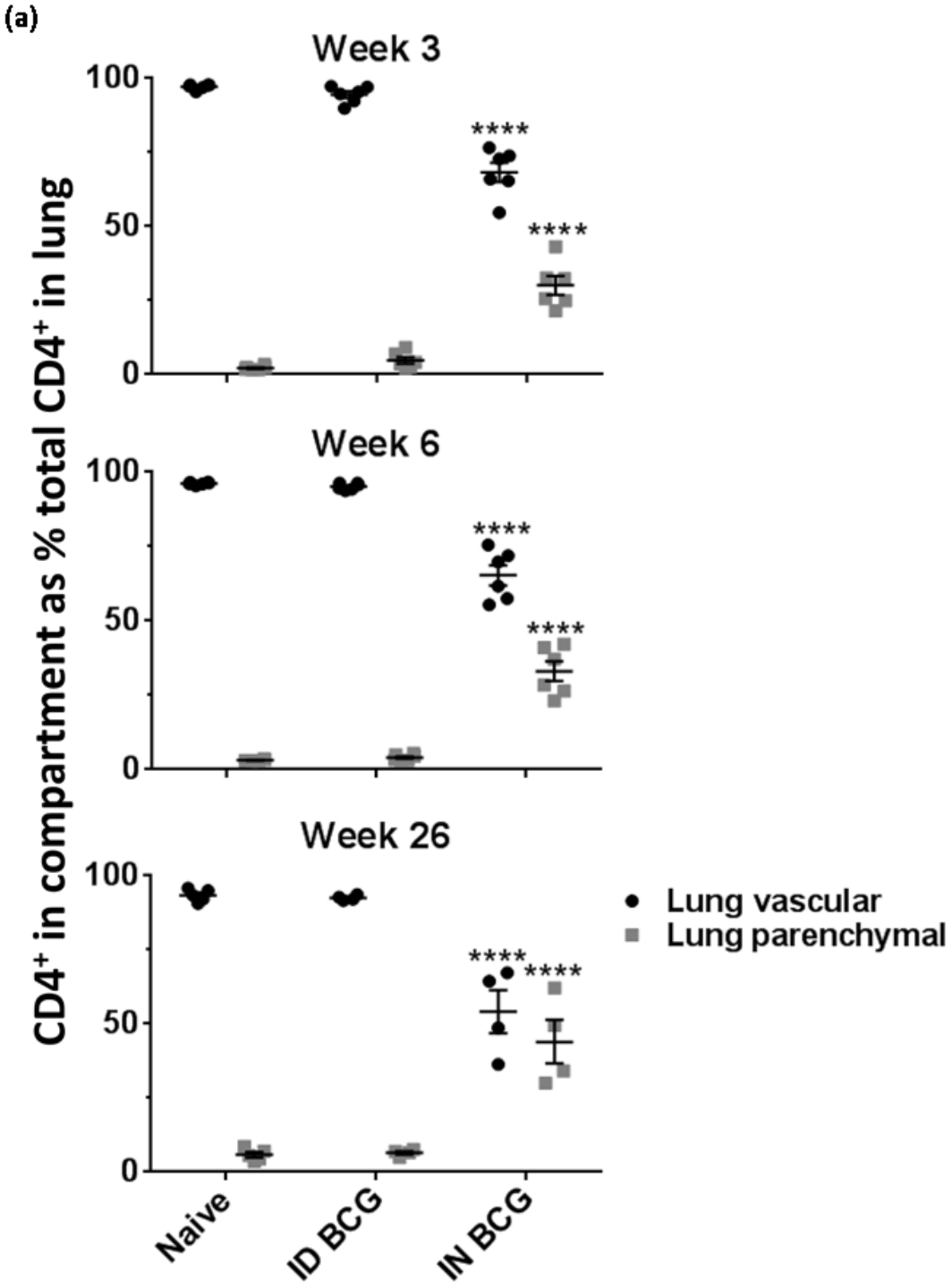
(a)
Week 3
Week 6
Week 26
CD4+ in compartment as % total CD4+ in lung
100
50
0
****
Naive
ID BCG
IN BCG
Lung vascular
Lung parenchymal

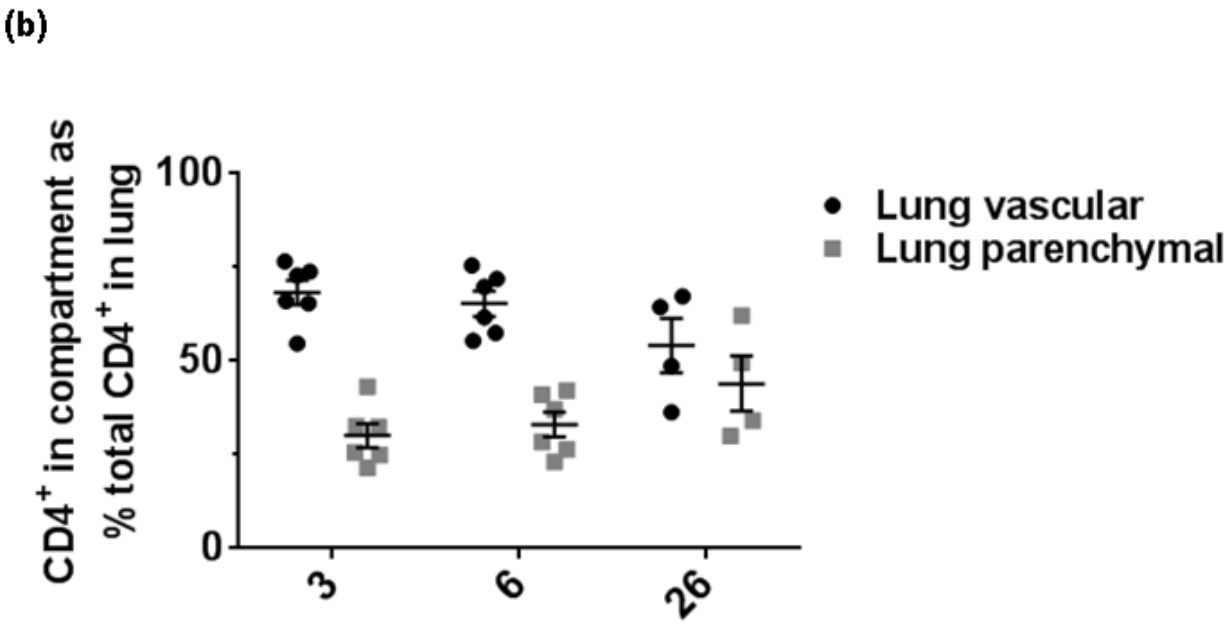

Figure 5.8 - Analysis of total $CD4^+$ T cells in lung-vascular and lung-parenchymal compartments at different time points following IN or ID BCG. BALB/c mice were immunised IN or ID with BCG. Three, 6 and 26 weeks later, intravascular staining was used to identify populations of lung-parenchymal and lung-vascular $CD4^+$ T cells. (a) Frequency of lung-parenchymal and lung-vascular $CD4^+$ T cells as a % of total $CD4^+$ T cells isolated from the lung at each time point. Statistical comparison is between frequency of $CD4^+$ T cells in each lung compartment with the same compartment across all groups. (b) Frequency of lung-parenchymal and lung-vascular $CD4^+$ T cells as a % of total $CD4^+$ T cells isolated from the lungs of IN-immunised mice at each time point. For all graphs, each dot represents an individual animal, bars represent mean values (n=6) and error bars show SEM. **** $\rho \leq 0.0001$, two-way ANOVA with Sidak's post-test.

5.2.4.2. IN BCG vaccination induces a greater frequency of cytokine$^+$ CD4$^+$ T cells in the lung-parenchyma and BAL at all time points

IN BCG induced a significantly greater frequency of cytokine$^+$ CD4$^+$ T cells in the lung-parenchyma and BAL than ID BCG at 3, 6 and 26 weeks post-vaccination (Figure 5.9a). When comparing IN-immunised mice at all time points, the frequency of cytokine$^+$ CD4$^+$ T cells was significantly greater in the lung-parenchyma at week 6 than week 26 (Figure 5.9b). The frequency of cytokine$^+$ CD4$^+$ T cells in the BAL was higher at week 26 than at either week 3 or week 6.

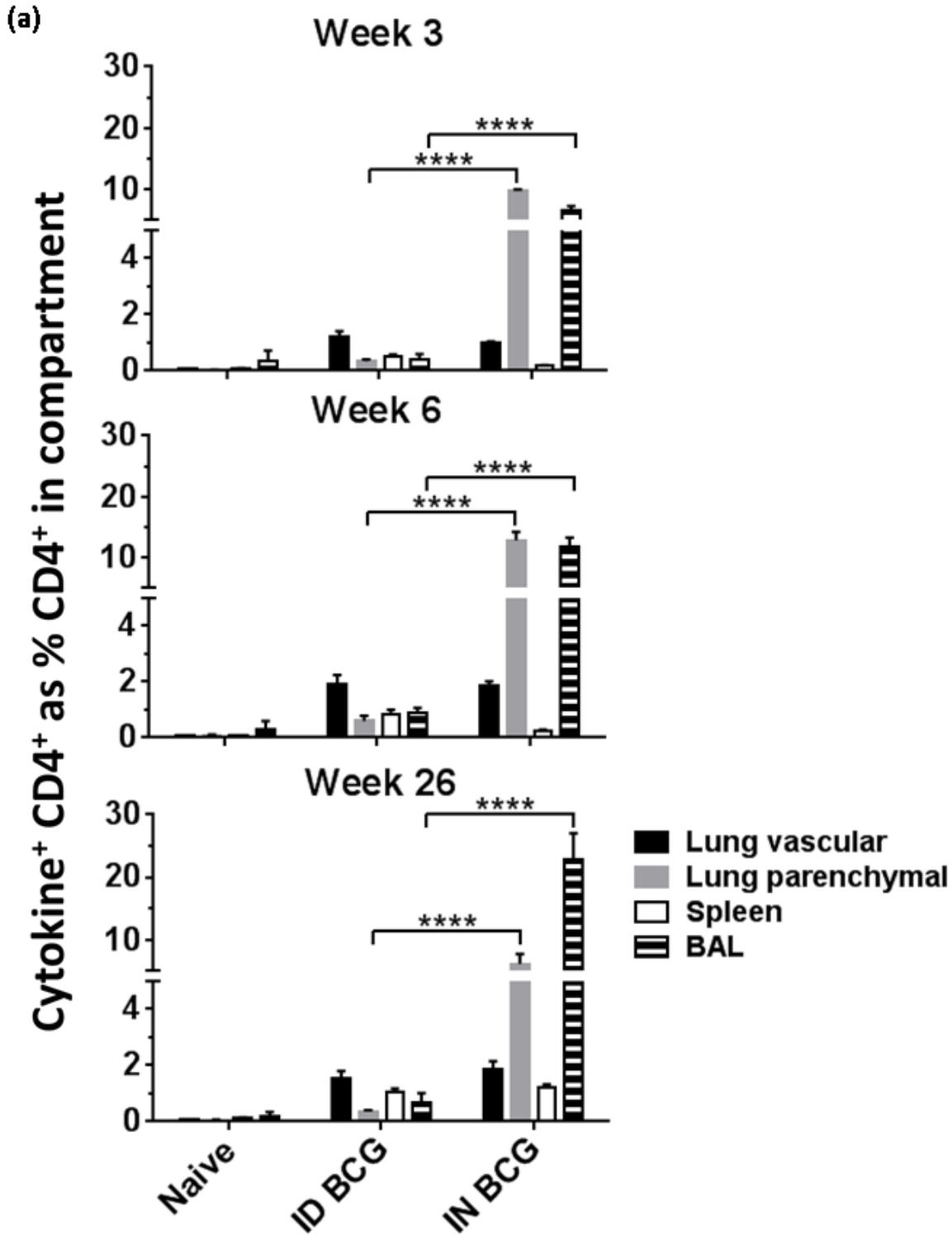
(a)
Week 3
Week 6
Week 26
Cytokine+ CD4+ as % CD4+ in compartment
30
20
10
4
2
0
****
****
Lung vascular
Lung parenchymal
Spleen
BAL
Naive
ID BCG
IN BCG

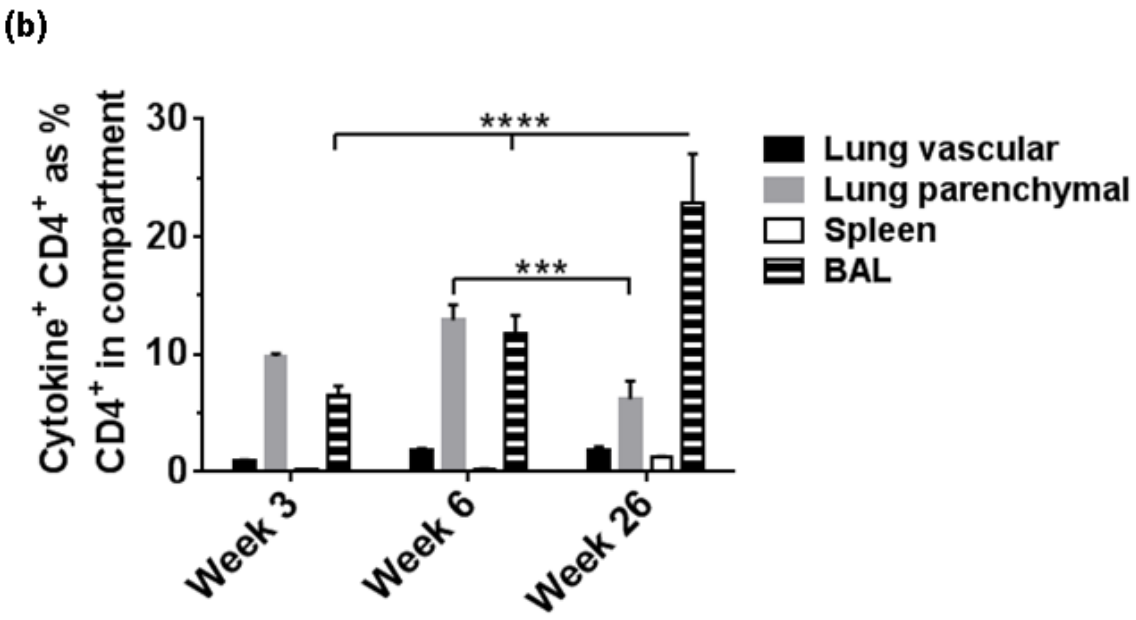

Figure 5.9 - Analysis of cytokine$^+$ CD4$^+$ T cells at different time points following ID or IN BCG. BALB/c mice were immunised IN or ID with BCG. Three, 6 and 26 weeks later, intravascular staining followed by ICS was used to identify populations of lung parenchymal and lung vascular PPD-T-specific CD4$^+$ T cells producing IFN-γ, TNF-α or IL-2 alone or in combination (cytokine$^+$). Spleen and BAL were also harvested for ICS. (a) Frequency of cytokine$^+$ CD4$^+$ T cells as a % of total CD4$^+$ T cells isolated from the same compartment. Statistical comparison is shown between IN and ID BCG for the same compartment. (b) Frequency of cytokine$^+$ CD4$^+$ T cells as a % of total CD4$^+$ T cells isolated from the same compartment of IN-immunised mice at each time point. Statistical comparison is shown between the same compartment at different time points. For all graphs, bars represent mean values (n=6) and error bars show SEM. **** $\rho \leq 0.0001$, two-way ANOVA with Sidak's post-test.

5.2.4.3. PD-1 KLRG1 cell-surface phenotype at different time points following IN or ID BCG

IN BCG induced a significant population of cytokine^{+} PD-1^{+} KLRG1^{-} CD4^{+} T cells in the lung-parenchyma at 3, 6 and 26 weeks post-vaccination, compared to naïve animals (Figure 5.10a). Significant populations of cytokine^{+} PD-1^{-} KLRG1^{+} CD4^{+} T cells were present in the lung-vascular compartment following ID BCG and both lung compartments following IN BCG at 3, 6 and 26 weeks post-vaccination, as well as in the spleen at 3 weeks and 26 weeks post-ID BCG vaccination, compared to naïve animals. In IN-immunised animals, the frequency of cytokine^{+} PD1^{+} KLRG1^{-} CD4^{+} T cells was highest in the lung-parenchymal compartment of IN-immunised mice at 3 weeks post-immunisation, compared to both 6 and 26 weeks post-immunisation (Figure 5.10b). At 26 weeks post-IN BCG, the frequency of cytokine^{+} PD1^{+} KLRG1^{-} CD4^{+} T cells in the lung-parenchyma was lower than at 3 or 6 weeks post-vaccination.

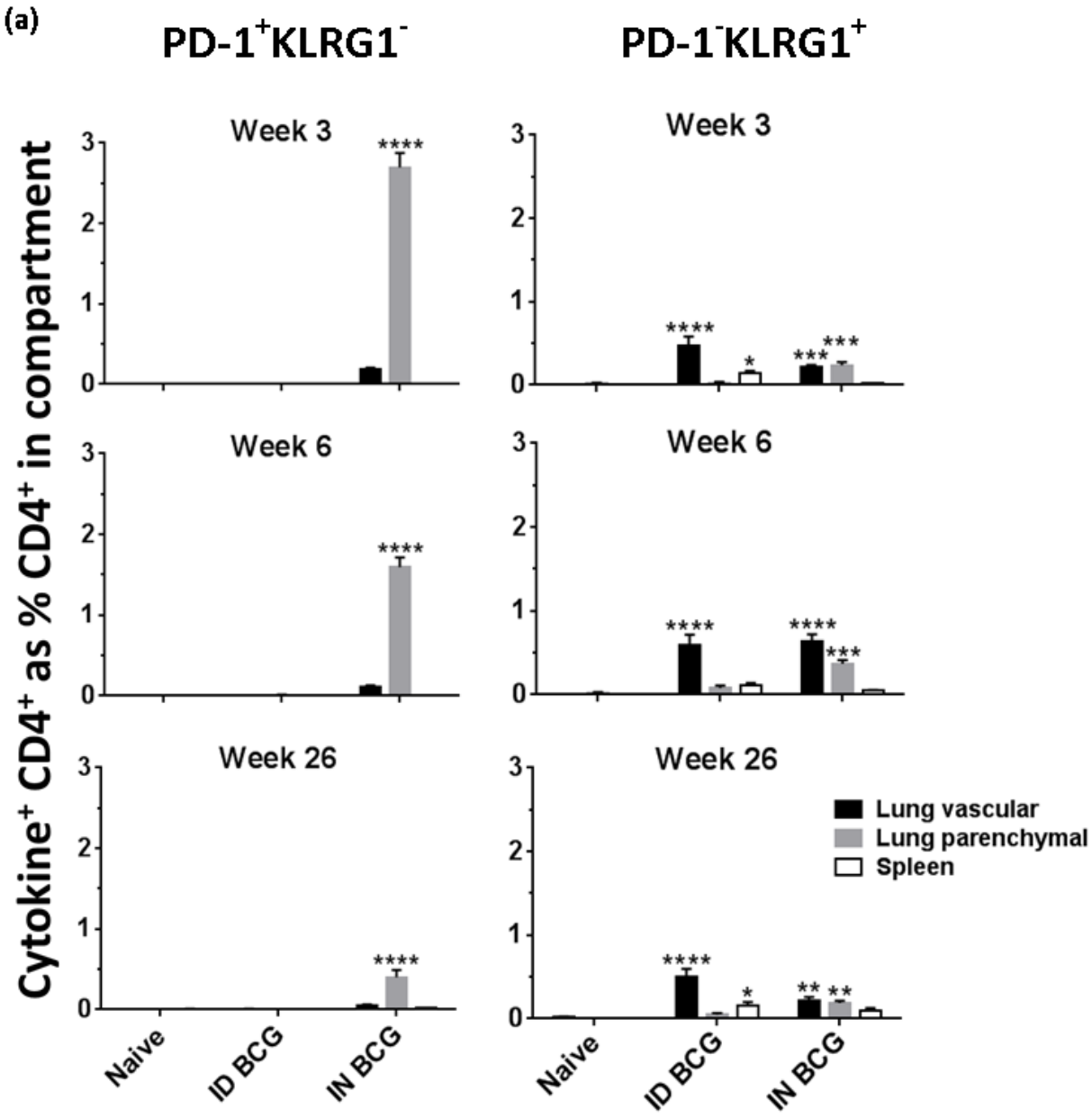
(a)
PD-1+KLRG1-
PD-1-KLRG1+
Week 3
Week 6
Week 26
Cytokine+ CD4+ as % CD4+ in compartment
Lung vascular
Lung parenchymal
Spleen
Naive
ID BCG
IN BCG

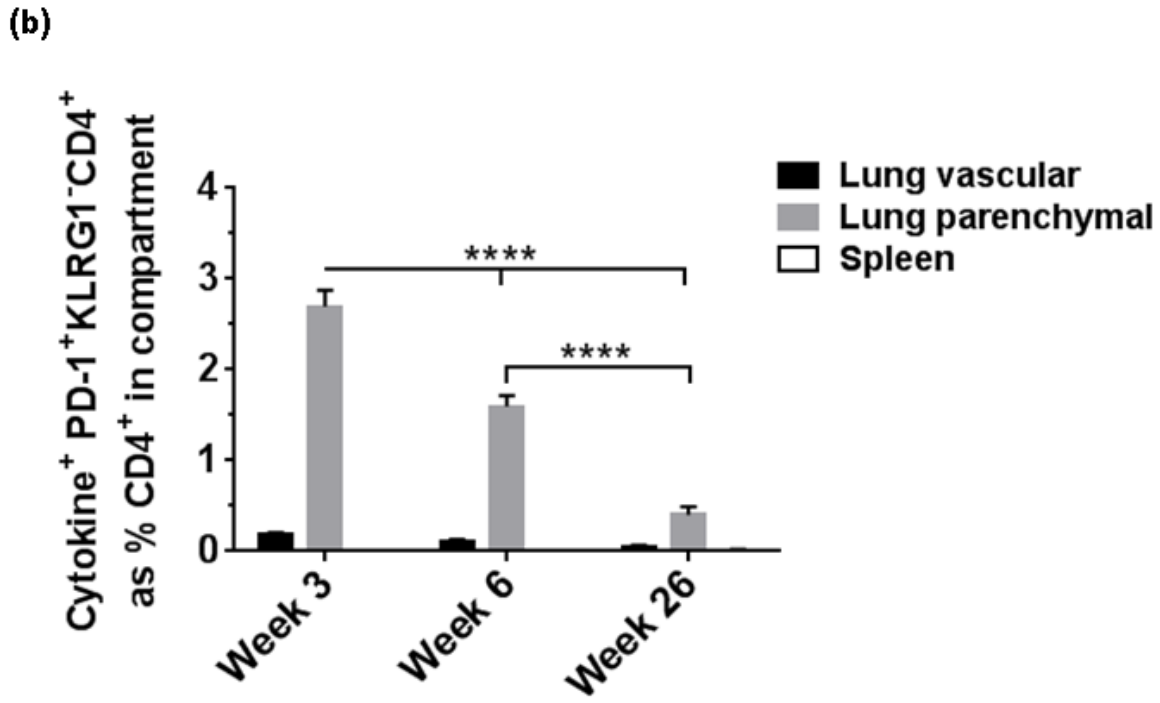

Figure 5.10 - Phenotype analysis of cytokine$^+$ CD4$^+$ T cells at different time points following ID or IN BCG. BALB/c mice were immunised IN or ID with BCG. Three, 6 and 26 weeks later, intravascular staining followed by ICS was used to identify populations of lung-parenchymal, lung-vascular and splenic PPD-T-specific CD4$^+$ T cells producing IFN-γ, TNF-α or IL-2 alone or in combination (cytokine$^+$). (a) Frequency of cytokine$^+$ CD4$^+$ T cells expressing a PD-1$^+$ KLRG1$^-$ or PD-1$^-$ KLRG1$^+$ phenotype in mice receiving IN or ID BCG. Statistical comparison is between naïve and BCG-immunised groups for the same compartment. (b) Frequency of cytokine$^+$ CD4$^+$ T cells expressing a PD-1$^+$ KLRG1$^-$ phenotype as a % of total CD4$^+$ T cells isolated from the same compartment of IN-immunised mice at each time point. Statistical comparison is between the same compartment at different time points. For all graphs, bars represent mean values (n=6) and error bars show SEM. * $\rho \leq 0.05$, ** $\rho \leq 0.01$, *** $\rho \leq 0.001$ **** $\rho \leq 0.0001$, two-way ANOVA with Sidak's post-test.

5.3. Discussion

Consistent with recent reports[217, 275], mucosal IN BCG vaccination conferred superior protection in the lungs of mice infected 4 weeks previously with *M.tb*, compared to mice receiving systemic ID BCG vaccination, when the animals were challenged 6 weeks post-immunisation. However, there was no significant difference in bacterial load in the spleens of mice receiving BCG by either route, suggesting that mucosal BCG induces locally protective mechanisms within the lungs, but does not afford additional protection against systemic dissemination of mycobacteria.

The mechanism for this additional local protection has yet to be determined, however, experiments in this chapter have demonstrated that delivery of BCG via the IN route results in recruitment of $CD4^+$ T cells from the periphery to the lung parenchyma, increasing the number of cells present at the primary site of infection. Additionally, within this larger population, there is an increased frequency of antigen-specific $CD4^+$ T cells. Impairment of DC-mediated antigen presentation in the lung and delay of DC migration to the draining lymph nodes are mechanisms of immune evasion employed by *M.tb* upon entry to the lungs[63, 129, 133-135]. This interference with the onset of an effective adaptive immune response allows the bacterial population to expand within the lung for up to 18-20 days before antigen-specific T cells have accumulated in sufficient numbers to inhibit further bacterial growth[78, 129, 131, 136, 137]. The influx of $CD4^+$ T cells into the parenchyma, observed in this chapter following mucosal BCG vaccination, may have been responsible for the enhanced protective efficacy against *M.tb* infection observed within this group, compared to systemically vaccinated animals. Having a greater number of local cells ready to respond

to bacterial invasion may help to control this early phase of *M.tb* growth. In accordance with this hypothesis, it has previously been shown that in the mouse, parenteral immunisation allowed *M.tb* to grow logarithmically in the lung for >10 days, while mucosal immunisation inhibited *M.tb* growth in the early phase after challenge[139, 140]. Srivastava *et al.*[295] have demonstrated that direct recognition of *M.tb*-infected cells by $CD4^+$ T cells is required for control of infection *in vivo*. Therefore, it is logical that a greater presence of antigen-specific $CD4^+$ T cells in the tissue of the lung, the initial entry point of bacteria, would facilitate control.

IN BCG, but not ID BCG, induced an antigen-specific $CD4^+$ T cell population in the BAL fluid. In agreement with this finding, several studies have demonstrated that TB vaccines delivered to the lung mucosa are able to elicit a T cell response within the airway lumen and restrict replication of *M.tb* in the first week following infection[140, 292, 294, 296-299]. These results indicate that airway luminal T cells may be able to provide a first line of defence against *M.tb* infection and should be considered as a target population when designing new vaccination regimes[294].

In order to further characterise the antigen-specific $CD4^+$ T cells induced locally in the lung and airways and peripherally in the spleen following IN and ID BCG, expression of the cell-surface markers PD-1 and KLRG1 was investigated. PD-1 and KLRG1 have been previously described as markers able to define different subsets of $CD4^+$ T cells present during *M.tb* infection. PD-1-expressing $CD4^+$ T cells have been shown to represent a subset of less-differentiated cells, exhibiting a greater proliferative and protective capacity than KLRG1-expressing cells[127, 289]. PD-1 is generally described as an inhibitory receptor which blocks T cell effector functions[202]. However, during *M.tb* infection, PD-1 deficiency leads to high

bacterial loads and rapid mortality following a low-dose aerosol challenge[300]. It has been suggested that this may be due to a requirement for the PD-1 pathway to control excessive inflammatory responses that lead to immunopathology[301]. Expression of KLRG1 has been associated with terminal differentiation[289], and an inability of *M.tb*-specific $CD4^+$ T cells to migrate into the lung-parenchyma and protect against *M.tb* infection[126]. One study describes a $CD4^+$ $KLRG1^-$ IL-2-secreting $CD4^+$ T cell population as a central memory subset with pronounced proliferative capacity and the ability to control bacterial growth in the later stages of *M.tb* infection[207].

PD-1 and KLRG1 expression has also been investigated in humans following TB treatment and BCG vaccination[302]. It was found that TB-treated individuals had increased levels of KLRG1 expression on $CD4^+$ T cells, whilst BCG-vaccinated individuals had increased levels of KLRG1 expression on $CD8^+$ T cells, and this correlated with decreased proliferative capacity. In contrast, $PD1^+$ T cells taken from BCG-vaccinated volunteers were able to proliferate following *in vitro* BCG-stimulation. This indicates that studying expression of these markers is valuable not only in animal models but also in human clinical trials, and suggests that comparisons may be able to be drawn between different study populations.

Data presented within this chapter reveal that an antigen-specific $CD4^+$ T cell population with $PD1^+$ $KLRG1^-$ cell-surface expression was only induced following IN BCG vaccination and was exclusively present within the lung-parenchyma and airways. This suggests that delivery of antigen via the mucosal route is critical for development of cells expressing this phenotypic combination, a subset of cells reportedly capable of providing enhanced protection against *M.tb* infection.

Expression of CXCR3 on antigen-specific $CD4^+$ T cells in the lung and spleen was also investigated, as this has been described as representing a population of $CD4^+$ T cells capable of localising to the lung-parenchyma during *M.tb* infection[126]. It was found that CXCR3 expression was only present on lung-parenchymal $CD4^+$ T cells following IN BCG vaccination. This is in contrast to recent studies by Woodworth *et al.*[218] and Jeyanathan *et al.*[292] which describe induction of antigen-specific T cells expressing CXCR3 following systemic immunisation. However, these studies used a subunit or viral-vectored TB vaccine rather than BCG, and it may be the case that these are better able to induce cells expressing this parenchyma-localising phenotype. This should be investigated further, as it has implications for future vaccine design.

The relationship between expression of PD-1, KLRG1 and CXCR3 on antigen-specific lung-parenchymal $CD4^+$ T cells following IN BCG was investigated, and it was found that whilst CXCR3 is expressed on cells with both a PD-1^+ $KLRG1^-$ and $PD1^-$ $KLRG1^+$ phenotype, there was a greater frequency of $CXCR3^+$ cells within the $PD1^+$ $KLRG1^-$ population. Based on existing studies within the literature, this suggests that IN BCG induces a population of cells with memory-like capacities, able to localise to the parenchyma of the lung.

Histopathology was performed to identify the location of lymphocytic infiltrates in the lung 6 weeks following mucosal BCG vaccination. This revealed that lymphocytes appeared to be accumulating in discrete clusters surrounding blood vessels, including those in association with the airways, rather than being present diffusely throughout the lung. However, the H&E staining used allows for identification of cells based on morphology alone and only reveals information about their location at a single point in time. It is also not possible to analyse these images quantifiably to generate data for statistical comparison. Use of

immunohistochemistry, both chromogenic and fluorescent, would provide valuable additional information to the images presented here, through allowing individual identification of $CD4^+$ and $CD8^+$ T cells as well as other cell-surface phenotypic markers of interest such as PD-1, KLRG1 and CXCR3. Other studies have utilised these techniques to study $CD4^+$ T_{RM} in the context of infection with *M.tb*[121, 126, 217] and influenza[123]. However, only one of these papers has utilised immunohistochemistry to identify cells in the lung following mucosal BCG vaccination[217]. Perdomo *et al.*[217] report that 60 days after intra-tracheal BCG vaccination, histological examination of the lungs revealed greater cell infiltration than in the lungs of naïve or systemically-vaccinated mice, with many of these infiltrating cells being identified as $CD4^+$ T cells. However, in contrast to data presented in this chapter, the authors describe this infiltration as a transient effect, reporting that 45 days later, no significant difference in the total number of T cells in the lung was observed between groups. Experiments in this chapter show that numbers of $CD4^+$ T cells in the lung-parenchyma remained significantly higher in mucosally BCG-vaccinated animals than systemically-vaccinated or control animals up to 182 days following immunisation. This difference between data from the aforementioned study and work included here may be accounted for by the fact that animals in the study were infected with *M.tb* 60 days after vaccination, and it was 45 days following infection that the second measurements of cellular infiltration were made. In the data from this thesis, cellular infiltration was only investigated following vaccination alone, not in the context of pathogenic challenge. The study suggests that infection changes the dynamics of this response, therefore future work could be conducted to investigate the population of lung-parenchymal $CD4^+$ T cells, identified by intravascular staining, following *M.tb* infection.

Protection against *M.tb* infection was also assessed 26 weeks post-BCG vaccination via IN and ID routes, in order to determine whether both routes of administration provided durable protection. There was significant protection compared to naïve animals in the lungs and spleens of mice in both immunised groups, however, there was no longer statistically significantly enhanced protection in the lungs of IN compared to ID-immunised mice, despite a trend towards this. This may be due to the fact that the frequency of antigen-specific $CD4^+$ T cells present in the lung-parenchyma of IN-immunised mice had significantly decreased from week 6 to week 26 post-vaccination, as well as the proportion of cells within this compartment expressing a PD-1^+ KLRG1^- phenotype, thought to be protective against *M.tb* infection. Interestingly, the frequency of antigen-specific $CD4^+$ T cells present in the BAL fluid of IN-immunised mice significantly increased from week 6 to week 26, suggesting that these cells alone are not sufficient for enhanced protection, and lung-parenchymal $CD4^+$ T cells do have a critical role to play.

In accordance with the protection data presented in this chapter, Derrick *et al.*[276] demonstrated significant improvements in protection in the lungs of IN BCG-immunised mice compared to ID-immunised mice at 2 and 4 months post-vaccination. When protection was investigated at 8 and 10 months post-vaccination, no significant differences in pulmonary protection were observed between the two groups. However, in contrast to the findings presented in this chapter, the authors of this study also report significantly elevated protective responses in the spleens of the IN-immunised mice at 2, 4, 8 and 10 months post-vaccination, compared to the ID-immunised mice. It is not clear why these differences exist. A similar dose of BCG was used in both experiments, delivered intranasally following a similar protocol, and all mice were challenged with *M.tb* via

aerosol. However, the study used Pasteur BCG rather than Danish, and C57BL/6 mice rather than BALB/c, as well as delivering double the dose of infectious *M.tb* to each animal. Further work is required to determine if these factors are responsible for the differing results. The study authors also report higher frequencies of $CD4^+$ and $CD8^+$ T cells producing IFN-γ in the spleens of the IN-immunised compared to the ID-immunised mice at all time points. Despite the fact that this was not observed in the experiments presented in this chapter, it does seem to confirm that the presence of higher frequencies of antigen-specific T cells within an organ correlates with enhanced protection in that organ. Further work is required to elucidate the underlying mechanisms behind these differences and to determine new vaccination approaches which may help to maintain the enhanced protection afforded in the lung by mucosal BCG, over longer periods of time post-vaccination.

In conclusion, results presented in this chapter reveal that mucosal delivery of BCG provides enhanced protection in the lungs of mice challenged with *M.tb* 6 weeks post-vaccination, when compared to mice immunised systemically with BCG. This enhanced local protection appears to correlate with the presence of larger numbers of $CD4^+$ T cells in the lung-parenchyma, a greater frequency of antigen-specific $CD4^+$ T cells within this population and the presence of antigen-specific $CD4^+$ T cells in the BAL fluid. A proportion of these IN BCG-induced antigen-specific $CD4^+$ T cells in the parenchyma and BAL expressed a $PD1^+$ $KLRG1^-$ cell-surface phenotype, associated with enhanced protection against *M.tb* infection. This suggests that mucosal BCG vaccination does induce specific local protective effects in the lung, and identifies lung-parenchymal $CD4^+$ T cells as a key component of this response.

Chapter 6.

Protective efficacy of lung tissue-resident $CD4^+$ T cells

6.1. Introduction

In the previous chapter, it was established that the presence of larger numbers of $CD4^+$ T cells in the lung-parenchyma appeared to correlate with enhanced protection against aerosol *M.tb* challenge in the lung. In light of this finding, it was important to further investigate potential mechanisms underlying this enhanced protection and to determine whether these cells were capable of conferring protection to a naïve mouse following adoptive transfer.

Work presented in the previous chapter revealed that a proportion of antigen-specific lung-parenchymal $CD4^+$ T cells displayed a $PD1^+KLRG1^-$ phenotype following intranasal BCG vaccination. This phenotype is described in the literature as 'memory-like', representing cells which are not terminally differentiated and retain the capacity to proliferate upon adoptive transfer[126, 127, 207, 289]. It is important to establish whether intranasal BCG vaccination does induce $CD4^+$ T cells within the lung-parenchymal compartment that are able to proliferate and to determine how the proliferative capacity of this compartment compares to the lung-vascular compartment and spleen. This may reveal an important difference between the populations of $CD4^+$ T cells found in different locations and may suggest a mechanism for the enhanced protection seemingly afforded by lung-parenchymal $CD4^+$ T cells. One of the aims of this chapter was to utilise expression of Ki67 to identify $CD4^+$ T cells from lung and spleen, following intranasal BCG vaccination, which actively proliferate upon stimulation with cognate antigen. Ki67 is a well-established marker of proliferation and has been shown to be expressed during all the active phases of the cell cycle, but not in resting cells, in both humans[303-307] and animal models[308-312].

Seminal work by Sakai *et al.* investigating the role of lung-parenchymal $CD4^+$ T cells during *M.tb* infection revealed that *M.tb*-specific lung-parenchymal $CD4^+$ T cells, taken from *M.tb*-infected mice, migrate back into the lung-parenchyma following adoptive transfer and provide greater control of *M.tb* infection compared to lung-vascular $CD4^+$ T cells[126]. A subsequent study by Moguche *et al.* also found that *M.tb*-specific lung-parenchymal $PD1^+KLRG1^-$ $CD4^+$ T cells confer superior protection against *M.tb* infection following adoptive transfer, when compared with lung-vascular $PD1^-KLRG1^+$ $CD4^+$ T cells[127].

To date, no data have been published on adoptive transfer of lung-parenchymal $CD4^+$ T cells, identified using intravascular staining, following vaccination against TB. Woodworth *et al.* recently published the first study describing adoptive transfer of vaccine-specific lung-vascular $CD4^+$ T cells following immunisation with a subunit TB vaccine, but this did not include any data on transfer of lung-parenchymal $CD4^+$ T cells[218]. The authors report that vaccine-specific lung-vascular $CD4^+$ T cells are able to traffic to the lung-parenchyma following adoptive transfer, but they do not assess protection against subsequent *M.tb* infection. Another recent paper by Perdomo *et al.* investigates adoptive transfer of lung airway but not parenchymal $CD4^+$ and $CD8^+$ T cells from mice following mucosal BCG vaccination[217]. They report that mucosal transfer of these airway populations confers protection against *M.tb* infection.

It is important to establish whether lung-parenchymal $CD4^+$ T cells, induced following mucosal BCG vaccination, display the same lung-homing characteristics as described in the context of *M.tb* infection. It is also critical to determine whether they are able to confer protection against *M.tb* infection following adoptive transfer into naïve recipients. Work contained within this chapter aims to address these questions with a series of adoptive

transfer experiments involving the use of congenic BALB/c mice and aerosol *M.tb* challenge experiments.

6.2. Results

6.2.1. Proliferative capacity of lung-parenchymal $CD4^+$ T cells following intranasal (IN) BCG vaccination

To investigate the proliferative capacity of lung-parenchymal $CD4^+$ T cells, expression of Ki67 was analysed in mice vaccinated IN with BCG. Six weeks post-immunisation, lungs and spleen were harvested following intravascular staining. Fluorescence activated cell sorting (FACS) was used to sort lung $CD4^+$ T cells based on intravascular staining. This enabled isolation of lung-parenchymal and lung-vascular $CD4^+$ T cells. Spleens were sorted by FACS to obtain $CD4^+$ T cells. Naïve control mice had total lungs and spleen cells sorted by FACS for $CD4^+$ T cells, without intravascular staining. After sorting, $CD4^+$ T cells were cultured with PPD-T for 3 days before staining for Ki67 and analysis by flow cytometry (Appendix – Flow cytometry Ki67 panel). The experiment was repeated three times with n=6 mice per group in each experiment, and pooled data from all three experiments, which all showed the same result, are presented.

6.2.1.1. IN BCG vaccination induces $Ki67^+$ $CD4^+$ T cells in the lung and spleen

IN BCG vaccination induced significant populations of $Ki67^+$ $CD4^+$ T cells in the lung-parenchyma (Figure 6.1a) and spleen (Figure 6.1b) compared to naïve controls. In the lung, the frequency of $Ki67^+$ $CD4^+$ T cells in the lung-parenchymal compartment was significantly greater than in the lung-vascular compartment (Figure 6.1a).

6.2.1.2. Frequency of Ki67^{+} CD4^{+} T cells is highest in the lung-parenchyma following IN BCG vaccination

IN BCG vaccination induced a significantly higher frequency of Ki67^{+} CD4^{+} T cells in the lung-parenchyma compared to the lung-vasculature and spleen (Figure 6.1c).

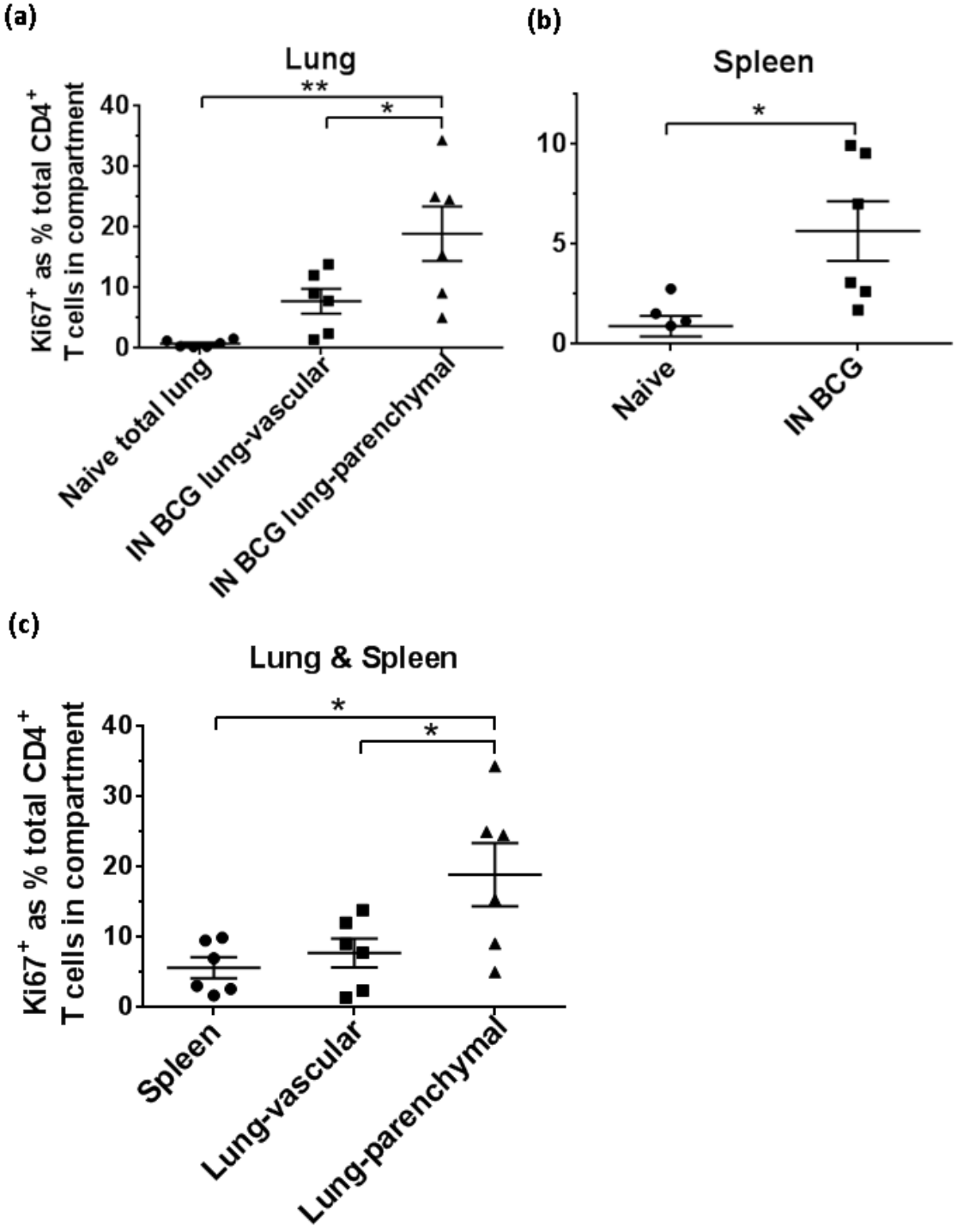

Figure 6.1 - Ki67 staining. BALB/c mice received IN BCG immunisation and were euthanased 6 weeks later following intravascular staining. Lungs were FACS sorted into lung-parenchymal and lung-vascular $CD4^+$ T cells. Spleens were sorted by FACS to obtain $CD4^+$ T cells. Naïve control animals had total lung and spleen sorted for $CD4^+$ T cells, without intravascular staining. Cells were cultured for 3 days with PPD-T (stimulated) or

without PPD-T (unstimulated) before staining for Ki67 as a marker of proliferation. For all graphs, each point respresents pooled cells from 3 mice. Data are pooled from 3 independent experiments. To account for non-specific expression of Ki67, unstimulated values were subtracted from stimulated. (a) Frequency of $Ki67^+$ $CD4^+$ T cells in the total lung of naïve mice and the lung-parenchyma and lung-vasculature of BCG-immunised mice. (b) Frequency of $Ki67^+$ $CD4^+$ T cells in the spleen of naïve and BCG-immunised mice. (c) Frequency of $Ki67^+$ $CD4^+$ T cells in the spleen and lung of BCG-immunised mice. For all graphs, bars represent mean values (n=6) and error bars show SEM. * $\rho \leq 0.05$, ** $\rho \leq 0.01$, one-way ANOVA with Tukey's post-test comparing BCG with control and all compartments with each other.

6.2.2. Homing capacity of $CD4^+$ T cells following adoptive transfer

In order to investigate whether lung-parenchymal $CD4^+$ T cells are able to return to the lung following adoptive transfer, congenic BALB/c mice expressing CD90.1 on T cells were vaccinated IN with BCG and euthanased 6 weeks later following intravascular staining. FACS was used to sort lung $CD4^+$ T cells based on intravascular staining. This enabled isolation of lung-parenchymal and lung-vascular $CD4^+$ T cells. Spleen cells were sorted by FACS to obtain $CD4^+$ T cells. Naïve control animals had lungs harvested and sorted by FACS to obtain total $CD4^+$ T cells, without intravascular staining. After sorting, $CD90.1^+$ $CD4^+$ T cells were transferred into naïve non-congenic recipient BALB/c mice via intravenous injection. Groups of recipient mice received $CD90.1^+$ $CD4^+$ T cells from the lung-vasculature, lung-parenchyma or spleen of immunised donor mice or $CD90.1^+$ $CD4^+$ T cells taken from the total lung of naïve mice. In the groups receiving lung-vascular or lung-parenchymal $CD90.1^+$ $CD4^+$ T cells, equal numbers of mice received cells from 1 donor mouse and from 2 donor mice. 24 hours following adoptive transfer, recipient mice were euthanased following intravascular staining and lungs and spleen were harvested and analysed by flow cytometry to identify donor $CD90.1^+$ $CD4^+$ T cells present in both organs (Appendix – Flow cytometry adoptive transfer panel).

6.2.2.1. Numbers of $CD90.1^+$ $CD4^+$ T cells found in the lungs and spleen of recipient mice following adoptive transfer varied between groups

Initial data analysis revealed that numbers of $CD90.1^+$ $CD4^+$ T cells found in the lungs and spleen of recipient mice following adoptive transfer varied between groups. The number of

donor splenic CD90.1$^+$ CD4$^+$ T cells found in the spleen of recipients was significantly higher than numbers of donor CD90.1$^+$ CD4$^+$ T cells from all other compartments (Figure 6.2a). Numbers of CD90.1$^+$ CD4$^+$ T cells transferred from the spleen of 1 donor mouse or lung-vasculature of 2 donor mice were significantly higher in the spleens of recipients than in either lung compartment.

6.2.2.2. Numbers of CD90.1$^+$ CD4$^+$ T cells transferred to each recipient differed between groups

The above analysis (Figure 6.2a) revealed that numbers of donor CD90.1$^+$ CD4$^+$ T cells found in the lungs and spleen of recipient animals, varied between groups. However, this finding is unable to take into account the fact that numbers of CD90.1$^+$ CD4$^+$ T cells transferred to recipients varied between groups, with numbers of splenic CD4$^+$ T cells transferred being significantly higher than all other groups (Figure 6.2b).

6.2.2.3. Frequency of CD90.1$^+$ CD4$^+$ T cells transferred from the lung-parenchyma of BCG-immunised mice was highest in the lung-parenchyma of recipient mice following adoptive transfer

In order to account for differences in the size of each compartment, CD90.1$^+$ CD4$^+$ T cells as a percentage of total CD4$^+$ T cells in each compartment are presented. In the lung-vasculature and spleen, the frequency of CD90.1$^+$ CD4$^+$ T cells transferred from the spleen was significantly higher than frequency of CD90.1$^+$ CD4$^+$ T cells transferred from the lung-vasculature, lung-parenchyma or total naïve lung (Figure 6.2c). In the lung-parenchyma, frequency of CD90.1$^+$ CD4$^+$ T cells transferred from the spleen was significantly higher than

frequency of CD90.1$^+$ CD4$^+$ T cells transferred from total naïve lung. In order to make a comparison between animals receiving equal numbers of CD90.1$^+$ CD4$^+$ T cells, groups receiving lung-parenchymal CD4$^+$ T cells from 2 donors, lung-vascular CD4$^+$ T cells from 1 donor or total naïve lung from 1 donor were analysed as they all received ~1.8x10^5 CD90.1$^+$ CD4$^+$ T cells (Figure 6.2d). In this analysis, frequency of CD90.1$^+$ CD4$^+$ T cells transferred from the lung-parenchyma was significantly higher in the recipient lung-parenchyma than frequency of CD90.1$^+$ CD4$^+$ T cells transferred from the lung-vasculature or total naïve lung. Frequencies of CD90.1$^+$ CD4$^+$ T cells found in the lung-vasculature and spleen were not significantly different regardless of whether they were transferred from lung-parenchyma, lung-vasculature or total naïve lung.

(a)

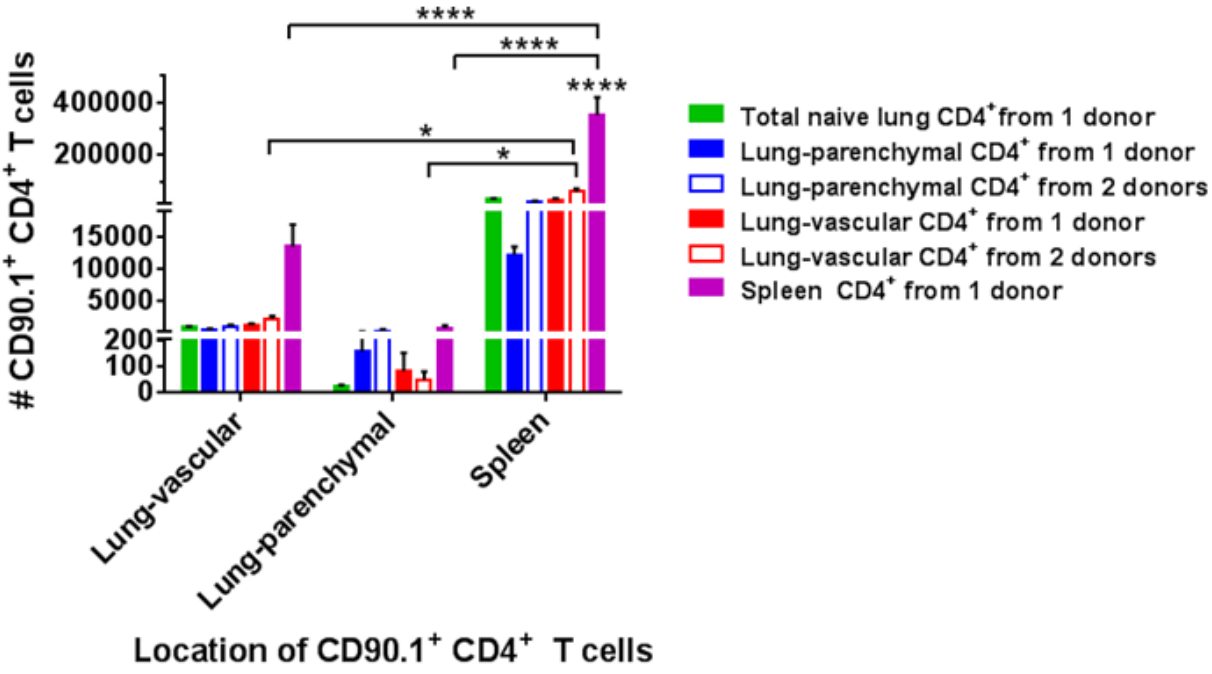
****
****
****
*
*
CD90.1+ CD4+ T cells
400000
200000
15000
10000
5000
200
100
0
Lung-vascular
Lung-parenchymal
Spleen
Location of CD90.1+ CD4+ T cells
Total naive lung CD4+from 1 donor
Lung-parenchymal CD4+ from 1 donor
Lung-parenchymal CD4+ from 2 donors
Lung-vascular CD4+ from 1 donor
Lung-vascular CD4+ from 2 donors
Spleen CD4+ from 1 donor

(b)

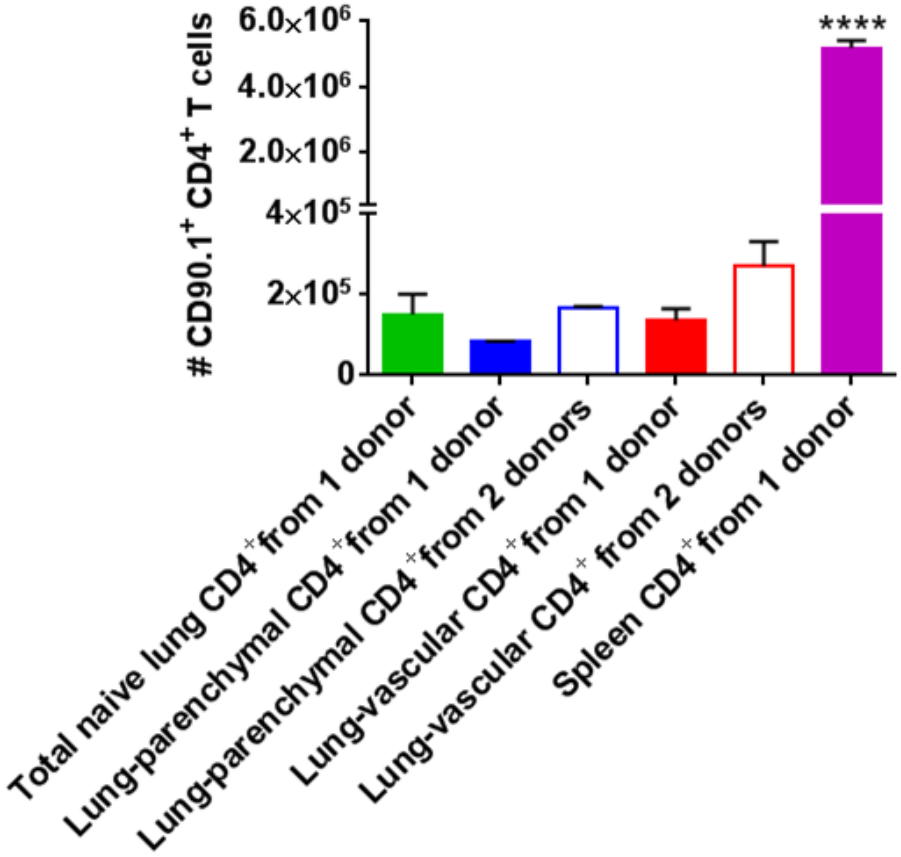
CD90.1+ CD4+ T cells
6.0×10^6
4.0×10^6
2.0×10^6
4×10^5
2×10^5
0
****
Total naive lung CD4+from 1 donor
Lung-parenchymal CD4+from 1 donor
Lung-parenchymal CD4+from 2 donors
Lung-vascular CD4+from 1 donor
Lung-vascular CD4+from 2 donors
Spleen CD4+from 1 donor

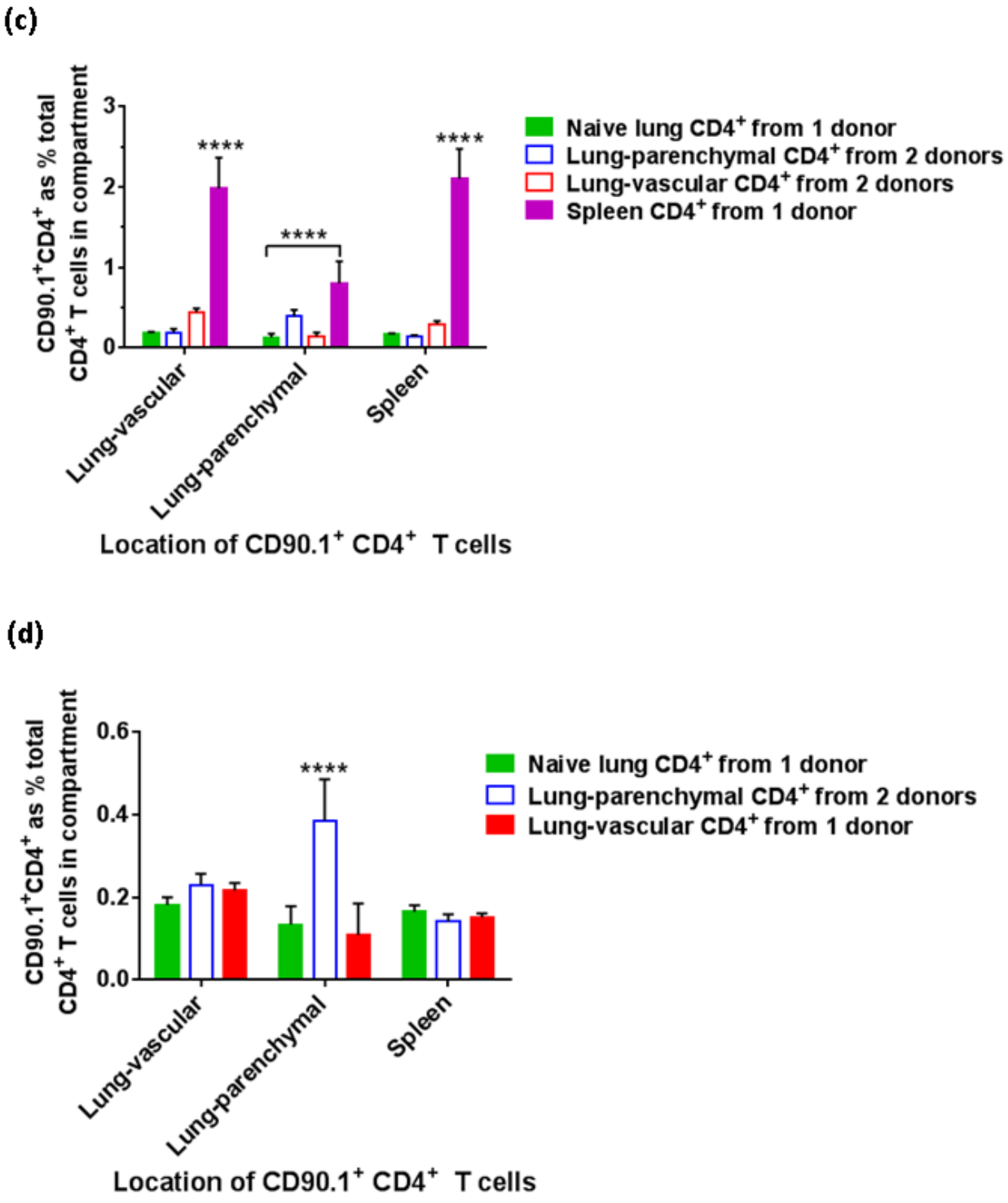

Figure 6.2 - Homing of $CD4^+$ T cells following adoptive transfer. Congenic BALB/c mice expressing CD90.1 on T cells received IN BCG immunisation and were euthanased 6 weeks later following intravascular staining. Lungs were FACS sorted into lung-parenchymal and lung-vascular $CD4^+$ T cells. Spleens were sorted by FACS to obtain $CD4^+$ T cells. Naïve control animals had total lung and spleen sorted for $CD4^+$ T cells, without intravascular staining.

$CD4^+$ T cells were transferred via intravenous injection into non-congenic recipient BALB/c mice. Groups of recipient mice received $CD4^+$ T cells from the lung-vasculature, lung-parenchyma or spleen of immunised donor mice or $CD4^+$ T cells taken from the total lung of naïve mice. In the groups receiving lung-vascular or lung-parenchymal $CD4^+$ T cells, equal numbers of mice received cells from 1 donor mouse and from 2 donor mice. Data shown is pooled from 2 independent experiments. (a) Numbers of $CD90.1^+$ $CD4^+$ T cells recovered from the lungs and spleen of recipient mice 24 hours after adoptive transfer. (b) Numbers of $CD90.1^+$ $CD4^+$ T cells transferred to recipient animals, measured through counting on a haemocytometer prior to adoptive transfer. (c) Frequency of $CD90.1^+$ $CD4^+$ T cells in the spleen and lungs of donor mice 24 hours after adoptive transfer as a % of total $CD4^+$ T cells in that compartment. (d) Frequency of $CD90.1^+$ $CD4^+$ T cells in the spleen and lungs of donor mice 24 hours after adoptive transfer as a % of total $CD4^+$ T cells in that compartment. Data shown just for mice receiving naïve lung $CD4^+$ from 1 donor, lung-parenchymal $CD4^+$ from 2 donors and lung-vascular $CD4^+$ from 1 donor, all receiving ~$1.8X10^5$ $CD90.1^+$ $CD4^+$ T cells. For all graphs except (b), bars represent mean values (n=6) and error bars show SEM. Two-way ANOVA with Sidaks post-test comparing groups receiving donor cells from different tissues within and between recipient organs. For graph (b), bars represent mean values (n=2) and error bars show SEM. One-way ANOVA with Tukey's post-test. * $\rho \leq 0.05$, **** $\rho \leq 0.0001$.

6.2.3. Protection against aerosol *M.tb* challenge in naïve mice receiving $CD4^+$ T cells adoptively transferred from BCG-immunised mice

In order to determine the protective capacity of $CD4^+$ T cells from the lung-parenchyma and lung-vasculature, BALB/c mice received BCG IN and were euthanased 6 weeks later following intravascular staining. FACS was used to sort lung $CD4^+$ T cells based on intravascular staining. This enabled isolation of lung-parenchymal and lung-vascular $CD4^+$ T cells. Naïve control animals also had lungs harvested without intravascular staining and sorted by FACS to obtain total $CD4^+$ T cells. After sorting, $CD4^+$ T cells were transferred into naïve recipient BALB/c mice via intravenous injection. Groups of recipient mice received $CD4^+$ T cells from the lung-vasculature or lung-parenchyma of immunised donor mice or $CD4^+$ T cells taken from the total lung of naïve mice. In the groups receiving lung-vascular or lung-parenchymal $CD4^+$ T cells, equal numbers of mice received cells from 1 donor mouse and from 2 donor mice. 24 hours following adoptive transfer, recipient mice were challenged with *M.tb* via aerosol. 4 weeks post-challenge, mice were euthanased and lungs and spleen were harvested for CFU enumeration.

6.2.3.1. Adoptive transfer of $CD4^+$ T cells from the lung-vasculature of BCG-immunised mice results in significantly reduced bacterial burden in the lungs following aerosol M.tb challenge

Following aerosol *M.tb* challenge, there was a significant reduction in bacterial burden in the lungs of mice receiving lung-vascular $CD4^+$ T cells from 2 donors compared to naïve

control animals (Figure 6.3a). The lungs of control mice had a bacterial burden of 7.0 $\log_{10}$ CFU *M.tb* compared to 6.5 $\log_{10}$ CFU in mice receiving lung-vascular $CD4^+$ T cells from 2 donors ($\rho \leq 0.05$), equating to a 0.5 $\log_{10}$ CFU reduction. There was no significant reduction in bacterial burden in the lungs of recipient mice in any other group or in the spleens of recipient mice in any group.

6.2.3.2. Numbers of $CD4^+$ T cells transferred to each recipient differed between groups

The numbers of $CD4^+$ T cells transferred to recipients was variable between groups (Figure 6.3b). Statistical analysis was not possible as cells were pooled prior to transfer so values shown on the graph indicate total number of $CD4^+$ T cells sorted divided by number of recipient animals.

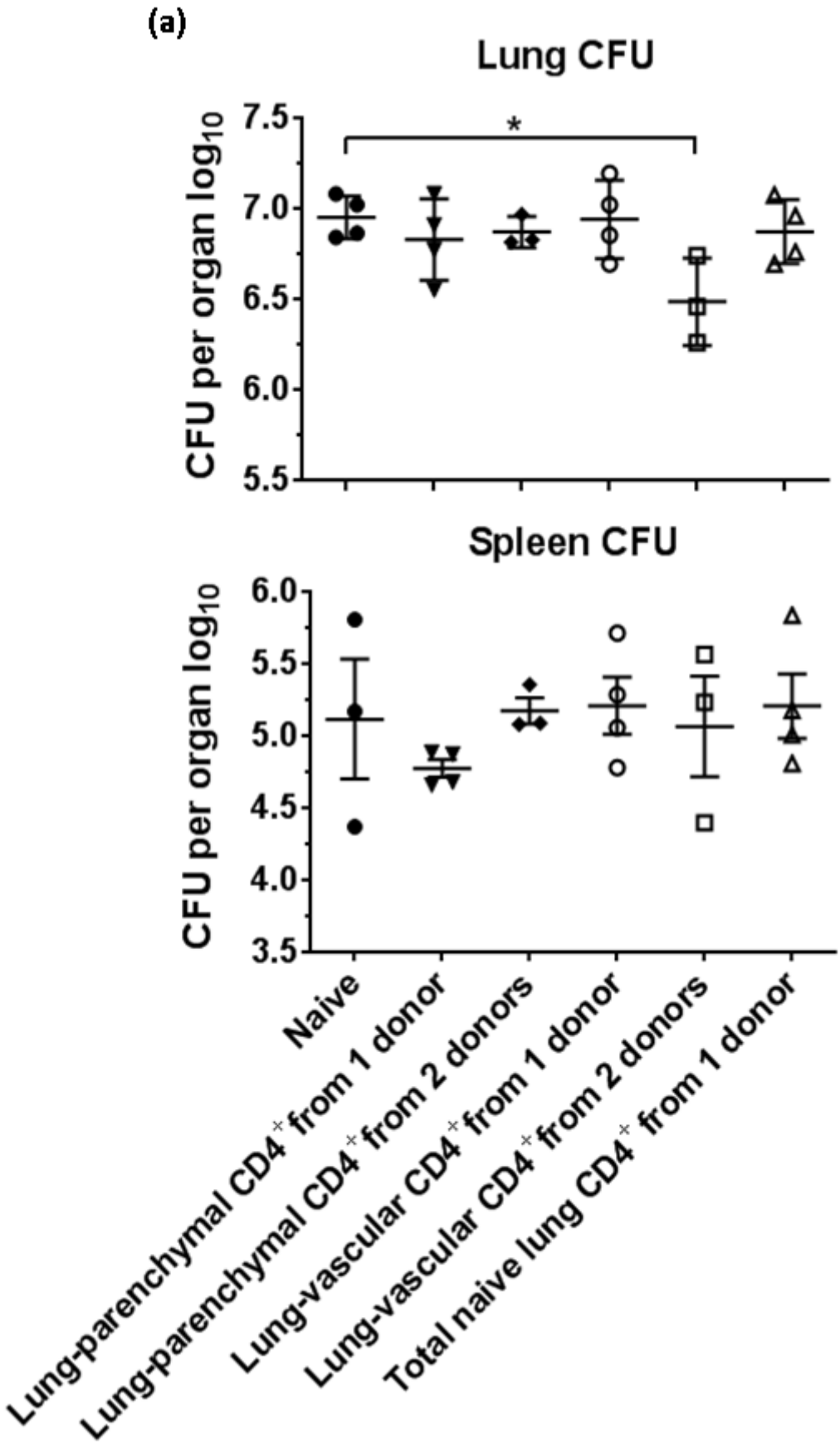
(a)
Lung CFU
CFU per organ log10
7.5
7.0
6.5
6.0
5.5
*
Spleen CFU
CFU per organ log10
6.0
5.5
5.0
4.5
4.0
3.5
Naive
Lung-parenchymal CD4+ from 1 donor
Lung-parenchymal CD4+ from 2 donors
Lung-vascular CD4+ from 1 donor
Lung-vascular CD4+ from 2 donors
Total naive lung CD4+ from 1 donor

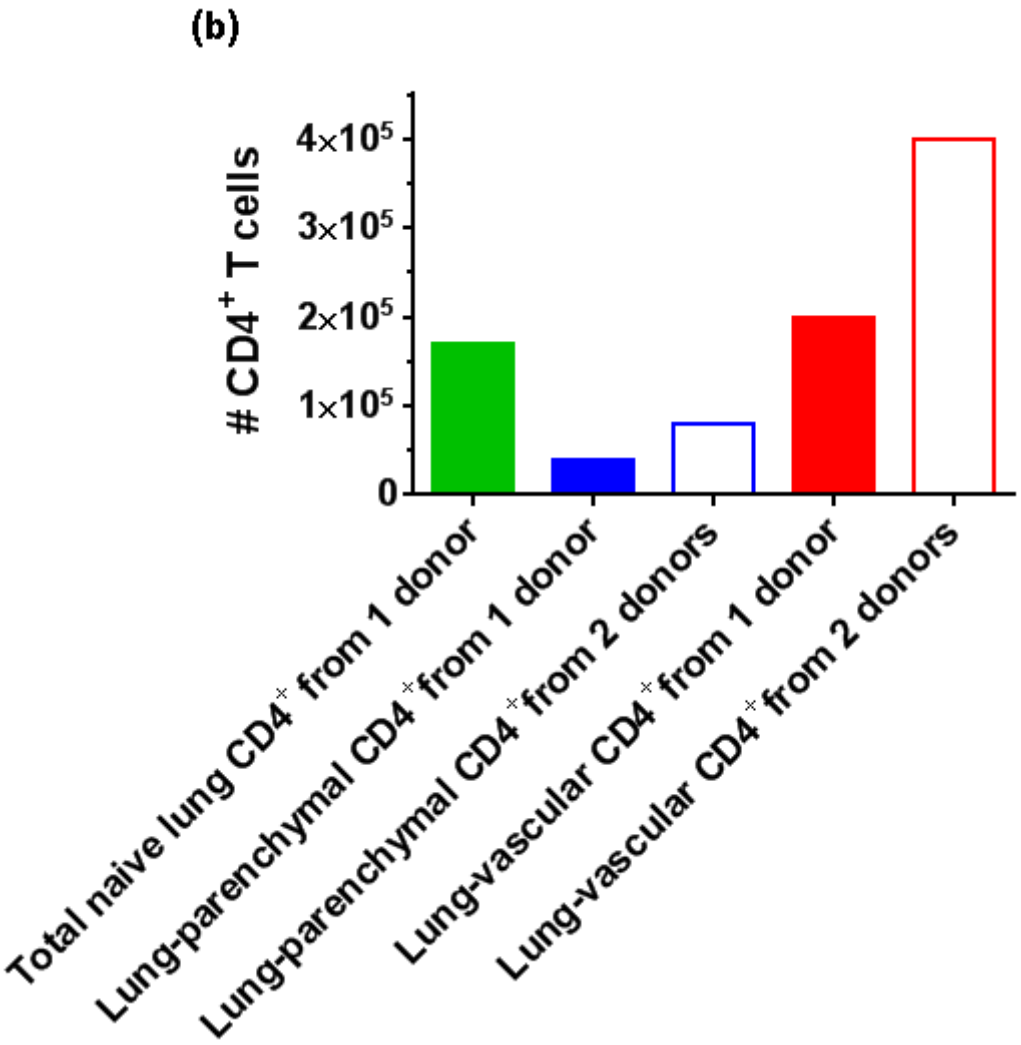

Figure 6.3 - Protection against aerosol *M.tb* challenge following adoptive transfer. BALB/c mice received IN BCG immunisation and were euthanased 6 weeks later following intravascular staining. Lungs were FACS sorted into lung-parenchymal and lung-vascular $CD4^+$ T cells. Naïve control animals had total lung sorted for $CD4^+$ T cells, without intravascular staining. $CD4^+$ T cells were transferred via intravascular injection into recipient BALB/c mice. Groups of recipient mice received $CD4^+$ T cells from the lung vasculature or lung parenchyma of immunised donor mice or $CD4^+$ T cells taken from the total lung of naïve mice. In the groups receiving lung-vascular or lung-parenchymal $CD4^+$ T cells, equal numbers of mice received cells from 1 donor mice and from 2 donor mice. 24 hours after adoptive transfer, recipient mice were challenged with *M.tb* via aerosol. Four weeks post-challenge, lungs and spleen were removed for CFU enumeration. (a) Individual $\log_{10}$ CFU counts are shown from the lungs and spleen with bars indicating mean and error bars

showing SEM (n ≥ 3 mice per group). * $\rho \leq 0.05$, one-way ANOVA with Tukey's post-test for significance. (b) Numbers of $CD90.1^{+}$ $CD4^{+}$ T cells transferred to recipient animals, measured through counting on a haemocytometer prior to adoptive transfer.

6.2.4. Protection against aerosol *M.tb* challenge in naïve mice receiving standardised numbers of $CD4^+$ T cells adoptively transferred from BCG-immunised mice

In Figure 6.3 it was shown that mice receiving $CD4^+$ T cells from the lung-vasculature of 2 donors had reduced bacterial burden in the lungs following aerosol challenge with *M.tb*, compared to naïve control mice. In order to determine whether this can be explained by the higher number of $CD4^+$ T cells transferred to recipient mice in this group, standardised numbers of $CD4^+$ T cells were transferred from the lung-vasculature, lung-parenchyma and total naïve lung of donor mice. BALB/c mice received BCG IN and were euthanased 6 weeks later following intravascular staining. FACS was used to sort lung $CD4^+$ T cells based on intravascular staining. This enabled isolation of lung-parenchymal and lung-vascular $CD4^+$ T cells. Naïve control animals also had lungs harvested without intravascular staining and sorted by FACS to obtain total $CD4^+$ T cells. After sorting, $CD4^+$ T cells were pooled and ~$5.5x10^5$ $CD4^+$ T cells were transferred into naïve recipient BALB/c mice via intravenous injection. Twenty-four hours following adoptive transfer, recipient mice were challenged with *M.tb* via aerosol. Four weeks post-challenge mice were euthanased and lungs and spleen were harvested for CFU enumeration.

6.2.4.1. Adoptive transfer of ~ 5.5x10^5 CD4$^+$ T cells from the lung-vasculature of BCG-immunised mice results in significantly reduced bacterial burden in the lungs following aerosol M.tb challenge

In the lungs of recipient mice following aerosol challenge, there was a significant reduction in bacterial burden in the group receiving lung-vascular CD4$^+$ T cells compared to naïve control animals (Figure 6.4). The lungs of control mice had a bacterial burden of 7.0 $\log_{10}$ CFU *M.tb* compared to 6.6 $\log_{10}$ CFU in mice receiving lung-vascular CD4$^+$ T cells from 2 donors ($\rho \leq 0.05$), equating to a 0.4 $\log_{10}$ CFU reduction. There was no significant reduction in bacterial burden in the lungs of recipient mice in any other group or in the spleens of recipient mice in any group.

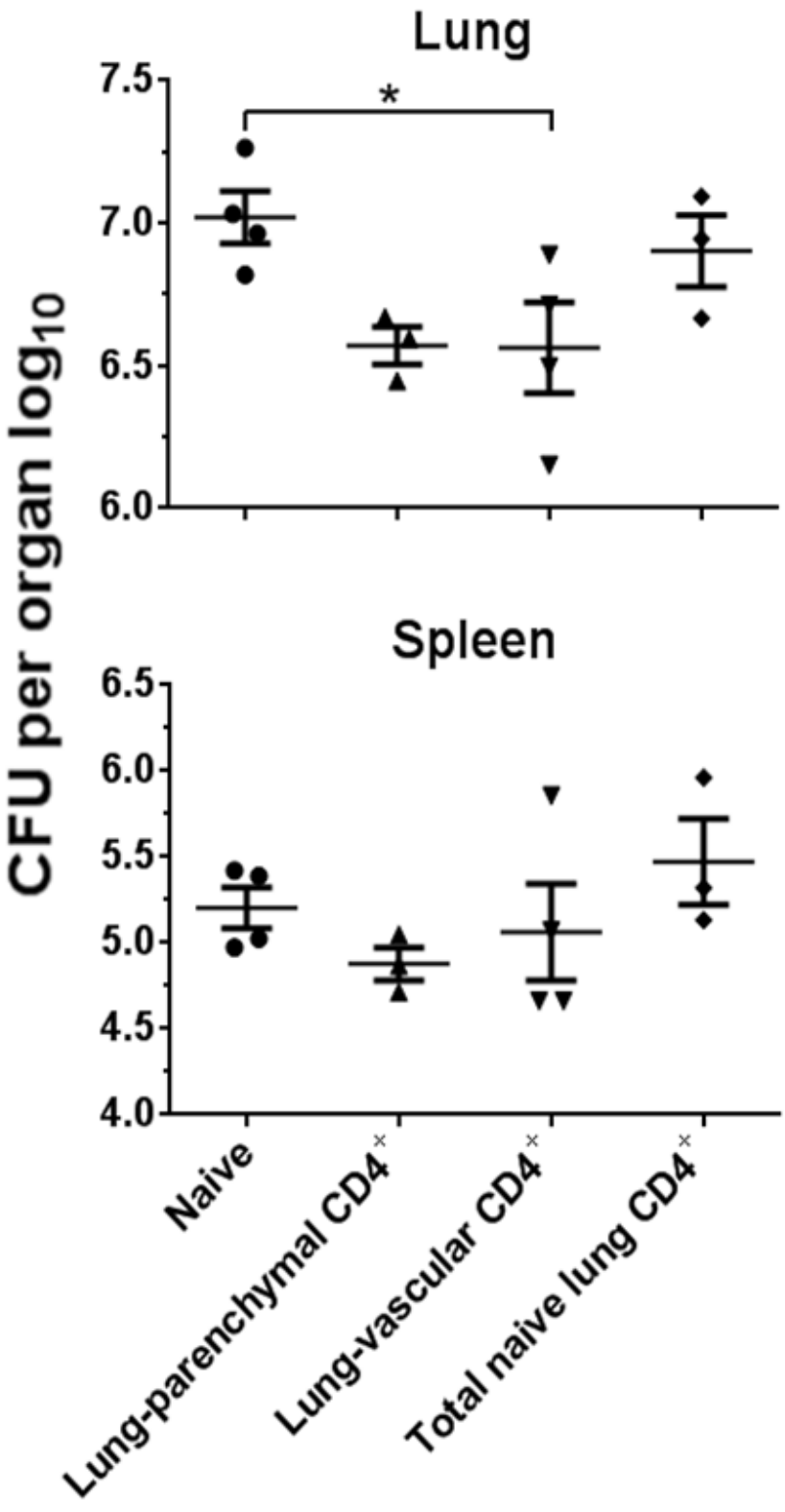

Figure 6.4 - Protection against aerosol *M.tb* challenge following adoptive transfer of standardised numbers of CD90.1$^+$ CD4$^+$ T cells. BALB/c mice received intranasal BCG

immunisation and were euthanased 6 weeks later following intravascular staining. Lungs were FACS sorted into lung-parenchymal and lung-vascular $CD4^+$ T cells. Naïve control animals had total lung sorted for $CD4^+$ T cells, without intravascular staining. $CD4^+$ T cells were transferred via intravenous injection into recipient BALB/c mice. Groups of recipient mice received ~ $5.5x10^5$ $CD4^+$ T cells from the lung vasculature or lung parenchyma of immunised donor mice or ~ $5.5x10^5$ $CD4^+$ T cells taken from the total lung of naïve mice. 24 hours after adoptive transfer, recipient mice were challenged with *M.tb* via aerosol. Four weeks post-challenge, lungs and spleen were removed for CFU enumeration. Individual $\log_{10}$ CFU counts are shown for the lung (a) and spleen (b) with bars indicating mean and error bars showing SEM (n≥3 mice per group). * $\rho \leq 0.05$, one-way ANOVA with Tukey's post-test for significance.

6.3. Discussion

Data included in this chapter reveals that $CD4^+$ T cells present within the lung-parenchyma following intranasal BCG vaccination have enhanced proliferative capacity compared to $CD4^+$ T cells present within the lung-vasculature or the spleen. The ability to proliferate suggests that these cells are memory, rather than terminally differentiated effector T cells. This is consistent with data included in the previous chapter describing in the lung-parenchyma the presence of antigen-specific $CD4^+$ T cells with a $PD1^+KLRG1^-$ phenotype, associated with non-terminal differentiation[126, 127, 207, 289]. The finding that lung-parenchymal $CD4^+$ T cells appear to have greater memory potential, as determined by proliferation, may explain the apparent correlation described in the previous chapter between presence of greater numbers of lung-parenchymal $CD4^+$ T cells and enhanced protection against *M.tb* infection in the lung. It suggests that mucosal BCG is able to induce a population of $CD4^+$ T cells within the lung tissue able to respond to pathogenic challenge *in situ* through clonal expansion.

In order to truly establish these lung-parenchymal $CD4^+$ T cells as the population responsible for enhanced protection against *M.tb* infection, a series of adoptive transfer experiments were conducted. Studies published in the existing literature describe adoptive transfer of lung-parenchymal $CD4^+$ T cells from *M.tb*-infected mice[126, 127]. In these studies, the cells are shown to be able to migrate back to the lung-parenchyma of the recipient mice and confer protection against subsequent *M.tb* infection. However, the transfer is performed into either infection-matched recipients or T cell-deficient recipients.

In infection-matched recipients, the lung will be undergoing a process of active inflammation which may result in non-specific recruitment of T cells. Thus it is unclear whether the migration of donor parenchymal T cells to the parenchyma is a result of inherent lung-homing capacity. It is for this reason that experiments presented in this chapter involve adoptive transfer into naïve recipients rather than infected animals. Sakai *et al.* do demonstrate increased efficiency of migration into the parenchyma by the parenchymal donor cells, compared to those taken from the lung-vasculature; however entry to the parenchyma is not exclusively restricted to cells originating in the parenchyma, with cells of lung-vascular origin also entering the tissue[126]. This is consistent with findings presented in this chapter, where $CD4^+$ T cells taken from the lung-parenchyma, lung-vasculature and spleen of BCG-immunised mice all entered the lung-parenchyma of naïve recipient animals following adoptive transfer.

A limitation of the experiment presented here was the difference in numbers of $CD4^+$ T cells from each tissue compartment transferred to recipients. In order to account for this, data from groups receiving naïve total lung $CD4^+$ T cells from 1 donor, lung-parenchymal $CD4^+$ T cells from 2 donors and lung-vascular $CD4^+$ T cells from 1 donor was analysed separately, as in these groups recipient animals received roughly equivalent numbers of cells. This analysis revealed a higher frequency of lung-parenchymal donor cells present in the lung-parenchyma of recipients, compared to lung-vascular or naïve total lung donor $CD4^+$ T cells. This is in keeping with the increased efficiency of migration reported by Sakai *et al*[126].

In order to determine the ability of transferred cells to confer protection against *M.tb* infection, experiments were performed in which recipient animals were challenged with *M.tb* via aerosol following adoptive transfer. In the published studies demonstrating

protection by lung-parenchymal $CD4^+$ T cells transferred from *M.tb*-infected donors, recipient animals were all T cell-deficient[126, 127]. Concerns have been raised over the validity of using immunodeficient mice as a model for studying $CD4^+$ T cell-mediated protection against tuberculosis[313]. Colitis and systemic chemokine response in immunodeficient recipients following transfer of $CD4^+$ T cells from either naïve or BCG-vaccinated mice has been reported, which may affect their responses to mycobacterial challenge. Another indication that this model may not reflect responses in immunocompetent animals is the observation that both $CD4^+$ T cells transferred from naïve mice and $CD62L^{hi}$ $CD4^+$ T cells transferred from BCG-immunised mice proliferated and developed an activated effector phenotype in the lungs of recipient mice, whether or not they were challenged with infectious mycobacteria[313].

In order to more accurately reflect the situation of natural infection in an immunocompetent host, adoptive transfer experiments conducted here were performed with fully immunocompetent naïve recipient mice. This may have made it more challenging to be able to observe protection in these recipient animals following aerosol *M.tb* challenge, however, it was observed in two separate experiments that $CD4^+$ T cells transferred from the lung-vasculature of BCG-immunised mice were able to confer some protection in the lungs of recipient mice post-challenge. The first challenge experiment described had the same limitation as the lung-homing experiment, as the numbers of $CD4^+$ T cells from each tissue compartment transferred to recipients differed between groups. Protection was observed in the lungs of mice receiving lung-vascular $CD4^+$ T cells from 2 donors, but not from 1 donor, implying that there is a minimum number of cells which must be transferred in order for protection to be detectable. In order to overcome this limitation

in the second challenge experiment, numbers of cells transferred were standardised between groups and increased in order to ensure that they exceeded the threshold determined by the previous experiment, below which protection was not observed. This introduced technical difficulties, as obtaining the required number of $CD4^+$ T cells for transfer into recipients was challenging, resulting in low group numbers. Therefore, whilst protection could again be observed in the group receiving lung-vascular $CD4^+$ T cells, statistically significant protection was not achieved in the group receiving lung-parenchymal $CD4^+$ T cells, despite a trend towards lower bacterial burden in the lungs.

These experiments suggest that $CD4^+$ T cells transferred from the lungs of mice immunised intranasally with BCG are able to confer protection against *M.tb* challenge in naïve mice, but do not demonstrate any enhancement of protection conferred by the transfer of $CD4^+$ T cells obtained specifically from the lung-parenchyma of donor animals. This may be explained by the observation in the lung-homing experiment that very few of the $CD4^+$ T cells transferred from either compartment of the lungs actually migrated into the lung-parenchyma of recipient animals. Experiments described in the previous chapter indicate that enhanced protection against *M.tb* infection in the lung appears to be related to increased numbers of $CD4^+$ T cells being present within the parenchyma. In these adoptive transfer experiments, recipient mice had comparatively few $CD4^+$ T cells present within the parenchyma. If protection is dependent on the number of antigen-specific $CD4^+$ T cells *in situ* within the parenchyma, ready to respond to pathogenic challenge, then this may explain the relative lack of protection observed in the experiments in this chapter when compared to levels of protection observed in the previous chapter.

One of the aims of this chapter was to demonstrate a tropism for lung tissue in the lung-parenchymal $CD4^+$ T cell population, therefore validating their description as a putative 'tissue-resident' population. However, upon adoptive transfer this population circulated to the lung-vasculature and spleen as well as the lung-parenchyma and didn't afford statistically significant protection against *M.tb* infection in recipient animals. Interestingly, Woodworth *et al.* recently described a population of circulating $CD4^+$ T cells, induced by a subunit vaccine against TB, which share phenotypic characteristics of lung-parenchymal $CD4^+$ T cells, with reduced KLRG1 and increased CXCR3 expression, and which efficiently traffic into *M.tb*-infected lung-parenchyma[218]. This may indicate that it is not necessary for $CD4^+$ T cells to be permanent residents in the lung in order for them to provide protection against *M.tb* infection. Indeed it may be enough for a vaccination to induce a population of $CD4^+$ T cells with the characteristics of lung-parenchymal cells, which are able to efficiently migrate to the lung when presented with a pathogenic challenge.

There were several general limitations of the adoptive transfer experiments presented here which could not be overcome. Firstly, the lack of an effective MHCII tetramer to identify antigen-specific $CD4^+$ T cells meant that the whole $CD4^+$ T cell population from each tissue compartment had to be sorted and transferred. Data presented in the previous chapter reveals that in fact only a small percentage of the total $CD4^+$ T cells found in each compartment, up to ~7%, produce cytokine upon stimulation with cognate antigen. The implications of this are unclear. The lung-homing experiment shows that only a very small percentage of the total number of $CD4^+$ T cells transferred into each recipient were recovered from the lungs and spleen 24 hours later. Some of the undetected cells may have been present in other tissues of the body, but it is also possible that a large proportion may

have died. It may be that transferring smaller numbers of purely antigen-specific $CD4^+$ T cells would have resulted in better survival of these cells. Another limitation was the use of total lung $CD4^+$ T cells from naïve animals as a negative control, rather than separating this into lung-parenchymal and lung-vascular populations. This was necessary because in the absence of IN BCG immunisation, only a very small proportion of the total $CD4^+$ T cells in the lung are present within the parenchyma, ~5%. In order to obtain sufficient cells from this compartment to transfer, numbers of donor animals would have to be increased dramatically, beyond the number that could be processed within the timeframe required for transfer. Even in immunised donor animals, numbers of $CD4^+$ T cells obtained from the lung-parenchyma and lung-vasculature were a limiting factor and this necessitated small group sizes for the challenge experiments. Logistically it was not possible to derive enough cells to transfer into larger numbers of recipient mice. This limited the possibility of detecting statistically significant protection in infected animals.

In conclusion, results presented in this chapter reveal an enhanced proliferative capacity of lung-parenchymal $CD4^+$ T cells present following IN BCG vaccination. This may explain the superior protection against *M.tb* infection in the lungs of intranasally-vaccinated animals described in the previous chapter, as this appeared to be associated with larger numbers of antigen-specific $CD4^+$ T cells in the lung-parenchyma, some of which exhibited a 'memory-like' $PD1^+KLRG1^-$ cell-surface phenotype. However, the results do not definitively prove an enhanced lung-homing capacity of these lung-parenchymal $CD4^+$ T cells, or the ability to confer enhanced protection against *M.tb* challenge to a naïve mouse following adoptive transfer. This may be due in part to some of the technical challenges involved in the adoptive transfer experiments, as described above, but could also be interpreted as

evidence in support of the theory suggested by Woodworth *et al.*[218] that these cells may not necessarily be permanent lung-residents but are able to circulate through the body and return to the lung when required, in response to pathogenic challenge. Further work is required in order to determine this conclusively.

Chapter 7.

Conclusions and future work

This project aimed to characterise the role of lung T_{RM} in protection provided by the BCG vaccine against *M.tb* infection, utilising an intravascular staining technique[121] to identify T_{RM}. Optimisation of the intravascular staining technique has allowed for clear discrimination between lung-parenchymal and lung-vascular $CD4^+$ T cells, enabling the independent study of these two populations distinct from one another. Recently, Kauffman *et al.* published the first report of intravascular staining in NHPs[314]. The prospect of expanding utilisation of this technique into other animal models apart from mice, particularly NHPs which more closely mimic humans in their response to *M.tb* infection[96, 97], is very exciting.

Despite the clarity afforded by the use of the intravascular staining technique, there have been some fundamental challenges to the classification of the lung-parenchymal $CD4^+$ T cell population as T_{RM}. These include: difficulty in proving permanent residency in the lung tissue, lack of definitive phenotype with which to identify this population, lack of understanding of the relationship between these T cells and other anatomically distinct, but possibly related, populations, for example airway luminal T cells, and finally difficulty in determining that they are truly memory T cells in spite of BCG persisting in the body for extended periods following vaccination. All of these challenges are discussed below, along with suggested approaches to address some of the issues raised and strengthen the data included in this thesis.

Data presented within this thesis reveal that both systemic and mucosal BCG immunisation induce populations of antigen-specific lung-parenchymal $CD4^+$ T cells, a putative tissue-resident population. One of the major challenges to defining this population as truly T_{RM} is

the difficulty in proving permanent residency in the lung tissue. Teijaro *et al.*[120] used parabiosis experiments to define a population of $CD4^+$ T cells specifically retained within the lungs following influenza infection. This retention was demonstrated for studies of up to 3 weeks in duration, but this sort of experiment cannot easily be performed for the study of chronic infections such as *M.tb*, as mice would have to remain surgically conjoined for much longer periods. Therefore, experiments in this thesis and in the TB literature have focussed on establishing 'residency' through physically locating cells in the lung-parenchyma, identifying cell-surface markers associated with residency and adoptively-transferring these cells into other mice to track their migration and establish a tropism for lung tissue.

Identification of a cell-surface phenotype with which to define the lung-parenchymal population has proven challenging. Several studies describe a number of phenotypic cell-surface markers as indicative of tissue-residence and, in particular, CD69 has been suggested to not only identify lung-residence but also to play a part in the mechanism of retention of T_{RM} in the tissue[215, 260, 262, 265]. Work described here examined a selection of these markers, including CD69, for their expression on BCG-induced antigen-specific lung-parenchymal and lung-vascular $CD4^+$ T cells, but it was not possible to define a phenotype uniquely expressed by one population or the other. Analysis of transcription factors rather than cell-surface markers may provide further information. Moguche *et al.*[127] used a murine model of *M.tb* infection to demonstrate that generation of lung-parenchymal $CD4^+$ T cells requires intrinsic expression of Bcl6 and that $PD1^+$ $KLRG1^-$ $CD4^+$ lung-parenchymal T cells express intermediate T-bet levels. Further work could be conducted to confirm these

findings in the context of BCG vaccination and to investigate additional transcription factors which may be differentially expressed by lung-parenchymal and lung-vascular populations.

Adoptive transfer experiments also failed to conclusively demonstrate selective lung-homing capacity in the lung-parenchymal $CD4^+$ T cell population. This may have been due to technical challenges experienced during the experimental process, discussed in greater detail in chapter 6. However, an alternative theory, presented by Woodworth *et al.*[218], suggests that certain characteristics of lung-parenchymal T cells may be shared with T cells present in the vasculature, allowing them to efficiently traffic into the lung tissue in response to pathogenic challenge. This theory aligns with data presented in this thesis, revealing that adoptively-transferred lung-vascular and splenic $CD4^+$ T cells could be recovered from the lung-parenchyma of recipients. This indicates that the parenchymal compartment is accessible to cells other than those originating there. However, this has not been tested in the context of *M.tb* infection as part of this project. Future work building on the findings of this thesis could include studies performing adoptive transfer experiments into recipient animals infected with *M.tb*.

A recent paper by *Kauffman et al.*[314] also supports this theory. This study, performed in rhesus macaques, reveals that all *M.tb*-specific $CD4^+$ T cells present in the granulomas of the lung following primary infection, had extravasated across the vascular endothelium to enter the parenchyma. The authors suggest that it is not lung-homing capacity which limits the ability of $CD4^+$ T cells to control *M.tb* infection, but the fact that the $CD4^+$ T cells in the lung are located within the outer lymphocyte cuff of the granulomas, rather than within the myeloid cell core containing the bacilli. This position within the granuloma limits $CD4^+$ T cell interactions with *M.tb*-infected macrophages, and direct contact has been shown to be a

requirement for killing of infected cells[295]. This implies that a successful vaccine would need to control *M.tb* infection rapidly, prior to the development of granulomas, in order to be effective.

It has been suggested that swift control of invading bacilli is aided by the presence of antigen-specific $CD4^+$ T cells *in situ* within the lung, ready to respond as soon as infection occurs[272]. This may explain the superior protection observed in this thesis in mucosally BCG-vaccinated compared to systemically BCG-vaccinated mice, which had greater numbers of antigen-specific $CD4^+$ T cells present within the lung-parenchyma and the BAL. This finding, that mucosal BCG appears to recruit $CD4^+$ T cells to the lung-parenchyma and airways, adds to our knowledge from existing studies in the literature, demonstrating that $CD4^+$ T cells from the periphery have the ability to enter the lung-parenchyma in response to *M.tb* infection[218, 314]. Future experiments could be performed to investigate whether other antigenic stimuli, for example viral-vectored TB vaccine candidates, could also recruit these cells to the lung if delivered mucosally. Future vaccination strategies could then be considered using a 'prime-pull' approach, whereby immune cells are primed in the periphery by an initial immunisation, before being drawn into the tissue by a second targeted immunisation.

Britton *et al.*[315] have already investigated this approach within a mouse model, using BCG and a lentiviral-vectored vaccine expressing antigen 85A (Ag85A), an immunodominant *M.tb* protein[316]. When the systemic 'prime' and mucosal 'pull' immunisations were both performed with the viral-vectored vaccine, antigen-specific $CD4^+$ and $CD8^+$ T cell responses were significantly enhanced within the lung, compared to animals receiving BCG prime followed by viral-vectored boost. However, it should be noted that this study doesn't use

the intravascular staining technique, so these results must be interpreted with the caveat that these cells may have been present within the vasculature of the lung rather than the tissue itself. The study finds that despite the enhanced antigen-specific responses, mice were not protected against mucosal BCG infection.

Stylianou *et al.* also used viral-vectored boost vaccines expressing Ag85A administered mucosally, following a systemic BCG prime[285]. Mice were boosted intranasally with a replication-deficient chimpanzee adenovirus expressing Ag85A (ChAdOx1.85A). As in the study by Britton *et al.*, this regime induced strong immune responses in the lung, yet failed to provide consistent protection against *M.tb* infection. However, the authors find that boosting again with a modified vaccinia virus Ankara also expressing Ag85A (MVA85A), not only induced strong immune responses but was able to significantly improve the protective efficacy of BCG alone. Interestingly, this second boost with MVA85A was equally protective when delivered either mucosally or systemically.

Jeyanathan *et al.* describe enhanced protective immunity in the lungs and spleen of mice receiving a subcutaneous BCG prime followed by an intranasal boost with a different replication-deficient chimpanzee adenovirus expressing Ag85A (AdCh68Ag85A)[284]. In contrast to the previously-described study, this regime did not require a second boost immunisation in order to achieve significantly improved protection against *M.tb* infection, compared to animals receiving systemic BCG alone. The differing findings from these studies suggest that further work is needed to investigate the immunological mechanisms underlying protection provided by prime and pull vaccination approaches against TB, and that careful antigen and vector selection is required in order to elicit the required responses in the lung. Separate analysis of lung-parenchymal and lung-vascular T cells,

through use of intravascular staining for future studies, may well provide new insight into these promising vaccination regimes.

Data presented in this thesis identify a cell-surface phenotype uniquely expressed on $CD4^+$ T cells present in the lung-parenchyma and BAL fluid of mice following mucosal BCG vaccination, $PD1^+$ $KLRG1^-$, suggesting that these two populations of cells may be related. If circulating T cells are able to enter the parenchyma in response to mucosal vaccination or pathogenic challenge, then it may be the case that these same cells are subsequently recruited to the airways from the tissue, providing immune responsiveness throughout the lung. Reutershan *et al.*[222] describe a similar process of sequential recruitment of neutrophils into the lung and BAL fluid of mice following acute LPS-induced lung injury. They track this recruitment of cells through performing intravascular staining at different time points post-injury to identify cells present initially in the vasculature, then in the parenchyma and finally in the BAL. This is possible for the study of an acute injury, where cells are migrating over a short time period, but would be more challenging in the context of studying a chronic infection such as *M.tb*. This approach also fails to identify movement of individual cells, and only reports changes in the total size of cell populations in each compartment.

If there is indeed a dynamic relationship between $CD4^+$ T cells in the periphery, the lung-parenchyma and the airways, it may be that a greater understanding of the mechanisms of immunological protection against *M.tb* infection is only possible when considering multiple tissue compartments and their relationship with one another. The focus of this project has been on lung T_{RM}, although airway luminal T cells, recovered in BAL fluid, have also been suggested to play an important role in protection against *M.tb* infection and may be an

important focus of future vaccination strategies[317]. In order to fully understand the migration of cells between different populations and their ability to traffic through the body, whole-body imaging techniques open up new possibilities. Adoptively-transferred T cells have been traced in recipient animals through use of magnetic resonance imaging (MRI), single photon emission computed tomography (SPECT) and positron emission tomography (PET) techniques[318]. Use of these techniques could provide insight into the migration of T cells from the periphery to the lung and then into the airways, in the context of BCG vaccination and *M.tb* infection.

Another challenge to the definitive characterisation of the BCG-induced lung-parenchymal $CD4^+$ T cell population as $T_{RM,}$ is the difficulty in proving that they are actually memory T cells rather than effector T cells. Memory can only truly be described when present in the absence of cognate antigen, and previous work demonstrates that BCG can persist for extended periods of at least 16 months in vaccinated mice[199]. For this reason, *ex-vivo* proliferation assays have been used within this thesis, as the ability to proliferate in response to cognate antigen suggests memory rather than terminally-differentiated effector T cells. Cells with proliferative capacity were present in the spleen and both lung compartments following mucosal BCG immunisation, with a greater frequency of these cells found in the parenchymal compartment. The assessment of proliferation provides functional information about these cells, but as the assays require 3 days of culture and stimulation it is impossible to reliably determine their phenotype at the end of this period without the caveat that it may have altered during culture. A further limitation of this work was the relatively large number of cells required for the assays, prohibiting inclusion of BAL T cells due to the limited number of these cells recovered from mice. Further work could be

performed to optimise analysis of proliferation in BAL cells, in order to determine whether airway luminal T cells also exhibit this hallmark of memory.

Other studies have determined memory through utilisation of antibiotic treatment to remove BCG or *M.tb* from immunised or infected animals, ensuring that all antigen-specific T cells remaining were not the product of a recent antigen interaction[199, 319-321]. These memory cells were reported to be long-lived[319], rapidly accumulate in the infected organs[320, 321] and mediate protection against subsequent *M.tb* challenge[199, 319-321]. No studies have investigated the location of these cells utilising the intravascular staining technique to separate lung-parenchymal and lung-vascular populations, or determined whether they are also present in the airways of the lung. Future work building on the findings of this thesis could be performed in order to determine whether these memory cells are retained within specific tissue niches in the lung and airways. This would provide valuable additional information, as these cells could undergo phenotyping and be quantified, both of which were not possible when using the techniques employed within this thesis to measure proliferation. However, Kaveh *et al.*[199] report that following antibiotic clearance of BCG in a mouse model, antigen-specific $CD4^+$ T cells were subsequently undetectable in the spleen and lung of these animals. It may be that so few memory T cells are maintained that they are below the limit of detection of the flow cytometric assay used.

An alternative method of identifying long-lived memory T cells could be achieved through adoptively-transferring T cells from BCG-immunised or *M.tb*-infected mice into naïve recipient mice, waiting for a period of time beyond which effector cells would not survive in the absence of antigenic stimulation, and then identifying the remaining antigen-specific T

cells. However, work conducted in this thesis describing adoptive transfer of T cells into naïve recipients found that only a very small proportion of those cells transferred were detectable in the recipient mouse just 24 hours after transfer. This loss could result in difficulties detecting the memory population at a later time point, due to the sensitivity of detection of our current methods for identifying antigen-specific T cells. Steinert *et al.*[322] have shown that there are many more lung lymphocytes identifiable histologically than are obtained through traditional tissue homogenisation techniques. If we are seeking to identify very small numbers of memory T cells, any loss of these through the harvesting process could result in the population being too small to detect. However, Moguche *et al.*[127] have successfully used this approach to identify antigen-specific $CD4^+$ T cells in the spleen of naïve recipient mice up to 28 days following their transfer from *M.tb*-infected donor mice. Therefore, future work could be performed to build on the findings of this study through identification of memory T cells in the lung and airways, as well as the spleen, following adoptive transfer.

In summary, work presented in this thesis identifies antigen-specific $CD4^+$ T cells in the parenchyma of the lung following BCG vaccination, a putative lung T_{RM} population. It has not been possible to definitively prove their long-term residence in the lung tissue or their true memory status, although further work described above could be conducted to address these points. This lung-parenchymal population is increased following mucosal BCG vaccination, correlating with improved protection against *M.tb* infection in mucosally-vaccinated compared to systemically-vaccinated animals. This finding highlights the potential of mucosal vaccination to elicit lung T_{RM}, and identifies this as a possible immunological mechanism underlying the enhanced protective efficacy of BCG delivered

mucosally. It is now important to determine the effect of delivery of new candidate TB vaccines or prime and boost regimes, via mucosal routes, on the lung-parenchymal population, and perform further evaluation in humans, with the ultimate goal of developing an efficacious vaccination regime to aid in the global fight against TB.

Appendix

8.1. Reagent details

1) Middlebrook 7H9 Broth[323]

4.7g Difco Middlebrook 7H9 broth (BD Biosciences)

0.5g Tween 80 (Sigma)

4.2g Sodium Pyruvate (Sigma)

900ml distilled water

100ml BBL Middlebrook OADC enrichment (BD Biosciences)

2) Modified 7H11 agar plates[323]

Produced by the Animal and Plant Health Agency media production department, Weybridge, according to this method:

16g Difco Middlebrook 7H11 Agar base (BD Biosciences)

4.2g Sodium Pyruvate

900ml distilled water

Autoclave (121°C/ 15min) then allow to cool to <50°C

100ml BBL Middlebrook OADC enrichment

Pour into sterile Petri dishes (~20ml)

3) Complete medium

Dulbecco's Modified Eagle Medium (DMEM) (Sigma)

10% Foetal bovine serum - heat inactivated (FBS) (Sigma)

2% Penicillin (100 units/ml) Streptomycin (100µg/ml) (Sigma)

4) Digestion medium

Complete media supplemented with:

150 units/ml Collagenase I (Gibco)

10 units/ml DNAse II (Sigma)

5) Flow wash buffer

HBSS (Gibco) supplemented with:

2% FBS

0.05% NaN_3 (Sigma)

8.2. Flow cytometry antibodies

Specificity	Fluorochrome	Clone	Supplier
CD4	APC-H7	GK1.5	BD Biosciences
	AF700	RM4-5	eBioscience
	APC	RM4-4	Biolegend
CD8	AF700	53-6.7	Biolegend
CD27	PerCP-Cy5.5	LG.7Fp	eBioscience
CD44	BV785	IM7	Biolegend
	BV421	IM7	Biolegend
CD45	PE	C363.16A	eBioscience
CD62L	FITC	MEL-14	BD Biosciences
	PerCP-Cy5.5	MEL-14	eBioscience
CD90.1	BV421	HIS51	Biolegend
CD90.2	eFluor450	30-H12	eBioscience
	FITC	30-H12	Biolegend
CD127	PE-Cy7	A7R34	Biolegend
CCR7	BV421	4B12	Biolegend
PD-1	FITC	29F.1A12	Biolegend
KLRG1	PerCP-Cy5.5	2FI/KLRG1	Biolegend
CXCR3	BV421	CXCR3-173	Biolegend

Ki67	PE	11F6	Biolegend
EdU	AF647		Invitrogen
Dead	Zombie Aqua		Biolegend
IFN-γ	PE-Cy7	XMG1.2	eBioscience
	BV605	XMG1.2	Biolegend
IL-2	APC	JES6-5H4	eBioscience
TNF-α	BV605	MP6-XT22	Biolegend
	PerCP-Cy5.5	MP6-XT22	eBioscience

8.3. Flow cytometry panels

Panel 1

CD62L-FITC, CD27-PerCP-Cy5.5, CD45-PE (intravascular stain), CD8-AF700, CD4-APC-H7, CD44-BV421, CD90.2-eFluor 450, dead-Zombie Aqua, IFN-γ-PE-Cy7, IL-2-APC, TNF-α-BV605

Tetramer panel

CD62L-FITC, CD27-PerCP-Cy5.5, CD45-PE (intravascular stain), CD8-AF700, CD4-APC-H7, CD44-BV421, CD90.2-eFluor 450, TB10.4-tetramer-APC dead-Zombie Aqua

Panel 2

CD127-PE-Cy7, CD62L-PerCP-Cy5.5, CD45-PE (intravascular stain), CD8-AF700, CD4-APC-H7, CD44-BV785, CCR7-BV421, dead-Zombie Aqua, IFN-γ-BV605, IL-2-APC

EdU panel

CD90.2-FITC, CD62L-PE-Cy7, EdU-AF647, CD8-AF700, CD4-APC-H7, CCR7-BV421, CD44-BV785, CD27-PerCP-Cy5.5, dead-Zombie Aqua

Panel 3

PD-1-FITC, CD44-BV785, CD8-AF700, CD4-APC-H7, KLRG1-PerCP-Cy5.5, CD45-PE (intravascular stain), CXCR3-BV421, dead-Zombie Aqua, IFN-γ-PE-Cy7, IL-2-APC, TNF-α-BV605

Adoptive transfer panel

CD90.2-eFluor 450, CD44-BV785, CD90.1-FITC, CD45-PE (intravascular stain in donor mice, CD4-APC (intravascular stain in recipient mice), CD4-AF700 (stain for sort), CD4-APC-H7, dead-Zombie Aqua, IFN-γ-BV605, IL-2-PE-Cy7, TNF-α-PerCP-Cy5.5

Ki67 panel

CD90.1-BV421, CD44-BV785, Ki67-PE, CD4-APC-H7, dead-Zombie Aqua

8.4. Flow cytometry gating strategy

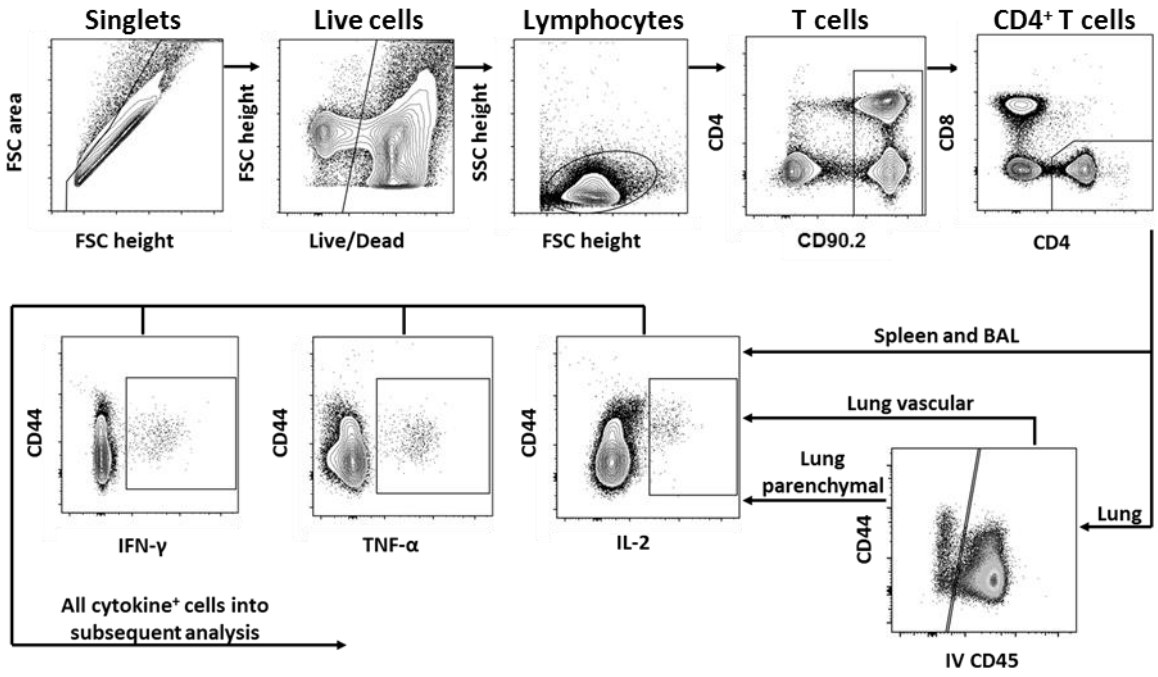

Figure 8.1 - Gating strategy for identification of $CD4^+$ T cells producing IFN-γ, TNF-α or IL-2 alone or in combination with each other. Cells are gated on singlets followed by live cells and then lymphocytes. T cells are identified as $CD90.2^+$ before gating on $CD4^+$ and identifying $CD44^{hi}$ cells producing IFN-γ, TNF-α or IL-2. Boolean gating is then used to identify all $CD4^+$ cells producing one or more of these cytokines ($cytokine^+$). For analysis of lung lymphocytes, an additional step of gating based on intravascular staining is performed prior to identification of $cytokine^+$ cells.

8.5. Representative flow cytometry plots

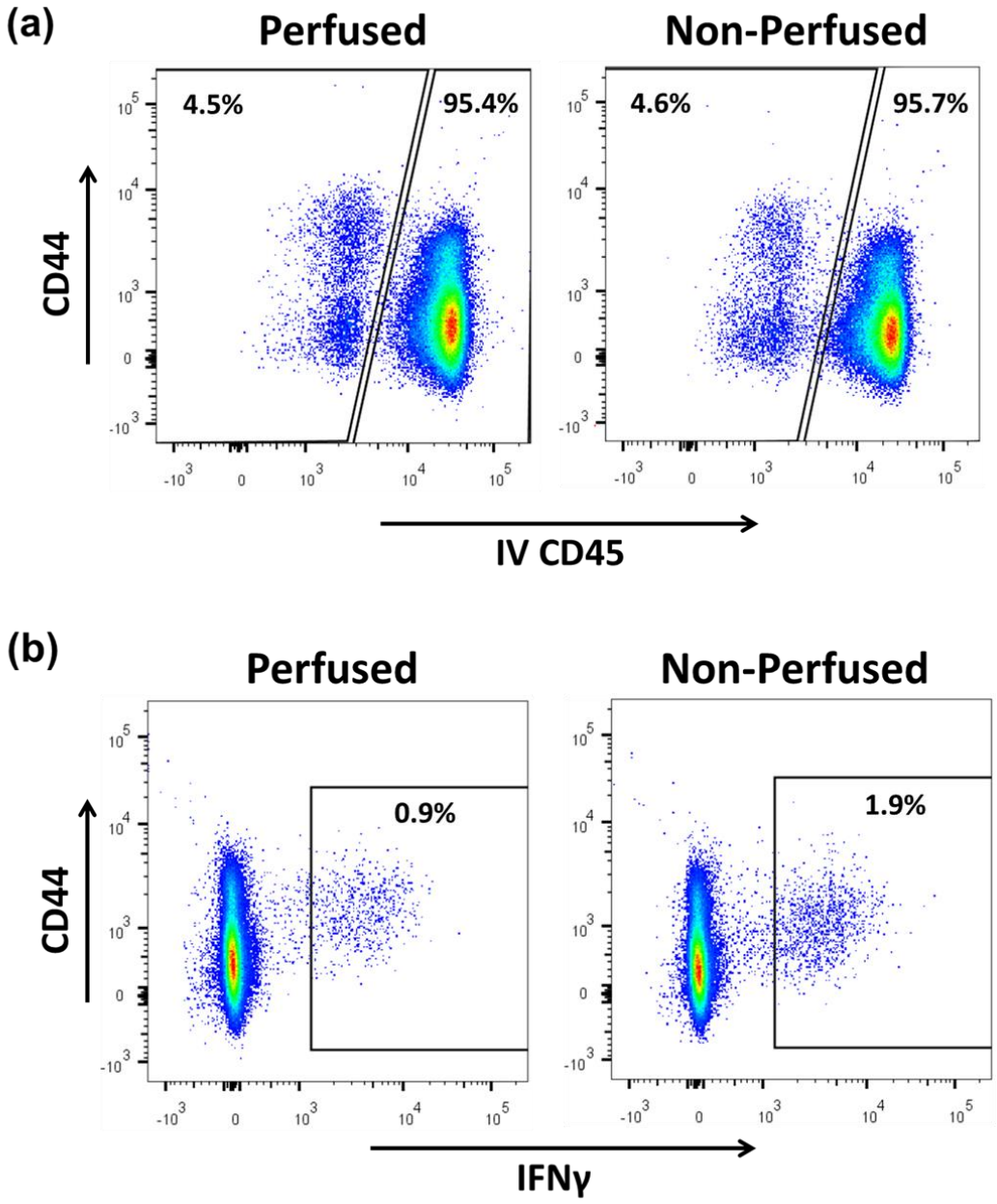

Figure 8.2 – Comparison between perfusion and non-perfusion of lungs. (a) Representative plots showing lungs from 2 BCG-immunised mice, following perfusion (left) or non-perfusion (right), pre-gated on $CD4^+$ T cells. Gates are drawn defining lung-parenchymal and lung-vascular populations, based on intravascular staining with anti-CD45 mAb. (b) Representative plots from 2 BCG-immunised mice, following perfusion (left) or

non-perfusion (right), showing IFNγ production by $CD4^+$ T cells, pre-gated on lung-vascular $CD4^+$ T cells.

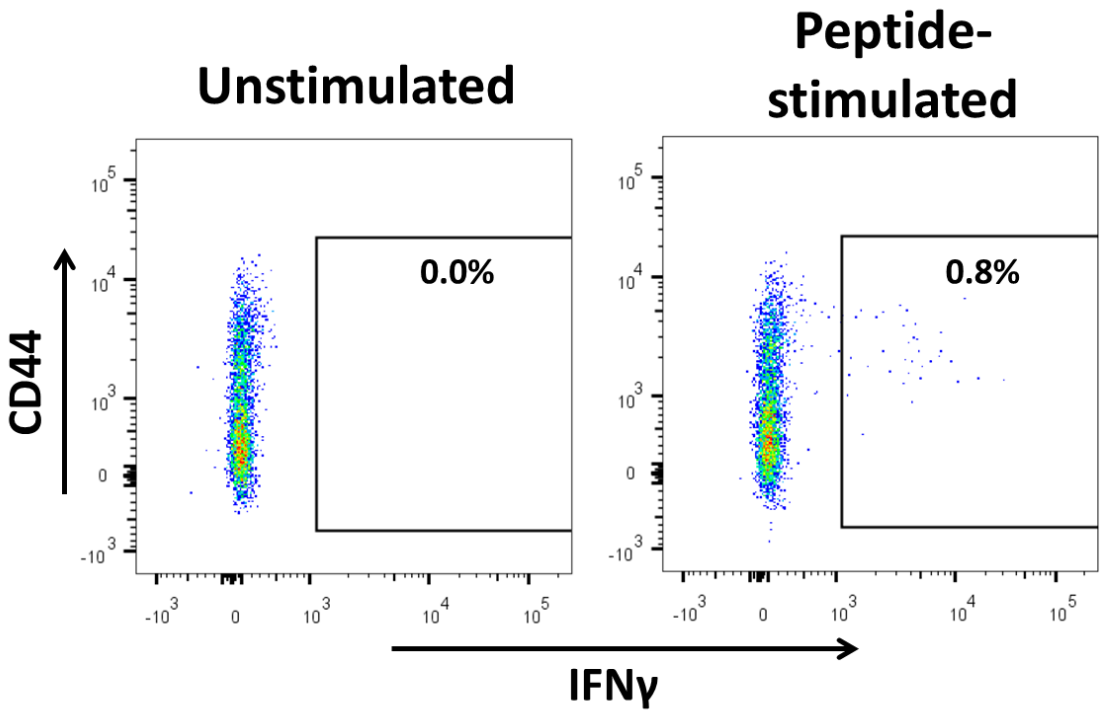

Figure 8.3 – IFNγ production by unstimulated and TB10.4 peptide-stimulated CD4$^+$ T cells. Representative plots showing production of IFNγ by lung-parenchymal CD4$^+$ T cells taken from the same BCG-immunised animal, either left unstimulated in overnight culture (left) or stimulated with TB10.4 peptides in overnight culture (right). Plots are pre-gated on lung-parenchymal CD4$^+$ T cells.

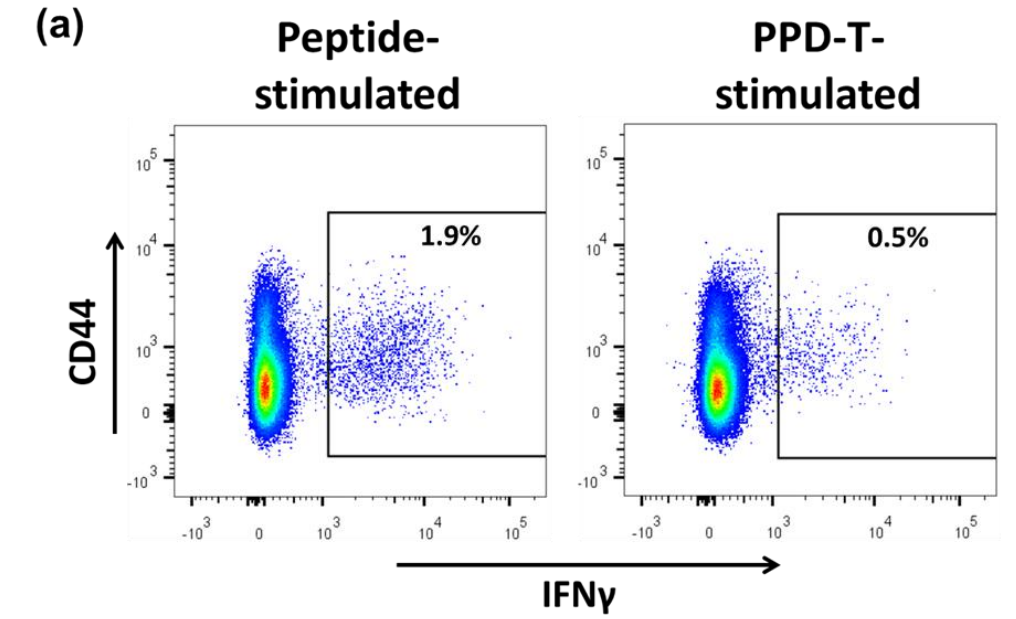
(a)
Peptide-stimulated
PPD-T-stimulated
1.9%
0.5%
CD44
IFNγ

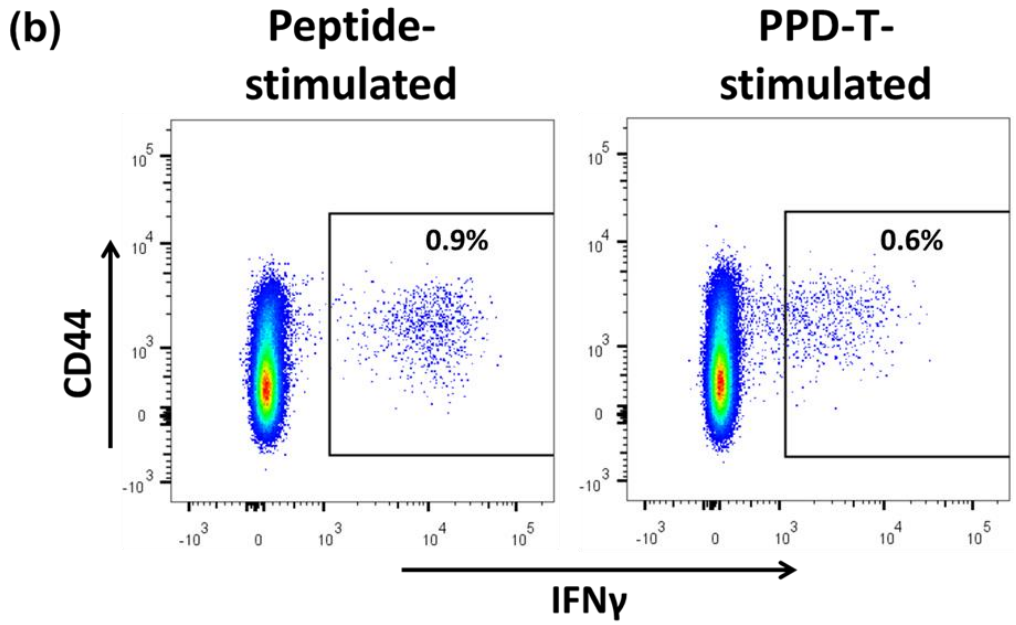
(b)
Peptide-stimulated
PPD-T-stimulated
0.9%
0.6%
CD44
IFNγ

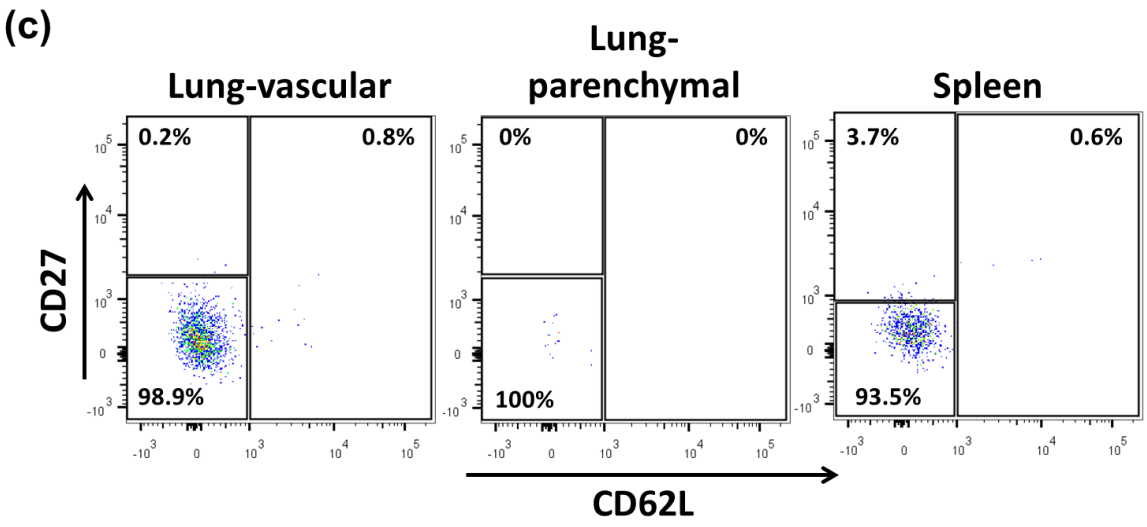

Figure 8.4 – Comparison between TB10.4 peptide-stimulation and PPD-T protein-stimulation. Representative plots showing IFNγ production by (a) lung-vascular and (b) splenic $CD4^+$ T cells harvested from the same BCG-immunised animal and stimulated with TB10.4 peptides (left) or PPD-T protein (right) in overnight culture. (c) Cell-surface expression of CD62L and CD27 on $cytokine^+$ $CD4^+$ T cells from the lung-vasculature, lung-parenchyma and spleen of the same BCG-immunised animal. Plots are pre-gated on $cytokine^+$ $CD4^+$ T cells.

Bibliography

1. WHO. *Global Tuberculosis Report 2016*. 2016 [cited 2017 22nd May]; Available from: http://www.who.int/tb/publications/global_report/en/.

2. Dye, C., S. Scheele, P. Dolin, V. Pathania, M.C. Raviglione, W.H.O.G.S. for the, and P. Monitoring, *Global burden of tuberculosis: Estimated incidence, prevalence, and mortality by country.* JAMA, 1999. **282**(7): p. 677-686.

3. Pareek, M., C. Greenaway, T. Noori, J. Munoz, and D. Zenner, *The impact of migration on tuberculosis epidemiology and control in high-income countries: a review.* BMC Medicine, 2016. **14**(1): p. 48.

4. WHO. *The End TB Strategy*. 2014 [cited 2017 22nd May]; Available from: http://www.who.int/tb/strategy/en/.

5. WHO. *Drug-resistant Tuberculosis*. 2017 [cited 2017 22nd May]; Available from: http://www.who.int/tb/areas-of-work/drug-resistant-tb/en/.

6. Corbett, E.L., C.J. Watt, N. Walker, and et al., *The growing burden of tuberculosis: Global trends and interactions with the hiv epidemic.* Archives of Internal Medicine, 2003. **163**(9): p. 1009-1021.

7. WHO. *TB and HIV*. 2017 [cited 2017 22nd May]; Available from: http://www.who.int/tb/areas-of-work/tb-hiv/en/.

8. Cosivi, O., J.M. Grange, C.J. Daborn, M.C. Raviglione, T. Fujikura, D. Cousins, R.A. Robinson, H.F. Huchzermeyer, I. de Kantor, and F.X. Meslin, *Zoonotic tuberculosis due to Mycobacterium bovis in developing countries.* Emerging Infectious Diseases, 1998. **4**(1): p. 59-70.

9. Olea-Popelka, F., A. Muwonge, A. Perera, A.S. Dean, E. Mumford, E. Erlacher-Vindel, S. Forcella, B.J. Silk, L. Ditiu, A. El Idrissi, M. Raviglione, O. Cosivi, P. LoBue, and P.I. Fujiwara, *Zoonotic tuberculosis in human beings caused by Mycobacterium bovis - a call for action.* The Lancet Infectious Diseases, 2017. **17**(1): p. e21-e25.

10. Cole, S.T., R. Brosch, J. Parkhill, T. Garnier, C. Churcher, D. Harris, S.V. Gordon, K. Eiglmeier, S. Gas, C.E. Barry, F. Tekaia, K. Badcock, D. Basham, D. Brown, T. Chillingworth, R. Connor, R. Davies, K. Devlin, T. Feltwell, S. Gentles, N. Hamlin, S. Holroyd, T. Hornsby, K. Jagels, A. Krogh, J. McLean, S. Moule, L. Murphy, K. Oliver, J. Osborne, M.A. Quail, M.A. Rajandream, J. Rogers, S. Rutter, K. Seeger, J. Skelton, R. Squares, S. Squares, J.E. Sulston, K. Taylor, S. Whitehead, and B.G. Barrell,

Deciphering the biology of Mycobacterium tuberculosis from the complete genome sequence. Nature, 1998. **393**(6685): p. 537-544.

11. Garnier, T., K. Eiglmeier, J.-C. Camus, N. Medina, H. Mansoor, M. Pryor, S. Duthoy, S. Grondin, C. Lacroix, C. Monsempe, S. Simon, B. Harris, R. Atkin, J. Doggett, R. Mayes, L. Keating, P.R. Wheeler, J. Parkhill, B.G. Barrell, S.T. Cole, S.V. Gordon, and R.G. Hewinson, *The complete genome sequence of Mycobacterium bovis.* Proceedings of the National Academy of Sciences, 2003. **100**(13): p. 7877-7882.

12. DEFRA. *A Strategy for Achieving Officially Bovine Tuberculosis Free status for England*. 2014 [cited 2017 22nd May]; Available from: https://www.gov.uk/government/publications/a-strategy-for-achieving-officially-bovine-tuberculosis-free-status-for-england.

13. de Lisle, G.W., C.G. Mackintosh, and R.G. Bengis, *Mycobacterium bovis in free-living and captive wildlife, including farmed deer.* Revue scientifique et technique (International Office of Epizootics), 2001. **20**(1): p. 86-111.

14. Zumla, A., P. Nahid, and S.T. Cole, *Advances in the development of new tuberculosis drugs and treatment regimens.* Nat Rev Drug Discov, 2013. **12**(5): p. 388-404.

15. Nathan, C. and C.E. Barry, 3rd, *TB drug development: immunology at the table.* Immunol Rev, 2015. **264**(1): p. 308-18.

16. Davies, P.D., *The role of DOTS in tuberculosis treatment and control.* Am J Respir Med, 2003. **2**(3): p. 203-9.

17. McNerney, R., J. Cunningham, P. Hepple, and A. Zumla, *New tuberculosis diagnostics and rollout.* International Journal of Infectious Diseases, 2015. **32**(Supplement C): p. 81-86.

18. Calmette, A., *Preventive Vaccination Against Tuberculosis with BCG.* Proceedings of the Royal Society of Medicine, 1931. **24**(11): p. 1481-1490.

19. Sakula, A., *BCG: who were Calmette and Guérin?* Thorax, 1983. **38**(11): p. 806-812.

20. Luca, S. and T. Mihaescu, *History of BCG Vaccine.* Mædica, 2013. **8**(1): p. 53-58.

21. Mangtani, P., I. Abubakar, C. Ariti, R. Beynon, L. Pimpin, P.E. Fine, L.C. Rodrigues, P.G. Smith, M. Lipman, P.F. Whiting, and J.A. Sterne, *Protection by BCG vaccine against tuberculosis: a systematic review of randomized controlled trials.* Clin Infect Dis, 2014. **58**(4): p. 470-80.

22. Trunz, B.B., P. Fine, and C. Dye, *Effect of BCG vaccination on childhood tuberculous meningitis and miliary tuberculosis worldwide: a meta-analysis and assessment of cost-effectiveness.* Lancet, 2006. **367**(9517): p. 1173-80.

23. Aronson, N.E., M. Santosham, G.W. Comstock, R.S. Howard, L.H. Moulton, E.R. Rhoades, and L.H. Harrison, *Long-term efficacy of BCG vaccine in American Indians and Alaska Natives: A 60-year follow-up study.* Jama, 2004. **291**(17): p. 2086-91.

24. Hewinson, R.G., H.M. Vordermeier, and B.M. Buddle, *Use of the bovine model of tuberculosis for the development of improved vaccines and diagnostics.* Tuberculosis, 2003. **83**(1–3): p. 119-130.

25. Roche, P.W., J.A. Triccas, and N. Winter, *BCG vaccination against tuberculosis: past disappointments and future hopes.* Trends Microbiol, 1995. **3**(10): p. 397-401.

26. Ottenhoff, T.H.M. and S.H.E. Kaufmann, *Vaccines against Tuberculosis: Where Are We and Where Do We Need to Go?* PLOS Pathogens, 2012. **8**(5): p. e1002607.

27. Oettinger, T., M. Jørgensen, A. Ladefoged, K. Hasløv, and P. Andersen, *Development of the Mycobacterium bovis BCG vaccine: review of the historical and biochemical evidence for a genealogical tree.* Tubercle and Lung Disease, 1999. **79**(4): p. 243-250.

28. Brewer, T.F., *Preventing Tuberculosis with Bacillus Calmette-Guérin Vaccine: A Meta-Analysis of the Literature.* Clinical Infectious Diseases, 2000. **31**(Supplement_3): p. S64-S67.

29. Miceli, I., I.N. De Kantor, D. ColaiÁCovo, G. Peluffo, I. Cutillo, R. Gorra, R. Botta, S. Hom, and H.G.T. Dam, *Evaluation of the Effectiveness of BCG Vaccination Using the Case Control Method in Buenos Aires, Argentina.* International Journal of Epidemiology, 1988. **17**(3): p. 629-634.

30. al-Kassimi, F.A., M.S. al-Hajjaj, I.O. al-Orainey, and E.A. Bamgboye, *Does the protective effect of neonatal BCG correlate with vaccine-induced tuberculin reaction?* American Journal of Respiratory and Critical Care Medicine, 1995. **152**(5): p. 1575-1578.

31. Chaparas, S.D., C.J. Maloney, and S.R. Hedrick, *Specificity of Tuberculins and Antigens from Various Species of Mycobacteria.* American Review of Respiratory Disease, 1970. **101**(1): p. 74-83.

32. Harboe, M., R.N. Mshana, O. Closs, G. Kronvall, and N.H. Axelsen, *Cross-reactions between Mycobacteria.* Scandinavian Journal of Immunology, 1979. **9**(2): p. 115-124.

33. Black, Gillian F., Hazel M. Dockrell, Amelia C. Crampin, S. Floyd, Rosemary E. Weir, L. Bliss, L. Sichali, L. Mwaungulu, H. Kanyongoloka, B. Ngwira, David K. Warndorff, and Paul E.M. Fine, *Patterns and Implications of Naturally Acquired Immune Responses to Environmental and Tuberculous Mycobacterial Antigens in Northern Malawi.* The Journal of Infectious Diseases, 2001. **184**(3): p. 322-329.

34. Weir, R.E., P.E.M. Fine, B. Nazareth, S. Floyd, G.F. Black, E. King, C. Stanley, L. Bliss, K. Branson, and H.M. Dockrell, *Interferon-γ and skin test responses of schoolchildren in southeast England to purified protein derivatives from Mycobacterium tuberculosis and other species of mycobacteria.* Clinical & Experimental Immunology, 2003. **134**(2): p. 285-294.

35. Brandt, L., J. Feino Cunha, A. Weinreich Olsen, B. Chilima, P. Hirsch, R. Appelberg, and P. Andersen, *Failure of the Mycobacterium bovis BCG Vaccine: Some Species of Environmental Mycobacteria Block Multiplication of BCG and Induction of Protective Immunity to Tuberculosis.* Infection and Immunity, 2002. **70**(2): p. 672-678.

36. Andersen, P. and T.M. Doherty, *The success and failure of BCG - implications for a novel tuberculosis vaccine.* Nat Rev Microbiol, 2005. **3**(8): p. 656-62.

37. Arregui, S., J. Sanz, D. Marinova, C. Martin, and Y. Moreno, *On the impact of masking and blocking hypotheses for measuring the efficacy of new tuberculosis vaccines.* PeerJ, 2016. **4**: p. e1513.

38. Barreto, M.L., D. Pilger, S.M. Pereira, B. Genser, A.A. Cruz, S.S. Cunha, C. Sant'Anna, M.A. Hijjar, M.Y. Ichihara, and L.C. Rodrigues, *Causes of variation in BCG vaccine efficacy: examining evidence from the BCG REVAC cluster randomized trial to explore the masking and the blocking hypotheses.* Vaccine, 2014. **32**(30): p. 3759-64.

39. Fletcher, H.A. and L. Schrager, *TB vaccine development and the End TB Strategy: importance and current status.* Transactions of The Royal Society of Tropical Medicine and Hygiene, 2016. **110**(4): p. 212-218.

40. Kaufmann, S.H., G. Hussey, and P.H. Lambert, *New vaccines for tuberculosis.* Lancet, 2010. **375**(9731): p. 2110-9.

41. Horwitz, M.A., *Recombinant BCG expressing Mycobacterium tuberculosis major extracellular proteins.* Microbes Infect, 2005. **7**(5-6): p. 947-54.

42. Grode, L., P. Seiler, S. Baumann, J. Hess, V. Brinkmann, A. Nasser Eddine, P. Mann, C. Goosmann, S. Bandermann, D. Smith, G.J. Bancroft, J.M. Reyrat, D. van Soolingen, B. Raupach, and S.H. Kaufmann, *Increased vaccine efficacy against tuberculosis of recombinant Mycobacterium bovis bacille Calmette-Guerin mutants that secrete listeriolysin.* J Clin Invest, 2005. **115**(9): p. 2472-9.

43. Aguilar, D., E. Infante, C. Martin, E. Gormley, B. Gicquel, and R. Hernandez Pando, *Immunological responses and protective immunity against tuberculosis conferred by vaccination of Balb/C mice with the attenuated Mycobacterium tuberculosis (phoP) SO2 strain.* Clin Exp Immunol, 2007. **147**(2): p. 330-8.

44. Hinchey, J., S. Lee, B.Y. Jeon, R.J. Basaraba, M.M. Venkataswamy, B. Chen, J. Chan, M. Braunstein, I.M. Orme, S.C. Derrick, S.L. Morris, W.R. Jacobs, Jr., and S.A. Porcelli, *Enhanced priming of adaptive immunity by a proapoptotic mutant of Mycobacterium tuberculosis.* J Clin Invest, 2007. **117**(8): p. 2279-88.

45. Elvang, T., J.P. Christensen, R. Billeskov, T. Thi Kim Thanh Hoang, P. Holst, A.R. Thomsen, P. Andersen, and J. Dietrich, *CD4 and CD8 T cell responses to the M. tuberculosis Ag85B-TB10.4 promoted by adjuvanted subunit, adenovector or heterologous prime boost vaccination.* PLoS One, 2009. **4**(4): p. e5139.

46. Skeiky, Y.A., J. Dietrich, T.M. Lasco, K. Stagliano, V. Dheenadhayalan, M.A. Goetz, L. Cantarero, R.J. Basaraba, P. Bang, I. Kromann, J.B. McMclain, J.C. Sadoff, and P. Andersen, *Non-clinical efficacy and safety of HyVac4:IC31 vaccine administered in a BCG prime-boost regimen.* Vaccine, 2010. **28**(4): p. 1084-93.

47. Tchilian, E.Z., C. Desel, E.K. Forbes, S. Bandermann, C.R. Sander, A.V. Hill, H. McShane, and S.H. Kaufmann, *Immunogenicity and protective efficacy of prime-boost regimens with recombinant (delta)ureC hly+ Mycobacterium bovis BCG and modified vaccinia virus ankara expressing M. tuberculosis antigen 85A against murine tuberculosis.* Infect Immun, 2009. **77**(2): p. 622-31.

48. Vordermeier, H.M., B. Villarreal-Ramos, P.J. Cockle, M. McAulay, S.G. Rhodes, T. Thacker, S.C. Gilbert, H. McShane, A.V. Hill, Z. Xing, and R.G. Hewinson, *Viral booster vaccines improve Mycobacterium bovis BCG-induced protection against bovine tuberculosis.* Infect Immun, 2009. **77**(8): p. 3364-73.

49. Whelan, K.T., A.A. Pathan, C.R. Sander, H.A. Fletcher, I. Poulton, N.C. Alder, A.V.S. Hill, and H. McShane, *Safety and Immunogenicity of Boosting BCG Vaccinated Subjects with BCG: Comparison with Boosting with a New TB Vaccine, MVA85A.* PLoS ONE, 2009. **4**(6): p. e5934.

50. Reed, S.G., R.N. Coler, W. Dalemans, E.V. Tan, E.C. DeLa Cruz, R.J. Basaraba, I.M. Orme, Y.A. Skeiky, M.R. Alderson, K.D. Cowgill, J.P. Prieels, R.M. Abalos, M.C. Dubois, J. Cohen, P. Mettens, and Y. Lobet, *Defined tuberculosis vaccine, Mtb72F/AS02A, evidence of protection in cynomolgus monkeys.* Proc Natl Acad Sci U S A, 2009. **106**(7): p. 2301-6.

51. Roth, A., P. Gustafson, A. Nhaga, Q. Djana, A. Poulsen, M.L. Garly, H. Jensen, M. Sodemann, A. Rodriques, and P. Aaby, *BCG vaccination scar associated with better childhood survival in Guinea-Bissau.* Int J Epidemiol, 2005. **34**(3): p. 540-7.

52. Roth, A., M. Sodemann, H. Jensen, A. Poulsen, P. Gustafson, C. Weise, J. Gomes, Q. Djana, M. Jakobsen, M.L. Garly, A. Rodrigues, and P. Aaby, *Tuberculin reaction, BCG scar, and lower female mortality.* Epidemiology, 2006. **17**(5): p. 562-8.

53. Storgaard, L., A. Rodrigues, C. Martins, B.U. Nielsen, H. Ravn, C.S. Benn, P. Aaby, and A.B. Fisker, *Development of BCG Scar and Subsequent Morbidity and Mortality in Rural Guinea-Bissau.* Clin Infect Dis, 2015. **61**(6): p. 950-9.

54. Kristensen, I., P. Aaby, and H. Jensen, *Routine vaccinations and child survival: follow up study in Guinea-Bissau, West Africa.* Bmj, 2000. **321**(7274): p. 1435-8.

55. Bhatt, K., S. Verma, J.J. Ellner, and P. Salgame, *Quest for correlates of protection against tuberculosis.* Clin Vaccine Immunol, 2015. **22**(3): p. 258-66.

56. Kaufmann, S.H., *Future vaccination strategies against tuberculosis: thinking outside the box.* Immunity, 2010. **33**(4): p. 567-77.

57. Nunes-Alves, C., M.G. Booty, S.M. Carpenter, P. Jayaraman, A.C. Rothchild, and S.M. Behar, *In search of a new paradigm for protective immunity to TB.* Nat Rev Microbiol, 2014. **12**(4): p. 289-99.

58. Orme, I.M., *Vaccines to prevent tuberculosis infection rather than disease: Physiological and immunological aspects.* Tuberculosis (Edinb), 2016. **101**: p. 210-216.

59. Evans, T.G., L. Schrager, and J. Thole, *Status of vaccine research and development of vaccines for tuberculosis.* Vaccine, 2016. **34**(26): p. 2911-2914.

60. Abu-Raddad, L.J., L. Sabatelli, J.T. Achterberg, J.D. Sugimoto, I.M. Longini, C. Dye, and M.E. Halloran, *Epidemiological benefits of more-effective tuberculosis vaccines, drugs, and diagnostics.* Proceedings of the National Academy of Sciences, 2009. **106**(33): p. 13980-13985.

61. Riley, R.L., C.C. Mills, W. Nyka, N. Weinstock, P.B. Storey, L.U. Sultan, M.C. Riley, and W.F. Wells, *Aerial dissemination of pulmonary tuberculosis: A two-year study of contagion in a tuberculosis ward.* American Journal of Epidemiology, 1995. **142**(1): p. 3-14.

62. Eum, S.-Y., J.-H. Kong, M.-S. Hong, Y.-J. Lee, J.-H. Kim, S.-H. Hwang, S.-N. Cho, L.E. Via, and C.E. Barry, *Neutrophils Are the Predominant Infected Phagocytic Cells in the Airways of Patients With Active Pulmonary TB.* Chest, 2010. **137**(1): p. 122-128.

63. Wolf, A.J., B. Linas, G.J. Trevejo-Nuñez, E. Kincaid, T. Tamura, K. Takatsu, and J.D. Ernst, *Mycobacterium tuberculosis Infects Dendritic Cells with High Frequency and Impairs Their Function In Vivo.* The Journal of Immunology, 2007. **179**(4): p. 2509-2519.

64. North, R.J. and Y.-J. Jung, *Immunity to Tuberculosis.* Annual Review of Immunology, 2004. **22**(1): p. 599-623.

65. Philips, J.A. and J.D. Ernst, *Tuberculosis Pathogenesis and Immunity.* Annual Review of Pathology: Mechanisms of Disease, 2012. **7**(1): p. 353-384.

66. Flynn, J.L. and J. Chan, *IMMUNOLOGY OF TUBERCULOSIS.* Annual Review of Immunology, 2001. **19**(1): p. 93-129.

67. Schlesinger, L.S., *Entry of Mycobacterium tuberculosis into Mononuclear Phagocytes*, in *Tuberculosis*, T.M. Shinnick, Editor. 1996, Springer Berlin Heidelberg: Berlin, Heidelberg. p. 71-96.

68. Flynn, J.L. and J. Chan, *Immune evasion by Mycobacterium tuberculosis: living with the enemy.* Current Opinion in Immunology, 2003. **15**(4): p. 450-455.

69. Fratti, R.A., J. Chua, I. Vergne, and V. Deretic, *Mycobacterium tuberculosis glycosylated phosphatidylinositol causes phagosome maturation arrest.* Proceedings of the National Academy of Sciences of the United States of America, 2003. **100**(9): p. 5437-5442.

70. Indrigo, J., R.L. Hunter, and J.K. Actor, *Cord factor trehalose 6,6 '-dimycolate (TDM) mediates trafficking events during mycobacterial infection of murine macrophages.* Microbiology-Sgm, 2003. **149**: p. 2049-2059.

71. Pieters, J., *Mycobacterium tuberculosis and the macrophage: maintaining a balance.* Cell Host Microbe, 2008. **3**(6): p. 399-407.

72. Fulton, S.A., S.M. Reba, R.K. Pai, M. Pennini, M. Torres, C.V. Harding, and W.H. Boom, *Inhibition of major histocompatibility complex II expression and antigen*

processing in murine alveolar macrophages by Mycobacterium bovis BCG and the 19-kilodalton mycobacterial lipoprotein. Infect Immun, 2004. **72**(4): p. 2101-10.

73. Nepal, R.M., S. Mampe, B. Shaffer, A.H. Erickson, and P. Bryant, *Cathepsin L maturation and activity is impaired in macrophages harboring M. avium and M. tuberculosis.* Int Immunol, 2006. **18**(6): p. 931-9.

74. Hanekom, W.A., M. Mendillo, C. Manca, P.A. Haslett, M.R. Siddiqui, C. Barry, 3rd, and G. Kaplan, *Mycobacterium tuberculosis inhibits maturation of human monocyte-derived dendritic cells in vitro.* J Infect Dis, 2003. **188**(2): p. 257-66.

75. Sturgill-Koszycki, S., P.H. Schlesinger, P. Chakraborty, P.L. Haddix, H.L. Collins, A.K. Fok, R.D. Allen, S.L. Gluck, J. Heuser, and D.G. Russell, *Lack of acidification in Mycobacterium phagosomes produced by exclusion of the vesicular proton-ATPase.* Science, 1994. **263**(5147): p. 678-81.

76. Clemens, D.L. and M.A. Horwitz, *Characterization of the Mycobacterium tuberculosis phagosome and evidence that phagosomal maturation is inhibited.* J Exp Med, 1995. **181**(1): p. 257-70.

77. O'Garra, A., P.S. Redford, F.W. McNab, C.I. Bloom, R.J. Wilkinson, and M.P.R. Berry, *The Immune Response in Tuberculosis.* Annual Review of Immunology, 2013. **31**(1): p. 475-527.

78. Orme, I.M., R.T. Robinson, and A.M. Cooper, *The balance between protective and pathogenic immune responses in the TB-infected lung.* Nat Immunol, 2014. **16**(1): p. 57-63.

79. Ramakrishnan, L., *Revisiting the role of the granuloma in tuberculosis.* Nat Rev Immunol, 2012. **12**(5): p. 352-66.

80. Russell, D.G., *Who puts the tubercle in tuberculosis?* Nat Rev Micro, 2007. **5**(1): p. 39-47.

81. Davis, J.M. and L. Ramakrishnan, *The Role of the Granuloma in Expansion and Dissemination of Early Tuberculous Infection.* Cell, 2009. **136**(1): p. 37-49.

82. Bold, T.D. and J.D. Ernst, *Who Benefits from Granulomas, Mycobacteria or Host?* Cell, 2009. **136**(1): p. 17-19.

83. van Rie , A., R. Warren , M. Richardson , T.C. Victor , R.P. Gie , D.A. Enarson , N. Beyers , and P.D. van Helden *Exogenous Reinfection as a Cause of Recurrent Tuberculosis after Curative Treatment.* New England Journal of Medicine, 1999. **341**(16): p. 1174-1179.

84. Verver, S., R.M. Warren, N. Beyers, M. Richardson, G.D. van der Spuy, M.W. Borgdorff, D.A. Enarson, M.A. Behr, and P.D. van Helden, *Rate of reinfection tuberculosis after successful treatment is higher than rate of new tuberculosis.* Am J Respir Crit Care Med, 2005. **171**(12): p. 1430-5.

85. Caminero, J.A., M.J. Pena, M.I. Campos-Herrero, J.C. Rodriguez, O. Afonso, C. Martin, J.M. Pavon, M.J. Torres, M. Burgos, P. Cabrera, P.M. Small, and D.A. Enarson, *Exogenous reinfection with tuberculosis on a European island with a moderate incidence of disease.* Am J Respir Crit Care Med, 2001. **163**(3 Pt 1): p. 717-20.

86. Barry, C.E., H.I. Boshoff, V. Dartois, T. Dick, S. Ehrt, J. Flynn, D. Schnappinger, R.J. Wilkinson, and D. Young, *The spectrum of latent tuberculosis: rethinking the biology and intervention strategies.* Nat Rev Micro, 2009. **7**(12): p. 845-855.

87. Young, D.B., H.P. Gideon, and R.J. Wilkinson, *Eliminating latent tuberculosis.* Trends in Microbiology, 2009. **17**(5): p. 183-188.

88. Guirado, E. and L.S. Schlesinger, *Modeling the Mycobacterium tuberculosis Granuloma - the Critical Battlefield in Host Immunity and Disease.* Front Immunol, 2013. **4**: p. 98.

89. Harisinghani, M.G., T.C. McLoud, J.-A.O. Shepard, J.P. Ko, M.M. Shroff, and P.R. Mueller, *Tuberculosis from Head to Toe.* RadioGraphics, 2000. **20**(2): p. 449-470.

90. Harris, S.A., J. Meyer, I. Satti, L. Marsay, I.D. Poulton, R. Tanner, A.M. Minassian, H.A. Fletcher, and H. McShane, *Evaluation of a Human BCG Challenge Model to Assess Antimycobacterial Immunity Induced by BCG and a Candidate Tuberculosis Vaccine, MVA85A, Alone and in Combination.* The Journal of Infectious Diseases, 2014. **209**(8): p. 1259-1268.

91. McShane, H. and A. Williams, *A review of preclinical animal models utilised for TB vaccine evaluation in the context of recent human efficacy data.* Tuberculosis (Edinb), 2014. **94**(2): p. 105-10.

92. Apt, A. and I. Kramnik, *Man and mouse TB: Contradictions and solutions.* Tuberculosis, 2009. **89**(3): p. 195-198.

93. Via, L.E., P.L. Lin, S.M. Ray, J. Carrillo, S.S. Allen, S.Y. Eum, K. Taylor, E. Klein, U. Manjunatha, J. Gonzales, E.G. Lee, S.K. Park, J.A. Raleigh, S.N. Cho, D.N. McMurray, J.L. Flynn, and C.E. Barry, *Tuberculous Granulomas Are Hypoxic in Guinea Pigs, Rabbits, and Nonhuman Primates.* Infection and Immunity, 2008. **76**(6): p. 2333-2340.

94. McMurray, D.N., *Disease model: pulmonary tuberculosis.* Trends Mol Med, 2001. **7**(3): p. 135-7.

95. Rhoades, E.R., A.A. Frank, and I.M. Orme, *Progression of chronic pulmonary tuberculosis in mice aerogenically infected with virulent Mycobacterium tuberculosis.* Tuber Lung Dis, 1997. **78**(1): p. 57-66.

96. Lin, P.L., S. Pawar, A. Myers, A. Pegu, C. Fuhrman, T.A. Reinhart, S.V. Capuano, E. Klein, and J.L. Flynn, *Early events in Mycobacterium tuberculosis infection in cynomolgus macaques.* Infect Immun, 2006. **74**(7): p. 3790-803.

97. Capuano, S.V., D.A. Croix, S. Pawar, A. Zinovik, A. Myers, P.L. Lin, S. Bissel, C. Fuhrman, E. Klein, and J.L. Flynn, *Experimental Mycobacterium tuberculosis Infection of Cynomolgus Macaques Closely Resembles the Various Manifestations of Human M. tuberculosis Infection.* Infection and Immunity, 2003. **71**(10): p. 5831-5844.

98. Flynn, J.L., J. Chan, K.J. Triebold, D.K. Dalton, T.A. Stewart, and B.R. Bloom, *An Essential Role for Interferon gamma in Resistance to Mycobacterium tuberculosis Infection.* J Exp Med, 1993. **178**: p. 2249-2254.

99. Cooper, A.M., J. Magram, J. Ferrante, and I.M. Orme, *Interleukin 12 (IL-12) is crucial to the development of protective immunity in mice intravenously infected with mycobacterium tuberculosis.* J Exp Med, 1997. **186**(1): p. 39-45.

100. Flynn, J.L., M.M. Goldstein, J. Chan, K.J. Triebold, K. Pfeffer, C.J. Lowenstein, R. Schrelber, T.W. Mak, and B.R. Bloom, *Tumor necrosis factor-α is required in the protective immune response against mycobacterium tuberculosis in mice.* Immunity, 1995. **2**(6): p. 561-572.

101. Keane, J., S. Gershon, R.P. Wise, E. Mirabile-Levens, J. Kasznica, W.D. Schwieterman, J.N. Siegel, and M.M. Braun, *Tuberculosis associated with infliximab, a tumor necrosis factor alpha-neutralizing agent.* N Engl J Med, 2001. **345**(15): p. 1098-104.

102. Jouanguy, E., S. Lamhamedi-Cherradi, D. Lammas, S.E. Dorman, M.C. Fondaneche, S. Dupuis, R. Doffinger, F. Altare, J. Girdlestone, J.F. Emile, H. Ducoulombier, D. Edgar, J. Clarke, V.A. Oxelius, M. Brai, V. Novelli, K. Heyne, A. Fischer, S.M. Holland, D.S. Kumararatne, R.D. Schreiber, and J.L. Casanova, *A human IFNGR1 small deletion hotspot associated with dominant susceptibility to mycobacterial infection.* Nature Genetics, 1999. **21**(4): p. 370-378.

103. Frucht, D.M. and S.M. Holland, *Defective monocyte costimulation for IFN-gamma production in familial disseminated Mycobacterium avium complex infection - Abnormal IL-12 regulation.* Journal of Immunology, 1996. **157**(1): p. 411-416.

104. Frucht, D.M., D.I. Sandberg, M.R. Brown, S.M. Gerstberger, and S.M. Holland, *IL-12 independent costimulation pathways for interferon-gamma production in familial dissemination Mycobacterium avium complex infection.* Clinical Immunology, 1999. **91**(2): p. 234-241.

105. Orme, I.M., *The kinetics of emergence and loss of mediator T lymphocytes acquired in response to infection with Mycobacterium tuberculosis.* The Journal of Immunology, 1987. **138**(1): p. 293-298.

106. Caruso, A.M., N. Serbina, E. Klein, K. Triebold, B.R. Bloom, and J.L. Flynn, *Mice Deficient in CD4 T Cells Have Only Transiently Diminished Levels of IFN-γ, Yet Succumb to Tuberculosis.* The Journal of Immunology, 1999. **162**(9): p. 5407-5416.

107. Mogues, T., M.E. Goodrich, L. Ryan, R. LaCourse, and R.J. North, *The Relative Importance of T Cell Subsets in Immunity and Immunopathology of Airborne Mycobacterium tuberculosis Infection in Mice.* The Journal of Experimental Medicine, 2001. **193**(3): p. 271-280.

108. Geldmacher, C., N. Ngwenyama, A. Schuetz, C. Petrovas, K. Reither, E.J. Heeregrave, J.P. Casazza, D.R. Ambrozak, M. Louder, W. Ampofo, G. Pollakis, B. Hill, E. Sanga, E. Saathoff, L. Maboko, M. Roederer, W.A. Paxton, M. Hoelscher, and R.A. Koup, *Preferential infection and depletion of Mycobacterium tuberculosis-specific CD4 T cells after HIV-1 infection.* J Exp Med, 2010. **207**(13): p. 2869-81.

109. Geldmacher, C., A. Schuetz, N. Ngwenyama, J.P. Casazza, E. Sanga, E. Saathoff, C. Boehme, S. Geis, L. Maboko, M. Singh, F. Minja, A. Meyerhans, R.A. Koup, and M. Hoelscher, *Early depletion of Mycobacterium tuberculosis-specific T helper 1 cell responses after HIV-1 infection.* J Infect Dis, 2008. **198**(11): p. 1590-8.

110. Geldmacher, C., A. Zumla, and M. Hoelscher, *Interaction between HIV and Mycobacterium tuberculosis: HIV-1-induced CD4 T-cell depletion and the development of active tuberculosis.* Current Opinion in HIV and AIDS, 2012. **7**(3): p. 268-274.

111. Chackerian, A.A. and S.M. Behar, *Susceptibility to Mycobacterium tuberculosis: lessons from inbred strains of mice.* Tuberculosis (Edinb), 2003. **83**(5): p. 279-85.

112. Marquis, J.F., A. Nantel, R. LaCourse, L. Ryan, R.J. North, and P. Gros, *Fibrotic response as a distinguishing feature of resistance and susceptibility to pulmonary infection with Mycobacterium tuberculosis in mice.* Infect Immun, 2008. **76**(1): p. 78-88.

113. Mitsos, L.M., L.R. Cardon, A. Fortin, L. Ryan, R. LaCourse, R.J. North, and P. Gros, *Genetic control of susceptibility to infection with Mycobacterium tuberculosis in mice.* Genes Immun, 2000. **1**(8): p. 467-77.

114. Dannenberg, A.M., Jr. and F.M. Collins, *Progressive pulmonary tuberculosis is not due to increasing numbers of viable bacilli in rabbits, mice and guinea pigs, but is due to a continuous host response to mycobacterial products.* Tuberculosis (Edinb), 2001. **81**(3): p. 229-42.

115. Neill, S.D., J.M. Pollock, D.B. Bryson, and J. Hanna, *Pathogenesis of Mycobacterium bovis infection in cattle.* Vet Microbiol, 1994. **40**(1-2): p. 41-52.

116. Van Rhijn, I., J. Godfroid, A. Michel, and V. Rutten, *Bovine tuberculosis as a model for human tuberculosis: advantages over small animal models.* Microbes Infect, 2008. **10**(7): p. 711-5.

117. Waters, W.R., M.F. Maggioli, J.L. McGill, K.P. Lyashchenko, and M.V. Palmer, *Relevance of bovine tuberculosis research to the understanding of human disease: historical perspectives, approaches, and immunologic mechanisms.* Vet Immunol Immunopathol, 2014. **159**(3-4): p. 113-32.

118. Waters, W.R., M.V. Palmer, T.C. Thacker, W.C. Davis, S. Sreevatsan, P. Coussens, K.G. Meade, J.C. Hope, and D.M. Estes, *Tuberculosis Immunity: Opportunities from Studies with Cattle.* Clinical and Developmental Immunology, 2011. **2011**: p. 11.

119. Giannakaki, S., L. Politi, E.M. Antonogiannaki, N. Spanakis, G. Arsenis, V. Filaditaki, S. Zakynthinos, N. Karagiannidis, and A. Tsakris, *Absence of human rhinovirus and respiratory syncytial virus from bronchoalveolar lavage and bronchial biopsies of selected patients with stable chronic obstructive pulmonary disease.* Respiratory Research, 2016. **17**(1): p. 11.

120. Teijaro, J.R., D. Turner, Q. Pham, E.J. Wherry, L. Lefrancois, and D.L. Farber, *Cutting edge: Tissue-retentive lung memory CD4 T cells mediate optimal protection to respiratory virus infection.* J Immunol, 2011. **187**(11): p. 5510-4.

121. Anderson, K.G., K. Mayer-Barber, H. Sung, L. Beura, B.R. James, J.J. Taylor, L. Qunaj, T.S. Griffith, V. Vezys, D.L. Barber, and D. Masopust, *Intravascular staining for discrimination of vascular and tissue leukocytes.* Nat Protoc, 2014. **9**(1): p. 209-22.

122. Anderson, K.G., H. Sung, C.N. Skon, L. Lefrancois, A. Deisinger, V. Vezys, and D. Masopust, *Cutting edge: intravascular staining redefines lung CD8 T cell responses.* J Immunol, 2012. **189**(6): p. 2702-6.

123. Turner, D.L., K.L. Bickham, J.J. Thome, C.Y. Kim, F. D'Ovidio, E.J. Wherry, and D.L. Farber, *Lung niches for the generation and maintenance of tissue-resident memory T cells.* Mucosal Immunol, 2014. **7**(3): p. 501-10.

124. Barletta, K.E., R.E. Cagnina, K.L. Wallace, S.I. Ramos, B. Mehrad, and J. Linden, *Leukocyte compartments in the mouse lung: distinguishing between marginated, interstitial, and alveolar cells in response to injury.* J Immunol Methods, 2012. **375**(1-2): p. 100-10.

125. Patel, B.V., K.C. Tatham, M.R. Wilson, K.P. O'Dea, and M. Takata, *In vivo compartmental analysis of leukocytes in mouse lungs.* Am J Physiol Lung Cell Mol Physiol, 2015. **309**(7): p. L639-52.

126. Sakai, S., K.D. Kauffman, J.M. Schenkel, C.C. McBerry, K.D. Mayer-Barber, D. Masopust, and D.L. Barber, *Cutting edge: control of Mycobacterium tuberculosis infection by a subset of lung parenchyma-homing CD4 T cells.* J Immunol, 2014. **192**(7): p. 2965-9.

127. Moguche, A.O., S. Shafiani, C. Clemons, R.P. Larson, C. Dinh, L.E. Higdon, C.J. Cambier, J.R. Sissons, A.M. Gallegos, P.J. Fink, and K.B. Urdahl, *ICOS and Bcl6-dependent pathways maintain a CD4 T cell population with memory-like properties during tuberculosis.* The Journal of Experimental Medicine, 2015. **212**(5): p. 715-728.

128. Cooper, A.M., K.D. Mayer-Barber, and A. Sher, *Role of innate cytokines in mycobacterial infection.* Mucosal Immunol, 2011. **4**(3): p. 252-60.

129. Wolf, A.J., L. Desvignes, B. Linas, N. Banaiee, T. Tamura, K. Takatsu, and J.D. Ernst, *Initiation of the adaptive immune response to Mycobacterium tuberculosis depends on antigen production in the local lymph node, not the lungs.* The Journal of Experimental Medicine, 2008. **205**(1): p. 105-115.

130. Kirman, J.R., M.I. Henao-Tamayo, and E.M. Agger, *The Memory Immune Response to Tuberculosis.* Microbiology Spectrum, 2016. **4**(6).

131. Chackerian, A.A., J.M. Alt, T.V. Perera, C.C. Dascher, and S.M. Behar, *Dissemination of Mycobacterium tuberculosis Is Influenced by Host Factors and Precedes the Initiation of T-Cell Immunity.* Infection and Immunity, 2002. **70**(8): p. 4501-4509.

132. Orme, I.M., A.D. Roberts, J.P. Griffin, and J.S. Abrams, *Cytokine secretion by CD4 T lymphocytes acquired in response to Mycobacterium tuberculosis infection.* The Journal of Immunology, 1993. **151**(1): p. 518-525.

133. Khader, S.A., S. Partida-Sanchez, G. Bell, D.M. Jelley-Gibbs, S. Swain, J.E. Pearl, N. Ghilardi, F.J. Desauvage, F.E. Lund, and A.M. Cooper, *Interleukin 12p40 is required for dendritic cell migration and T cell priming after Mycobacterium tuberculosis infection.* J Exp Med, 2006. **203**(7): p. 1805-15.

134. Urdahl, K.B., S. Shafiani, and J.D. Ernst, *Initiation and regulation of T-cell responses in tuberculosis.* Mucosal Immunol, 2011. **4**(3): p. 288-93.

135. Cooper, A.M., *Cell-mediated immune responses in tuberculosis.* Annu Rev Immunol, 2009. **27**: p. 393-422.

136. Reiley, W.W., M.D. Calayag, S.T. Wittmer, J.L. Huntington, J.E. Pearl, J.J. Fountain, C.A. Martino, A.D. Roberts, A.M. Cooper, G.M. Winslow, and D.L. Woodland, *ESAT-6-specific CD4 T cell responses to aerosol Mycobacterium tuberculosis infection are initiated in the mediastinal lymph nodes.* Proceedings of the National Academy of Sciences, 2008. **105**(31): p. 10961-10966.

137. Gallegos, A.M., E.G. Pamer, and M.S. Glickman, *Delayed protection by ESAT-6-specific effector CD4$^+$ T cells after airborne M. tuberculosis infection.* J Exp Med, 2008. **205**(10): p. 2359-68.

138. Griffiths, K.L., M. Ahmed, S. Das, R. Gopal, W. Horne, T.D. Connell, K.D. Moynihan, J.K. Kolls, D.J. Irvine, M.N. Artyomov, J. Rangel-Moreno, and S.A. Khader, *Targeting dendritic cells to accelerate T-cell activation overcomes a bottleneck in tuberculosis vaccine efficacy.* Nat Commun, 2016. **7**: p. 13894.

139. Tchilian, E.Z., E.O. Ronan, C. de Lara, L.N. Lee, K.L. Franken, M.H. Vordermeier, T.H. Ottenhoff, and P.C. Beverley, *Simultaneous immunization against tuberculosis.* PLoS One, 2011. **6**(11): p. e27477.

140. Ronan, E.O., L.N. Lee, P.C.L. Beverley, and E.Z. Tchilian, *Immunization of Mice with a Recombinant Adenovirus Vaccine Inhibits the Early Growth of Mycobacterium tuberculosis After Infection.* PLOS ONE, 2009. **4**(12): p. e8235.

141. Cooper, A.M., D.K. Dalton, T.A. Stewart, J.P. Griffin, D.G. Russell, and I.M. Orme, *Disseminated tuberculosis in interferon gamma gene-disrupted mice.* J Exp Med, 1993. **178**(6): p. 2243-7.

142. Levin, M., M.J. Newport, S. Dsouza, P. Kalabalikis, I.N. Brown, H.M. Lenicker, P.V. Agius, E.G. Davies, A. Thrasher, N. Klein, and J.M. Blackwell, *FAMILIAL DISSEMINATED ATYPICAL MYCOBACTERIAL INFECTION IN CHILDHOOD - A HUMAN MYCOBACTERIAL SUSCEPTIBILITY GENE.* Lancet, 1995. **345**(8942): p. 79-83.

143. and, J.-L.C. and L. Abel, *GENETIC DISSECTION OF IMMUNITY TO MYCOBACTERIA: The Human Model.* Annual Review of Immunology, 2002. **20**(1): p. 581-620.

144. Ni Cheallaigh, C., F.J. Sheedy, J. Harris, N. Munoz-Wolf, J. Lee, K. West, E.P. McDermott, A. Smyth, L.E. Gleeson, M. Coleman, N. Martinez, C.H. Hearnden, G.A. Tynan, E.C. Carroll, S.A. Jones, S.C. Corr, N.J. Bernard, M.M. Hughes, S.E. Corcoran, M. O'Sullivan, C.M. Fallon, H. Kornfeld, D. Golenbock, S.V. Gordon, L.A. O'Neill, E.C. Lavelle, and J. Keane, *A Common Variant in the Adaptor Mal Regulates Interferon Gamma Signaling.* Immunity, 2016. **44**(2): p. 368-79.

145. Chan, J., Y. Xing, R.S. Magliozzo, and B.R. Bloom, *Killing of virulent Mycobacterium tuberculosis by reactive nitrogen intermediates produced by activated murine macrophages.* The Journal of Experimental Medicine, 1992. **175**(4): p. 1111-1122.

146. MacMicking, J.D., G.A. Taylor, and J.D. McKinney, *Immune Control of Tuberculosis by IFN-γ-Inducible LRG-47.* Science, 2003. **302**(5645): p. 654-659.

147. Gutierrez, M.G., S.S. Master, S.B. Singh, G.A. Taylor, M.I. Colombo, and V. Deretic, *Autophagy Is a Defense Mechanism Inhibiting BCG and Mycobacterium tuberculosis Survival in Infected Macrophages.* Cell, 2004. **119**(6): p. 753-766.

148. MacMicking, J.D., R.J. North, R. LaCourse, J.S. Mudgett, S.K. Shah, and C.F. Nathan, *Identification of nitric oxide synthase as a protective locus against tuberculosis.* Proceedings of the National Academy of Sciences, 1997. **94**(10): p. 5243-5248.

149. Fabri, M., S. Stenger, D.-M. Shin, J.-M. Yuk, P.T. Liu, S. Realegeno, H.-M. Lee, S.R. Krutzik, M. Schenk, P.A. Sieling, R. Teles, D. Montoya, S.S. Iyer, H. Bruns, D.M. Lewinsohn, B.W. Hollis, M. Hewison, J.S. Adams, A. Steinmeyer, U. Zügel, G. Cheng, E.-K. Jo, B.R. Bloom, and R.L. Modlin, *Vitamin D Is Required for IFN-γ–Mediated Antimicrobial Activity of Human Macrophages.* Science Translational Medicine, 2011. **3**(104): p. 104ra102-104ra102.

150. Liu, P.T., S. Stenger, D.H. Tang, and R.L. Modlin, *Cutting Edge: Vitamin D-Mediated Human Antimicrobial Activity against Mycobacterium tuberculosis Is Dependent on the Induction of Cathelicidin.* The Journal of Immunology, 2007. **179**(4): p. 2060-2063.

151. Fletcher, H.A., M.A. Snowden, B. Landry, W. Rida, I. Satti, S.A. Harris, M. Matsumiya, R. Tanner, M.K. O'Shea, V. Dheenadhayalan, L. Bogardus, L. Stockdale, L. Marsay, A. Chomka, R. Harrington-Kandt, Z.R. Manjaly-Thomas, V. Naranbhai, E. Stylianou, F. Darboe, A. Penn-Nicholson, E. Nemes, M. Hatheril, G. Hussey, H. Mahomed, M. Tameris, J.B. McClain, T.G. Evans, W.A. Hanekom, T.J. Scriba, and H. McShane, *T-cell*

activation is an immune correlate of risk in BCG vaccinated infants. Nat Commun, 2016. **7**: p. 11290.

152. Mayer-Barber, K.D., D.L. Barber, K. Shenderov, S.D. White, M.S. Wilson, A. Cheever, D. Kugler, S. Hieny, P. Caspar, G. Nunez, D. Schlueter, R.A. Flavell, F.S. Sutterwala, and A. Sher, *Caspase-1 independent IL-1beta production is critical for host resistance to mycobacterium tuberculosis and does not require TLR signaling in vivo.* J Immunol, 2010. **184**(7): p. 3326-30.

153. Gonzalez-Juarrero, M., J.M. Hattle, A. Izzo, A.P. Junqueira-Kipnis, T.S. Shim, B.C. Trapnell, A.M. Cooper, and I.M. Orme, *Disruption of granulocyte macrophage-colony stimulating factor production in the lungs severely affects the ability of mice to control Mycobacterium tuberculosis infection.* J Leukoc Biol, 2005. **77**(6): p. 914-22.

154. Ladel, C.H., C. Blum, A. Dreher, K. Reifenberg, M. Kopf, and S.H. Kaufmann, *Lethal tuberculosis in interleukin-6-deficient mutant mice.* Infection and Immunity, 1997. **65**(11): p. 4843-9.

155. Leal, I.S., B. Smedegaard, P. Andersen, and R. Appelberg, *Failure to induce enhanced protection against tuberculosis by increasing T-cell-dependent interferon-gamma generation.* Immmunology, 2001. **104**: p. 157-161.

156. Mittrucker, H.W., U. Steinhoff, A. Kohler, M. Krause, D. Lazar, P. Mex, D. Miekley, and S.H. Kaufmann, *Poor correlation between BCG vaccination-induced T cell responses and protection against tuberculosis.* Proc Natl Acad Sci U S A, 2007. **104**(30): p. 12434-9.

157. Vordermeier, H.M., M.A. Chambers, P.J. Cockle, A.o. Whelan, J. Simmons, and R.G. Hewinson, *Correlation of ESAT-6-Specific Gamma Interferon Production with Pathology in Cattle following Mycobacterium bovis BCG Vaccination against Experimental Bovine Tuberculosis.* Infection and Immunity, 2002. **70**(6): p. 3026-3032.

158. Kagina, B.M., B. Abel, T.J. Scriba, E.J. Hughes, A. Keyser, A. Soares, H. Gamieldien, M. Sidibana, M. Hatherill, S. Gelderbloem, H. Mahomed, A. Hawkridge, G. Hussey, G. Kaplan, and W.A. Hanekom, *Specific T cell frequency and cytokine expression profile do not correlate with protection against tuberculosis after bacillus Calmette-Guerin vaccination of newborns.* Am J Respir Crit Care Med, 2010. **182**(8): p. 1073-9.

159. Hoft, D.F., S. Worku, B. Kampmann, C.C. Whalen, J.J. Ellner, C.S. Hirsch, R.B. Brown, R. Larkin, Q. Li, H. Yun, and R.F. Silver, *Investigation of the Relationships between Immune-Mediated Inhibition of Mycobacterial Growth and Other Potential*

Surrogate Markers of Protective Mycobacterium tuberculosis Immunity. J Infect Dis, 2002. **186**: p. 1448-1457.

160. Elias, D., H. Akuffo, and S. Britton, *PPD induced in vitro interferon gamma production is not a reliable correlate of protection against Mycobacterium tuberculosis.* Trans R Soc Trop Med Hyg, 2005. **99**(5): p. 363-8.

161. Fletcher, H.A., *Correlates of immune protection from tuberculosis.* Curr Mol Med, 2007. **7**(3): p. 319-25.

162. Saunders, B.M., H. Briscoe, and W.J. Britton, *T cell-derived tumour necrosis factor is essential, but not sufficient, for protection against Mycobacterium tuberculosis infection.* Clin Exp Immunol, 2004. **137**(2): p. 279-87.

163. Bermudez, L.E. and L.S. Young, *Recombinant granulocyte-macrophage colony-stimulating factor activates human macrophages to inhibit growth or kill Mycobacterium avium complex.* J Leukoc Biol, 1990. **48**(1): p. 67-73.

164. Rothchild, A.C., P. Jayaraman, C. Nunes-Alves, and S.M. Behar, *iNKT Cell Production of GM-CSF Controls Mycobacterium tuberculosis.* PLoS Pathogens, 2014. **10**(1): p. e1003805.

165. Jayaraman, P., I. Sada-Ovalle, T. Nishimura, A.C. Anderson, V.K. Kuchroo, H.G. Remold, and S.M. Behar, *IL-1beta promotes antimicrobial immunity in macrophages by regulating TNFR signaling and caspase-3 activation.* J Immunol, 2013. **190**(8): p. 4196-204.

166. Martineau, A.R., K.A. Wilkinson, S.M. Newton, R.A. Floto, A.W. Norman, K. Skolimowska, R.N. Davidson, O.E. Sorensen, B. Kampmann, C.J. Griffiths, and R.J. Wilkinson, *IFN-gamma- and TNF-independent vitamin D-inducible human suppression of mycobacteria: the role of cathelicidin LL-37.* J Immunol, 2007. **178**(11): p. 7190-8.

167. Verway, M., M. Bouttier, T.T. Wang, M. Carrier, M. Calderon, B.S. An, E. Devemy, F. McIntosh, M. Divangahi, M.A. Behr, and J.H. White, *Vitamin D induces interleukin-1beta expression: paracrine macrophage epithelial signaling controls M. tuberculosis infection.* PLoS Pathog, 2013. **9**(6): p. e1003407.

168. Vilchèze, C., T. Hartman, B. Weinrick, and W.R. Jacobs Jr, *Mycobacterium tuberculosis is extraordinarily sensitive to killing by a vitamin C-induced Fenton reaction.* Nature Communications, 2013. **4**: p. 1881.

169. Chen, C.Y., D. Huang, R.C. Wang, L. Shen, G. Zeng, S. Yao, Y. Shen, L. Halliday, J. Fortman, M. McAllister, J. Estep, R. Hunt, D. Vasconcelos, G. Du, S.A. Porcelli, M.H. Larsen, W.R. Jacobs, Jr., B.F. Haynes, N.L. Letvin, and Z.W. Chen, *A critical role for CD8 T cells in a nonhuman primate model of tuberculosis.* PLoS Pathog, 2009. **5**(4): p. e1000392.

170. Skinner, M.A., N. Parlane, A. McCarthy, and B.M. Buddle, *Cytotoxic T-cell responses to Mycobacterium bovis during experimental infection of cattle with bovine tuberculosis.* Immunology, 2003. **110**(2): p. 234-241.

171. Woodworth, J.S. and S.M. Behar, *Mycobacterium tuberculosis-specific CD8+ T cells and their role in immunity.* Crit Rev Immunol, 2006. **26**(4): p. 317-52.

172. Woodworth, J.S., Y. Wu, and S.M. Behar, *Mycobacterium tuberculosis-specific $CD8^+$ T cells require perforin to kill target cells and provide protection in vivo.* J Immunol, 2008. **181**(12): p. 8595-603.

173. Umemura, M., A. Yahagi, S. Hamada, M.D. Begum, H. Watanabe, K. Kawakami, T. Suda, K. Sudo, S. Nakae, Y. Iwakura, and G. Matsuzaki, *IL-17-mediated regulation of innate and acquired immune response against pulmonary Mycobacterium bovis bacille Calmette-Guerin infection.* J Immunol, 2007. **178**(6): p. 3786-96.

174. Khader, S.A., G.K. Bell, J.E. Pearl, J.J. Fountain, J. Rangel-Moreno, G.E. Cilley, F. Shen, S.M. Eaton, S.L. Gaffen, S.L. Swain, R.M. Locksley, L. Haynes, T.D. Randall, and A.M. Cooper, *IL-23 and IL-17 in the establishment of protective pulmonary $CD4^+$ T cell responses after vaccination and during Mycobacterium tuberculosis challenge.* Nat Immunol, 2007. **8**(4): p. 369-77.

175. Gopal, R., Y. Lin, N. Obermajer, S. Slight, N. Nuthalapati, M. Ahmed, P. Kalinski, and S.A. Khader, *IL-23-dependent IL-17 drives Th1-cell responses following Mycobacterium bovis BCG vaccination.* Eur J Immunol, 2012. **42**(2): p. 364-73.

176. Sousa, A.O., R.J. Mazzaccaro, R.G. Russell, F.K. Lee, O.C. Turner, S. Hong, L. Van Kaer, and B.R. Bloom, *Relative contributions of distinct MHC class I-dependent cell populations in protection to tuberculosis infection in mice.* Proceedings of the National Academy of Sciences, 2000. **97**(8): p. 4204-4208.

177. Hernandez-Pando, R., M. Jeyanathan, G. Mengistu, D. Aguilar, H. Orozco, M. Harboe, G.A. Rook, and G. Bjune, *Persistence of DNA from Mycobacterium tuberculosis in superficially normal lung tissue during latent infection.* Lancet, 2000. **356**(9248): p. 2133-8.

178. Stenger, S., D.A. Hanson, R. Teitelbaum, P. Dewan, K.R. Niazi, C.J. Froelich, T. Ganz, S. Thoma-Uszynski, A. Melian, C. Bogdan, S.A. Porcelli, B.R. Bloom, A.M. Krensky, and R.L. Modlin, *An antimicrobial activity of cytolytic T cells mediated by granulysin.* Science, 1998. **282**(5386): p. 121-5.

179. Caccamo, N., S. Meraviglia, C. La Mendola, G. Guggino, F. Dieli, and A. Salerno, *Phenotypical and functional analysis of memory and effector human CD8 T cells specific for mycobacterial antigens.* J Immunol, 2006. **177**(3): p. 1780-5.

180. Bellamy, R., C. Ruwende, T. Corrah, K.P.W.J. McAdam, M. Thursz, H.C. Whittle, and A.V.S. Hill, *Tuberculosis and Chronic Hepatitis B Virus Infection in Africans and Variation in the Vitamin D Receptor Gene.* The Journal of Infectious Diseases, 1999. **179**(3): p. 721-724.

181. Bellamy , R., C. Ruwende , T. Corrah , K.P.W.J. McAdam , H.C. Whittle , and A.V.S. Hill *Variations in the NRAMP1 Gene and Susceptibility to Tuberculosis in West Africans.* New England Journal of Medicine, 1998. **338**(10): p. 640-644.

182. Wilkinson, R.J., M. Llewelyn, Z. Toossi, P. Patel, G. Pasvol, A. Lalvani, D. Wright, M. Latif, and R.N. Davidson, *Influence of vitamin D deficiency and vitamin D receptor polymorphisms on tuberculosis among Gujarati Asians in west London: a case-control study.* The Lancet, 2000. **355**(9204): p. 618-621.

183. Wilkinson, R.J., P. Patel, M. Llewelyn, C.S. Hirsch, G. Pasvol, G. Snounou, R.N. Davidson, and Z. Toossi, *Influence of Polymorphism in the Genes for the Interleukin (IL)-1 Receptor Antagonist and IL-1β on Tuberculosis.* The Journal of Experimental Medicine, 1999. **189**(12): p. 1863-1874.

184. Iho, S., T. Yamamoto, T. Takahashi, and S. Yamamoto, *Oligodeoxynucleotides Containing Palindrome Sequences with Internal 5'-CpG-3' Act Directly on Human NK and Activated T Cells to Induce IFN-γ Production In Vitro.* The Journal of Immunology, 1999. **163**(7): p. 3642-3652.

185. García, V.E., K. Uyemura, P.A. Sieling, M.T. Ochoa, C.T. Morita, H. Okamura, M. Kurimoto, T.H. Rea, and R.L. Modlin, *IL-18 Promotes Type 1 Cytokine Production from NK Cells and T Cells in Human Intracellular Infection.* The Journal of Immunology, 1999. **162**(10): p. 6114-6121.

186. van Crevel, R., T.H.M. Ottenhoff, and J.W.M. van der Meer, *Innate Immunity to Mycobacterium tuberculosis.* Clinical Microbiology Reviews, 2002. **15**(2): p. 294-309.

187. Moreira-Teixeira, L., J. Sousa, F.W. McNab, E. Torrado, F. Cardoso, H. Machado, F. Castro, V. Cardoso, J. Gaifem, X. Wu, R. Appelberg, A.G. Castro, A. O'Garra, and M.

Saraiva, *Type I IFN Inhibits Alternative Macrophage Activation during Mycobacterium tuberculosis Infection and Leads to Enhanced Protection in the Absence of IFN-γ Signaling.* The Journal of Immunology, 2016. **197**(12): p. 4714-4726.

188. McNab, F., K. Mayer-Barber, A. Sher, A. Wack, and A. O'Garra, *Type I interferons in infectious disease.* Nat Rev Immunol, 2015. **15**(2): p. 87-103.

189. Ordway, D., M. Henao-Tamayo, M. Harton, G. Palanisamy, J. Troudt, C. Shanley, R.J. Basaraba, and I.M. Orme, *The hypervirulent Mycobacterium tuberculosis strain HN878 induces a potent TH1 response followed by rapid down-regulation.* J Immunol, 2007. **179**(1): p. 522-31.

190. Stanley, S.A., J.E. Johndrow, P. Manzanillo, and J.S. Cox, *The Type I IFN response to infection with Mycobacterium tuberculosis requires ESX-1-mediated secretion and contributes to pathogenesis.* J Immunol, 2007. **178**(5): p. 3143-52.

191. Manca, C., L. Tsenova, S. Freeman, A.K. Barczak, M. Tovey, P.J. Murray, C. Barry, and G. Kaplan, *Hypervirulent M. tuberculosis W/Beijing strains upregulate type I IFNs and increase expression of negative regulators of the Jak-Stat pathway.* J Interferon Cytokine Res, 2005. **25**(11): p. 694-701.

192. Kaech, S.M., E.J. Wherry, and R. Ahmed, *Effector and memory T-cell differentiation: implications for vaccine development.* Nat Rev Immunol, 2002. **2**(4): p. 251-62.

193. Pennock, N.D., J.T. White, E.W. Cross, E.E. Cheney, B.A. Tamburini, and R.M. Kedl, *T cell responses: naïve to memory and everything in between.* Advances in Physiology Education, 2013. **37**(4): p. 273-283.

194. Sathaliyawala, T., M. Kubota, N. Yudanin, D. Turner, P. Camp, Joseph J.C. Thome, Kara L. Bickham, H. Lerner, M. Goldstein, M. Sykes, T. Kato, and Donna L. Farber, *Distribution and Compartmentalization of Human Circulating and Tissue-Resident Memory T Cell Subsets.* Immunity, 2013. **38**(1): p. 187-197.

195. Whitmire, J.K., M.S. Asano, K. Murali-Krishna, M. Suresh, and R. Ahmed, *Long-Term CD4 Th1 and Th2 Memory following Acute Lymphocytic Choriomeningitis Virus Infection.* Journal of Virology, 1998. **72**(10): p. 8281-8288.

196. Kotturi, M.F., J.A. Swann, B. Peters, C.L. Arlehamn, J. Sidney, R.V. Kolla, E.A. James, R.S. Akondy, R. Ahmed, W.W. Kwok, M.J. Buchmeier, and A. Sette, *Human $CD8^+$ and $CD4^+$ T Cell Memory to Lymphocytic Choriomeningitis Virus Infection.* Journal of Virology, 2011. **85**(22): p. 11770-11780.

197. Seder, R.A. and R. Ahmed, *Similarities and differences in CD4$^+$ and CD8$^+$ effector and memory T cell generation.* Nat Immunol, 2003. **4**(9): p. 835-842.

198. Vollers, S.S. and L.J. Stern, *Class II major histocompatibility complex tetramer staining: progress, problems, and prospects.* Immunology, 2008. **123**(3): p. 305-13.

199. Kaveh, D.A., M. Carmen Garcia-Pelayo, and P.J. Hogarth, *Persistent BCG bacilli perpetuate CD4 T effector memory and optimal protection against tuberculosis.* Vaccine, 2014. **32**(51): p. 6911-6918.

200. Fritz, C., S. Maass, A. Kreft, and F.C. Bange, *Dependence of Mycobacterium bovis BCG on anaerobic nitrate reductase for persistence is tissue specific.* Infect Immun, 2002. **70**(1): p. 286-91.

201. Wherry, E.J., *T cell exhaustion.* Nat Immunol, 2011. **12**(6): p. 492-499.

202. Behar, S.M., S.M. Carpenter, M.G. Booty, D.L. Barber, and P. Jayaraman, *Orchestration of pulmonary T cell immunity during Mycobacterium tuberculosis infection: Immunity interruptus.* Semin Immunol, 2014. **26**(6): p. 559-577.

203. Sallusto, F., D. Lenig, R. Forster, M. Lipp, and A. Lanzavecchia, *Two subsets of memory T lymphocytes with distinct homing potentials and effector functions.* Nature, 1999. **401**: p. 708-712.

204. Andersen, P. and B. Smedegaard, *CD4$^+$ T-Cell Subsets That Mediate Immunological Memory to Mycobaterium tuberculosis Infection in Mice.* Infection and Immunity, 2000. **68**(2): p. 621-629.

205. Kipnis, A., S. Irwin, A.A. Izzo, R.J. Basaraba, and I.M. Orme, *Memory T lymphocytes generated by Mycobacterium bovis BCG vaccination reside within a CD4 CD44lo CD62 ligand(hi) population.* Infect Immun, 2005. **73**(11): p. 7759-64.

206. Vogelzang, A., C. Perdomo, U. Zedler, S. Kuhlmann, R. Hurwitz, M. Gengenbacher, and S.H. Kaufmann, *Central Memory CD4+ T Cells Are Responsible for the Recombinant Bacillus Calmette-Guerin DeltaureC::hly Vaccine's Superior Protection Against Tuberculosis.* J Infect Dis, 2014. **210**(12): p. 1928-37.

207. Lindenstrom, T., N.P. Knudsen, E.M. Agger, and P. Andersen, *Control of chronic mycobacterium tuberculosis infection by CD4 KLRG1- IL-2-secreting central memory cells.* J Immunol, 2013. **190**(12): p. 6311-9.

208. Orme, I.M., *The Achilles heel of BCG.* Tuberculosis (Edinb), 2010. **90**(6): p. 329-32.

209. White, A.D., C. Sarfas, K. West, L.S. Sibley, A.S. Wareham, S. Clark, M.J. Dennis, A. Williams, P.D. Marsh, and S.A. Sharpe, *Evaluation of the Immunogenicity of Mycobacterium bovis BCG Delivered by Aerosol to the Lungs of Macaques.* Clinical and Vaccine Immunology, 2015. **22**(9): p. 992-1003.

210. Gebhardt, T., L.M. Wakim, L. Eidsmo, P.C. Reading, W.R. Heath, and F.R. Carbone, *Memory T cells in nonlymphoid tissue that provide enhanced local immunity during infection with herpes simplex virus.* Nat Immunol, 2009. **10**(5): p. 524-30.

211. Masopust, D., D. Choo, V. Vezys, E.J. Wherry, J. Duraiswamy, R. Akondy, J. Wang, K.A. Casey, D.L. Barber, K.S. Kawamura, K.A. Fraser, R.J. Webby, V. Brinkmann, E.C. Butcher, K.A. Newell, and R. Ahmed, *Dynamic T cell migration program provides resident memory within intestinal epithelium.* J Exp Med, 2010. **207**(3): p. 553-64.

212. Wakim, L.M., A. Woodward-Davis, and M.J. Bevan, *Memory T cells persisting within the brain after local infection show functional adaptations to their tissue of residence.* Proc Natl Acad Sci U S A, 2010. **107**(42): p. 17872-17879.

213. Jiang, X., R.A. Clark, L. Liu, A.J. Wagers, R.C. Fuhlbrigge, and T.S. Kupper, *Skin infection generates non-migratory memory CD8^{+} T(RM) cells providing global skin immunity.* Nature, 2012. **483**(7388): p. 227-31.

214. Shin, H. and A. Iwasaki, *A vaccine strategy that protects against genital herpes by establishing local memory T cells.* Nature, 2012. **491**(7424): p. 463-7.

215. Sallin, M.A., S. Sakai, K.D. Kauffman, H.A. Young, J. Zhu, and D.L. Barber, *Th1 Differentiation Drives the Accumulation of Intravascular, Non-protective CD4 T Cells during Tuberculosis.* Cell Reports. **18**(13): p. 3091-3104.

216. Connor, L.M., M.C. Harvie, F.J. Rich, K.M. Quinn, V. Brinkmann, G. Le Gros, and J.R. Kirman, *A key role for lung-resident memory lymphocytes in protective immune responses after BCG vaccination.* Eur J Immunol, 2010. **40**(9): p. 2482-92.

217. Perdomo, C., U. Zedler, A.A. Kühl, L. Lozza, P. Saikali, L.E. Sander, A. Vogelzang, S.H.E. Kaufmann, and A. Kupz, *Mucosal BCG Vaccination Induces Protective Lung-Resident Memory T Cell Populations against Tuberculosis.* mBio, 2016. **7**(6).

218. Woodworth, J.S., S.B. Cohen, A.O. Moguche, C.R. Plumlee, E.M. Agger, K.B. Urdahl, and P. Andersen, *Subunit vaccine H56/CAF01 induces a population of circulating CD4 T cells that traffic into the Mycobacterium tuberculosis-infected lung.* Mucosal Immunol, 2017. **10**(2): p. 555-564.

219. Purwar, R., J. Campbell, G. Murphy, W.G. Richards, R.A. Clark, and T.S. Kupper, *Resident memory T cells (T(RM)) are abundant in human lung: diversity, function, and antigen specificity.* PLoS One, 2011. **6**(1): p. e16245.

220. Walrath, J., L. Zukowski, A. Krywiak, and R.F. Silver, *Resident Th1-like effector memory cells in pulmonary recall responses to Mycobacterium tuberculosis.* Am J Respir Cell Mol Biol, 2005. **33**(1): p. 48-55.

221. Walrath, J.R. and R.F. Silver, *The alpha4beta1 integrin in localization of Mycobacterium tuberculosis-specific T helper type 1 cells to the human lung.* Am J Respir Cell Mol Biol, 2011. **45**(1): p. 24-30.

222. Reutershan, J., A. Basit, E.V. Galkina, and K. Ley, *Sequential recruitment of neutrophils into lung and bronchoalveolar lavage fluid in LPS-induced acute lung injury.* Am J Physiol Lung Cell Mol Physiol, 2005. **289**(5): p. L807-15.

223. Galkina, E., J. Thatte, V. Dabak, M.B. Williams, K. Ley, and T.J. Braciale, *Preferential migration of effector CD8+ T cells into the interstitium of the normal lung.* The Journal of Clinical Investigation, 2005. **115**(12): p. 3473-3483.

224. Carmen Garcia-Pelayo, M., V.S. Bachy, D.A. Kaveh, and P.J. Hogarth, *BALB/c mice display more enhanced BCG vaccine induced Th1 and Th17 response than C57BL/6 mice but have equivalent protection.* Tuberculosis, 2014.

225. Kaveh, D.A., V.S. Bachy, G.R. Hewinson, and P.J. Hogarth, *Systemic BCG Immunization Induces Persistent Lung Mucosal Multifunctional CD4 TEM Cells which Expand Following Virulent Mycobaterial Challenge.* PLoS One, 2011. **6**(6): p. e21566.

226. Cosmi, L., L. Maggi, V. Santarlasci, F. Liotta, F. Frosali, R. Angeli, M. Mazzetti, A. Vultaggio, A. Matucci, E. Maggi, S. Romagnani, and F. Annunziato, *Detection by Flow Cytometry of ESAT-6- and PPD-Specific Circulating $CD4^+$ T Lymphocytes as a Diagnostic Tool for Tuberculosis.* International Archives of Allergy and Immunology, 2007. **143**(1): p. 1-9.

227. Smith, S.G., K. Smits, S.A. Joosten, K.E. van Meijgaarden, I. Satti, H.A. Fletcher, N. Caccamo, F. Dieli, F. Mascart, H. McShane, H.M. Dockrell, T.H.M. Ottenhoff, and T.T.B.W. Group, *Intracellular Cytokine Staining and Flow Cytometry: Considerations for Application in Clinical Trials of Novel Tuberculosis Vaccines.* PLOS ONE, 2015. **10**(9): p. e0138042.

228. Geissmann, F., T.O. Cameron, S. Sidobre, N. Manlongat, M. Kronenberg, M.J. Briskin, M.L. Dustin, and D.R. Littman, *Intravascular immune surveillance by $CXCR6^+$ NKT cells patrolling liver sinusoids.* PLoS Biol, 2005. **3**(4): p. e113.

229. Lee, W., T.J. Moriarty, C.H.Y. Wong, H. Zhou, R.M. Strieter, N. van Rooijen, G. Chaconas, and P. Kubes, *An intravascular immune response to Borrelia burgdorferi involves Kupffer cells and invariant NKT cells.* Nat Immunol, 2010. **11**: p. 295-302.

230. Thomas, S.Y., S.T. Scanlon, K.G. Griewank, M.G. Constantinides, A.K. Savage, K.A. Barr, F. Meng, A.D. Luster, and A. Bendelac, *PLZF induces an intravascular surveillance program mediated by long-lived LFA-1-ICAM-1 interactions.* J Exp Med, 2011. **208**(6): p. 1179-88.

231. Scanlon, S.T., S.Y. Thomas, C.M. Ferreira, L. Bai, T. Krausz, P.B. Savage, and A. Bendelac, *Airborne lipid antigens mobilize resident intravascular NKT cells to induce allergic airway inflammation.* J Exp Med, 2011. **208**(10): p. 2113-24.

232. Schaible, U.E., F. Winau, P.A. Sieling, K. Fischer, H.L. Collins, K. Hagens, R.L. Modlin, V. Brinkmann, and S.H. Kaufmann, *Apoptosis facilitates antigen presentation to T lymphocytes through MHC-I and CD1 in tuberculosis.* Nat Med, 2003. **9**(8): p. 1039-46.

233. Eddine, A.N. and S.H.E. Kaufmann, *Improved protection by recombinant BCG.* Microbes and Infection, 2005. **7**(5): p. 939-946.

234. Kaufmann, S.H. and A.J. McMichael, *Annulling a dangerous liaison: vaccination strategies against AIDS and tuberculosis.* Nat Med, 2005. **11**(4 Suppl): p. S33-44.

235. Majlessi, L., M.J. Rojas, P. Brodin, and C. Leclerc, *CD8+-T-cell responses of Mycobacterium-infected mice to a newly identified major histocompatibility complex class I-restricted epitope shared by proteins of the ESAT-6 family.* Infect Immun, 2003. **71**(12): p. 7173-7.

236. Smith, S.M., A.S. Malin, T. Pauline, Lukey, S.E. Atkinson, J. Content, K. Huygen, and H.M. Dockrell, *Characterization of human Mycobacterium bovis bacille Calmette-Guerin-reactive CD8+ T cells.* Infect Immun, 1999. **67**(10): p. 5223-30.

237. Hervas-Stubbs, S., L. Majlessi, M. Simsova, J. Morova, M.J. Rojas, C. Nouze, P. Brodin, P. Sebo, and C. Leclerc, *High frequency of CD4$^+$ T cells specific for the TB10.4 protein correlates with protection against Mycobacterium tuberculosis infection.* Infect Immun, 2006. **74**(6): p. 3396-407.

238. Billeskov, R., M.V. Grandal, C. Poulsen, J.P. Christensen, N. Winther, C. Vingsbo-Lundberg, T.T. Hoang, B. van Deurs, Y.H. Song, C. Aagaard, P. Andersen, and J. Dietrich, *Difference in TB10.4 T-cell epitope recognition following immunization with recombinant TB10.4, BCG or infection with Mycobacterium tuberculosis.* Eur J Immunol, 2010. **40**(5): p. 1342-54.

239. Yang, H., N.A. Kruh-Garcia, and K.M. Dobos, *Purified Protein Derivatives of Tuberculin - Past, Present, and Future.* FEMS immunology and medical microbiology, 2012. **66**(3): p. 273-280.

240. Hewitt, C.R. and M. Feldmann, *Human T cell clones present antigen.* The Journal of Immunology, 1989. **143**(2): p. 762-769.

241. Nisini, R., P.M. Matricardi, A. Fattorossi, R. Biselli, and R. D'Amelio, *Presentation of superantigen by human T cell clones: A model of T-T cell interaction.* European Journal of Immunology, 1992. **22**(8): p. 2033-2039.

242. Wyss-Coray, T., H. Gallati, I. Pracht, A. Limat, D. Mauri, K. Frutig, and W.J. Pichler, *Antigen-presenting human T cells and antigen-presenting B cells induce a similar cytokine profile in specific T cell clones.* Eur J Immunol, 1993. **23**(12): p. 3350-7.

243. LaSalle, J.M., K. Ota, and D.A. Hafler, *Presentation of autoantigen by human T cells.* The Journal of Immunology, 1991. **147**(3): p. 774-780.

244. Gerrard, T.L., D.J. Volkman, C.H. Jurgensen, and A.S. Fauci, *Activated human T cells can present alloantigens but cannot present soluble antigens.* Cell Immunol, 1985. **95**(1): p. 65-74.

245. Cole, D.K., N.J. Pumphrey, J.M. Boulter, M. Sami, J.I. Bell, E. Gostick, D.A. Price, G.F. Gao, A.K. Sewell, and B.K. Jakobsen, *Human TCR-binding affinity is governed by MHC class restriction.* J Immunol, 2007. **178**(9): p. 5727-34.

246. Knudson, C.J., K.A. Weiss, S.M. Hartwig, and S.M. Varga, *The Pulmonary Localization of Virus-Specific T Lymphocytes Is Governed by the Tissue Tropism of Infection.* Journal of Virology, 2014. **88**(16): p. 9010-9016.

247. Zens, K.D., J.K. Chen, and D.L. Farber, *Vaccine-generated lung tissue–resident memory T cells provide heterosubtypic protection to influenza infection.* JCI Insight, 2016. **1**(10): p. e85832.

248. Hogan, R.J., W. Zhong, E.J. Usherwood, T. Cookkenham, A.D. Roberts, and D.L. Woodland, *Potection from Respiratory Virus Infections Can Be Mediated by Antigen-specific CD4$^+$ T Cells That Persist in the Lungs.* J Exp Med, 2001. **193**(8): p. 981-986.

249. Cauley, L.S., T. Cookenham, T.B. Miller, Sadams, P. S., K.M. Vignali, D.A.A. Vignali, and D.L. Woodland, *Cutting Edge: Virus-Specific CD4$^+$ Memory T Cells in Nonlymphoid Tissues Express a Highly Activated Phenotype.* J Immunol, 2002. **169**: p. 6655-6658.

250. Sakai, S., K.D. Kauffman, M.A. Sallin, A.H. Sharpe, H.A. Young, V.V. Ganusov, and D.L. Barber, *CD4 T Cell-Derived IFN-γ Plays a Minimal Role in Control of Pulmonary Mycobacterium tuberculosis Infection and Must Be Actively Repressed by PD-1 to Prevent Lethal Disease.* PLOS Pathogens, 2016. **12**(5): p. e1005667.

251. Pabst, R., R.M. Binns, S.T. Licence, and M. Peter, *Evidence of a selective major vascular marginal pool of lymphocytes in the lung.* Am Rev Respir Dis, 1987. **136**(5): p. 1213-8.

252. Doerschuk, C.M., N. Beyers, H.O. Coxson, B. Wiggs, and J.C. Hogg, *Comparison of neutrophil and capillary diameters and their relation to neutrophil sequestration in the lung.* J Appl Physiol (1985), 1993. **74**(6): p. 3040-5.

253. Hogg, J.C., H.O. Coxson, M.L. Brumwell, N. Beyers, C.M. Doerschuk, W. MacNee, and B.R. Wiggs, *Erythrocyte and polymorphonuclear cell transit time and concentration in human pulmonary capillaries.* J Appl Physiol (1985), 1994. **77**(4): p. 1795-800.

254. Shirai, A., *Modeling neutrophil transport in pulmonary capillaries.* Respir Physiol Neurobiol, 2008. **163**(1-3): p. 158-65.

255. Thommasen, H.V., B.A. Martin, B.R. Wiggs, M. Quiroga, E.M. Baile, and J.C. Hogg, *Effect of pulmonary blood flow on leukocyte uptake and release by dog lung.* J Appl Physiol Respir Environ Exerc Physiol, 1984. **56**(4): p. 966-74.

256. Hogg, J.C., C.M. Doerschuk, B. Wiggs, and D. Minshall, *Neutrophil retention during a single transit through the pulmonary circulation.* J Appl Physiol (1985), 1992. **73**(4): p. 1683-5.

257. Baaten, B.J., C.R. Li, M.F. Deiro, M.M. Lin, P.J. Linton, and L.M. Bradley, *CD44 regulates survival and memory development in Th1 cells.* Immunity, 2010. **32**(1): p. 104-15.

258. Schiott, A., M. Lindstedt, B. Johansson-Lindbom, E. Roggen, and C.A. Borrebaeck, *CD27- CD4+ memory T cells define a differentiated memory population at both the functional and transcriptional levels.* Immunology, 2004. **113**(3): p. 363-70.

259. Pepper, M., J.L. Linehan, A.J. Pagan, T. Zell, T. Dileepan, P.P. Cleary, and M.K. Jenkins, *Different routes of bacterial infection induce long-lived TH1 memory cells and short-lived TH17 cells.* Nat Immunol, 2010. **11**(1): p. 83-9.

260. Mackay, L.K., A. Rahimpour, J.Z. Ma, N. Collins, A.T. Stock, M.L. Hafon, J. Vega-Ramos, P. Lauzurica, S.N. Mueller, T. Stefanovic, D.C. Tscharke, W.R. Heath, M. Inouye, F.R. Carbone, and T. Gebhardt, *The developmental pathway for*

CD103(+)CD8+ tissue-resident memory T cells of skin. Nat Immunol, 2013. **14**(12): p. 1294-301.

261. Masopust, D., V. Vezys, E.J. Wherry, D.L. Barber, and R. Ahmed, *Cutting Edge: Gut Microenvironment Promotes Differentiation of a Unique Memory CD8 T Cell Population.* J Immunol, 2006. **176**: p. 2079-2083.

262. Skon, C.N., J.Y. Lee, K.G. Anderson, D. Masopust, K.A. Hogquist, and S.C. Jameson, *Transcriptional downregulation of S1pr1 is required for the establishment of resident memory CD8+ T cells.* Nat Immunol, 2013. **14**(12): p. 1285-93.

263. Arnon, T.I., Y. Xu, C. Lo, T. Pham, J. An, S. Coughlin, G.W. Dorn, and J.G. Cyster, *GRK2-dependent S1PR1 desensitization is required for lymphocytes to overcome their attraction to blood.* Science, 2011. **333**(6051): p. 1898-903.

264. Matloubian, M., C.G. Lo, G. Cinamon, M.J. Lesneski, Y. Xu, V. Brinkmann, M.L. Allende, R.L. Proia, and J.G. Cyster, *Lymphocyte egress from thymus and peripheral lymphoid organs is dependent on S1P receptor 1.* Nature, 2004. **427**(6972): p. 355-60.

265. Shiow, L.R., D.B. Rosen, N. Brdickova, Y. Xu, J. An, L.L. Lanier, J.G. Cyster, and M. Matloubian, *CD69 acts downstream of interferon-alpha/beta to inhibit S1P1 and lymphocyte egress from lymphoid organs.* Nature, 2006. **440**(7083): p. 540-4.

266. Schenkel, Jason M. and D. Masopust, *Tissue-Resident Memory T Cells.* Immunity, 2014. **41**(6): p. 886-897.

267. Henao-Tamayo, M.I., D.J. Ordway, S.M. Irwin, S. Shang, C. Shanley, and I.M. Orme, *Phenotypic definition of effector and memory T-lymphocyte subsets in mice chronically infected with Mycobacterium tuberculosis.* Clin Vaccine Immunol, 2010. **17**(4): p. 618-25.

268. Kondrack, R.M., J. Harbertson, J.T. Tan, M.E. McBreen, C.D. Surh, and L.M. Bradley, *Interleukin 7 regulates the survival and generation of memory CD4 cells.* J Exp Med, 2003. **198**(12): p. 1797-806.

269. Lenz, D.C., S.K. Kurz, E. Lemmens, S.P. Schoenberger, J. Sprent, M.B. Oldstone, and D. Homann, *IL-7 regulates basal homeostatic proliferation of antiviral CD4+T cell memory.* Proc Natl Acad Sci U S A, 2004. **101**(25): p. 9357-62.

270. Rosenblum, M.D., S.S. Way, and A.K. Abbas, *Regulatory T cell memory.* Nat Rev Immunol, 2016. **16**(2): p. 90-101.

271. Kurtulus, S., P. Tripathi, and D. Hildeman, *Protecting and rescuing the effectors: roles of differentiation and survival in the control of memory T cell development.* Frontiers in Immunology, 2013. **3**(404).

272. Beverley, P.C., S. Sridhar, A. Lalvani, and E.Z. Tchilian, *Harnessing local and systemic immunity for vaccines against tuberculosis.* Mucosal Immunol, 2014. **7**(1): p. 20-6.

273. Clapp, B., X. Yang, T. Thornburg, N. Walters, and D.W. Pascual, *Nasal Vaccination Stimulates CD8(+) T Cells for Potent Protection Against Mucosal Brucella melitensis Challenge.* Immunology and cell biology, 2016. **94**(5): p. 496-508.

274. Rose, M.A., S. Zielen, and U. Baumann, *Mucosal immunity and nasal influenza vaccination.* Expert Rev Vaccines, 2012. **11**(5): p. 595-607.

275. Aguilo, N., S. Alvarez-Arguedas, S. Uranga, D. Marinova, M. Monzon, J. Badiola, and C. Martin, *Pulmonary but Not Subcutaneous Delivery of BCG Vaccine Confers Protection to Tuberculosis-Susceptible Mice by an Interleukin 17-Dependent Mechanism.* J Infect Dis, 2016. **213**(5): p. 831-9.

276. Derrick, S.C., K. Kolibab, A. Yang, and S.L. Morris, *Intranasal administration of Mycobacterium bovis BCG induces superior protection against aerosol infection with Mycobacterium tuberculosis in mice.* Clin Vaccine Immunol, 2014. **21**(10): p. 1443-51.

277. Aguilo, N., A.M. Toledo, E.M. Lopez-Roman, E. Perez-Herran, E. Gormley, J. Rullas-Trincado, I. Angulo-Barturen, and C. Martin, *Pulmonary Mycobacterium bovis BCG Vaccination Confers Dose-Dependent Superior Protection Compared to That of Subcutaneous Vaccination.* Clinical and Vaccine Immunology, 2014. **21**(4): p. 594-597.

278. Chen, L., J. Wang, A. Zganiacz, and Z. Xing, *Single intranasal mucosal Mycobacterium bovis BCG vaccination confers improved protection compared to subcutaneous vaccination against pulmonary tuberculosis.* Infect Immun, 2004. **72**(1): p. 238-46.

279. Giri, P.K., I. Verma, and G.K. Khuller, *Protective efficacy of intranasal vaccination with Mycobacterium bovis BCG against airway Mycobacterium tuberculosis challenge in mice.* J Infect, 2006. **53**(5): p. 350-6.

280. Price, D.N., D.F. Kusewitt, C.A. Lino, A.A. McBride, and P. Muttil, *Oral Tolerance to Environmental Mycobacteria Interferes with Intradermal, but Not Pulmonary, Immunization against Tuberculosis.* PLOS Pathogens, 2016. **12**(5): p. e1005614.

281. Garcia-Contreras, L., Y.-L. Wong, P. Muttil, D. Padilla, J. Sadoff, J. DeRousse, W.A. Germishuizen, S. Goonesekera, K. Elbert, B.R. Bloom, R. Miller, P.B. Fourie, A. Hickey, and D. Edwards, *Immunization by a bacterial aerosol.* Proceedings of the National Academy of Sciences, 2008. **105**(12): p. 4656-4660.

282. Barclay, W.R., W.M. Busey, D.W. Dalgard, R.C. Good, B.W. Janicki, J.E. Kasik, E. Ribi, C.E. Ulrich, and E. Wolinsky, *Protection of monkeys against airborne tuberculosis by aerosol vaccination with bacillus Calmette-Guerin.* Am Rev Respir Dis, 1973. **107**(3): p. 351-8.

283. Santosuosso, M., S. McCormick, X. Zhang, A. Zganiacz, and Z. Xing, *Intranasal boosting with an adenovirus-vectored vaccine markedly enhances protection by parenteral Mycobacterium bovis BCG immunization against pulmonary tuberculosis.* Infect Immun, 2006. **74**(8): p. 4634-43.

284. Jeyanathan, M., N. Thanthrige-Don, S. Afkhami, R. Lai, D. Damjanovic, A. Zganiacz, X. Feng, X.D. Yao, K.L. Rosenthal, M. Fe Medina, J. Gauldie, H.C. Ertl, and Z. Xing, *Novel chimpanzee adenovirus-vectored respiratory mucosal tuberculosis vaccine: overcoming local anti-human adenovirus immunity for potent TB protection.* Mucosal Immunol, 2015. **8**(6): p. 1373-1387.

285. Stylianou, E., K.L. Griffiths, H.C. Poyntz, R. Harrington-Kandt, M.D. Dicks, L. Stockdale, G. Betts, and H. McShane, *Improvement of BCG protective efficacy with a novel chimpanzee adenovirus and a modified vaccinia Ankara virus both expressing Ag85A.* Vaccine, 2015. **33**(48): p. 6800-8.

286. Ancelet, L.R., F.E. Aldwell, F.J. Rich, and J.R. Kirman, *Oral Vaccination with Lipid-Formulated BCG Induces a Long-lived, Multifunctional CD4^{+} T Cell Memory Immune Response.* PLOS ONE, 2012. **7**(9): p. e45888.

287. Lai, X., Y. Shen, D. Zhou, P. Sehgal, L. Shen, M. Simon, L. Qiu, N.L. Letvin, and Z.W. Chen, *Immune biology of macaque lymphocyte populations during mycobacterial infection.* Clin Exp Immunol, 2003. **133**(2): p. 182-92.

288. Kaushal, D., T.W. Foreman, U.S. Gautam, X. Alvarez, T. Adekambi, J. Rangel-Moreno, N.A. Golden, A.-M.F. Johnson, B.L. Phillips, M.H. Ahsan, K.E. Russell-Lodrigue, L.A. Doyle, C.J. Roy, P.J. Didier, J.L. Blanchard, J. Rengarajan, A.A. Lackner, S.A. Khader, and S. Mehra, *Mucosal vaccination with attenuated Mycobacterium tuberculosis induces strong central memory responses and protects against tuberculosis.* 2015. **6**: p. 8533.

289. Reiley, W.W., S. Shafiani, S.T. Wittmer, G.s. Tucker-Heard, J.J. Moon, M.K. Jenkins, K.B. Urdahl, G.M. Winslow, and D.L. Woodland, *Distinct functions of antigen-specific*

CD4 T cells during murine Mycobacterium tuberculosis infection. Proceedings of the National Academy of Sciences, 2010. **107**(45): p. 19408-19413.

290. Torrado, E., J.J. Fountain, M. Liao, M. Tighe, W.W. Reiley, R.P. Lai, G. Meintjes, J.E. Pearl, X. Chen, D.E. Zak, E.G. Thompson, A. Aderem, N. Ghilardi, A. Solache, K.K. McKinstry, T.M. Strutt, R.J. Wilkinson, S.L. Swain, and A.M. Cooper, *Interleukin 27R regulates CD4^{+} T cell phenotype and impacts protective immunity during Mycobacterium tuberculosis infection.* The Journal of Experimental Medicine, 2015. **212**(9): p. 1449-1463.

291. Moguche, A.O., M. Musvosvi, A. Penn-Nicholson, C.R. Plumlee, H. Mearns, H. Geldenhuys, E. Smit, D. Abrahams, V. Rozot, O. Dintwe, S.T. Hoff, I. Kromann, M. Ruhwald, P. Bang, R.P. Larson, S. Shafiani, S. Ma, D.R. Sherman, A. Sette, C.S. Lindestam Arlehamn, D.M. McKinney, H. Maecker, W.A. Hanekom, M. Hatherill, P. Andersen, T.J. Scriba, and K.B. Urdahl, *Antigen Availability Shapes T Cell Differentiation and Function during Tuberculosis.* Cell Host & Microbe. **21**(6): p. 695-706.e5.

292. Jeyanathan, M., S. Afkhami, A. Khera, T. Mandur, D. Damjanovic, Y. Yao, R. Lai, S. Haddadi, A. Dvorkin-Gheva, M. Jordana, S.L. Kunkel, and Z. Xing, *CXCR3 Signaling Is Required for Restricted Homing of Parenteral Tuberculosis Vaccine–Induced T Cells to Both the Lung Parenchyma and Airway.* The Journal of Immunology, 2017.

293. Satti, I., J. Meyer, S.A. Harris, Z.R. Manjaly Thomas, K. Griffiths, R.D. Antrobus, R. Rowland, R.L. Ramon, M. Smith, S. Sheehan, H. Bettinson, and H. McShane, *Safety and immunogenicity of a candidate tuberculosis vaccine MVA85A delivered by aerosol in BCG-vaccinated healthy adults: a phase 1, double-blind, randomised controlled trial.* Lancet Infect Dis, 2014. **14**(10): p. 939-46.

294. Jeyanathan, M., A. Heriazon, and Z. Xing, *Airway luminal T cells: a newcomer on the stage of TB vaccination strategies.* Trends Immunol, 2010. **31**(7): p. 247-52.

295. Srivastava, S. and J.D. Ernst, *Cutting edge: Direct recognition of infected cells by CD4 T cells is required for control of intracellular Mycobacterium tuberculosis in vivo.* J Immunol, 2013. **191**(3): p. 1016-20.

296. Santosuosso, M., X. Zhang, S. McCormick, J. Wang, M. Hitt, and Z. Xing, *Mechanisms of mucosal and parenteral tuberculosis vaccinations: adenoviral-based mucosal immunization preferentially elicits sustained accumulation of immune protective CD4 and CD8 T cells within the airway lumen.* J Immunol, 2005. **174**(12): p. 7986-94.

297. Wang, J., L. Thorson, R.W. Stokes, M. Santosuosso, K. Huygen, A. Zganiacz, M. Hitt, and Z. Xing, *Single mucosal, but not parenteral, immunization with recombinant*

adenoviral-based vaccine provides potent protection from pulmonary tuberculosis. J Immunol, 2004. **173**(10): p. 6357-65.

298. Horvath, C.N., C.R. Shaler, M. Jeyanathan, A. Zganiacz, and Z. Xing, *Mechanisms of delayed anti-tuberculosis protection in the lung of parenteral BCG-vaccinated hosts: a critical role of airway luminal T cells.* Mucosal Immunol, 2012. **5**(4): p. 420-31.

299. Jeyanathan, M., J. Mu, S. McCormick, D. Damjanovic, C.L. Small, C.R. Shaler, K. Kugathasan, and Z. Xing, *Murine airway luminal antituberculosis memory CD8 T cells by mucosal immunization are maintained via antigen-driven in situ proliferation, independent of peripheral T cell recruitment.* Am J Respir Crit Care Med, 2010. **181**(8): p. 862-72.

300. Lazar-Molnar, E., B. Chen, K.A. Sweeney, E.J. Wang, W. Liu, J. Lin, S.A. Porcelli, S.C. Almo, S.G. Nathenson, and W.R. Jacobs, Jr., *Programmed death-1 (PD-1)-deficient mice are extraordinarily sensitive to tuberculosis.* Proc Natl Acad Sci U S A, 2010. **107**(30): p. 13402-7.

301. Barber, D.L., K.D. Mayer-Barber, C.G. Feng, A.H. Sharpe, and A. Sher, *CD4 T cells promote rather than control tuberculosis in the absence of PD-1-mediated inhibition.* J Immunol, 2011. **186**(3): p. 1598-607.

302. Boer, M.C., K.E. van Meijgaarden, D. Goletti, V. Vanini, C. Prins, T.H.M. Ottenhoff, and S.A. Joosten, *KLRG1 and PD-1 expression are increased on T-cells following tuberculosis-treatment and identify cells with different proliferative capacities in BCG-vaccinated adults.* Tuberculosis, 2016. **97**(Supplement C): p. 163-171.

303. Scholzen, T. and J. Gerdes, *The Ki-67 protein: from the known and the unknown.* J Cell Physiol, 2000. **182**(3): p. 311-22.

304. Gerdes, J., U. Schwab, H. Lemke, and H. Stein, *Production of a mouse monoclonal antibody reactive with a human nuclear antigen associated with cell proliferation.* Int J Cancer, 1983. **31**(1): p. 13-20.

305. Gerdes, J., H. Lemke, H. Baisch, H.H. Wacker, U. Schwab, and H. Stein, *Cell cycle analysis of a cell proliferation-associated human nuclear antigen defined by the monoclonal antibody Ki-67.* J Immunol, 1984. **133**(4): p. 1710-5.

306. Schluter, C., M. Duchrow, C. Wohlenberg, M.H. Becker, G. Key, H.D. Flad, and J. Gerdes, *The cell proliferation-associated antigen of antibody Ki-67: a very large, ubiquitous nuclear protein with numerous repeated elements, representing a new kind of cell cycle-maintaining proteins.* J Cell Biol, 1993. **123**(3): p. 513-22.

307. Soares, A., L. Govender, J. Hughes, W. Mavakla, M. de Kock, C. Barnard, B. Pienaar, E. Janse van Rensburg, G. Jacobs, G. Khomba, L. Stone, B. Abel, T.J. Scriba, and W.A. Hanekom, *Novel application of Ki67 to quantify antigen-specific in vitro lymphoproliferation.* Journal of Immunological Methods, 2010. **362**(1-2): p. 43-50.

308. Gerlach, C., M. Golding, L. Larue, M.R. Alison, and J. Gerdes, *Ki-67 immunoexpression is a robust marker of proliferative cells in the rat.* Lab Invest, 1997. **77**(6): p. 697-8.

309. Starborg, M., K. Gell, E. Brundell, and C. Hoog, *The murine Ki-67 cell proliferation antigen accumulates in the nucleolar and heterochromatic regions of interphase cells and at the periphery of the mitotic chromosomes in a process essential for cell cycle progression.* Journal of Cell Science, 1996. **109**(1): p. 143-153.

310. Sharma, S.K., N.K. Chintala, S.K. Vadrevu, J. Patel, M. Karbowniczek, and M.M. Markiewski, *Pulmonary alveolar macrophages contribute to the premetastatic niche by suppressing antitumor T cell responses in the lungs.* J Immunol, 2015. **194**(11): p. 5529-38.

311. Ohta, Y. and K. Ichimura, *Proliferation Markers, Proliferating Cell Nuclear Antigen, Ki67, 5-Bromo-2'-Deoxyuridine, and Cyclin D1 in Mouse Olfactory Epithelium.* Annals of Otology, Rhinology & Laryngology, 2000. **109**(11): p. 1046-1048.

312. Winking, H., J. Gerdes, and W. Traut, *Expression of the proliferation marker Ki-67 during early mouse development.* Cytogenetic and Genome Research, 2004. **105**(2-4): p. 251-256.

313. Ancelet, L., F.J. Rich, B. Delahunt, and J.R. Kirman, *Dissecting memory T cell responses to TB: concerns using adoptive transfer into immunodeficient mice.* Tuberculosis (Edinb), 2012. **92**(5): p. 422-33.

314. Kauffman, K.D., M.A. Sallin, S. Sakai, O. Kamenyeva, J. Kabat, D. Weiner, M. Sutphin, D. Schimel, L. Via, C.E. Barry Iii, T. Wilder-Kofie, I. Moore, R. Moore, and D.L. Barber, *Defective positioning in granulomas but not lung-homing limits CD4 T-cell interactions with Mycobacterium tuberculosis-infected macrophages in rhesus macaques.* Mucosal Immunol, 2017.

315. Britton, G., D.C. MacDonald, J.S. Brown, M.K. Collins, and A.L. Goodman, *Using a prime and pull approach, lentivector vaccines expressing Ag85A induce immunogenicity but fail to induce protection against Mycobacterium bovis bacillus Calmette–Guérin challenge in mice.* Immunology, 2015. **146**(2): p. 264-270.

316. McShane, H., A.A. Pathan, C.R. Sander, S.M. Keating, S.C. Gilbert, K. Huygen, H.A. Fletcher, and A.V. Hill, *Recombinant modified vaccinia virus Ankara expressing antigen 85A boosts BCG-primed and naturally acquired antimycobacterial immunity in humans.* Nat Med, 2004. **10**(11): p. 1240-4.

317. Jeyanathan, M., A. Heriazon, and Z. Xing, *Airway luminal T cells: A newcomer on the stage of TB vaccination strategies.* Trends in Immunology. **31**(7): p. 247-252.

318. Leech, J.M., E. Sharif-Paghaleh, J. Maher, L. Livieratos, R.I. Lechler, G.E. Mullen, G. Lombardi, and L.A. Smyth, *Whole-body imaging of adoptively transferred T cells using magnetic resonance imaging, single photon emission computed tomography and positron emission tomography techniques, with a focus on regulatory T cells.* Clin Exp Immunol, 2013. **172**(2): p. 169-77.

319. Orme, I.M., *Characteristics and specificity of acquired immunologic memory to Mycobacterium tuberculosis infection.* J Immunol, 1988. **140**(10): p. 3589-93.

320. Andersen, P., A.B. Andersen, A.L. Sorensen, and S. Nagai, *Recall of long-lived immunity to Mycobacterium tuberculosis infection in mice.* J Immunol, 1995. **154**(7): p. 3359-72.

321. Griffin, J.P. and I.M. Orme, *Evolution of CD4 T-cell subsets following infection of naive and memory immune mice with Mycobacterium tuberculosis.* Infect Immun, 1994. **62**(5): p. 1683-1690.

322. Steinert, E.M., J.M. Schenkel, K.A. Fraser, L.K. Beura, L.S. Manlove, B.Z. Igyarto, P.J. Southern, and D. Masopust, *Quantifying Memory CD8 T Cells Reveals Regionalization of Immunosurveillance.* Cell, 2015. **161**(4): p. 737-49.

323. Gallagher, J. and D.M. Horwill, *A selective oleic acid albumin agar medium for the cultivation of Mycobacterium bovis.* J Hyg (Lond), 1977. **79**(1): p. 155-60.